Alma Mater Studiorum – Università di Bologna

DOTTORATO DI RICERCA IN

CHIMICA

Ciclo XXX

Settore Concorsuale di afferenza: 03/C2

Settore Scientifico disciplinare: CHIM/04

Exploring the gas-phase catalytic transfer hydrogenation as a tool for the production of fuels and chemicals from renewables

Presentata da: **Lorenzo Grazia**

Coordinatore Dottorato   **Supervisore**

Prof. Aldo Roda   **Prof.ssa Stefania Albonetti**

                                                                    Prof. Fabrizio Cavani

Esame finale anno 2018

"La volontà, abdicando, aveva ceduto lo scettro agli istinti;
il senso estetico aveva sostituito il senso morale.
Ma codesto senso estetico a punto,
sottilissimo e potentissimo e sempre attivo,
gli manteneva nello spirito un certo equilibrio;
cosìche si poteva dire che la sua vita fosse una continua lotta di forze contrarie
chiusa ne' limiti d'un certo equilibrio.
Li uomini d'intelletto, educati al culto della Bellezza,
conservano sempre,
anche nelle peggiori depravazioni,
una specie di ordine.
La concezione della Bellezza è, dirò così,
l'asse del loro essere interiore,
intorno al quale tutte le loro passioni gravitano."

"Il piacere"
Gabriele D'Annunzio

"Professore, un'ultima cosa. È vero tutto questo?
O sta succedendo dentro la mia testa?"
"Certo che sta succedendo dentro la tua testa, Harry.
Dovrebbe voler dire che non è vero?"

H. J. P and A. P. W. B. S.

"...volontà, istinti, equilibrio, intelletto, la bellezza del bilanciamento nonchè quella del simmetrico e asimmetrico, desideri, verità, immaginazione, passione... Per me non porre limiti a tutto ciò e alla propria mente è basilare per farci piacere quello che ci piace fare."

ABSTRACT

Over the past decade, great efforts have been devoted in the field of biomass valorization to the development of reductive processes for the sustainable production of bio-fuel additives and chemicals. Catalytic transfer hydrogenation, which uses alcohols as the hydrogen source, offers an interesting approach that avoids the use of both high H_2 pressure and precious metal catalysts. In this work, the vapour-phase production of furfuryl alcohol (FAL) and 2-methylfuran (MF) from biomass-derived furfural (FU), using methanol as the H-transfer agent was studied. Two class of catalysts were employed: basic-based systems such as MgO, Mg/Fe/O, Mg/Al/O and CaO; and a mixed iron-vanadium oxide $FeVO_4$. With the latter at the temperature of 320°C it was possible to achieve 80% yield to 2-methylfuran, with small amounts of 2,5-dimethylfuran (DMF) and 2-vinylfuran (VINFU) as by-products. Catalyst characterization highlighted that $FeVO_4$ reduction took place under the studied conditions, leading to the in-situ development of the true active phase. The study of the reaction network permitted us to infer on the relative contribution of H-transfer and hydrogenation, the latter from the in-situ generated formaldehyde and H_2, to 2-methylfuran formation. On the other hand, with the basic-base catalysts, it was demonstrated that both the pristine systems MgO and CaO were totally selective towards the formation of the unsaturated alcohol FAL as the only reduction product of FU at mild temperature condition, thus allowing selective H-transfer from methanol to the substrate. Conversely, the distribution of compounds obtained with Mg/Fe/O was significantly different, with 2-methylfuran formation prevailing when the reaction was carried out between 300 and 400 °C. In this temperature range, upon tuning the reaction conditions, a very high yield of 2-methylfuran was produced, thus indicating that the mixed oxide allows efficient sequential transfer hydrogenation/hydrogenolysis reactions. Furthermore the use of different hydrogen sources such as 2-propanol, acetone, acetaldehyde, formaldehyde and molecular hydrogen allow to identify the complete reaction network for the vapor-phase transformation of FU, demonstrating that both the in-situ produced molecular hydrogen and formaldehyde played a direct role in MF formation.

The reported results indicate the potential application of the catalytic transfer hydrogenation reaction as an efficient process for the selective de-oxygenation of biomass-derived molecules.

Negli ultimi decenni sempre maggiori sforzi sono stati effettuati nel campo della valorizzazione di prodotti derivanti da biomasse, in particolar modo lo sviluppo di processi sostenibili volti alla riduzione di building-block derivanti da fonti rinnovabili per la produzione di molecole base per l'industria chimica e additivi per bio-barburanti risulta un argomento di grande interesse. La reazione di Hydrogen Transfer, che prevede l'utilizzo di un alcol come fonte di idrogeno, costituisce un approccio interesante ed alternativo che evita l'utilizzo di H_2 ad alte pressioni e catalizzatori contenenti metalli nobili. Nel presente lavoro viene studiata la produzione in fase gassosa di alcol furfurilico (FAL) e 2-metilfurano (MF) per riduzione selettiva della molecola piattaforma furfurale (FU), ottenibile da biomasse di seconda generazione, utilizzando metanolo come reagente di Hydrogen Transfer. Nello specifico lo studio è stato basato sull'utilizzo di due categorie di catalizzatori eterogenei: la prima è costituita da catalizzatori basici come il MgO, Mg/Fe/O, Mg/Al/O e CaO; in secondo luogo l'attività dell'ossido misto $FeVO_4$ è stata studiata. Con l'ossido misto a base di ferro e vanadio è stato possibile ottenere, alla temperatura di 320°C, rese dell'80% in MF, con piccole tracce di 2,5-dimetilfurano (DMF) e 2-vinilfurano come principali coprodotti. La caratterizzazione effettuata sul catalyzzatore ha permesso di evidenziare come la riduzione del $FeVO_4$ nelle condizioni di reazione porti alla formazione della reale fase attiva. Lo studio del meccaniso di reazione ha inoltre permesso di dedurre come la produzione di MF in elevate quantità derivi dal contemporaneo effetto della reazione di hydrogen transfer, dell'attivazione dell'H_2 molecolare e della formaldeide prodotte in situ dalla de-idrogenazione del metanolo. D'altro canto con i catalizzatori basici è stato dimostrato come i sistemi puri MgO e CaO siano completamente selettivi nella conversione della FU ad alcol furfurilico come unico prodotto di riduzione in condizioni blande di temperatura. Al contrario la distribuzione dei prodotti otteuta con il catalizzatore Mg/Fe/O si dimostra profondamente differente in quanto il MF viene ottenuto come prodotto principale nel caso in cui la reazione venga condotta nell'intervallo di temperatura compreso tra 300 e 400°C. Nel menzionato intervallo di temperatura il MF viene ottenuto con rese elevate indicando come il catalizzatore contenente ferro presenti un'elevata attività verso la reazione di idrogenolisi consecutiva. L'utilizzo di fonti di idrogeno alternative come 2-propanolo, acetone, acetaldeide, formaldeide e idrogeno molecolare hanno permesso inoltre di identificare il meccanismo completo tramite il quale avviene la conversione, in fase gassosa, della FU utilizzando metanolo come reagente di H-Transfer dimostrando che sia

la formaldeide che l'idrogeno molecolare prodotti in situ influenzano direttamente la produzione di MF.

I risultati ottenuti sottolineano come la reazione di Hydrogen Transfer possa costituire un efficiente processo da utilizzare per diminuire il ocntenuto di ossigeno nelle molecole piattaforma derivanti da biomasse.

KEY WORDS

Catalytic transfer hydrogenation

Lignocellulose biomass

Furfural

Basic catalysts

FeVO$_4$

Methanol

SUMMARY

AIM OF THE WORK

In recent decades the continuing growing global demand for petrochemical products and fossil fuels, with the associated increase in CO_2 emission, has forced researchers to seek some renewable alternative feedstock for the production of chemicals and fuels[1,2]. In this field, the conversion of non-food lignocellulosic second-generation biomasses such as wood chips and agricultural and municipal wastes into chemicals and fuels has gained increasingly more importance. Indeed, lignocellulose can be converted into different chemicals and liquid fuels via biological and chemical pathways[3]. Furan derivatives play an important role in the transformation of this renewable feedstock[4,5,6,7]. For instance furfural (FU), which is available on an industrial scale via the hydrolysis–dehydration of the hemicellulose part of lignocellulosic biomass[8,9], is a key precursor for the synthesis of derivatives with applications in the fuel and polymer industries[10]. The FU upgrade processes involve the selective hydrogenation of the carbonyl group into the corresponding unsaturated furfuryl alcohol (FAL), which finds application in industry for the production of resins and fine chemicals[11,12], and into 2-methylfuran (MF) (**Scheme 1**), used as a renewable fuel. Indeed, this furan compound has superior properties as compared to bio-ethanol because of its higher energy density and octane values[13]. The octane number of MF is higher than that of gasoline (103 vs. 97 RON), while their energy densities are very close (28.5 MJ L^{-1} vs. 31.9 MJ L^{-1}), which means that with the same volume of fuel, MF contains 34% more energy than the market-leading biofuel ethanol[14].
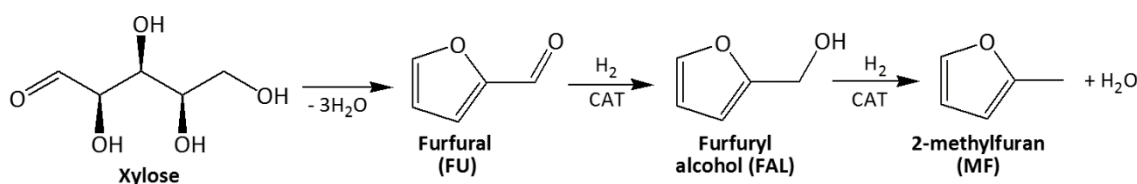
Scheme 1. Production of furfuryl alcohol (FAL) and 2-methylfuran (MF) from xylose and furfural (FU).

For the synthesis of MF from FU, the selective hydrodeoxygenation of the formyl group is necessary, avoiding the opening or hydrogenation of the furan ring. Indeed, one of the key challenges for upgrading FU is product selectivity, since the hydrogenation of FU often results in a mixture of side-chain and ring-hydrogenated products along with ring-opening products. Nickel-, copper-, and noble metal-based catalysts have been reported to be active in the conversion of FU to MF[15,16]. Zheng et al. reported an 87% yield to MF

with a catalyst of composition Cu/Zn/Al/Ca/Na=59:33:6:1:1[17]. A SiO$_2$-supported Cu/Fe bimetallic catalyst at 1 bar H$_2$ is reported to produce a 98% yield to MF[18]. On the other hand, a comparison of silica-supported monometallic Ni and bimetallic Ni-Fe catalysts for the conversion of FU at 1 bar of H$_2$ and 210-250°C showed that FAL is the primary reduction product obtained in high yield through the monometallic system. The introduction of Fe leads to an increased MF yield; indeed, Fe suppresses the decarbonylation activity of Ni and promotes the hydrogenation-hydrogenolysis of the FU carbonyl group[19].

An alternative approach for the reduction of the FU carbonyl group to produce FAL and MF, bypassing the need for high hydrogen pressure and noble metal-based catalysts, is the Meerwein–Ponndorf–Verley (MPV) reaction, in which an alcohol is used as the hydrogen source. The catalytic transfer hydrogenation is indeed a classic organic chemistry reaction discovered at the beginning of the XXth century by Meerwein, Ponndorf and Verley, who discover that carbonyl compounds are reduced in the presence of 2-propanol while, Oppenauer finds that secondary alcohols are oxidized in the presence of acetone. Under appropriate conditions, the reaction can be highly chemo-selective towards carbonyl groups[20,21,22].

Catalysts studied for this reaction may be divided into three main groups: Lewis basic, Lewis acid, and metal-supported catalysts[23,24,25].

Di Cosimo and co-workers reported on the use of MgO as selective catalyst for the conversion of a wide range of unsaturated ketones to the corresponding alcohols using isopropanol as the hydrogen source[26].

Dumesic and co-workers have demonstrated that ZrO$_2$ can be used as a catalyst with isopropanol as the H-donor to hydrogenate levulinic acid and ethyl levulinate for the production of γ-valerolactone. They also reported a systematic computational study on the MPV reaction applied to biomass derived molecules such as ethyl levulinate and FU[27]. Hermans et al. have reported that Cu, Ni and Pd supported on Fe$_2$O$_3$ are active in the catalytic transfer hydrogenation of FU to produce a mixture of FAL, MF and 2-methyltetahydrofuran (MTHF) both in batch and continuous flow reactor, using 2-propanol as the hydrogen donor. They demonstrated that the high activity of Pd/Fe$_2$O$_3$ is due to strong metal-support interaction[28].

Additionally, Vlachos and co-workers reported on the vapour-phase hydrodeoxygenation of FU to MF with 50-60% selectivity using MoC as the catalyst[29]. They also described a

liquid-phase catalytic transfer hydrogenation of FU over Ru/C and Ru/RuO catalysts, using various alcohols as hydrogen sources[30].

Nevertheless, there are only a few studies in literature concerning the vapour-phase production of MF from FU with heterogeneous catalysts, and most of them require noble metal-supported catalysts, together with high hydrogen pressure and reaction temperature. Therefore, the development of a continuous catalytic process based on non-noble metal catalysts for the hydrodeoxygenation of FU to MF is a very attractive topic. Moreover, the use of H-transfer instead of classical hydrogenation could make it possible to use bio-alcohols as hydrogen sources, thus increasing the sustainability of the entire process.

In this specific field, our research group recently reported on the use of methanol as a clean and efficient H-transfer reactant for carbonyl reduction in the liquid phase[31]. Compared to other molecules used in H-transfer, methanol showed the advantage of producing gaseous components as the only co-products. Using high-surface area MgO as a simple, easily recoverable and reusable catalyst for FU reduction, a 100% FAL yield was obtained.

As an alternative, mixed iron-vanadium mixed oxides could be used for the catalytic transfer hydrogenation on FU. Indeed, these materials were reported to be able to activate methanol in several reactions, for potential industrial applications. For example, Asahi Company reported that $FeVO_4$ is a very active and stable catalyst for the gas-phase methylation of phenol to *o*-cresol using methanol as the alkylating agent[32]. It was demonstrated that the strong de-hydrogenating properties of the catalyst make possible the in-situ formation of a high quantity of formaldehyde, which is the real (hydroxyl)alkylating agent. Furthermore, Andersson and co-workers reported that $FeVO_4$ is very active and selective in methanol oxidation to formaldehyde[33].

In this view, the aim of the present PhD Thesis is focused on the development of a new continuous gas-phase process, based on the catalytic transfer hydrogenation reaction, for the valorization of the second generation lignocellulose biomass-derived platform molecule furfural (FU). In particular the attention has been focused on the possibility to produce, as the target products, furfuryl alcohol (FAL) and 2-methylfuran (MF) using methanol as alternative hydrogen source and two main class of catalysts.

The first considered class of catalysts consists in the basic-based systems such as MgO, CaO and the Mg/Fe/O-Mg/Al/O mixed oxides. The second catalyst consists in the bulk mixed iron-vanadium oxide $FeVO_4$.

More in detail the work could be resumed as follow:

- ❖ Synthesis and characterization of the catalysts with the main techniques such as:
    - determination of the specific surface area through the single point model BET;
    - powder X-ray diffraction (XRD) for the determination of the crystalline structure;
    - thermogravimetric and differential thermal analysis (TGA-DTA) for the investigation of the catalyst's precursor decomposition and the determination of the heavy carbonaceous compounds formed during the catalytic tests;
    - Raman spectroscopy for the determination of the carbon deposits nature;
    - elemental analysis by-means of atomic adsorption;
    - in-situ DRIFT (Diffuse Reflectance Infrared Fourier Transform Spectroscopy) for the study of the interaction between the catalyst and the reagents;
    - temperature programmed-desorption-reduction-oxidation (TPDRO) for the determination of the acid-base and reducibility properties of the catalysts.
- ❖ Evaluation of the catalytic activity of the synthesized systems in the gas-phase catalytic transfer hydrogenation of FU to FAL and MF using methanol as hydrogen transfer reactant;
- ❖ Study of the overall reaction network in order to explain the role of the in-situ produced formaldehyde and molecular H_2 and the relationship between their direct involvement in the transformation of FU and the features of the catalysts in terms of acid-base, de-hydrogenating and de-oxygenating properties. Nevertheless, the study of the reaction mechanism for the formation of both the reduced product FAL and MF and the main side-products of the process has been evaluated feeding the possible reaction intermediates.

[1] R. Sheldon, *Green Chem.*, 2014, **16**, 950

[2] L. Hu, G. Zhao, W. Hao, X. Tang, Y. Sun, L. Lin and S. Liu, *RSC Adv.,* 2012, **2**, 11184

[3] Recommendations for Biofuels in the Aviation Industry; U.S. Department of Energy, Office of Energy Efficiency and Renewable Energy: Washington, DC, June 28, 2013

[4] A. Corma, S. Iborra and A. Velty, *Chem. Rev.*, 2007, **107**, 2411

[5] M. J. Climent, A. Corma and S. Iborra, *Green Chem.,* 2014, **16**, 516

[6] B. Liu and Z. Zhang, *ChemSusChem,* 2016, **9**,2015

[7] L. Hu, L. Lin, Z. Wu, S. Zhou and S. Liu, *Renew. Sust. Energ. Rev.,* 2017, **74**, 230

[8] H. Nguyen, R. F. DeJaco, N. Mittal, J. I. Siepmann, M. Tsapatsis, M. A. Snyder, W. Fan, B. Saha and D. G. Vlachos, *Annu. Rev. Chem. Biomol. Eng.*, 2017, 6.1

[9] N. K. Gupta, A. Fukuoka and K. Nakajima, *ACS Catal.,* 2017, **7**, 2430

[10] J. P. Lange, E. van der Heide, J. van Buijtenen and R. Price, *ChemSusChem*, 2012, **5**, 150

[11] J. Kijenski, P. Winiarek, T. Paryjczak, A. Lewicki, A. Mikołajska, *Appl. Catal. A: Gen.* 2002, **233**, 171

[12] B.M. Nagaraja, A.H. Padmasri, B. David Raju, K.S. Rama Rao, *J. Mol. Catal. A: Chem.,* 2007, **265**, 90

[13] M. Thewes, M. Muether, S. Pischinger, M. Budde, A. Brunn, A. Sehr, P. Adomeit, J. Klankermayer, *Energy & Fuels,* 2011, **25** (12), 5549

[14] X. Ma, C. Jiang, H. Xu, H. Ding and S. Shuai, *Fuel,* 2014, **116**, 281

[15] Y. Nakagawa, M. Tamura and K. Tomishige, *ACS Catal.*, 2013, **3**, 2655

[16] P. Gallezot, *Chem. Soc. Rev.,* 2012, **41**, 1538

[17] H. Y. Zheng, Y. L. Zhu, B. T. Teng, Z. Q. Bai, C. H. Zhang, H. W. Xiang and Y. W. Li, *J. Mol. Catal. A Chem.*, 2006, **246**, 18

[18] J. Lessard, J. F. Morin, J. F. Wehrung, D. Magnin, E. Chornet, *Top Catal.,* 2010, **53**, 1231

[19] S. Sitthisa, W. An, D. E. Resasco, *J. Catal.,* 2011, **284**,90

[20] G. Brieger and T. Nestrick, *Chem. Rev.,* 1974, **74**, 567

[21] J. R. Ruiz and C. Jiménez-Sanchidrián, *Curr. Org. Chem.,* 2007, **11**, 1113

[22] a) M. J. Gilkey and B. Xu, *ACS Catal.,* 2016, **6**, 1420; b) F. Cavani, S, Albonetti, F. Basile and A. Gandini, (eds.) *"Chemicals and Fuels from Bio-Based Building Blocks"* 2016, ISBN 978-3-527-33897-9 Wiley-VCH, Weinheim; c) B. Cai, X-C. Zhou, Y.-C. Miao, J.-Y. Luo, H. Pan, Y.-B. Huang *ACS Sustain. Chem. Eng.* 2017, **5** (2), 1322

[23] F. Wang, Z. Zhang, *ACS Sust. Chem. Eng.,* 2017, **5**, 942

[24] M. M. Villaverde, T. F. Garetto, A. J. Marchi, *Catal. Commun.,* 2015, **58**, 6

[25] J. Li, J. I. Liu, H. Zhou, Y. Fu, *ChemSusChem,* 2016, **9**, 1339

[26] J.J. Ramos, V.K. Diez, C.A. Ferretti, P.A. Torresi, C.R. Apesteguia, J.I. Di Cosimo, *Catal. Today,* 2011, **172**, 41

[27] R. S. Assary, L. A. Curtiss and J. A. Dumesic, *ACS Catal.,* 2013, 3, 2694

[28] D. Scholz, C. Aellig, and I. Hermans, *ChemSusChem,* 2014, **7**, 268

[29] W. S. Lee, Z. Wang, Z. Weiqing, D. G. Vlachos, B. Aditya, *Catal. Sci. Technol.,* 2014, **4**, 2340

[30] a) P. Panagiotopoulou, N. Martin, D. G. Vlachos, *J. Mol. Catal. A: Chem.,* 2014, **392**, 223; b) A.V. Mironeko, D.G. Vlachos *J. Am. Chem. Soc.* 2016, **138**, 8104; c) M. J. Gilkey, P. Panagiotopoulou, A. V. Mironenko, G. R. Jenness, D. G. Vlachos and B. Xu, *ACS Catal.* 2015**, 5(7),** 3988

[31] T. Pasini, A. Lolli, S. Albonetti, F. Cavani, M. Mella, *J. Catal.,* 2014, **317**, 206

[32] Nakajima et al., United State Patent 3937669, 1976

[33] A. Andersson, J. Holmberg, R. Haggblad, *Top Catal.,* 2016, **59**, 1589

CHAPTER 1   IInd generation lignocellulose biomass upgrading

1.1. Introduction

In the last decades the continue increase of global demand for petrochemical products and fossil fuels associated with the increase of CO_2 emission have forced the researchers to find renewable alternative feedstock for the production of chemicals and fuels[1,2]. Nowadays more than 75% of the energy produced all over the world derives from fossil sources as carbon coke, oil and natural gas[3]. In this field the conversion of biomass into fuels and chemicals has been considered one the most attractive alternative to the use of the fossil sources. Indeed, the use of these renewable material allow to decrease the CO_2 emission in the atmosphere considering that carbon dioxide is involved itself in the process of biomass re-generation. In 2002 a report published from 26 experts and named "Roadmap for Biomass Technologies" has predicted that within the 2030 the 20% of the fuels and the 25% of the chemicals would be produced from biomass[4]. Taking into account this, the challenge for the researcher is the development of new economic and environmentally friendly process for the conversion of biomass-derived materials into fuels and high value chemicals. The use of renewable starting materials represent an attractive route for the production of chemicals due to the high functionalization degree of the platform molecules deriving from their transformation. For instance, the valorization processe involve a less number of step with the result of minimize the by-products[5,6].

At the moment the biomass feedstock could be divided into three different groups depending on the origin. The first generation (1G), comprising corn, sugar cane, oily seed and bagasse shows an high potential in terms of valorization but, at the same time, presents reasonable ethic drawbacks related to the competition with food culture. On the contrary, the second generation (2G), based on the use of wood chips, agricultural and municipal wastes represents a promising alternative considering the non-ethic problem. Finally, in the last years, the use of the third generation (3G) biomass, such as algae, become always more relevant[7].

In order to reach the mentioned targets, consisting in the development of process for the valorization and the production of fuels and chemical from renewable sources, a biomass-transformation industry layout has been proposed on the base of the classic refinery. The National Renewable Energy Laboratory (NREL) creates the bio-refinery industry model, a new concept in which the process for the conversion of biomass into fuels, chemicals and energy are integrated.

1.2. The integrated Biorefinery

As introduced above the main challenge for the biorefinery consists in the possibility to produce fine chemicals and fuels starting from renewable sources optimizing and integrating to these process the production of energy, in order to improve the balance between the input of energy and raw materials required for the biomass transformation and the output (chemicals, energy and waste treatment)[8,9].

Figure 1-1 shows the simplified scheme of an integrated biorefinery, in which the conversion of the biomass into fuels, chemicals energy and added value products are integrated in order to maximized the raw materials used and the gain deriving from the sale of the products.
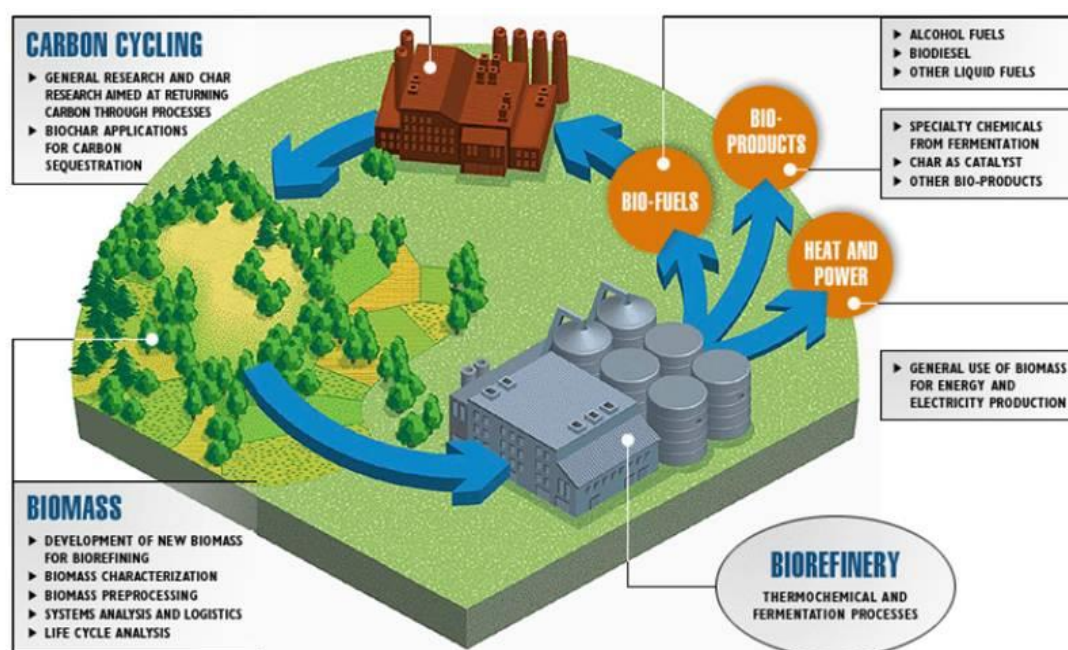
Figure 1-1. *Simplified scheme of integrated biorefinery*

One of the main drawback connected to the production of biofuels, bioethanol and fine chemicals from renewable sources in the biorefinery plant is that the transformation process are not still sustainable from the economic point of view. Indeed, the thermo-catalytic process for the oil transformation into fuels and starting materials for the chemical industries have been developed from more than a century, with optimized technologies and an economic feasibility related to the possibility to build big plants in terms of annual production.

To make up for that drawback the development of an economically sustainable biorefinery has to be made on the integration idea. That means to place side by side the production of fuels and energy, process that bring to a loss of money at the moment, and the production of high value chemicals that allow to reach an overall positive economic balance. In this field, the production process that take place in an integrated biorefinery for the transformation of the biomass could be summarized as follow:

- ❖ production of syn-gas and bio-oil through gasification and pyrolysis process;
- ❖ production of high value chemicals from carbohydrates such as glucose, fructose and xylose through catalytic or enzymatic process;
- ❖ production of chemicals through new synthetic strategies based on single step transformation in order to minimize the cost of the process, the formation of by or co-products and the waste treatment.

In the last years, a list of the 12 most important building blocks deriving from sugar transformation has been published (**Figure 1-2**); these compounds could be transformed into an high number of products with direct application in the polymer industry or as fuels. On the other hand, for some of them a direct application as monomer for the production of polymers is possible.
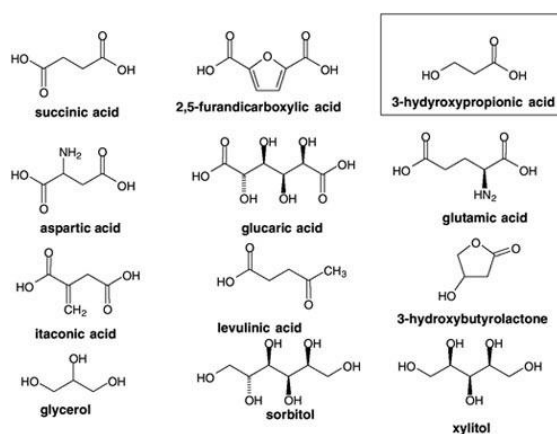
Figure 1-2. *Most promising buiding blocks deriving from sugars.*

1.3. Lignocellulose materials

In the prospective for the development of an integrated and economically sustainable biorefinery, lignocellulose biomass has been considered one of the main alternative to the fossil sources for the production of fuels and chemicals thanks to its abundance and to the non-food-based renewable carbon availability[10]. In the family of the lignocellulose materials could be considered the agricultural and municipal wastes, the wood chips produced from the wood industry. These kind of second generation biomass has attracted the researcher's interest thanks to their composition. Indeed, these materials are composed by three main fractions: cellulose, hemicellulose and lignin (**Figure 1-3**). These could be treated and transformed into platform molecules and high value chemicals by-means of thermos-catalytic and enzymatic process.
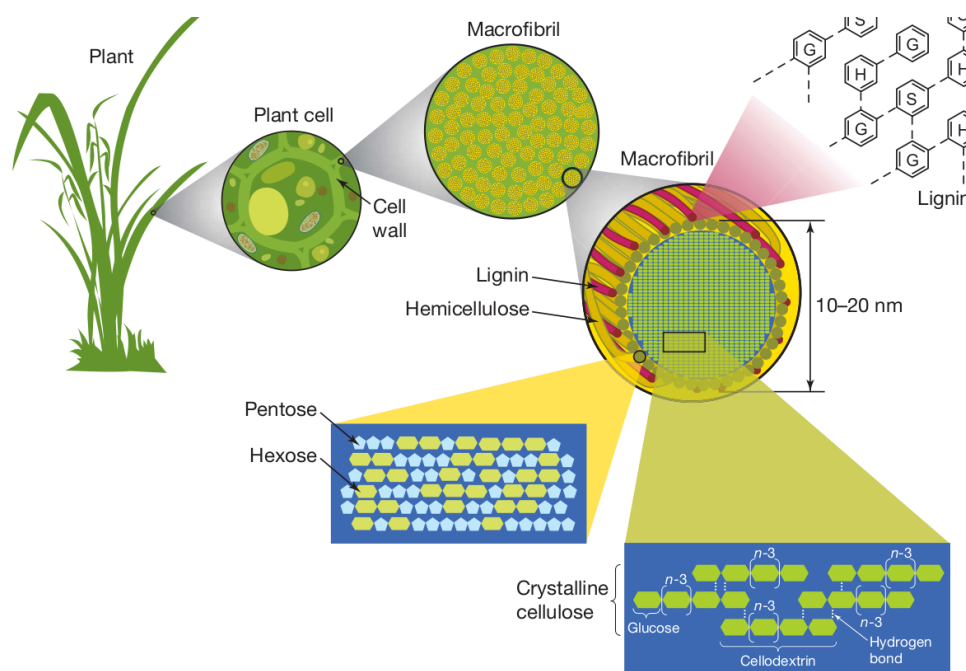
Figure 1-3. *Structure of lignocellulose materials.*

Considered one of the most attractive renewable resource, lignocellulose is extremely stable against chemical and biochemical processing due to its rigid structure. To date, different strategies have been proposed for the valorization of cellulose and hemicellulose such as the complete gasification, high temperature pyrolysis, as well as stepwise transformation through fractionation and depolymerization of the lignocellulosic polysaccharides[8,11,12]. A potential bio-refinery scheme aiming for a controlled fractionation and depolymerization of lignocellulose comprehends a sequence of the following steps:

1. fractionation of lignocellulose into biopolymers: cellulose, hemicelluloses and lignin;
2. depolymerization of the biopolymers into the forming monomers;
3. transformation of the monomers into value-added products.

Due to distinct differences of structure and reactivity of cellulose, hemicelluloses and lignin, they have to be processed under different reaction conditions[13]. A general approach toward fractionation is a selective solubilization of lignin or hemicelluloses leaving the least-reactive cellulose intact[14]. Examples of potential fractionation processes include steam explosion for solubilization of hemicelluloses or alkaline treatment for dissolution of lignin and partial defunctionalization of hemicelluloses[15,16]. In any case, it is important to note that the structure and composition of lignocellulosic biomass is highly dependent on the plant type. For instance, hardwoods contain more cellulose and hemicellulose, but softwoods are reported to contain more lignin[17]. **Table 1-1** shows the typical compositional characteristics of various common lignocellulosic biomass resources.

Biomass	Composition (%)			Method of analysis
	Cellulose	**Hemicellulose**	**Lignin**	
Corn stover	40.8	20.6	21.3	NREL: LAP[a]
Hardwood barks	39-44	19-25	18-22	
Miscanthus straw	44.5	26.2	26.5	
Poplar wood	49.3	21.5	25.4	TAPPI method[b]
Rice straw	36.5	20.8	16.9	NREL: LAP
Softwood barks	16-41	18-21	23-40	
Sugarcane bagasse	41.0	30.1	21.1	
Switchgrass	34.8	28.5	23.5	
Wheat straw	35.2	22.2	22.1	

[a] NREL: LAP stands for "National Renewable Energy Laboratoty: Laboratory Analytical Procedure"

[b] TAPPI method stands for "Technical Association of the Pulp and Paper Industry Methods"

Table 1-1. *Typical compositional properties for various common lignocellulosic biomass. Adapted from [18]*

1.3.1. Structure of cellulose, hemicellulose and lignin

Cellulose is the most abundant homo-polysaccharide in nature representing about 1.5×10^{12} tons of the annual biomass production. The cellulose macromolecule is composed of D-glucose monomer units connected to each other via α-1,4-glycosidic bonds (**Figure 1-4**).The degree of polymerization of cellulose depending from the cellulose source. Cellulose chains in primary plant cell walls, have a degree of polymerization (DP) ranging from 5000 to 7500 glucose units, and in wood and cotton-based materials between 10,000 and 15,000[19]. Each repeating unit of cellulose contains three hydroxyl groups which are involved in networking of the units with hydrogen bonds (**Figure 1-4**). The intra-chain hydrogen bonding between hydroxyl groups and oxygen of the adjacent ring molecules makes the linkage stable and results in the linear configuration of the cellulose chains[20].The cellulose structure consists of crystalline and amorphous domains. The hydroxyl groups in cellulose chains form intra-and intermolecular hydrogen bonds constituting the crystalline structure.
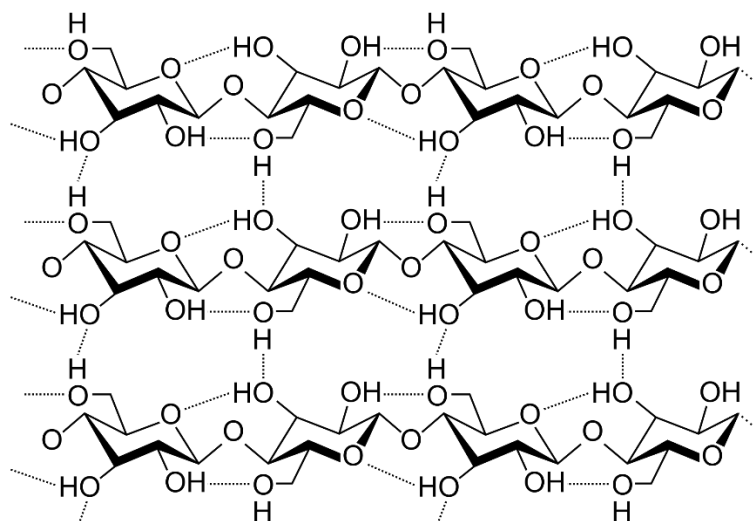
Figure 1-4. *Schematic structure of cellulose.*

The arrangement of cellulose molecules with respect to each other and to the fiber axis determines the physical and chemical properties of cellulose. The fiber structure of cellulose provides its high chemical stability. Crystalline domains of cellulose are less accessible to chemical reactants. On the other hand, amorphous regions are easily penetrated by reactants during chemical reactions[20].The reactivity of cellulose can be determined by several factors such as hydrogen bonding, the length of chains, the distribution of chain length, the crystallinity and the distribution of functional groups within the repeating units and along the polymer chains[19].

Hemicelluloses are the second major polysaccharides in plant cell. Unlike cellulose, hemicelluloses are hetero-polymers, they are composed of different monomeric units. Hemicelluloses are often branched (**Figure 1-5**): they have a main chain and side groups attached to it. A number of monosaccharides and organic acids can be produced by hydrolysis of hemicelluloses, e.g. xylose, arabinose, mannose, galactose, acetic acid, glucuronic acid, etc.
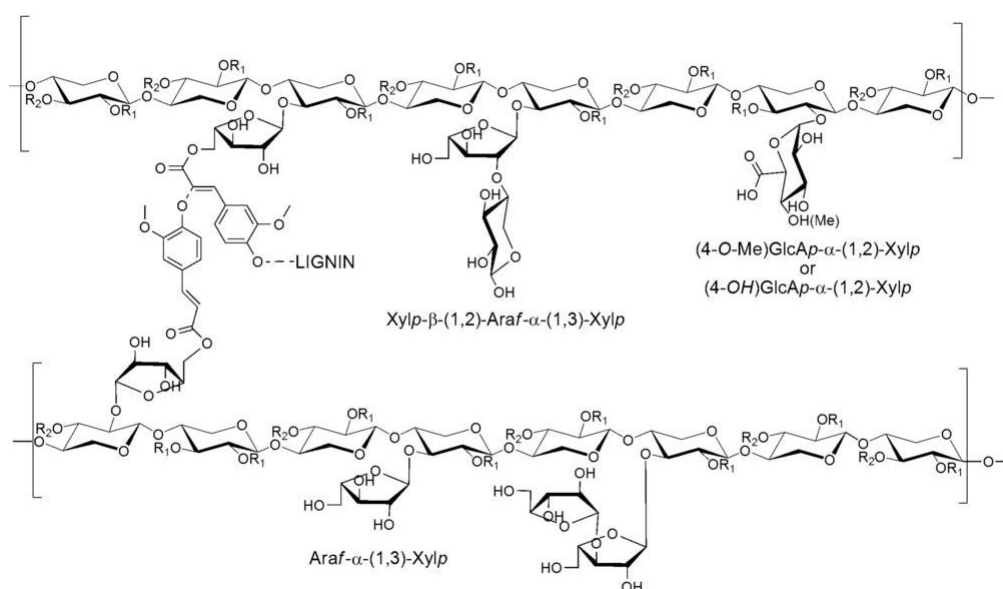
Figure 1-5. *Schematic structure of hemicellulose.*

Importantly, the sub-class and polymerization degree of hemi-celluloses depends on not only the plant species, but also the tissue type and development stage[21,22]. Hemicelluloses were reported to be chemically associated with lignin, cellulose or proteins. Spectroscopic data suggest that most probably hemi-celluloses are not connected to cellulose via chemical bonding, but rather via hydrogen bonds or van der Waals forces[21]. On the contrary, chemical association of hemicelluloses with phenolic lignin compounds has been known for a long time. As shown below, such chemical association is considered as a reason for existence of slow-reacting xylan. Alike cellulose, backbones of hemicelluloses consist of β-(1,4)-linked monomers, but the branched structure of hemicelluloses prevents extensive formation of hydrogen bonds. Hence, in contrast to cellulose, hemicelluloses are amorphous, and therefore exhibit higher reactivity for hydrolysis.

Lignin is an amorphous phenolic bio-polymer composed by an high heterogeneity of phenolic-based molecules, and it plays a vital role in the recalcitrance of biomass by acting as a physical barrier that protects the biomass against attack from microorganisms

as well as chemical degradation[23,24,25]. In short, the impermeability of lignocellulosic biomass towards mechanical and biological degradation is contributed by the complex structure of cellulose that provides strength over cell walls, hemicellulose that serve as wire mesh that circulate around cellulose, while lignin fills up any remaining space and prevents the polysaccharide environment from water[26].
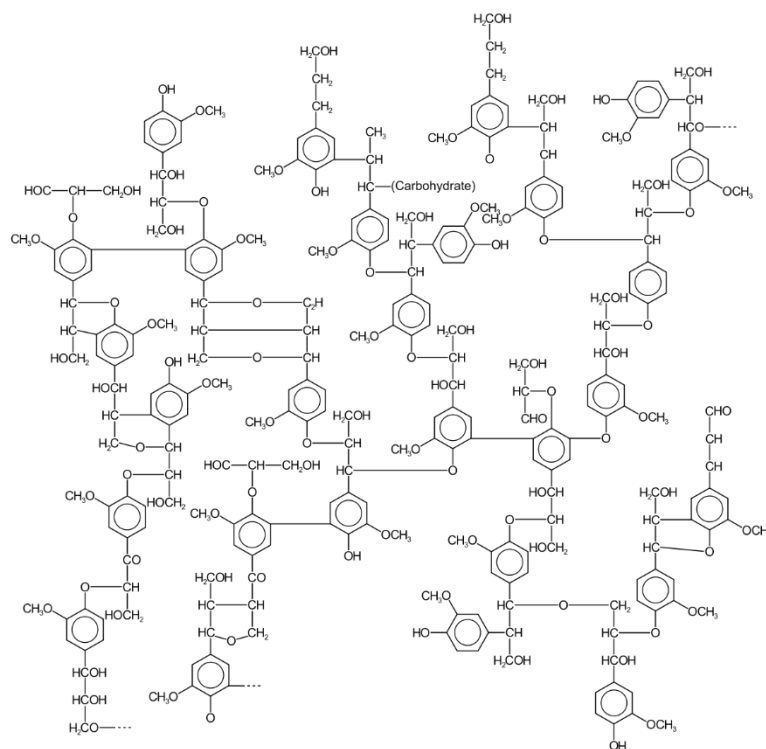
***Figure 1-6.** Schematic structure of lignin.*

1.3.2. Strategies for cellulose and hemicellulose hydrolysis

According to the recent scientific reports, a large portfolio of chemical compounds can be synthesized based on monosaccharides[8,11,12]. Several carbohydrate-based processes have already been commercialized, but the majority of them relies on monosaccharides derived from edible resources such as starch or sucrose[27]. Obviously, hydrolysis of cellulose and hemicelluloses still poses challenges, which need to be solved. Different techniques can be applied for depolymerization of polysaccharides, e.g. acid-catalyzed aqueous-phase hydrolysis[28], hydrolysis using ionic liquids[29], enzymatic depolymerization[30], and solubilization in super-critical water with subsequent hydrolysis[31,32]. Known for a long time, acid hydrolysis of cellulose and hemicelluloses still receives great attention due to high attractiveness for commercial application. Indeed. It is well known that from the hydrolysis of cellulose glucose could be obtained as the

main product while, from the hemicellulose fraction, xylose is the main produced monosaccharide. A further acid de-hydration process over these monosaccharides allow to form two of the most considered platform molecules deriving from renewable sources: 5-hydroxymethylfurfural (HMF) and 2-furaldehyde or furfural (FU)[33,34].

One of the attempts to utilize the polysaccharides comprising lignocellulose considered the treatment of wood with an acid to conduct simultaneous hydrolysis of hemicelluloses and cellulose[13]. However, amorphous hemicelluloses undergo hydrolysis under milder conditions than crystalline cellulose. In addition, under the harsh reaction conditions required for acid hydrolysis of cellulose, monosaccharides derived from hemicelluloses suffer from decomposition. Elaboration of two-step processes improved the overall yield of derived monosaccharides[13]. The first step of such processes is treatment of wood with diluted acids under mild conditions to accomplish hydrolysis of hemicelluloses leaving solid cellulose and lignin unaltered. Dissolved hemicellulosic monosaccharides can be easily isolated with the liquid phase. The second step of the process is hydrolysis of cellulose under harsher conditions. Processes for "wood saccharification" are known for a longtime including examples such as the two-step Scholler process or the Noguchi process[35].

Cellulose

Hydrolysis of cellulose with dilute or concentrated sulfuric acid and HCl has been used since the 1940s[36.37,38]. Two different methods have been applied for acid hydrolysis of cellulose. The first method uses a high concentration of mineral acids (e.g.,15–16 N HCl or 31–70 wt% H_2SO_4) and low operation temperatures(20–50°C). The major drawbacks of this method are the high cost of acid recovery and the need for expensive construction materials. In the second method, a highly diluted acid (pH 1.5–2.5) at high operation temperatures (200–230°C) is utilized. This method is more favorable and most frequently applied[39,40]. Reaction conditions dramatically influence the yield of glucose. An optimization of reaction parameters requires considering conditions such as reaction time, initial concentration, reactor con-figuration (CSTR, plug flow, percolation reactor), operation mode (batch, continuous), the applied temperature and acid concentration. For example, the yield of glucose was about 50% when using a plug flow reactor with short residence time of 0.22 min and 1 wt% of sulfuric acid at 240◦C. In batch operation with 0.07 wt% of sulfuric acid, 65% yield of glucose could be obtained after 30 min. It should

be noted that harsh reaction conditions, i.e. high temperature and long time, lead to enhanced degradation to dehydration products including HMF, furfural and levulinic acid. Due to the presence of minerals in cellulose, partial neutralization of acidic catalysts takes place[41,42,43]. Therefore, several investigators proposed including the neutralization capacity of cellulose into the rate of hydrolysis[44,45].

Although mineral liquid acids are highly active even under mild conditions for many acid-catalyzed reactions including the hydrolysis of cellulose, their fatal problem is the difficulty in recycling the acids and the consequent costly post-treatments such as neutralization and effluent processing, which is environmentally unfriendly. Therefore, highly active and stable solid acid catalysts are very fascinating for numerous "green" chemical processes. Hara et al.[46,47,48,49] recently developed a type of carbon-based solid acid with a high density of Brönsted acid sites (SO$_3$H and COOH) to pyrolytically carbonize sugars such as glucose, sucrose, or cellulose and subsequently sulfonate the as-prepared carbons. It is interesting that these sulfonated carbon materials are very active for the hydrolysis of microcrystalline cellulose to produce water-soluble saccharides even at a low reaction temperature (100 °C), and conventional strong solid Brönsted acid catalysts such as niobic acid, H-mordenite, Nafion, and Amberlyst-15 had no activity[47]. The specific surface area of the sulfonated carbon was only around 2 m^2/g but the yield of soluble saccharides reached nearly 70%. Using sulfonated silica-carbon nanocomposites Van de Vyver et al.[50] improved the glucose yield to 50% at 61% conversion of cellulose under similar reaction conditions. Furthermore, Pang et al.[51] reported a 75% glucose yield with 94% conversion of cellulose on sulfonated mesoporous carbon CMK-3. Although many other solid acid catalysts such as layered niobium molybdate (HNbMoO6)[52] and wormhole-type mesoporous TaxW10-x oxides[53] in addition to conventional solid acids like sulfonated zirconia, Amberlyst and Nafion were used for cellulose conversion, low catalytic activities have been obtained until now.

Hemicellulose

For the recent 20–30 years, the attention to acid hydrolysis of hemicellulosic components of lignocellulose has increased. This development is connected with novel "bio-refinery concepts" and growing interest in microbial synthesis of bioethanol[28].Switching from a starch, sucrose and glucose-based production of bioethanol to lignocellulosic bioethanol is very beneficial from an economical point. However, cellulose as a part of lignocellulose

is strongly associated with lignin and hemicelluloses dramatically hampering the access of microorganisms to cellulose[28,30]. The accessibility of cellulose can be increased by treating lignocellulose with diluted acids[28,30]. Efficient removal of hemi-celluloses prior to fermentation is crucial, because the cellulose enzyme is significantly inhibited by xylose, xylan and especially xylo-oligosaccharides[54,55,56]. In this case, the process can be considered both as a pre-treatment technique and as a way to recover hemicellulosic monosaccharides. Therefore, such approaches are sometimes referred to as "acid pre-hydrolysis". Acid pre-hydrolysis of lignocellulose is carried out in the presence of diluted acids with a concentration of 0.25–6 wt.%[57,58,59]. Investigations mainly focus on H_2SO_4 as catalyst, but other mineral acids such as HCl[60], H_3PO_4[61], or HNO3[62], and organic acids, e.g. maleic[63], oxalic[64], acetic[65] or trifluroacetic acids were also tested. At pH 2 and lower, the rate of hydrolysis is a function of proton concentration and does not depend on the nature of the acid catalyst.The reaction is usually conducted in a temperature range of 70 to 220°C. At low temperatures, hydrolysis is too slow, while at high temperature, also cellulose starts to hydrolyse. Many efforts were made preventing monosaccharide decomposition. A high selectivity toward monosaccharides is crucial, as side products such as furfural inhibit subsequent fermentation. Hydrolysis at high temperature is often complete within less than 2 h but is associated with the mentioned by-products formation[66]. Lowering the temperature to 90◦C increases selectivity to 100%. However, up to 24 hare required for full conversion of hemicelluloses under these conditions.

Hydrolysis of hemicelluloses using pure water is also the focus of numerous investigations[67]. The main motivation for using non-acid aqueous hydrolysis is exclusion of soluble acids. Although diluted sulfuric acid is an extremely cheap reagent, its exploitation dramatically increases the capital costs, as it requires a corrosion resistant construction. Furthermore, classic removal of sulfuric acid from monosaccharide hydrolysates proceeds via precipitation with calcium ions. Consequently, lime is produced as side product and needs disposal. Aqueous hydrolysis can be performed as e.g. treatment of lignocellulose with hot water or applying steam explosion. The process is usually conducted at 150–220°C[68], i.e. it requires higher temperatures compared to acid hydrolysis.

1.4. Furanic sugar-derived platform molecules: 5-hydroxymethylfurfural (HMF) and 2-furaldehyde or furfural (FU)

The de-hydration of the 5 or 6 carbon atoms monosaccharides obtained from the depolymerization of the cellulose and hemicellulose fraction of lignocellulose materials bring to the formation of the 5-hydroxymethylurfural (HMF) and 2-furaldehyde or furfural (FU). These compounds have been considered two of the most important platform molecules deriving from renewable sources due to the possibility to produce, from their transformation, several molecules with application as fuels, monomer for the polymer industry and as fine chemical.

1.4.1. 5-hydroxymethylfurfural (HMF)

As mentioned above, the possibility to produce HMF in high yield starting from renewable lignocellulose feedstock represent one of the most attractive route for the production of fuels, fine chemicals and monomers for the polymer industry as alternative to the classic fossil sources. In particular HMF could be synthesized from different starting monosaccharides or oligo-saccharides mainly deriving from the cellulose fraction of the lignocellulose feedstock. Fructose, glucose, sucrose inulin and starch itself compose the main raw materials used as starter for the production of HMF[33]. The general strategy applied for the conversion of these sugars into the desired six carbon atoms furanic platform molecule involve the use of an acid catalyst, both homogeneous mineral acids and heterogeneous acid catalysts have been used, that is able to promote the hydrolysis and the de-hydration of the monosaccharides. Obviously different type of acid catalysts are used depending on the initial substrate used. For instance, starting from fructose and inulin the possibility to obtain HMF yield between 24 and 97% was claimed. Qi et al.[69,70] studied the dehydration of fructose in the presence of a strong acidic resin Dowex 50wx8-100 in water–acetone and acetone–DMSO, HMF yields of 73.4 and 89.8% were achieved, respectively. Nafion-H was used for the dehydration of fructose in DMSO, HMF yield was 75%. When the reaction was performed under mild evacuation, the yield of HMF could be improved to 94%[71]. Subsequently, another acidic resin Amberlyst-15 was also tested for the formation of HMF from fructose, and yield of 83.3% was reached[72].

Moreau et al.[73] examined the application of H-form mordenite for the dehydration of fructose and obtained 74% HMF yield in water/MIBK. When H-ZSM-5 and Hβ-zeolite were used in the same solvent, HMF yields of 45 and 32% were achieved, respectively[74]. Recently, SBA-15-SO_3H was also synthesized and used for the dehydration of fructose, 81% HMF yield was obtained. Moreover, the evaluation of these catalysts indicated that the acidity and pore size of zeolites have a large effect on catalytic activities in the synthesis of HMF[75].

Yang found that Nb_2O_5 and Ta_2O_5 also possessed good performance on fructose dehydration and the latter was more effective than the former. More importantly, H_3PO_4–modified Ta_2O_5 (TA-p) exhibited stronger acidity, which is highly favorable for the synthesis of HMF, and a yield of 90% was obtained in water/2-butanol. When inulin was used as feedstock, 87% HMF yield was achieved[76].

As can be seen from the above description, the dehydration of fructose into HMF is very easy and efficient. However, it should be pointed out that fructose is not abundant in nature because it mainly exists only in fruit and honey. Moreover, fructose is very expensive because its manufacturing process is very complicated. Thus, the two major problems limit the large-scale and sustainable production of HMF from fructose. On the contrary, glucose, which is the most abundant and the cheapest monosaccharide, has been considered as the preferred feedstock for the production of HMF. Disappointingly, many catalytic systems in which fructose is readily converted into HMF are normally ineffective for glucose, which is attributed to the stable pyranoside ring structure of glucose[33].

The synthesis of HMF from glucose in the presence of solid acid catalysts is now also established. TiO_2 and ZrO_2 were employed in various solvents including water, DMSO, NMP, water/MIBK and [BMIM]Cl–water for the dehydration of glucose into HMF. The results indicated that TiO_2 and ZrO_2 could not only promote the isomerization of glucose into fructose acting as base catalysts, but also promote the dehydration of fructose into HMF acting as acid catalysts[77,78].

Sulfonated-ZrO_2 and Sulfonated-ZrO_2–Al_2O_3 were also prepared and used for the synthesis of HMF from glucose. The results demonstrated that the latter was more effective than the former in DMSO, this might be ascribed to the introduction of Al, which resulted in an increase in basicity that promoted the isomerization of glucose into fructose[79]. Nakajima et al.[80] and Yang et al.[81] investigated the dehydration of glucose into

HMF using H_3PO_4-modified Nb_2O_5 (NA-p) as catalyst in water and water/2-butanol, yields of 52.1 and 49% were obtained, respectively.
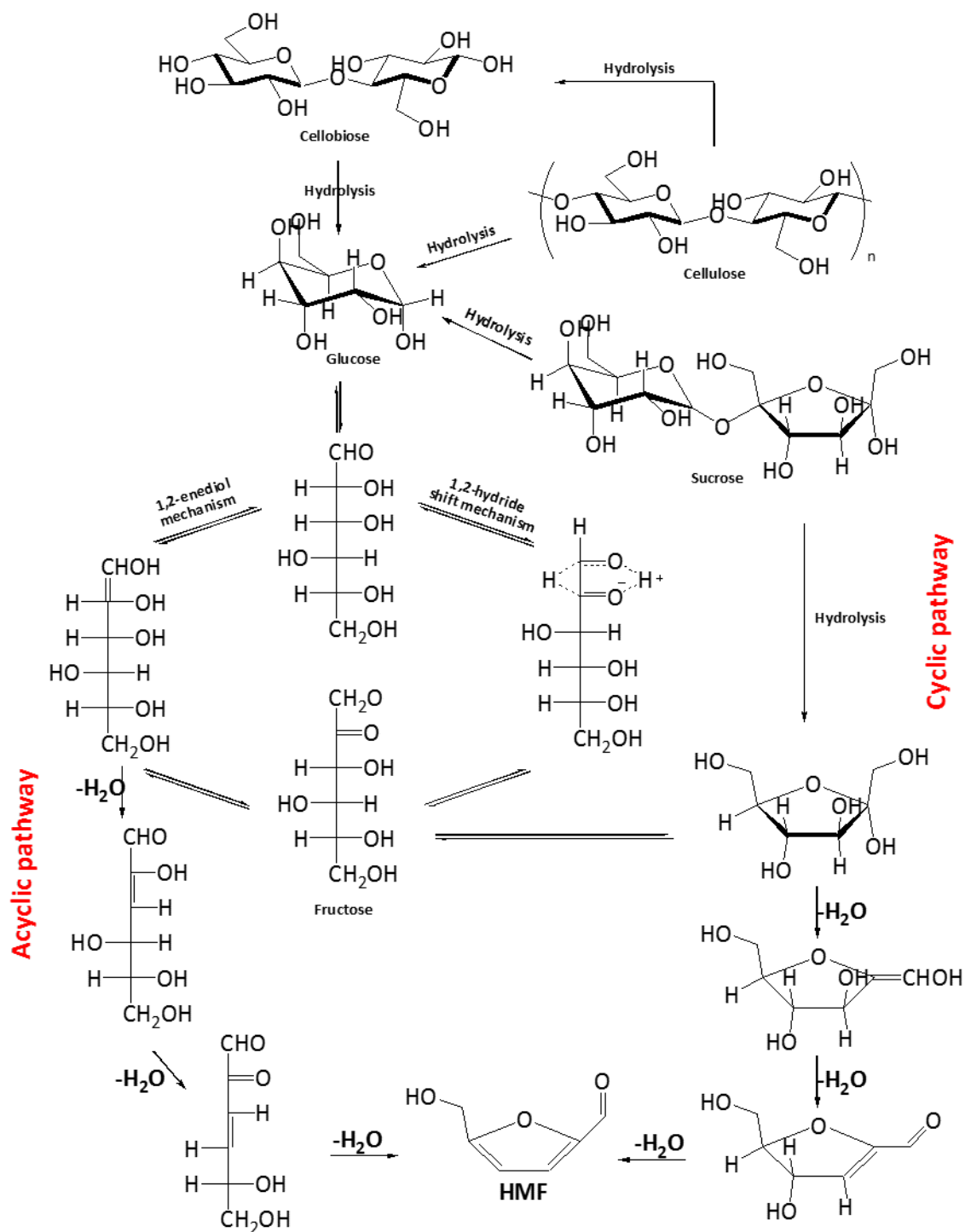
Scheme 1-1. *Proposed mechanisms for the production of HMF from glucose. Adapted from [82,83].*

The mechanism for the production of HMF from glucose (**Scheme 1-1**) with acid catalysts involves a cyclic pathway and an acyclic pathway. However, in recent years, an increasing number of studies suggested that the cyclic pathway may be dominant, especially in ionic liquids using metal chlorides as catalysts. In this pathway, the isomerization of glucose into fructose through the 1,2-enediol mechanism or 1,2-hydride shift mechanism is the rate-controlling step. As a consequence, the conversion of glucose into HMF is much slower than fructose, indicating that once fructose is formed, the subsequent dehydration of fructose into HMF is readily accomplished[82,83].

Among various biomass-derived products, 5-hydroxymethylfurfural (HMF), is considered to be one of the most appealing and promising platform compounds[84,85], this is because that it contains a marvelous and reactive structure involving an aldehyde group, a hydroxyl group and a furan ring and then can be further transformed into higher added value molecules that find application mainly as fuels or as monomers for the polymer industry (**Scheme 1-2**).
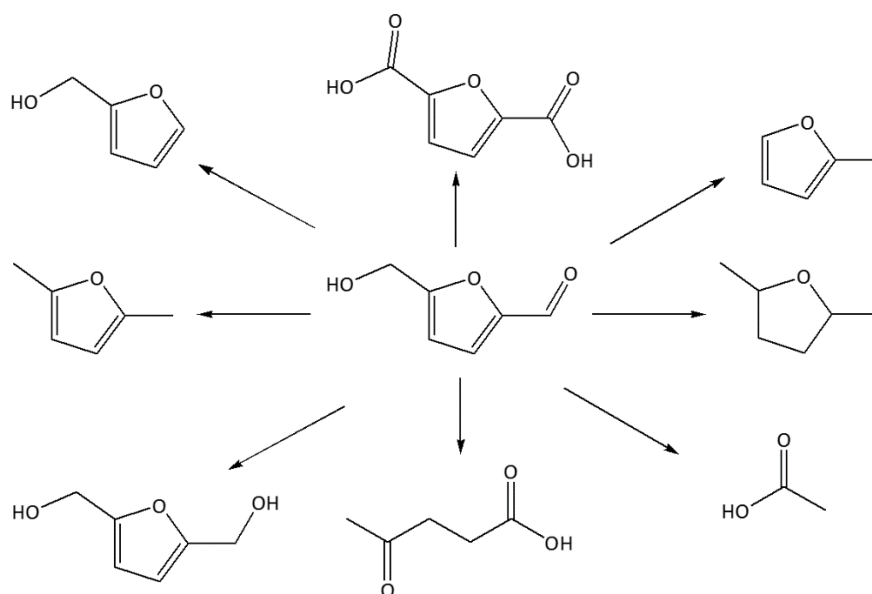
Scheme 1-2. *Main HMF derivatives with application as fuels or as monomers for the polymer industry.*

To obtained high quality fuels additive such as 2,5-dimethylfuran (DMF), 2,5-dimethyltetrahydrofuran (DMTHF) or ethyl levulinate (EL) the hydro-deoxygenation of the main oxygenates functionality of HMF is the main applied strategy.

Indeed, DMF, possessing excellent energy density, boiling point, octane value, hydrophobic property and production efficiency, is considered to be very promising liquid fuels or excellent additive for gasoline[86], and can be produced from the selective

hydrogenation of HMF involving the hydrogenation-hydrogenolysis of both the aldehyde and the hydroxyl preserving the aromatic function of furan ring (which otherwise lead to unnecessary hydrogen consumption). However, it should be noted that DMF can be further hydrogenated into DMTHF, which is also an excellent liquid fuel (**Scheme 1-3**). In 2007, Roman-Leshkov et al.[86] reported the synthesis of DMF from HMF using Cu–Ru/C as catalyst, a yield of 71% was achieved in 1-butanol at 220°C for 10 h with 6.8 bar H_2. Two years later, in the same reaction conditions, Binder et al.7 studied the hydrogenation of crude HMF obtained from corn straw in the presence of Cu–Ru/C, leading to 49% DMF yield.
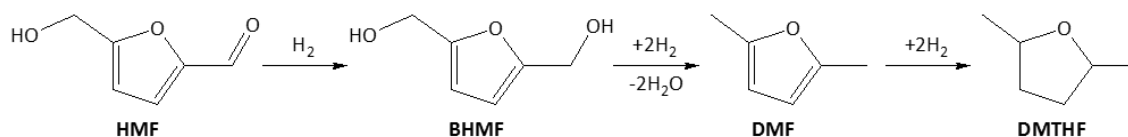
Scheme 1-3. *General pathway for the production of DMF and DMTHF from HMF.*

More importantly, a breakthrough in the synthesis of DMF was reported by Thananatthanachon et al.[87] An excellent yield of DMF with up to 95% from HMF was reached in the presence of HCOOH, H_2SO_4, THF and Pd/C under reflux for 15 h. When the reaction was started from fructose, a DMF yield of 51% was also achieved. In this one-pot synthesis of DMF, HCOOH could be used not only as an acid catalyst for the dehydration of fructose into HMF and as a hydrogen source for the hydrogenation of HMF into DHMF but also as a reagent for the deoxygenation of furanylmethanols.

Another interesting HMF derivative obtained from the selective reduction of the aldehyde group is the 2,5-bishydroxymethylfuran (BHMF) which is widely used as an intermediate for the synthesis of resins[88], fibers[89], foams[90], drugs[91], polymers[92] and crown ethers[93]. Traditionally, DHMF is readily obtained by the stoichiometric hydrogenation of HMF with the help of sodium borohydride (NaBH4)[94]. However, this strategy has some problems such as the treatment of reductive agents and the production of equivalent salts. To overcome these drawbacks, considerable efforts have been devoted to seek the appropriate catalytic systems that are able to effectively and selectively hydrogenate HMF into DHMF.

In 2012, Balakrishnan et al.[93] studied the selective hydrogenation of HMF over carbon-supported platinum (Pt/C) in ethanol. Under 14 bar molecular hydrogen (H_2), the moderate DHMF yield of 82.0% was obtained at 23 °C for 18 h.

Similarly, in the same reaction medium, titania-supported iridium (Ir/TiO$_2$), zeolite-supported platinum (Pt/MCM-41) and iron oxide-supported gold (Au/FeOx) were also adopted by Cai et al.[95], Chatterjee et al.[96] and Satsuma et al.[97] as catalysts for the selective hydrogenation of HMF in 2014 and 2016. After 3, 2 and 2 h at 50, 35 and 80 °C, the yields of DHMF were up to 94.9%, 98.9% and 96.0% under 60, 8 and 30 bar H$_2$, respectively. Recently, the selective hydrogenation of HMF was investigated by Pasini et al. in the presence of toluene and Shvo's catalyst, an excellent DHMF yield of 99.0% was achieved at 90 °C for 1 h under 10 bar H$_2$[98].

On the other hand, one of the most important HMF derivative consists in 2,5-furandicarboxylic acid (FDCA), obtained from the oxidation of both the aldehyde and the hydroxyl group, used as a monomer for the synthesis of a new class of polymers, alternative to those obtained from terephthalic acid. The Department of Energy identifies FDCA as a key platform molecule serving as a starting point for the synthesis of various polymers. The preparation of FDCA from HMF has been studied widely over the past 20 years and various methods have been proposed for this oxidative process. Studied paths range from the use of stoichiometric oxidants to heterogeneous metal catalysts or biochemical production[99,100]. At the present time, there is no commercial process available for producing FDCA. However Avantium, among others, is pursuing the use of FDCA to produce polyethylene furandicarboxylate (PEF) by replacing terephthalic acid (**Scheme 1-4**).
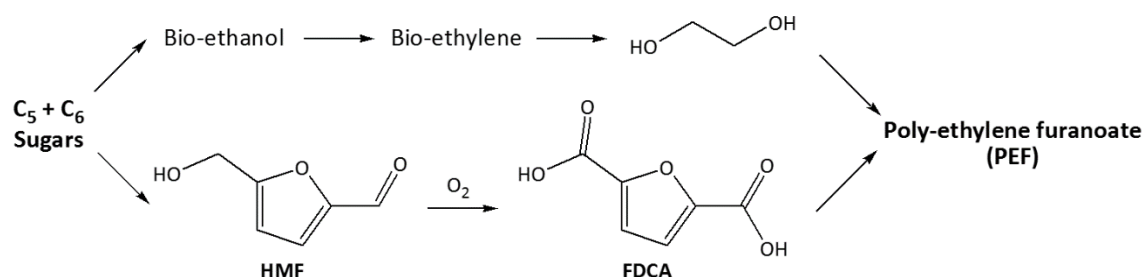
Scheme 1-4. Simplified scheme for the production of PEF from renewable sources.

Recently, Au-supported catalysts have been found to be very active for HMF oxidation to FDCA[101,102]. Many researchers have focused their attention on the study of the best supports and reaction conditions for improving FDCA yield. For instance Au/CeO$_2$, Au/TiO$_2$, and bimetallic Au–Cu supported over the same materials showed to be highly active in FDCA formation in mild reaction conditions[103].

1.4.2. 2-furaldehyde or furfural (FU)

In the last years FU, together with the previously mentioned HMF, has been considered one of the most attractive platform molecule deriving from renewable lignocellulose feedstock due to the possibility to upgrade it to a numerous molecules with application as bio-fuels or as monomers for the polymer industry. FU, instead of HMF, is just produced at large scale industrial process that allow an annual production of more 300000 tonn, the most of which are produced in China. The purification and separation steps are easier and so the final cost of FU is much lower than that of HMF, addressing FU as the most important platform molecule for the production of bio-fuels in the optic of the future bio-refinery scenario.

Furfural is typically derived from xylose that is mainly present as xylan in the hemicellulose. The traditional processes for the production of furfural are based on homogeneous acid catalysts such as $HCOOH$, CH_3COOH, HCl, H_2SO_4, HNO_3 and H_3PO_4 in aqueous solution[104,105,106]. However, these homogeneous acid catalysts are very corrosive and possess higher environmental risks[107,108]. Recently, numerous modifications based on the use of solid acids, Lewis acids and various solvents have been proposed to design a cleaner and more environmental friendly process. For example, O'Neill et al.[109] studied the dehydration of xylose in water by the use of H-ZSM-5 catalyst, 46% furfural yield was obtained at 200°C over 18 min. Dhepe and Sahu[110] reported a one-pot conversion of hemicellulose into furfural using K10 and HUSY in aqueous media, gave 12% yields at 170 °C for 3 h, respectively. In addition, Sn-beta, MSHS-SO_3H, graphene, graphene oxide (GO), sulfonated graphene (SG) and sulfonated graphene oxide (SGO) are also synthesized and used for furfural formation, and yields of 14.3, 43.5, 51, 53, 55 and 62% have been achieved, respectively[111,112]. It is worth noting that water is the most economical solvent for the synthesis of furfural.

In recent years, ionic liquids, which possess some specific properties such as low melting point, negligible vapor pressure, non-flammability, high thermal stability, remarkable solubilizing ability and close to infinite structural variation[113,114], have been successfully used for the production of furfural from xylose and xylan. Lima et al.[115] and Tao et al.[116] found that acidic ionic liquids 1-ethyl-3-methylimidazolium hydrogen sulfate ([EMIM][HSO4]) and 1-(4-sulfonic acid)butyl-3-methylimidazolium hydrogen sulfate ([SBMIM][HSO4]) as both solvents and catalysts were effective for the conversion of xylose into furfural, and yields of 84 and 91.5% could be reached, respectively. Neutral

ionic liquid 1-butyl-3-methylimidazolium chloride ([BMIM]Cl) as solvent was also active when H_2SO_4 was used as catalyst.
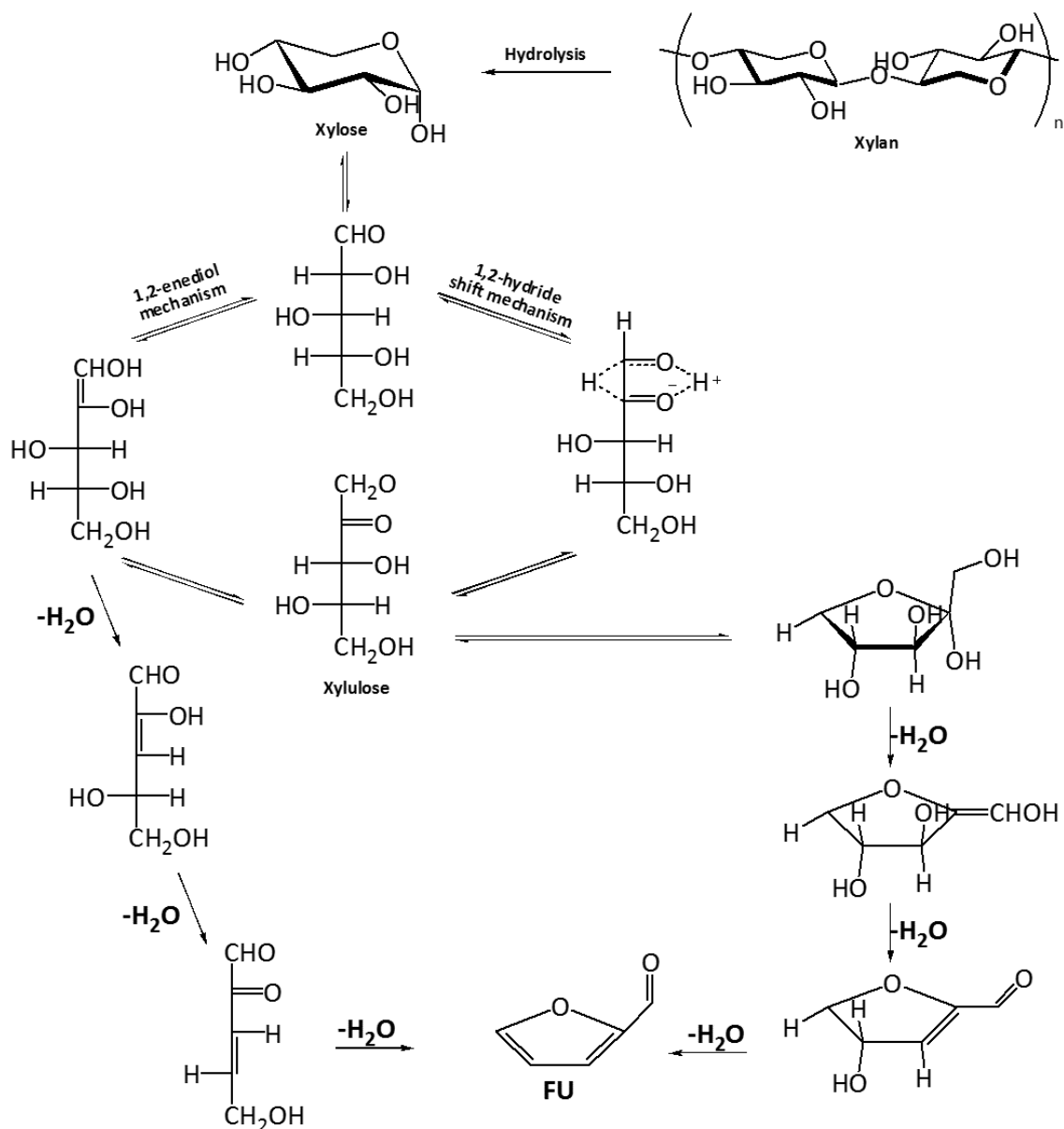
Scheme 1-5. *Proposed mechanisms for the production of FU from xylose. Adapted from [82,83].*

According to considerable previous studies, the conversion of xylose into furfural involves two possible pathways (**Scheme 1-5**): one is based on cyclic intermediates, while the other is based on acyclic intermediates. The isomerization of xylose into xylulose involving hydrogen transfer, which is much slower than the dehydration of xylulose and is thought to be the rate-limiting step in the formation of furfural can occur not only through the 1,2-enediol mechanism but also through a 1,2- hydride shift mechanism. To be specific, in the former mechanism, the hydrogen atom is first removed from C2 and a proton from the solvent is subsequently incorporated into O1 to form the 1,2-enediol

intermediate. Then, the hydrogen atom of O2 is deprotonated and another proton from the solvent is incorporated into C1 to form xylulose. In the latter mechanism, the deprotonation in O2 is first required; then, the hydrogen atom located in C2 moves to C1. Finally, the proton from O2 goes back to O1 to form xylulose. However, the mechanism for furfural production is still debated, and may be dependent on various catalysts, solvents or reaction conditions. Thus, this aspect remains to be further investigated[82,83].

As mentioned above FU could be considered the most promising biomass-derived platform molecule for the future bio-refinery scenario due to the low cost of production, the easy handling and storing and the possibility to produce from the upgrade of it functionalities chemicals that find application as fuels, fuels-additive or monomers for the synthesis of polymers.

Among various biomass-derived products, FU, is considered to be one of the most appealing and promising platform compounds, this is because that it contains a marvelous and reactive structure involving an aldehyde group, a hydroxyl group and a furan ring and then can be further transformed into higher added value molecules that find application mainly as fuels or as monomers for the polymer industry (**Scheme 1-6**).
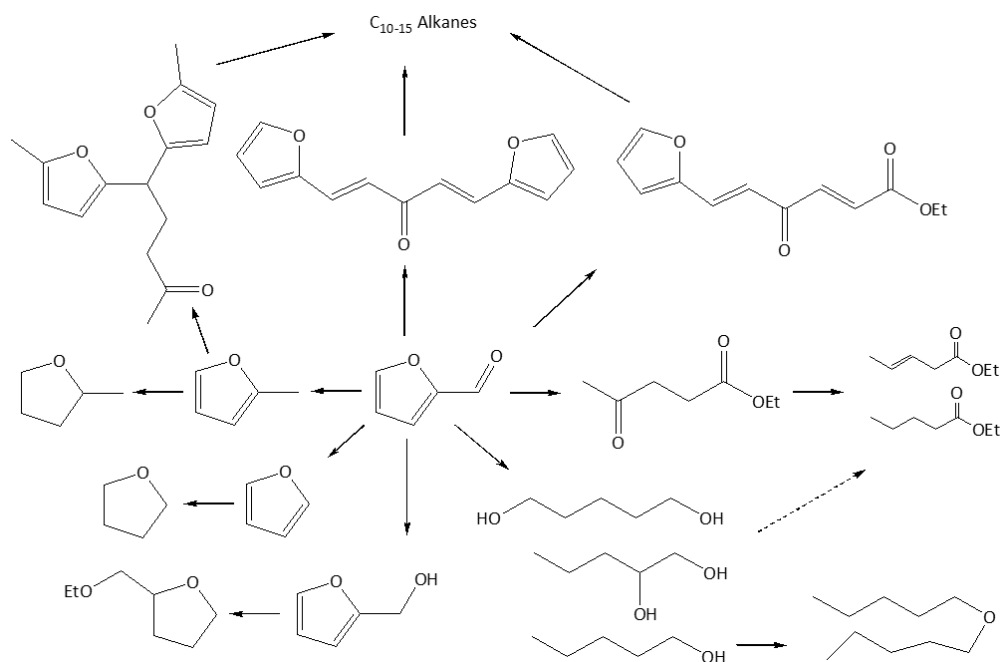
Scheme 1-6. *Main FU derivatives with application as fuels or as monomers for the polymer industry.*

In the case of FU the most of the derivatives with application as a fuels, fuel-additives or as monomer for the polymer industry are produced by-means of hydrogenation process that involved the aldehyde group or the aromatic furanic double bonds. In this scenario

furfuryl alcohol (FAL), 2-methylfuran (MF), 2-methyltetrahydrofuran (MTHF) represent the most attractive derivative of FU.

FAL derives from the selective reduction of the aldehyde group of FU and is used for the production of thermostatic resins or as intermediate in the fine chemical industry; The most of the reported production process are performed in batch reactor[117,118].

On the other hand, MF, as well as MTHF, is considered one of the most appealing bio-fuels thanks to its properties such as an excellent energy density, boiling point, octane value, hydrophobic property and production efficiency.

Cu-based catalysts are generally used for the hydrogenation of furfural into MF through furfuryl alcohol as an intermediate. In the earlier studies, Raney-Cu, Cu-chromite, Cu–Zn–Al–Ca–Na, Cu/Al_2O_3, $Cu–Fe/SiO_2$ and Cu-chromite/C showed 87–98% MF yields at 200–300°C with 0.15–0.3 h-1 LHSV (liquid hourly space velocity), 0.1 MPa and 5–25 H_2/furfural molar ratio[119,120]. However, these catalysts were reported to deactivate rapidly, which is most likely caused by thermal polymerization and coking of furfuryl alcohol on the surface of catalysts under high temperature[34]. Subsequently, a novel process involving the coupling of the dehydrogenation of 1,4-butanediol (BDO) or cyclohexanol (CHL) and the hydrogenation of furfural using Cu–Zn or Cu–Zn–Al as catalysts has been reported, respectively[121122]. The coupled process could be conducted at a lower temperature (typically lower by 10–20°C) than conventional processes while also leading to higher MF yields of 96.5 and 92.8%, respectively, which was thought to be ascribed to that the rich activated hydrogen species on the surface of catalysts from BDO or CHL dehydrogenation may promote furfural hydrogenation reaction. More recently, a few papers reported the hydrogenation of furfural into MF under milder temperatures. Sun et al.[123] claimed that a yield of MF of 100% from furfural at 18°C for 57 min with 0.1 MPa H_2 using Pd complex/SiO_2 as catalyst. At the same time, a variety of solvents was screened, and the best results were obtained from small, polar alcohols such as methanol and ethanol. Lange et al. studied the synthesis of MF from furfural, 50% yield was observed in ethanol at 30°C for 1 h with 0.25 MPa H_2 by the use of Pd/C or Pd/SiO_2 in the presence of a small amount of HCl that could depress undesired side reactions. More interestingly, Li et al.[124] investigated the electrocatalytic hydrogenation of furfural into MF using the cathode metal as catalysts. Among the tested anode and cathode metals, a combination of Ni anode and Ni cathode exhibited the best result. In addition, the formation of MF was favored at pH 1.0.

[1] R. Sheldon, *Green Chem.*, 2014, **16**, 950

[2] L. Hu, G. Zhao, W. Hao, X. Tang, Y. Sun, L. Lin and S. Liu, *RSC Adv.,* 2012, **2**, 11184

[3] J.N. Chieda, G.W. Huber and J.A. Dumesic, *Angew. Chem. Int. Ed.,* 2007, **46**, 7164

[4] *The Roadmap for Biomass Technologies in the U.S.*, Biomass R&D Technical Advisory Committee, US Departement of Energy, Accession No ADA 436527, 2002

[5] P. Gallezot, "Catalysis of renewables: from feedstock to energy production", edited by Gabriele Centi e Ritger A. Van Santen, Wiley-VCH Verlag GmbH & Co KgaA Weinheim, 2007, **53**

[6] P.T. Anastas and J.C. Warne; *Green Chem.*; 1998, **30**

[7] A. Bohre, S. Dutta, B. Saha, and M. M. Abu-Omar, *ACS Sustainable Chem. Eng*. **2015**, 3, 1263−1277

[8] .J. Climent, A. Corma and S. Iborra; *Green Chem.;* 2011, **13**, 520

[9] J. C. Serrano-Ruiz, R. L. and A. Sepulveda-Escribano; *Chem. Soc. Rev.;* 2011, **40**, 5266

[10] M. J. Gilkey and B. Xu, *ACS Catal.,* 2016, **6**, 1420

[11] G.W. Huber, S. Iborra, A. Corma, *Chem. Rev.,* 2006, **106**, 4044

[12] I. Delidovich, K. Leonhard, R. Palkovits, *Energy Environ. Sci.,* 2014, **7**, 2803

[13] F. Carrasco, C. Roy, *Wood Sci. Technol.,* 1992, **26**, 189

[14] F. Carvalheiro, L.C. Duarte, F.M. Gírio, *J. Sci. Ind. Res.,* 2008, **67**, 849

[15] N. Mosier, C. Wyman, B. Dale, R. Elander, Y.Y. Lee, M. Holtzapple, M. Ladisch, *Bioresour. Technol.,* 2005, **96**, 673

[16] J.Q. Bond, A.A. Upadhye, H. Olcay, G.A. Tompsett, J. Jae, R. Xing, D.M. Alonso,D. Wang, T. Zhang, R. Kumar, A. Foster, S.M. Sen, C.T. Maravelias, R. Malina,S.R.H. Barrett, R. Lobo, C.E. Wyman, J.A. Dumesic, G.W. Huber, *Energy Environ. Sci.,* 2014, **7**, 1500

[17] Balat A., *Energy Source Part A,* 2009, **31**, 516

[18] Y.-L. Loow et Al., *Cellulose,* 2016, **23**, 1491

[19] S. Dumitriu, *Polysaccharides: structural diversity and functional versatility, 2nd ed,* Marcel Dekker, New York, 2005

[20] D. Klemm, B., Heublein, H.P., Fink, A., Bohn, *AngewandteChemie–International Edition,* 2005, **44**, 3358

[21] C.E. Wyman, S.R. Decker, M.E. Himmel, J.W. Brady, C.E. Skopec, L. Viikari, Hydrolysis of Cellulose and Hemicellulose, in: Polysaccharides: Structural Diversity and Functional Versatility, 2nd ed., Marcel Dekker, New York,2004, pp. 995

[22] K. Bunnell, A. Rich, C. Luckett, Y.-J. Wang, E. Martin, D.J. Carrier, *ACS Sus.Chem. Eng.,* 2013, **1**, 649

[23] K. Kotarska, A. Swierczynska, W. Dziemianowicz, *Renew Energy,* 2015, **75**,389

[24] T. Manavalan, A. Manavalan, K. Heese, *Curr Microbiol.,* 2015, **70**, 485

[25] C. H. Pang, S. Gaddipatti, G. Tucker, E. Lester, T. Wu, *Bioresour. Technol.,* 2014, **172**, 312

[26] Y. L. Loow, T. Y. Wu, K. A. Tan, Y. S. Lim, L. F. Siow, J. M. Jahim, A. W. Mohammad, W. H. Teoh, *J. Agric. Food Chem.,* 2015, **63**, 8349

[27] G.-Q. Chen, M.K. Patel, *Chem. Rev.,* 2011, **112**, 2082

[28] S. Jacobsen, C. Wyman, Cellulose and hemicellulose hydrolysis models for application to current and novel pretreatment processes, in: M. Finkelstein,B. Davison (Eds.), Twenty-First Symposium on Biotechnology for Fuels and Chemicals, Humana Press, 2000, pp. 81

[29] C. Li, Z.K. Zhao, *Adv. Synth. Catal.,* 2007, **349**, 1847

[30] C.E. Wyman, S.R. Decker, M.E. Himmel, J.W. Brady, C.E. Skopec, L. Viikari, Hydrolysis of Cellulose and Hemicellulose, in: Polysaccharides: Structural Diversity and Functional Versatility, 2nd ed., Marcel Dekker, New York,2004, pp. 995

[31] M. Sasaki, B. Kabyemela, R. Malaluan, S. Hirose, N. Takeda, T. Adschiri, K.Arai, *J. Supercrit. Fluids,* 1998, **13**, 261

[32] M. Sasaki, Z. Fang, Y. Fukushima, T. Adschiri, K. Arai, *Ind. Eng. Chem. Res.,* 2000, **39**, 2883

[33] L. Hu et Al., *Renewable and Sustainable Energy Reviews,* 2017, **74**, 230

[34] J.P. Lange et al.; *ChemSusChem,* 2012, **5**, 150

[35] P. Mäki-Arvela, T. Salmi, B. Holmbom, S. Willför, D.Y. Murzin, *Chem. Rev.,* 2011, **111**, 5638

[36] J.F. Saeman, *Ind. Eng. Chem.,* 1945, **37**, 43

[37] R. Aguilar, J.A. Ramı́ırez, G. Garrote, M. Vázquez, *J Food Eng.,* 2002, **55**, 309

[38] F. Camacho, P. González-Tello, E. Jurado, A. Robles, *J.Chem. Technol. Biotechnol.,* 1996, **67**, 350

[39] J. Kim, Y.Y. Lee, R. Torget, *Appl. Biochem. Biotechnol.,* 2001, **91**, 331

[40] N.S. Mosier, C.M. Ladisch, M.R. Ladisch, *Biotechnol. Bioeng.,* 2002, **79**, 610

[41] A. Esteghlalian, A.G. Hashimoto, J.J. Fenske, M.H. Penner, *Bioresour. Technol.,* 1997, **59**, 129

[42] J. Bouchard, G. Garnier, P. Vidal, E. Chornet, R.P. Overend, *Wood Sci. Technol.,* 1990, **24**, 159

[43] D.R. Cahela, Y.Y. Lee, R.P. Chambers, *Biotechnol. Bioeng.,* 1983, **25**, 3

[44] A.H. Conner, B.F. Wood, C.G. Hill, J.F. Harris, *J. Wood Chem. Technol.,* 1985, **5**, 461

[45] I.A. Malester, M. Green, G. Shelef, *Ind. Engin. Chem. Res.,* 1992, **31**, 1998

[46] M. Toda, A. Takagaki, M. Okamura, J. N. Kondo, S. Hayashi, K. Domen, M. Hara. *Nature*, 2005, **438**: 178

[47] S. Suganuma, K. Nakajima, M. Kitano, D. Yamaguchi, H. Kato, S. Hayashi, M. Hara., *J. Am. Chem. Soc.*, 2008, **130**, 12787

[48] M. Okamura, A. Takagaki, M. Toda, J. N. Kondo, K. Domen, T. Tatsumi, M. Hara, S. Hayashi, *Chem. Mater.*, 2006, **18**, 3039

[49] D. Yamaguchi, M. Kitano, S. Suganuma, K. Nakajima, H. Kato, M. Hara., *J. Phys. Chem. C*, 2009, **113**, 3181

[50] S. Van de Vyver, L. Peng, J. Geboers, H. Schepers, F. De Clippel, C. J. Gommes, B. Goderis, P. A. Jacobs, *Green Chem.*, 2010, **12**, 1560

[51] J. Pang, A. Wang, M. Zheng, T. Zhang, *Chem. Commun.*, 2010, **46**, 6935

[52] A. Takagaki, C. Tagusagawa, K. Domen, *Chem. Commun.*, 2008, 5363

[53] C. Tagusagawa, A. Takagaki, A. Iguchi, K. Takanabe, J. N. Kondo, K. Ebitani, T. Tatsumi, K. Domen, *Chem. Mater.*, 2010, **22**, 3072

[54] Q. Qing, B. Yang, C.E. Wyman, *Bioresour. Technol.,* 2010, **101**, 9624

[55] Y. Kim, E. Ximenes, N.S. Mosier, M.R. Ladisch, *Enzyme Microb. Technol.,* 2011, **48**, 408

[56] E. Ximenes, Y. Kim, N. Mosier, B. Dien, M. Ladisch, *Enzyme Microb. Technol.,* 2010, **46**, 170

[57] J.E. Morinelly, J.R. Jensen, M. Browne, T.B. Co, D.R. Shonnard, *Ind. Eng. Chem. Res.,* 2009, **48**, 9877

[58] J. Shen, C.E. Wyman, *Bioresour. Technol.,* 2011, **102**, 9111

[59] I.S.M. Rafiqul, A.M. Mimi Sakinah, *Chem. Eng. Sci.,* 2012, **71**, 431

[60] G. Marcotullio, E. Krisanti, J. Giuntoli, W. de Jong, *Bioresour. Technol.,* 2011, **102**, 5917

[61] S. Gámez, J.J. González-Cabriales, J.A. Ramírez, G. Garrote, M. Vázquez, *J. Food Eng.,* 2006, **74**, 78

[62] A. Rodríguez-Chong, J. Alberto Ramírez, G. Garrote, M. Vázquez, *J. Food Eng.,* 2004, **61**, 143

[63] Y. Kim, T. Kreke, M.R. Ladisch, *AIChE J.,* 2013, **59**, 188

[64] B.T. Kusema, T. Tönnov, P. Mäki-Arvela, T. Salmi, S. Willför, B. Holmbom, D.Y.Murzin, *Catal. Sci. Technol.,* 2013, **3**, 116

[65] J. Xu, M.H. Thomsen, A.B. Thomsen, *BiomassBioenerg.,* 2009, **33** 1660

[66] G. Garrote, H. Domínguez, J.C. Parajó, *J. Chem. Technol. Biotechnol.,* 1999, **74**, 1101

[67] G. Garrote, H. Domínguez, J.C. Parajó, *J. Food Eng.,* 2002, **52**, 211

[68] Y. Kim, R. Hendrickson, N. Mosier, M. Ladisch, Liquid Hot WaterPretreat-ment of Cellulosic Biomas, in: J.R. Mielenz (Ed.), Biofuels, HumanaPress, 2009, pp. 93

[69] X. H. Qi, M. Watanabe, T. M. Aida and R. L. Smith, *Green Chem.,* 2008, **10**, 799

[70] X. H. Qi, M. Watanabe, T. M. Aida and R. L. Smith, *Ind. Eng. Chem. Res.,* 2008, **47**, 9234

[71] K. I. Shimizu, R. Uozumi and A. Satsuma, *Catal. Commun.,* 2009, **10**, 1849

[72] X. H. Qi, M. Watanabe, T. M. Aida and R. L. Smith, *Green Chem.,* 2009, **11**, 1327

[73] C. Moreau, R. Durand, S. Razigade, J. Duhamet, P. Faugeras, P. Rivalier, P. Ros and G. Avignon, *Appl. Catal., A,* 1996, **145**, 211

[74] V. V. Ordomsky, J. van der Schaaf, J. C. Schouten and T. A. Nijhuis, *J. Catal.,* 2012, **287**, 68

[75] X. C. Guo, Q. Cao, Y. J. Jiang, J. Guan, X. Y. Wang and X. D. Mu, *Carbohydr. Res.,* 2012, **351**, 35

[76] F. L. Yang, Q. S. Liu, M. Yue, X. F. Bai and Y. G. Du, *Chem. Commun.,* 2011, **47**, 4469

[77] X. H. Qi, M. Watanabe, T. M. Aida and R. L. Smith, *Catal. Commun.,* 2008, **9**, 2244

[78] S. Dutta, S. De, A. K. Patra, M. Sasidharan, A. Bhaumik and B. Saha, *Appl. Catal., A*, 2011, **409–410,** 133

[79] H. P. Yan, Y. Yang, D. M. Tong, X. Xiang and C. W. Hu, *Catal. Commun.,* 2009, **10**, 1558

[80] K. Nakajima, Y. Baba, R. Noma, M. Kitano, J. N. Kondo, S. Hayas and M. Hara, *J. Am. Chem. Soc.,* 2011, **133**, 4224

[81] F. L. Yang, Q. S. Liu, X. F. Bai and Y. G. Du, *Bioresour. Technol.*, 2011, **102**, 3424

[82] J. Guan, Q. Cao, X. C. Guo and X. D. Mu, *Comput. Theor. Chem.,* 2011, **963**, 453

[83] Y. Roma´n-Leshkov, M. Moliner, J. A. Labinger and M. E. Davis, *Angew. Chem., Int. Ed., 2010,* **49**, 8954

[84] O. Yemis and G. Mazza, *Bioresour. Technol.,* 2012, **109**, 215

[85] A. Takagaki, M. Ohara, S. Nishimura and K. Ebitani, *Chem. Lett.,* 2010, **39**, 838

[86] N. K. Gupta, S. Nishimura, A. Takagaki and K. Ebitani, *Green Chem.,* 2011, **13**, 824

[87] T. Thananatthanachon and T. B. Rauchfuss, *Angew. Chem., Int. Ed.,* 2010, **49**, 6616

[88] I. Delidovich, P. J. Hausoul, L. Deng, R. Pfutzenreuter, M. Rose, R, Palkovits, *Chem. Rev.,* 2016, **116**, 1540

[89] A. Gelmini, S. Albonetti, F. Cavani, C. Cesari, A. Lolli, V. Zanotti, *Appl. Catal. B: Environ.,* 2016, **180**, 38

[90] Y. Nakagawa, M. Tamura, K. Tomishige, *ACS Catal.,* 2013, **3**, 2655

[91] Y. Kwon, E. De Jong, S. Raoufmoghaddam, M. T. Koper, *ChemSusChem ,*2013, **6**, 1659

[92] A. Gandini, *Green Chem.,* 2011, **13**, 1061

[93] M. Balakrishnan, E. R. Sacia, A. T. Bell, *Green Chem.,* 2012, **14**, 1626

[94] B. Saha, C. M. Bohn, M. M. Abu-Omar, *ChemSusChem,* 2014, **7**, 3095

[95] H. L. Cai, C. Z. Li, A. Q. Wang, T. Zhang, *Catal. Today,* 2014, **234**, 59

[96] M. Chatterjee, T. Ishizaka, H. Kawanami, *Green Chem.,* 2014, **16**, 4734

[97] J. Ohyama, Y. Hayashi, K. Ueda, Y. Yamamoto, S. Arai, A. Satsuma, *J. Phys. Chem. C,* 2016, **120**, 15129

[98] R. Mazzoni, T. Pasini, G. Solinas, V. Zanotti, S. Albonetti, F. Cavani, *Dalton Trans.,* 2014, **43**, 10224

[99] F. Koopman, N. Wierckx, J.H. de Winde, H.J. Ruijssenaars, *Bioresour. Technol.,* 2010, **101**, 6291

[100] W.P. Dijkman, D.E. Groothuis, M.W. Fraaije, *Angew. Chem. Int. Ed.,* 2014, **53**, 6515

[101] Y.Y. Gorbanev, S.K. Klitgaard, J.M. Woodley, C.H. Christensen, A. Riisager, *ChemSusChem,* 2009, **2**, 672

[102] S.E. Davis, B.N. Zope, R.J. Davis, *Green Chem.,* 2012, **14**, 143

[103] S. Albonetti et al., *Applied Catalysis B: Environmental,* 2015, **163**, 520

[104] A. S. Mamman, J. M. Lee, Y. C. Kim, I. T. Hwang and N. J. Park, *Biofuels, Bioprod. Biorefin.,* 2008, **2**, 438

[105] J. N. Chheda, Y. Roma´n-Leshkov and J. A. Dumesic, *Green Chem.,* 2007, **9**, 342

[106] R. Weingarten, J. Cho, W. C. Conner and G. W. Huber, *Green Chem.,* 2010, **12**, 1423

[107] J. C. Serrano-Ruiz, R. Luque and A. Sepulveda-Escribano, *Chem. Soc. Rev.,* 2011, **40**, 5266

[108] E. Lam, J. H. Chong, E. Majid, Y. L. Liu, S. Hrapovic, A. C. W. Leung and J. H. T. Luong, *Carbon,* 2012, **50**, 1033

[109] R. O'Neill, M. N. Ahmad, L. Vanoye and F. Aiouache, *Ind. Eng. Chem. Res.,* 2009, **48**, 4300

[110] P. L. Dhepe and R. A. Sahu, *Green Chem.,* 2010, **12**, 2153

[111] V. Choudhary, A. B. Pinar, S. I. Sandler, D. G. Vlachos and R. F. Lobo, *ACS Catal.,* 2011, **1**, 1724

[112] G. H. Jeong, E. G. Kim, S. B. Kim, E. D. Park and S. W. Kim, *Microporous Mesoporous Mater.,* 2011, **144**, 134

[113] S. Lima, M. M. Antunes, M. Pillinger and A. A. Valente, *ChemCatChem,* 2011, **3**, 1686

[114] M. E. Zakrzewska, E. Bogel-Lukasik and R. Bogel-Lukasik, *Chem. Rev.,* 2011, **111**, 397

[115] S. Lima, P. Neves, M. M. Antunes, M. Pillinger, N. Ignatyev and A. A. Valente, *Appl. Catal. A,* 2009, **363**, 93

[116] F. R. Tao, H. L. Song and L. J. Chou, *Can. J. Chem.*, 2011, **89**, 83

[117] J. Kijenski, P. Winiarek, T. Paryjczak, A. Lewicki, A. Mikołajska, *Appl. Catal. A: Gen.;* 2002, **233**, 171

[118] B.M. Nagaraja, A.H. Padmasri, B. David Raju, K.S. Rama Rao, *J. Mol. Catal. A: Chem.,* 2007, **265**, 90

[119] J. Lessard, J. F. Morin, J. F. Wehrung, D. Magnin and E. Chornet, *Top. Catal.,* 2010, **53**, 1231

[120] H. Y. Zheng, Y. L. Zhu, B. T. Teng, Z. Q. Bai, C. H. Zhang, H. W. Xiang and Y. W. Li, *J. Mol. Catal. A: Chem.,* 2006, **246**, 18

[121] Y. L. Zhu, H. W. Xiang, Y. W. Li, H. J. Jiao, G. S. Wu, B. Zhong and G. Q. Guo, *New J. Chem.,* 2003, **27**, 208

[122] H. Y. Zhang, Y. L. Zhu, Z. Q. Bai, L. Huang, H. W. Xiang and Y. W. Li, *Green Chem.,* 2006, **8**, 107

[123] Q. Sun, S. F. Liu, X. H. Yao, Y. C. Su and Z. Q. Zhang, *Chin. J. Syn. Chem.,* 1996, **4**, 146

[124] G. C. A. Luijkx, N. P. M. Huck, F. Van Rantwijk, L. Maat and H. Van Bekkum, *Heterocycles,* 2009, **77**, 1037

CHAPTER 2   Hydrogen-Transfer reaction as a tool for the catalytic reduction of bio-based building block

2.1. Introduction

In the former chapter it has been reported on the importance and the appeal for the possibility to produce fuels, fuel-additives, chemicals and high added value chemicals for the fine industry starting from short-life cycle renewable sources in order to decrease the dependency from the fossil sources. Indeed, the continue increase for fuels and chemicals for the industries demand, coupled with continued increase of the pollutant emission in the atmosphere, have forced in the researcher community to find renewable alternatives on which in the future the chemical industries could find their feedstock. In this scenario, the second generation lignocellulose biomass materials, mainly composed by wood chips, agricultural and municipal wastes, have been identified as one of the min alternative to the fossil sources thanks to the possibility to produce from their thermo-chemical treatment new platform molecules considered highly appealing. Indeed, after further transformation, fuels, fuel-additives, monomer for the polymer industry and fine chemicals could be obtained.

HMF and FU, respectively produced by the acidic hydrolysis-dehydration of the cellulose and hemicellulose fraction of the lignocellulose biomass, have been considered, in the last years, two of the most appealing platform molecules deriving from renewable sources. As reported previously mainly fuels and monomers could be produced from their transformation. DMF and MF, produced as a consequence of the selective hydrogenation-hydrogenolysis of the hydroxyl and aldehyde functionality of HMF and FU are considered two of the most promising bio-fuels or fuel-additives considering their excellent energy density, boiling point, octane value, hydrophobic property and production efficiency.

So their production represent an extremely interesting route for the production of liquid renewable fuels. Indeed these furan compounds are superior compared to bio-ethanol because of the higher energy density and higher octane values[1]. **Table 2-1** summarize the

main fuel properties of MF and DMF compared with that of bio-ethanol, commercial 95 octane gasoline. The octane number of both MF and DMF are higher than that of gasoline (103 and 101 respectively vs. 96.8 RON), while their energy densities are very close (28.5 and 30 MJ L−1 vs. 31.9 MJ L−1), which means that with the same volume of fuel, MF and DMF contains 34% more energy compared to the market-leading biofuel ethanol[2]. Thewes et al. have performed combustion tests on bench engines to compare MF and DMF with bio-ethanol and 95-octane gasoline. The reported results confirm that the two furanic compounds could be considered a promising bio-fuels. Indeed they have a faster initial evaporation compared to that of ethanol and similar to that of 95-octane gasoline; furthermore both the particulate emission and partially combusted species are lower compared to that obtained with the other fuels [1].
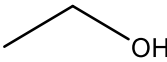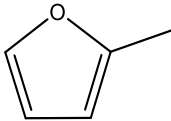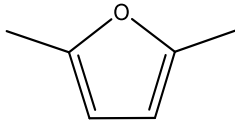
Feature	95-octane gasoline	Ethanol	MF	DMF
Chemical formula	C_6-C_9			
H/C ratio	1,795	3	1,2	1,3
O/C ratio	0	0,5	0,2	0,17
Density @ 20°C (kg/m^3)	745	791	913	890
Research Octane Number (RON)	97	107	103	101
Motor Octane Number (MON)	85,7	89	86	88
Energy density (MJ/L)	31,9	21	28,5	30
Initial boiling point (°C)	32,8	78,4	64,7	93
Autoignition Temperature (°C)	257	363	450	286
Water miscibility at 25°C (g/l)	Miscible	Miscible	3	2,3

Table 2-1. *Comparison of the fuel properties of MF and DMF versus Gasoline and ethanol. Adapted from [1, 2].*

The main applied strategy for the production of fuels such as MF and DMF from the renewable platform molecules FU and HMF is the classic catalytic hydro-de-oxygenation (HDO); indeed, the aim is the removal of the oxygen-containing functional groups (**Figure 2-1**). As reported above, the most of the patented or literature process involve the use of molecular hydrogen as reducing agent at high pressure and temperature in liquid-phase batch set-up reactors.
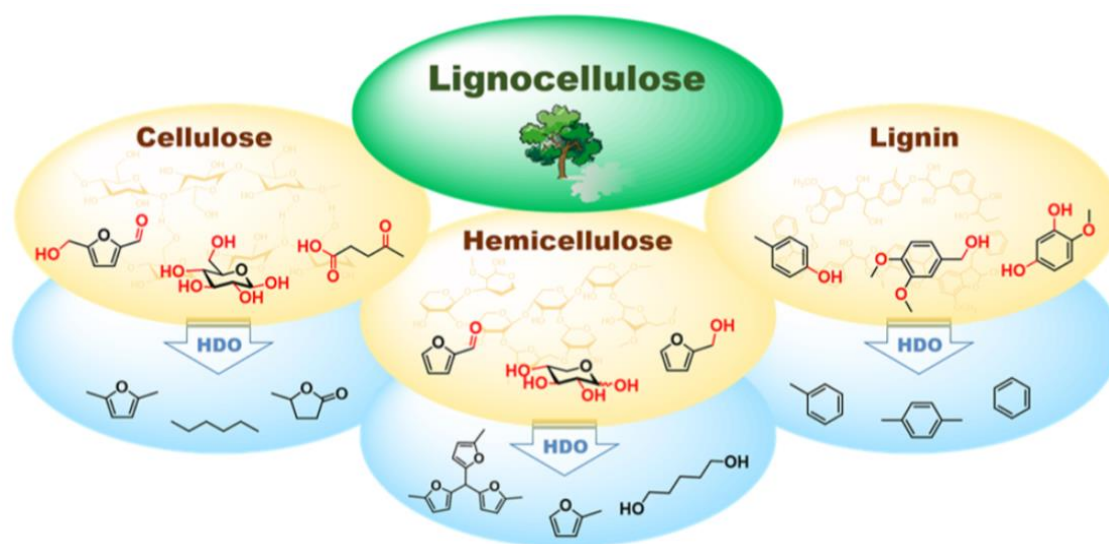
Figure 2-1. *HDO strategy for the production of fuel-range target molecules from lignocellulose biomass.*

The use of molecular hydrogen as reducing agent decrease the overall sustainability of the process considering that nowadays more than 95% of the produced H_2 derives from fossil sources by-means of CH_4 steam reforming, CPO, dry-reforming or from carbon gasification. On the other hand, the catalysts reported to be active in the HDO process of FU and HMF are mainly based on noble metal supported catalysts or on transition-metal oxides such as Cu, Cr, Ni and Fe. In the case of noble metal based catalysts and systems containing Cr and Ni the main drawbacks are represented by the high cost of the active phase or by the toxicity of the used metal oxide.

Taking into account these information, a completely different approach for the reduction process of the biomass-derived building block could be the catalytic transfer hydrogenation reaction (CTH) or Meerwein-Ponndorf-Verley reaction (MPV). In brief, that alternative process consists in a classic organic chemistry reaction developed in the first years of the XXth century in which, usually, an alcohol is used as hydrogen-source or hydrogen-donor for the selective reduction of a carbonyl group. In terms of biomass upgrading the possibility to use an alcohol as hydrogen source for the HDO process opens

to the possible use of bio-alcohols, obtained from biomass fermentation or enzymatic transformation of simple sugars, increasing the overall sustainability of the process and untying to the use of molecular hydrogen.

2.2. The catalytic transfer hydrogenation reaction (CTH)

The catalytic transfer hydrogenation reaction (CTH) or Meerwein-Ponndorf-Verley (MPV) reaction is a catalytic carbonyl reduction performed in the presence of an alcohol as a hydrogen donor. It has been independently discovered in the early years of XXth century by Meerwein, Ponndorf and Verley when they found that, in the proper conditions and with the proper catalyst, carbonyl group-containing compounds were reduced in the presence of 2-propanol[3]. Later, Oppenauer found that secondary alcohols were oxidized in the presence of acetone[4] (**Scheme 2-1**).
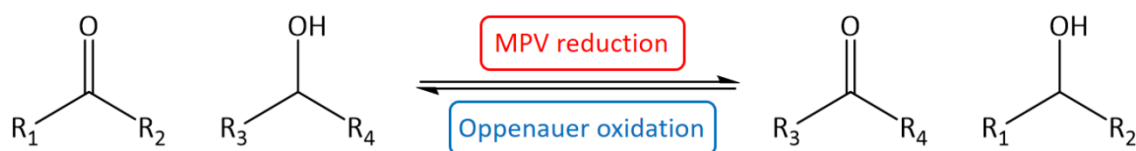
Scheme 2-1. *Meerwein-Ponndorf-Verley reduction and Oppenauer oxidation.*

CTH is effective in reducing functional groups by adding hydrogen to either unsaturated bonds (hydrogenation), e.g., C-C double and triple bonds, carbonyl group, nitro group, N-N triple bonds, and C-N triple bonds, or single bonds leading to bond cleavage (hydrogenolysis), e.g., C−O, C−N, C−S, and C−X (halogen)[5].

The first catalysts employed are homogeneous: Lewis acids such as Al, B, or Zr alkoxides salts and complexes of Pd, Pt, Ru, Ir, Rh, Fe, Ni and Co. Then heterogeneous catalysts with acid properties such as Lewis acid cations such as Al^{3+}, Zr^{4+}, or Sn^{4+} incorporated in zeolite framework or supported on oxides are employed in CTH as well as basic or amphoteric oxides (MgO, ZrO_2)[6].

The efficiency of the reduction is determined in part by thermodynamic considerations. Indeed, secondary alcohols are stronger reductants than primary ones and aldehydes are more easily reduced than ketones. As a consequence, iso-propanol is the most commonly used H-donor. The reaction is an equilibrium and it is usually driven to the right by using a large excess of reductant; this is the reason why in liquid phase processes alcohols are often used both as H-donor and as the solvent.

Transfer hydrogenation has the advantages of operational simplicity and environmental friendliness: no hydrogen pressure is used and no special equipment is required. In addition, no hazardous waste is produced, as in the case of stoichiometric reduction by borane reagents. When 2-propanol is used as hydrogen donor, the only side product formed is acetone, which is easily removed by distillation during workup. 2-Propanol and formic acid, which are both often used as hydrogen donors, are non-toxic and also inexpensive reactants. One drawback of the use of this reaction is that each step in the cycle is reversible and the selectivity is driven by the thermodynamic properties of products and intermediates. This disadvantage can be overcome by the use of a formate, since the reaction in this case is irreversible, with loss of CO_2. Pasini et al. recently report on the use of methanol as hydrogen source in the liquid-phase CTH using MgO as highly active catalyst; the C1 alcohol is less active as hydrogen source compared to iso-propanol but shows the advantage to produced only gaseous co-products (CO. CO_2 and CH_4) deriving from formaldehyde degradation. The formation of gaseous light compounds consist in an optimal thermodynamic driving force that push the CTH equilibrium to the right[7].

2.2.1. CTH with homogeneous catalysts

The CTH with homogeneous catalysts have been deeply studied[8] and it has been demonstrated that could proceed through two main mechanisms:

- The direct hydrogen transfer route (MPV);
- The metal hydride route[9,10].

When an alcohol acts as the hydrogen donor in reducing a carbonyl group following the direct hydrogen transfer pathway, the α-H is transferred from the α-C of the alcohol to the carbonyl carbon in a concerted step via a six-membered-ring intermediate, without forming a metal hydride. This is also commonly referred to as the Meerwein−Ponndorf−Verley (MPV) mechanism (**Scheme 2-2**).
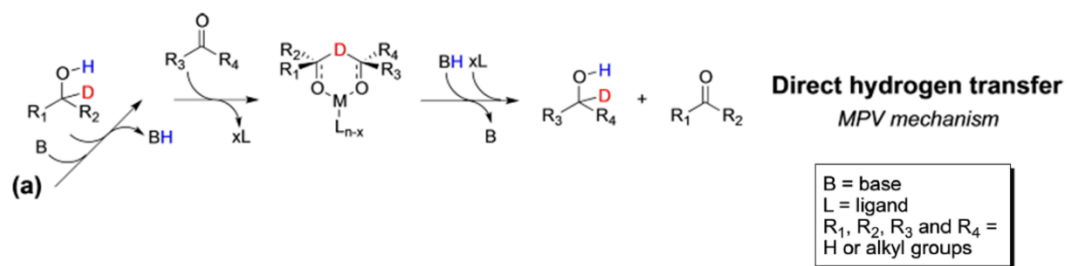
Scheme 2-2. *Direct hydrogen transfer mechanism with homogeneous catalysts. Adapted from [5].*

On the other hand, the formation of metal hydride is the signature of the metal hydride route (**Scheme 2-3**), which could be grouped into two subcategories: i.e., the monohydride and di-hydride mechanisms. In the monohydride route, only the hydrogen on the α-C of the hydrogen donor, e.g., alcohols and formic acid, is transferred to the metal. In contrast, the di-hydride mechanism entails that both the hydrogen atom in the hydroxyl group and that bonded to the α-C are transferred to the metal. The key difference between these two pathways is whether the hydrogen atoms in O−H and C−H maintain their identity in the product.
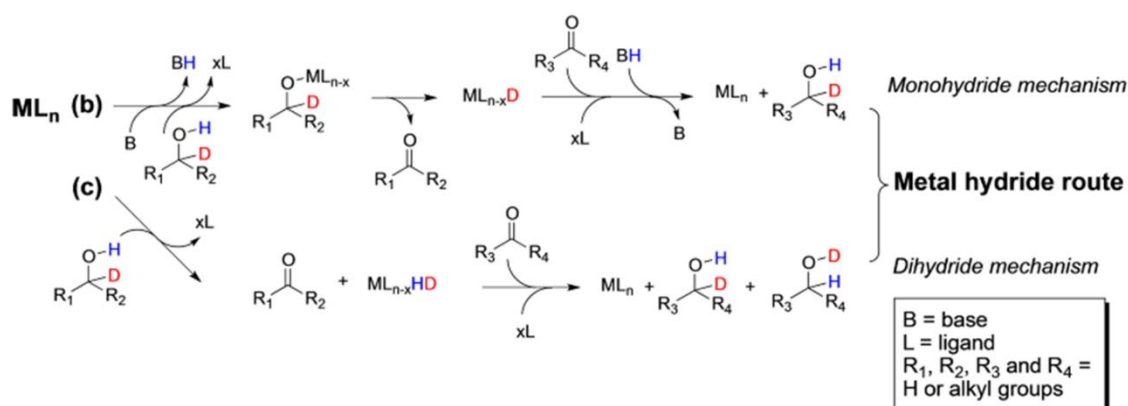
Scheme 2-3. *Metal hydride route hydrogen transfer mechanism with homogeneous catalysts. Adapted from [5].*

One of the main advantages in the use of MPV reaction for the reduction of carbonyl compounds, is its high selectivity for C=O double bond. As a matter of fact, α,β-unsaturated carbonyl compounds can be selectively reduced via MPV reaction, leaving C=C untouched.

Besides aluminum complexes, the zirconium complex, bis(cyclopentadienyl)zirconium di-hydride, has also been reported to be active in the MPV reaction for several carbonyl compounds such as benzaldehyde, acetone and benzophenone. Different linear (e.g. butanol, octanol, dodecanol, allyl alcohol) and cyclic alcohols (cyclohexanol, benzyl

alcohol) were used as hydrogen donor and they were all active in the hydrogen transfer reaction[11].

Shvo's catalyst has also been demonstrated to be a powerful catalyst for transfer hydrogenation[98]. 5-hydroxymethylfurfural (HMF) reduction to 2,5-bishydroxymethylfuran (BHMF) occurred under mild conditions (10 bar H_2, 90°C) and with complete selectivity towards the formation of the desired product. Catalyst has been successfully recycled, after removing the product from the reaction mixture by precipitation and filtration.

In addition to these homogeneous catalysts some others alternative materials have also been reported, based on either non-precious metals, such as $Fe^{12,13,14}$ or alkali metal ions, such as Li alkoxides[15,16] or KOH^{17}.

2.2.2. CTH with heterogeneous catalysts

The requirement of a large amount of reagents and the presence of undesired side reactions are the main drawbacks of the MPV reduction using homogeneous catalysts. To overcome these problems, the reaction has been investigated over different heterogeneous catalysts, including metal oxides, hydrous zirconia, hydrotalcites, zeolites and even metal alkoxides immobilized on mesoporous materials. As a matter of fact, H-transfer reduction by means of hydrogen donors on heterogeneous catalysts has many interesting advantages, if compared to the classical reduction procedure, which requires molecular hydrogen. Using the H-transfer reaction, no gas tank is necessary, avoiding any possible hazards connected to the presence of a gas with a low molecular weight and high diffusibility in a chemical plant. Therefore, over the past two decades, an increasing number of reports on heterogeneous catalysts for the MPV reaction have been published[18].

Most of the solid catalysts reported in literature are based on alkali and alkaline earth oxides, which sometimes are characterized by the insertion of metal atoms, bringing Lewis acid properties. The solid catalysts, which have been investigated for this kind of reaction, can be divided into three main groups: Lewis base or Lewis acid catalysts and metal supported catalysts.

Metal doped zeolites are included in Lewis acid type catalysts together with Zr containing systems. In particular, beta zeolite has been found to be highly stereoselective catalysts in the MPV reduction especially when some guest element such as Ti, Sn and Zr was

introduced in the structure. For example, zeolites such as H-beta[19,20,21] and alumina[22] were used in the H-transfer reaction using isopropanol, ethanol, or cyclopentanol as donor. Furthermore, high surface area mesoporous materials should be included: Ti or Sn incorporated in MCM[23,24,25] were used as catalysts with isopropanol or 2-butanol as the reducing agents.

As far as the Zr based systems are concerned, the most relevant results were obtained with ZrO_2 and hydrous zirconia, either doped or as it is, anchored/grafted Zr over supports[26,27].

In the field of solid base materials, magnesium oxide has been widely used in H- transfer reactions. More specifically, examples include: (a) MgO, either doped or as it is and Mg/M mixed oxides, which have been used for the reduction of substrates such as citral, cyclohexanone, acetophenone, hexenone, acetone, benzaldehyde, crotonaldehyde, and, in general, for various aliphatic aldehydes and ketones or aralkylketones. In most of the cases, isopropanol was used as the H-transfer reactant, with a few exceptions in which ethanol and other C_4 alcohols were taken into consideration. The majority of these processes were carried out in liquid phase.

Some gas phase reactions over MgO were reported by Cosimo and coworkers[28]. The author concluded that the unsaturated ketone conversion pathways toward unsaturated alcohols and other compounds also depended on the ketone structure. Unsaturated alcohols were formed on MgO as a primary product from both 2-cyclohexenone and mesityl oxide. However, the saturated alcohol can be produced by a consecutive reaction of unsaturated alcohols in the presence of 2-cyclohexenone and not with mesityl oxide. The reduction of the C=C bond was negligible regardless the reactant structure, whereas competing reactions such as the C=C bond shift were more likely to contribute during reduction of the acyclic reactant.

Among the heterogeneous catalytic systems, supported noble metal catalysts such as Pt[29,30], Au[31,32], Pd[33], and Ir[34] acted as effective and reusable heterogeneous catalyst for the same reaction. Au supported onto different support (TiO_2, Fe_2O_3, Carbon) and Pd/C were used as catalyst for H-transfer hydrogenation of acetophenone and many other carbonyl compounds, using 2-propanol as H-donor.

Concerning the investigation of the reaction mechanism for the CTH over heterogeneous catalysts numerous studies have been performed and the general conclusion reached consists in the possibility, for the solid materials, to follow three main pathways:

- The general acid-base pair mechanism;
- The basic oxide catalysts "direct" hydrogen transfer route (likely MPV);
- The basic oxide hydride route.

Although both Lewis acidic and basic materials have been reported to be active in mediating CTH processes following the MPV mechanism, it is important to recognize that both Lewis acid and base sites are necessary to catalyze the reaction. The role of the Lewis acid site, typically an electron-deficient metal center, is to bond with the electron-rich oxygen in the hydroxyl and carbonyl groups in the hydrogen donor and acceptor, respectively, whereas the adjacent base site attracts the proton in the hydroxyl and weakens the O−H bond. The stronger the interaction between the hydroxyl oxygen and the Lewis acid site, the more acidic the hydroxyl hydrogen in the hydrogen donor becomes, which facilitates the abstraction of the hydrogen by the base site. Conversely, strongly basic sites can effectively abstract the hydrogen from the hydroxyl group of the alcohol, leading to the formation of an alkoxide adsorbed on the adjacent Lewis acid site, thus promoting the hydride transfer. Thus, both strong acids and strong bases facilitate CTH, but it is unlikely that strong Lewis acid and base sites can coexist on the same catalyst. Although either the acid or base property of a catalyst could dominate, an acid−base pair is needed to complete the catalytic cycle and allow the formation of the six-membered-ring intermediate (**Scheme 2-4**).
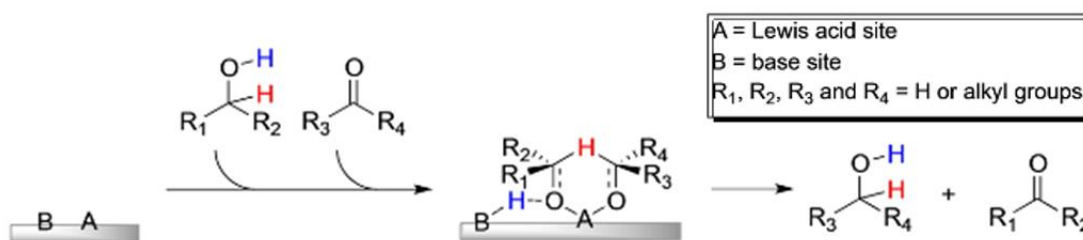
Scheme 2-4. *General acid-base pair heterogeneous catalysts CTH mechanism. Adapted from [5].*

On the other hand, in the case of the basic oxide catalysts that proceed through a mechanism that could be assimilated to the classic "direct" hydrogen transfer route described above for the homogeneous systems. In this case it has to be highlighted that the reaction is driven by the basic sites on the catalyst surface and can be divided into two following steps. The first consists in the coordination of the hydrogen source over the catalyst surface with the results of the proton abstraction from the R-OH specie by-means of the basic site (generally the O^{2-} anion). The second step consists in the coordination of

the carbonyl group through the C-O⁻ over the acidic site (generally an M^{2+} cation). Also in this case the neighboring presence of both acid and base sites are necessary in order to allow the formation of the six-membered-ring intermediate that then evolves in the formation of the reduced product after the transfer of hydrogen (**Scheme 2-5**).
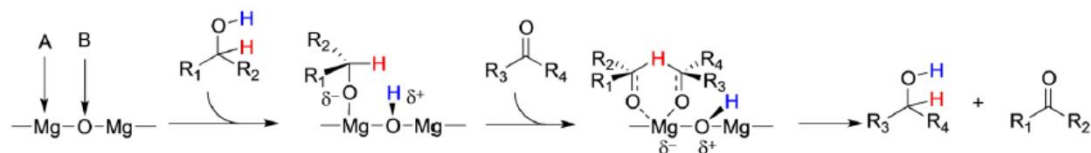
Scheme 2-5. *CTH mechanism for the basic catalysts that follow an MPV-like mechanism. Adapted from [5].*

Finally, it has been discovered another pathway through which the CTH could proceed with the heterogeneous basic catalysts. This is the case of that kind of basic catalysts for which the behavior are similar to that exhibited by the metal hydride-route homogeneous systems. Base-mediated CTH reactions are proposed to proceed through a two-step process: the alcohol (hydrogen donor) dissociates to form the corresponding alkoxide on a weekly acidic metal cation, e.g., Mg^{2+}, while the hydroxyl proton resides on the basic O^{2-} anion. The α-H of the alkoxide and the proton adsorbed on the base site are then transferred to the carbon and oxygen atoms in the carbonyl group, respectively. This pathway is quite different from the typical MPV mechanism because the six-membered-ring intermediate does not involve the metal site (**Scheme 2-6**).
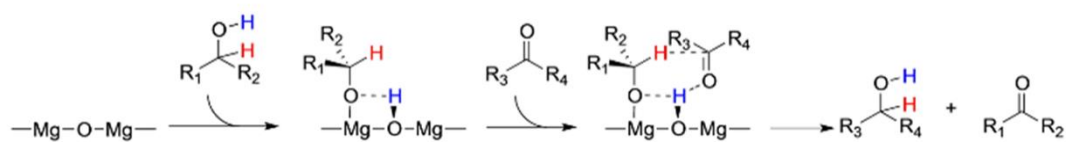
Scheme 2-6. *CTH mechanism for the basic catalysts that follow the hydride-like mechanism. Adapted from [5].*

2.3. CTH as new strategy for the upgrade of biomass-derived platform molecules

It has just been reported in the former sections of this work that the in the last years the second generation lignocellulose biomass feedstock has been considered one of the most appealing alternative to the fossil sources for the production of fuels and chemicals. In order to upgrade and valorize the platform molecules produced from the cellulose and hemicellulose fraction of the renewable feedstock it is necessary to set up an oxygen removal step targeted to the decrease of the high oxygen content characterizing these new platform molecules. In this part of the work are summarized the main catalytic strategies involved in the use of the CTH as a tool for the upgrade of the biomass-derived building block.

The renewable-feedstock building block can be divided into two main groups on the base of the relevance and the appealing found in the scientific community:

- HMF, FU and levulinic acid are the most used platform due to the possibility to produce from their direct transformation numerous target molecules with application as monomers, fuels or fuel-additives;
- Lignin, vanillin, sorbitol and glycerol that started to became attractive, from the CTH upgrade point of view, only in the last years.

2.3.1. CTH upgrade of furanic-platform molecules: HMF and FU

As deeply described in the first chapter, furfuryl alcohol (FAL) and methylfuran (MeF) as well as 2,5-bishydroxymethylfuran (BHMF) and 2,5-dimethylfuran (DMF), which are respectively produced from the selective hydrogenation of biomass-derived FU and HMF, have been considered as new-fashioned monomers for the polymer industry or liquid bio-fuels for transportation, receiving much more attention from many researchers in the world. Furfural and HMF are considered the most important platform molecules obtained from the dehydration of C_5 and C_6 sugars, which are present in the hemicellulose and cellulose part of the biomass feedstock (**Scheme 2-7**).
The most of the reported process for the production of these interesting furanic derivatives involve the use of molecular hydrogen as reductant and metal supported catalysts. At the

best of our knowledge these process are not yet competitive, from an economical point of view, with the petrochemical technologies. Hence, the development of new approaches which decreases the number of reaction and purification processes is becoming fundamental. The hydrogen transfer approach could be considered as a relevant approach to produce biofuels, avoiding molecular hydrogen and in some cases also an expensive metal based catalyst.
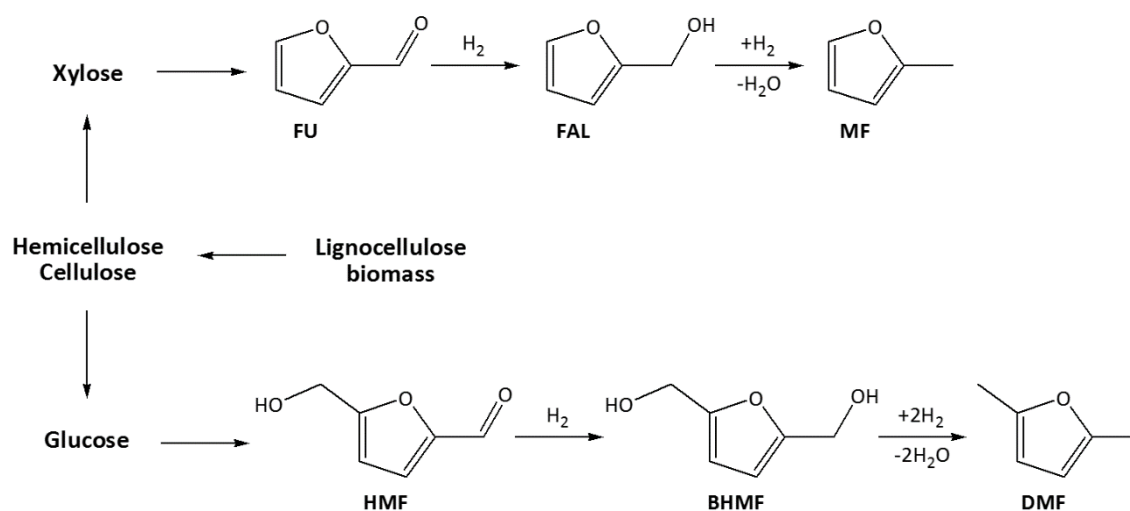
Scheme 2-7. *Production of FAL, MF, BHMF and DMF from lignocellulose biomass.*

In this field, at the beginning, the researcher has focused their attention on the development of process for the production of BHMF and DMF from HMF, highlighting the different reactivity and catalysts performances as a function of the alcohol used as hydrogen source and discussing the possible reaction mechanism. It has also to be highlighted that one of the key challenges for upgrading furans is product selectivity; a mixture of side chain ring-hydrogenated and ring-opened products is often formed.

In 2010, Rauchfuss and coworkers[35] proposed a mild catalytic system, in which formic acid (FA) was first used as a hydrogen donor for the selective hydrogenation of HMF. When the reaction was carried out in THF over the Pd/C catalyst, more than 95% DMF yield with 100% HMF conversion was observed at 70°C after 15 h. Furthermore, a one-pot process for the synthesis of DMF from fructose was also investigated. In the presence of FA, H_2SO_4, Pd/C and THF, fructose was initially dehydrated at 150°C for 2 h, and the generated HMF was subsequently hydrogenated at 70°C for 15 h, obtaining 51% DMF yield. It is worth noting that using FA as catalyst it is possible to perform three different reactions, thanks to its peculiar characteristics: it is an acid catalyst for the dehydration of

fructose into HMF and a reagent for the deoxygenation of furanylmethanols as well as a hydrogen donor for the hydrogenation of HMF into DHMF.

The use of FA for these processes is very attractive because it can be derived from biomass and it can be regenerated by hydrogenation of formed CO_2. Furthermore, its presence was reported to inhibit the decarbonylation of molecules, which can occur quite easily at 120°C in the presence of Pd/C even at low reaction time (2-8 hours)[36]. On the other hand the main drawback related to the use of FA consists in the necessity for a special corrosion-resistant equipment, in the view of an industrial scale-up, that surely increases the cost of the possible investment.

Beside formic acid, some alcohols can also be used as H-donor in HMF reduction.

The use of isopropyl alcohol, as hydrogen donor as well as reaction medium, was alternatively studied by Vlachos and coworkers[37] for HMF reduction. When the reaction was conducted over the Ru/C based catalyst, 100% conversion of HMF and a 81% of yield in DMF were achieved at 190°C after 6 h. Unfortunately, when the recovered Ru/C was reused in the second cycle, HMF conversion and DMF yield were significantly decreased to 47% and 13% respectively,, showing a considerable deactivation of Ru/C even after its first use, which might be due to the formation of high molecular weight by-products on ruthenium surfaces. More recently, Pd and Rh supported onto carbon were used for HMF hydrogenation in the presence of MeOH at 150°C and 20 bar of H_2 pressure[38]. $ZrCl_2$ was used as co-catalyst since it is claimed to improve DMF selectivity thanks to the presence of a strong synergistic effect between Pd and Zr; the addition of Zr salt to the reaction mixture has been fundamental also when Ru/C was used as catalyst. DMF yield reached 39% in 2 hours with a conversion of HMF around 75%. However, in the presence of methanol HMF etherification occurred, forming 5-methoxymethylfurfural; this reaction was catalyzed by Lewis acid sites, that belonged to the used catalyst. On the contrary, the use of THF as solvent led to 85% yield of DMF in 8h with a complete conversion of HMF, demonstrating the inability of these systems to transform completely HMF into DMF in the presence of an alcoholic solution.

Another stable catalyst based on Pd supported on Fe_2O_3 was prepared and used by Hermans and coworkers[39]. The yield of DMF reached 72% when a continuous-flow reactor at 180 °C was used. Due to its similarity to HMF, furfural can be easily reduced via H-transfer using the same methodology already reported for this molecule. In fact, in the same paper it is reported that 2-propanol on Fe_2O_3-supported Cu, Ni and Pd catalysts can carry out the sequential transfer hydrogenation/hydrogenolysis of furfural to 2-

methylfuran. An optimal yield of 57% of furfuryl alcohol and the formation of 10% of MF were observed in a batch reactor at 180°C after 7.5 hours of reaction with Pd/Fe_2O_3. The remarkable activity of Pd/Fe_2O_3 in both transfer hydrogenation and hydrogenolysis is attributed to a strong metal-support interaction. Using a noble metal catalyst, the active site for H-production seems to be the same used for substrate hydrogenation.

An unconventional H-transfer reactant was used by Cavani and coworkers[40], who reported that HMF could be selectively reduced to BHMF (100% yield) over MgO using methanol as both H-donor and reaction solvent, under mild condition (160°C). In the same reaction conditions, furfural was hydrogenated reaching 97% of furfuryl alcohol yield. MgO was demonstrated to be an excellent catalyst because it was able to activate methanol at low temperature, which is the key step of this process; moreover, the only formed by-products were gaseous (CO, CO_2, CH_4) easily separable for the reaction mixture.

In the last years the development of CTH process for the production of FAL and MF from FU takes place, demonstrating the increase appealing for the large-scale production of these interesting biomass derivatives with several and appealing application.

Recently a recent paper has been published by Marchi and coworkers[41] on furfural hydrogenation by means of H-transfer with copper based catalyst (Cu/SiO_2 and Cu-Mg-Al) prepared by co-precipitation. The authors investigated the effect of metal-support interaction and concluded that smaller particles with stronger interaction with the spinel-like matrix had higher capability for transferring hydrogen than large ones. Under the optimal conditions (150°C, 8 hours), 100% conversion of furfural to furfuryl alcohol can be obtained. Moreover, ethanol, propanol and isopropanol have been tested as H-donor and the last one showed better performances. Vlachos and coworkers[42] studied the effect of H-donor on $Ru/RuO_x/C$ catalyst, using different primary and secondary alcohols. Secondary alcohols have shown greater activity in MF production and it has been discovered that alcohol polarity can affect the hydrogenolysis reaction. The optimum methyl furan yield of 76% was achieved using 2-butanol and 2-pentanol (180°C, 10 hours). Meanwhile, the author indicated that methylfuran yield increased with increasing alcohol dehydrogenation activity and decreasing alcohol polarity. Another paper has just been published by Vlachos and co-workers[43] with the aim of clarifying the reaction mechanism in MF formation when $Ru/RuO_x/C$ was used as catalyst and 2-propanol as H-donor. The reaction mechanism was studied using isotopically labeled chemicals and performing a mass fragmentation analysis. These mechanistic investigations highlighted

the presence of a MPV Lewis acid mediated pathway for furfural hydrogenation. The usual six-member intermediate was formed and the β-H of 2-propanol was transferred to the carbonyl carbon atom of the substrate in a concerted step without transferring the hydrogen to the surface of the catalyst, as it usually happens in metal-mediated hydrogenation.

Chen and coworkers[44] prepared a series of metal supported carbon nitrile catalyst (M/CN, where M = Ag, Pt, Au and Pd) which could proceed the reduction of unsaturated compounds including furfural at room temperature in water using formic acid as the hydrogen source. The author indicated that the reusability of such a hybrid catalyst is high due to the strong Mott–Schottky effect present between the metal nanoparticles and the carbon nitride support. The highest conversion of furfural was 64% with 99% selectivity towards MF.

2.3.2. CTH for levulinic acid (LA) reduction

The acid hydrolysis of lignocellulosic materials led to levulinic acid (LA) formation. The hydrogenation of LA then gives γ-valerolactone (GVL), which is a sustainable liquid for energy and carbon based chemicals. In **Scheme 2-8**, the main products that can be obtained from GVL are reported, with application in fuels, additive for fuels and chemicals production.
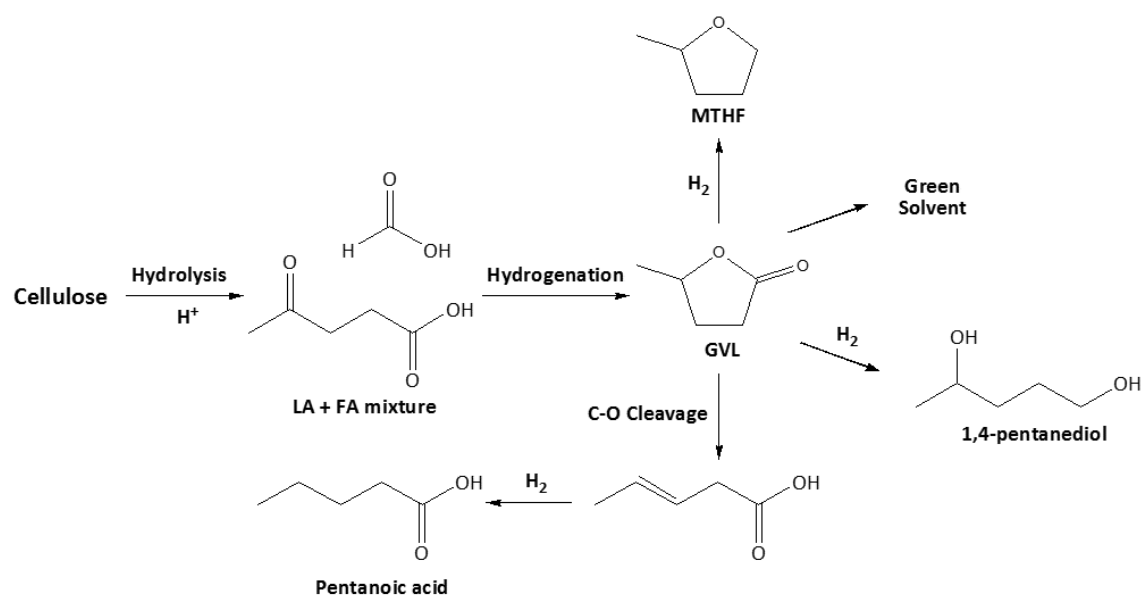
Scheme 2-8. Reaction pathways for conversion of γ-valerolactone (GVL) into fuels and chemicals.

Many processes have been reported for hydrogenation of levulinic acid (LA) to GVL using gaseous H_2 and metal based catalyst (Ru, Pd, Pt) either in homogeneous or in heterogeneous conditions. However, reaction parameters must be carefully controlled to prevent further hydrogenation reaction, forming MTHF and pentanoic acid, even if they are both products with a high added value[45,46]. GVL can also be synthesized by catalytic transfer hydrogenation, using alcohols as hydrogen donor. Several catalytic systems have recently been reported for the production of GVL *via* the H-transfer process. Dumesic and coworker[47] compared different metal oxides in H-transfer reduction of levulinate derivatives to GVL and ZrO_2 was found to be a highly active material for H-transfer in both batch reactions and continuous flow reactor. Using isopropanol/isobutanol as H-donors at 150°C under pressurized inert gas flow the reaction reached a yield of 84% in 16 hours. Analogously, Lin and coworkers[48] investigated an H-transfer reaction of ethyl levulinate (EL) over ZrO_2 catalyst in a supercritical ethanol. Using ethanol as H-donor, an integrated biomass utilization chain will be created, since ethanol can also be produced from biomass feedstock.

Microporous zirconosilicate molecular sieves (Zr-beta) have recently been reported to be more active and stable catalysts if compared to bulk zirconia. Chuah and co-workers[49] developed Zr–Beta zeolite as a robust and active catalyst for the hydrogen transfer reduction of levulinic acid to γ-valerolactone using 2-propanol as H-donor. They also explained its high activity with the presence of both Lewis acid sites with moderate strength and relatively few basic sites. The presence of a low amount of basic sites prevented catalyst poisoning due to the absorption of the acid reactant. In a batch reactor, γ-valerolactone was formed with the selectivity higher than 96% and 100% LA conversion, whereas quantitative conversion with > 99% yield of GVL was obtained with a steady generation rate of 0.46 $mol_{GVL}g_{Zr}^{-1}h^{-1}$.

Besides Zr based oxide, some noble metal supported catalysts were also investigated in LA transformation using H-transfer processes.

Fujitani and coworkers[50] reported LA reduction via H-transfer over a cheap noble metal supported catalyst, Ru hydroxide supported on anatase. Since Ru in the form of hydroxide had already been reported as an efficient catalyst in carbonyl compounds hydrogenation, this study demonstrated that it worked as well for biomass-derived carbonyl compounds reduction. Further improvements were obtained by Yamashita and coworkers[51], using a catalyst made up of uniformly dispersed Ru nanoparticles supported on Zr-containing spherical mesoporous silica. This system showed a superior activity for the hydrogenation

of both LA and its ester under mild conditions; the Zr sites embedded within the spherical mesoporous silica were demonstrated to have the ability to disperse and stabilize the Ru NPs, giving rise to an improved catalyst stability and reusability, and to provide acidity, which highly improved GLV selectivity. Cao and coworkers studied Au-ZrO$_2$ catalyst to catalyze the hydrogenation of levulinic acid to γ-valerolactone using formic acid (FA) or butyl formate[52,53] as H-donor. The superior performance of Au catalysts for formate-mediated transfer reduction was attributed to the nature of gold nanoparticles, which had been demonstrated to be an excellent catalyst in formate media decomposition. Indeed, they can directly convert a 1:1 aqueous mixture of LA and FA into GVL with high yields. This means that GVL can be synthesized from an integrated process, which starts from the solution of LA and FA derived from HMF synthesis and decomposition in acidic aqueous medium.

[1] M. Thewes, M. Muether, S. Pischinger, M. Budde, A. Brunn, A. Sehr, P. Adomeit, J. Klankermayer, *Energy & Fuels,* 2011, **25 (12)**, 5549

[2] X. Ma, C. Jiang, H. Xu, H. Ding and S. Shuai, *Fuel*, 2014, **116**, 281

[3] T. Laue, A. Plagens, *Namen- und Schlagwort-Reaktionen der Organischen Chemie*, Vieweg Teubner Verlag, 1994, pp. 221

[4] W. Ponndorf, Angew. Chem., 1926, **39**, 138

[5] M. J. Gilkey, B. Xu, ACS Catal. 2016, 6**,** 1420

[6] F. Cavani, S. Albonetti et al. "Beyond H_2: Exploiting H-Transfer Reaction as a Tool for the Catalytic Reduction of Biomass" in "**Chemicals and Fuels from Bio-Based Building Blocks**" **2016** Wiley-VCH Verlag

[7] F. Cavani, S. Albonetti et al., *J. Catal.,* 2014, **317**, 206

[8] R. Noyori, M. Yamakawa, S. Hashiguchi, *J. Org.Chem.,* 2001, **66**, 7931

[9] T. C Johnson, D. J. Morris, M. Wills, *Chem. Soc. Rev.,* 2010, **39**,81

[10] J. S. Samec, J. E. Bäckvall, P. G. Andersson, P. Brandt, *Chem. Soc. Rev.,* 2006, **35**, 237

[11] Y. Ishii, T. Nakano, A. Inada, Y. Kishigami, K. Sakurai, M. Ogawa, *J. Org. Chem.,* 1986, **51**, 240

[12] S. Enthaler, K. Junge, M. Beller, *Angew. Chem. Int. Ed.,* 2008, **47**, 3317

[13] C. Bolm, J. Legros, J. Le Paih, L. Zani, *Chem. Rev.,* 2004, **104**, 6217

[14] R.M. Bullock, *Angew.Chem. Int. Ed.,* 2007, **46**, 7360

[15] J. Ekström, J. Wettergren, H. Adolfsson, *Adv. Synth. Catal.,* 2007, **349**, 1609

[16] J. Sedelmeier, S.V. Ley, I.R. Baxendale, *Green Chem.,* 2009, **11**, 683

[17] V. Polshettiwar, R.S. Varma, *Green Chem.,* 2009, **11**, 1313-

[18] M. Geeta Pamar, P. Govender, K. Muthusamy, R. W. M. Krause and H.M. Nanjundaswamy Orient. *J. Chem.,* 2013, *29(3)*, 969

[19] A. Ramanathan, M.C. Castro Villalobos, C. Kwakernaak, S. Telalovic, U. Hanefeld, *Chem. Eur. J., 2008,* **14**, 961

[20] D. Klomp, T. Maschmeyer, U. Hanefeld, J.A. Peters, *Chem. Eur. J.,* 2004, **10**, 2088

[21] O. Bortnovsky, Z. Sobalík, B. Wichterlová, Z. Bastl, *J. Catal,.* 2002, **210**, 171

[22] S. Carre, N.S. Gnep, R. Revel, P. Magnoux, *Appl. Catal. A: General.,* 2008, **348**, 71

[23] M. Boronat, A. Corma, M. Renz, P.M. Viruela, *Chem. Eur. J.,* 2006*,* **12***,* 7067

[24] P.P. Samuel, S. Shylesh, A.P. Singh, *J. Mol. Catal. A Chem.,* 2007, **266**, 11

[25] C. van der Waal, P.J. Kunkeler, K. Tan, H. van Bekkum, *J. Catal.,* 1998, **173**, 74

[26] S. Axpuac, M.A. Aramendía, J. Hidalgo-Carrillo, A. Marinas, J.M. Marinas, V. Montes-Jiménez, F.J. Urbano, V. Borau, *Catal. Today,* 2012, **187**, 183

[27] B. Zhang M. Tang, J. Yuan, L. Wu Chin. *J. Catal*., 2012, **33**, 914

[28] J.J. Ramos, V.K. Díez, C.A. Ferretti, P.A. Torresi, C.R. Apesteguía, J.I. Di Cosimo, *Catal. Today,* 2011*,* **172**, 41

[29] F. Alonso, P. Riente, F. Rodríguez-Reinoso, J. Ruiz-Martínez, A. Sepúlveda-Escribano, M. Yus, *J. Catal.,* 2008, **260**, 113

[30] F. Alonso, P. Riente, F. Rodríguez-Reinoso, J. Ruiz-Martínez, A. Sepúlveda-Escribano, M. Yus, *ChemCatChem,* 2009, **1**, 75

[31] F.-Z. Su, L. He, J. Ni, Y. Cao, H.-Y. He, K.-N. Fan, *Chem. Commun.,* 2008, 3531

[32] L. He, J. Ni, L.-C. Wang, F.-J. Yu, Y. Cao, H.-Y. He, K.-N. Fan, *Chem. Eur. J.,* 2009*,* **15**, 11833

[33] J.-Q. Yu, H.-C. Wu, C. Ramarao, J.B. Spencer, S.V. Ley, *Chem. Commun.,* 2003, 678

[34] C. Hammond, M.T. Schümperli, S. Conrad, I. Hermans, *ChemCatChem,* 2013*,* **5**, 2983

[35] T.Thananatthanachon, T.B. Rauchfuss, Angew. *Chem. Int. Ed.,* 2010, **49**, 6616

[36] J. Mitra, X. Zhou, T. Rauchfuss, *Green Chem.,* 2015, **17**, 307

[37] J. Jae, W. Zheng, R.F. Lobo, D.G. Vlachos, *ChemSusChem,* 2013*,* **6**, 1158

[38] Saha, B., Abu-Omar, *ChemSusChem,* 2015, **8**, 1133

[39] D. Scholz, C. Aellig, I. Hermans, *ChemSusChem,* 2014*,* **7**, 268

[40] T. Pasini, A. Lolli, S. Albonetti, F. Cavani, M. Mella, *J. Catal.,* 2014, **317**, 206

[41] M.M. Villaverde, T.F. Garetto, A.J. Marchi, *Catal. Commun.,* 2015*,* **58**, 6

[42] P. Panagiotopoulou, N. Martin, D.G. Vlachos, *J. Mol. Catal. A Chem.,* 2014, **392**, 223

[43] M.J. Gilkey, P. Panagiotopoulou, A.V. Mironenko, G.R. Jenness, D.G. Vlachos, B. Xu, *ACS Catal.* 2015 DOI: 10.1021/acscatal.5b00586.

[44] L.-H. Gong, Y.-Y. Cai, X.-H. Li, Y.-N. Zhang, J. Su, J.-S. Chen, *Green Chem.*, 2014*,* **16**, 3746

[45] D.M. Alonso, S.G. Wettstein, J.A. Dumesic, *Green Chem.,* 2013*,* **15**, 584

[46] J.-P. Lange, R. Price, P.M. Ayoub, J. Louis, L. Petrus, L. Clarke, H. Gosselink, *Angew. Chem. Int. Ed.,* 2010*,* **49**, 4479

[47] M. Chia, J.A. Dumesic, *Chem. Commun.,* 2011*,* **47**, 12233

[48] X. Tang, L. Hu, Y. Sun, G. Zhao, W. Hao, L. Lin, *RSC Adv.,* 2013*,* **3**, 10277

[49] Wang, S. Jaenicke, G.-K. Chuah, *RSC Adv.,* 2014*,* **4**, 13481

[50] Y. Kuwahara, W. Kaburagi, T. Fujitani, *RSC Adv.,* 2014*,* **4**, 45848

[51] Y. Kuwahara, Y. Magatani, H. Yamashita, *Catal. Today,* 2015, doi:10.1016/j.cattod.2015.01.015

[52] X.-L. Du, L. He, S. Zhao, Y.-M. Liu, Y. Cao, H.-Y. He, K.-N. Fan, *Angew. Chem. Int.Ed.,* 2011*,* **50**, 7815

[53] X.-L. Du, Q.-Y. Bi, Y.-M. Liu, Y. Cao, K.-N. Fan, *ChemSusChem,* 2011,**4**,1838

CHAPTER 3   Heterogeneous basic catalysis

3.1. Introduction

Acid and base are paired concepts; a number of chemical interactions have been understood in terms of acid-base interaction. Among chemical reactions which involve acid-base interactions are acid-catalyzed and base-catalyzed reactions which are initiated by acid-base interactions between the catalyst and the substrate followed by catalytic cycles. In acid-catalyzed reactions, reactants act as bases toward catalysts which act as acids. On the contrary in base-catalyzed reactions reactants act as acids toward catalysts which act as bases.

In homogeneous systems, a huge number of acid-catalyzed reactions and base-catalyzed reactions are known. In heterogeneous systems, a limited number of reactions are recognized as acid or base-catalyzed reactions. In particular, base-catalyzed reactions have been studied to a lesser extent as compared to acid-catalyzed reactions in heterogeneous systems. Heterogeneous acid catalysis attracted much attention primarily because heterogeneous acidic catalysts act as catalysts in petroleum refinery and are known as a main catalyst in the cracking process which is the largest process among the industrial chemical processes. Extensive studies of heterogeneous cracking catalysts undertaken in the 1950s revealed that the essential nature of cracking catalysts are acidic, and generation of acidic sites on the solids was extensively studied. As a result, amorphous silica-alumina was utilized as a cracking catalyst, and then crystalline aluminosilicate (zeolite) was used afterward.

In contrast to these extensive studies on heterogeneous acidic catalysts, fewer studies have been performed over heterogeneous basic catalysts. The beginning of the heterogeneous basic-catalysts-era could be pointed after the studies of Pines et al. that demonstrated the ability of supported metal Na to acts as electrons donor acting as a basic system[1].

In a second moment it has been reported that certain metal oxides, composed by a single metal cation, act as heterogeneous basic catalysts in the absence of such alkali metals as Na and K.

In the 1970s, Kokes et al. reported that hydrogen molecules were adsorbed on zinc oxide by acid-base interaction to form proton and hydride on the surface. They proved that the heterolytically dissociated hydrogens act as intermediates for alkene hydrogenation. In the same period, Hattori et al. reported that calcium oxide and magnesium oxide exhibited high activities for 1-butene isomerization. The reaction is recognized as a base-catalyzed reaction in which the reaction was initiated by abstraction of a proton from 1-butene by the basic site on the catalyst surfaces.

Type of material	Examples of heterogeneous basic catalyst
Single component metal oxides	alkaline-earth oxides
	alkali-metal oxides
	rare-earth oxides
	ThO_2, ZrO_2, ZnO, TiO_2
Zeolites	alkali-ion-exchanged zeolites
	alkali-ion-added zeolites
Supported alkali-metal ions	alkali-metal ions on alumina
	alkali-metal ions on silica
	alkali-metal on alkaline-earth oxides
	alkali-metal and alkali-metal hydroxides on alumina
Clay minerals	hydrotalcite
	chrysotile
	sepiolite
Non-oxides	KF supported on alumina
	lanthanide imide and nitride in zeolite

Table 3-1. *Types of heterogeneous basic catalysts. Adapted from [2].*

In addition to the acid-zeolites, that find several application as industrial catalyst in the oil refinery process, in early 1970s have been developed basic-type zeolites. For instance, Yashima et al. reported that side chain alkylation of toluene was catalyzed by alkali ion-exchanged X and Y type zeolites.j The reaction is a typical base-catalyzed reaction, and the activity varied with the type of exchanged alkali cation and with type of zeolite, suggesting that the basic properties can be controlled by selecting the exchanged cation and the type of zeolite.

In addition to the above mentioned catalysts, a number of materials have been reported to act as heterogeneous basic catalysts (**Table 3-1**). Except for non-oxide catalysts, the basic sites are believed to be surface O^{2-} atoms[2].

In the last years have been identified, as a general rule, 4 main features that an heterogeneous catalysts should present in order to be considered an heterogeneous basic catalyst:

1. Characterizations of the surfaces by various methods such as color change of the acid-base indicators adsorbed, surface reactions, adsorption of acidic molecules, and spectroscopies indicate that basic sites exist on the surfaces;

2. There is a parallel relation between catalytic activity and the amount and/or strength of the basic sites: The catalytic activities correlate well with the amount of basic sites or with the strength of the basic sites measured by various methods. Furthermore, the active sites could be poisoned by acidic molecules such as HC1, H_2O, and CO_2;

3. The material has similar activities to those of homogeneous basic catalysts for "base-catalyzed reactions" well-known in homogeneous systems. There are a number of reactions known as base-catalyzed reactions in homogeneous systems. Certain solid materials also catalyze these reactions to give the same products. The reaction mechanisms occurring on the surfaces are suggested to be essentially the same as those in homogeneous basic solutions;

4. There are indications of anionic intermediates participating in the reactions: Mechanistic studies of the reactions, product distributions, and spectroscopic observations of the species adsorbed on certain materials indicate that anionic intermediates are involved in the reactions.

3.2. Generation of basic sites

One of the reasons why the studies of heterogeneous basic catalysts are not as extensive as those of heterogeneous acidic catalysts seems to be the requirement for severe pretreatment conditions to allow the formation of the basic sites over the catalysts surface. Indeed, in the most of the cases, the surface of the synthesized heterogeneous basic systems are covered by simple molecules such as carbon dioxide, water, oxygen, etc. thus,

the generation of the basic sites usually requires an high-temperature pretreatment to remove the mentioned adsorbed molecules. Furthermore, the nature of the basic sites generated by the removal of the adsorbed molecules mainly depends by the desorption temperature; the lower is the desorption temperature the lower is the strength of the generated basic site. For instance, the molecules weakly interacting with the surfaces are desorbed at lower pretreatment temperatures, and those strongly interacting are desorbed at higher temperatures. The sites that appeared on the surfaces by pretreatment at low temperatures are suggested to be different from those that appeared at high temperatures. If simple desorption of molecules occurs during pretreatment, the basic sites that appeared at high temperatures should be strong.

However, rearrangement of surface and bulk atoms also occurs during pretreatment in addition to the desorption of the molecules, which is evidenced by a decrease in the surface area with an increase in the pretreatment temperature.
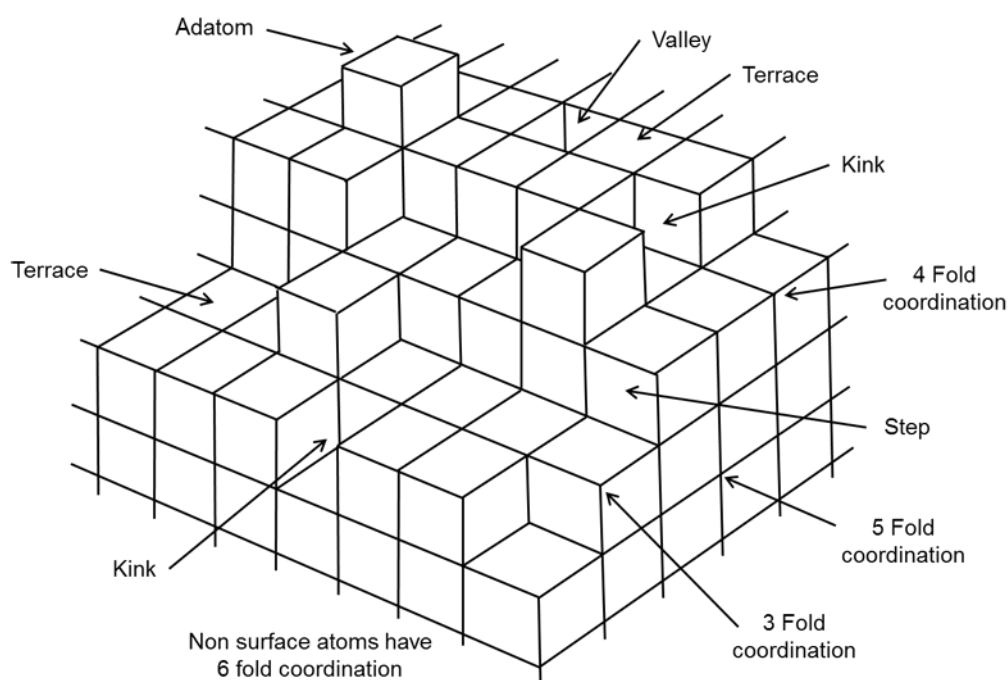
Figure 3-1. Schematic representation of the low-coordinated atoms over the surface of an heterogeneous basic catalyst.

Coluccia and Tench proposed a surface model for MgO (**Figure 3-1**)[3]. There exist several Mg-O ion pairs of different coordination numbers. Ion pairs of low coordination numbers exist at corners, edges, step or kink. The different strength and nature of the basic sites generated at he increase of the pre-treatment temperature could be related to the coordination degree of the atoms on the surface. However, the correspondence between

the catalytically active sites for different reaction types and the coordination number of the ion pairs is not definite yet.

In the case of MgO, considered as an example, the ion pair of 3-fold Mg^{2+}-3-fold O^{2-} (Mg^{2+}_{3C}-O^{2-}_{3C}) is most reactive and adsorbs carbon dioxide most strongly. To reveal the ion pair Mg^{2+}_{3C}-O^{2-}_{3C} the highest pretreatment temperature is required. At the same time, the ion pair Mg^{2+}_{3C}-O^{2-}_{3C} is most unstable and tend to rearrange easily at high temperature. Thus, the formation of these high active basic sites as the consequence of carbon dioxide desorption is in competition with their rearrangement to more stable coordination sites.

Although the surface model shown in **Figure 3-1** is proposed for MgO, the other metal oxide heterogeneous bases may be in a situation similar to that of MgO. The nature of basic sites varies with the severity of the pretreatment conditions for most heterogeneous basic catalysts.

3.3. Catalytic application of heterogeneous basic catalyst

In the next few pages an overall review of the main catalytic application of the heterogeneous basic catalysts is reported. Despite the era of the heterogeneous basic catalysis is young, numerous application have been developed in the recent years, creating always more appeal in the scientific community. The main reaction in which the heterogeneous basic catalysts have found application is reported as follows:

- Double bond migration/alkene isomerization;
- Dehydration and dehydrogenation reactions;
- Hydrogenation reaction;
- Amination reaction;
- Dehydrocyclodimerization of conjugated diens;
- Alkylation;
- Aldol addition and condensation;
- The Tishchenko Reaction;
- Michael Addition;
- The Wittig-Horner Reaction and Knoevenagel Condensation;
- Synthesis of ag-Unsaturated Compound by use of methanol;
- Meerwein-Ponndorf-Verley Reduction.

3.3.1. Double bond migration/alkene isomerization

1-Butene isomerization to 2-butenes has been extensively studied over many heterogeneous basic catalysts to elucidate the reaction mechanisms and to characterize the surface basic properties. The reaction proceeds at room temperature or below over most of heterogeneous basic catalysts. Over MgO, for example, the reaction occurs even at 223 K if the catalyst is properly activated. The reaction mechanisms for 1-butene isomerization are shown in **Scheme 3-1**[4]. The reaction starts by abstraction of allylic H by basic sites to form cis or trans forms of the allyl anion. In the form of the allyl anion, the cis form is more stable than the trans one. Therefore, *cis-2*-butene is predominantly formed at the initial stage of the reaction. A high cis to trans ratio observed for the base-catalyzed isomerization is in contrast to the value close to unity for acid-catalyzed isomerization. The cis to trans ratio in 2-butenes produced could be used to judge whether the reaction is a base-catalyzed or acid-catalyzed one.
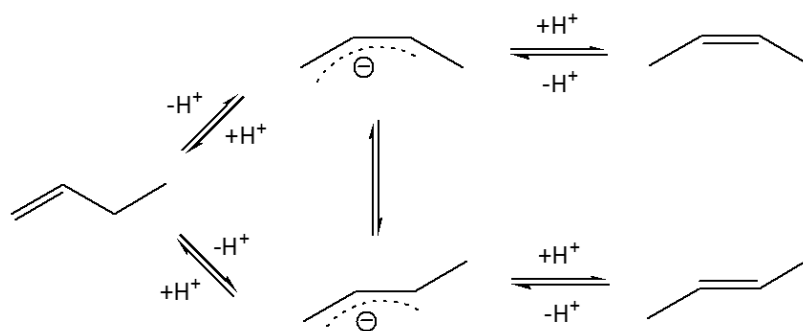
Scheme 3-1. *Reaction pathway for the 1-butene isomerization to cis-trans-2-butene mixture.*

The fundamental studies of 1-butene double bond isomerization over heterogeneous basic catalysts were extended to the double bond migration of olefins having more complex structures such as pinene, carene, protoilludene, illudadiene[5,6,7]. These olefins contain three-membered and four-membered rings. If acidic catalysts were used, the ring-opening reactions would easily occur, and the selectivities for double bond migration should markedly decrease. A characteristic feature of heterogeneous basic catalysts is a lack of C-C bond cleavage ability. Thus, the double bond migration selectively occurs without C-C bond cleavages over heterogeneous basic catalysts. This particular behavior showed by the basic catalysts represent an advantage in the case of thermal unstable olefins that can indeed isomerized at low temperature by means of heterogeneous basic catalysts preventing the degradation phenomena. For instance, because of this advantage, the

heterogeneous basic catalyst, $Na/NaOH/Al_2O_3$, is used for an industrial process for the selective double bond migration of 5-vinylbicyclo[2.2.l]heptane[8].

Finally, the heterogeneous basic catalysts show to have another advantage in double bonds migration process compared to the acid systems. Indeed, in the isomerization of heteroatoms-containing olefins, such as nitrogen-containing, heterogeneous basic systems are much more efficient than the acidic ones. That feature of the basic systems is connected to the low interaction established between the basic active site and the heteroatoms, interaction that are strongly in the case of the acid catalysts and that bring to the catalysts inactivity[9].

3.3.2. Dehydration and dehydrogenation

In general, alcohols undergo dehydration to olefins and ethers over acidic catalysts, and dehydrogenation to aldehydes or ketones over basic catalysts. In some cases, however, heterogeneous basic catalysts promote dehydration of alcohols in which the mechanisms and product distribution differ from those for acid-catalyzed dehydration. The characteristic features of base-catalyzed dehydration are observed for 2-butanol dehydration. The products consist mainly of 1-butene over the rare earth oxides[10], ThO_2[11], and ZrO_2[12]. This is in contrast to the preferential formation of 2-butenes over acidic catalysts. The initial step in the base-catalyzed dehydration is the abstraction of an H^+ at C-1 and 2-butanol to form anion. Dehydration of 1-cyclohexylethanol to vinylcyclohexane has been industrialized by use of ZrO_2 as a catalyst. In the dehydration of 2-alcohols to the corresponding 1-olefins over ZrO_2, the selectivity for 1-olefins depends on the amount of Si contained in ZrO_2 as an impurity. Indeed, silicon contamination in ZrO_2 generate acidic sites. By treatment of ZrO with NaOH to eliminate the acidic sites, the byproducts of 2-olefins are markedly reduced and the selectivity for 1-olefins is increased.

3.3.3. Hydrogenation

The use of the heterogeneous basic catalysts to catalyze hydrogenation reaction starts from the observation that MgO pretreated at 1273 K exhibits olefin hydrogenation activities[13]. The hydrogenation occurring on heterogeneous basic catalysts present fundamental differences with the classic hydrogenation performed with supported metals catalysts, supported transition metals or transition metals oxides. The main features of the base-catalyzed hydrogenation process are reported as follows:

1. A deep difference between the hydrogenation rate of olefins and conjugated-dienes has been observed. The latter undergo into hydrogenation with a much higher rate compared to the olefins; furthermore, the main reduction product for the dienes hydrogenation consist in the olefin;

2. The hydrogenation of conjugated dienes, such as 1,3-butadiene, takes mainly place as 1,4-hydrogen addition over the heterogeneous basic systems instead of the most common 1,2-hydrogen addition that occur over the classic hydrogenation catalysts. The main consequence is the preferable formation of 2-butenes over the basic systems while, with the conventional systems 1-butenes are the predominant products;

3. There is retention of the molecular identity of the H atoms during the reaction. This means that either two the hydrogen atoms added to the olefin or diene molecule are provided from the same molecule of hydrogen that dissociates over the surface of the catalyst.

Direct hydrogenation (or reduction) of aromatic carboxylic acids to corresponding aldehydes has been industrialized by use of ZrO_2. Although the reaction mechanism is not clear at present, the hydrogenation and dehydration abilities, which are associated with the basic properties of ZrO_2, seem to be important for promoting the reaction. The catalytic properties are improved by modification with the metal ions such as Cr^{3+} and Mn^{4+} ions. Crystallization of ZrO_2 is suppressed and coke formation is avoided by addition of the metal ions[14].

3.3.4. Dehydrocyclodimerization of conjugated dienes

Conjugated dienes such as 1,3-butadiene and 2-methyl-1,3-butadiene (isoprene) react over ZrO_2 and MgO to yield aromatics at 643 K[15,16]. Heterogeneous basic catalysts other than ZrO_2 and MgO scarcely exhibit appreciable activities. For the formation of aromatics from dienes, two kinds of mechanisms are possible. One involves the Diels-Alder reaction followed by double bond migration and dehydrogenation. The other involves anionic intermediates. Over MgO 1,3-butadiene mainly produces *o-* and p-xylenes, which will not be formed via the Diels- Alder reaction. On the other hand, over ZrO_2, the main product from1,3-butadiene is ethylbenzene which will be formed via the Diels-Alder reaction. For instance, two mechanisms for dehydrocyclodimerization are shown in

Scheme 3-2: the former one, involving the Diels-Alder reaction, takes place over ZrO_2 while the anionic one takes place over MgO.
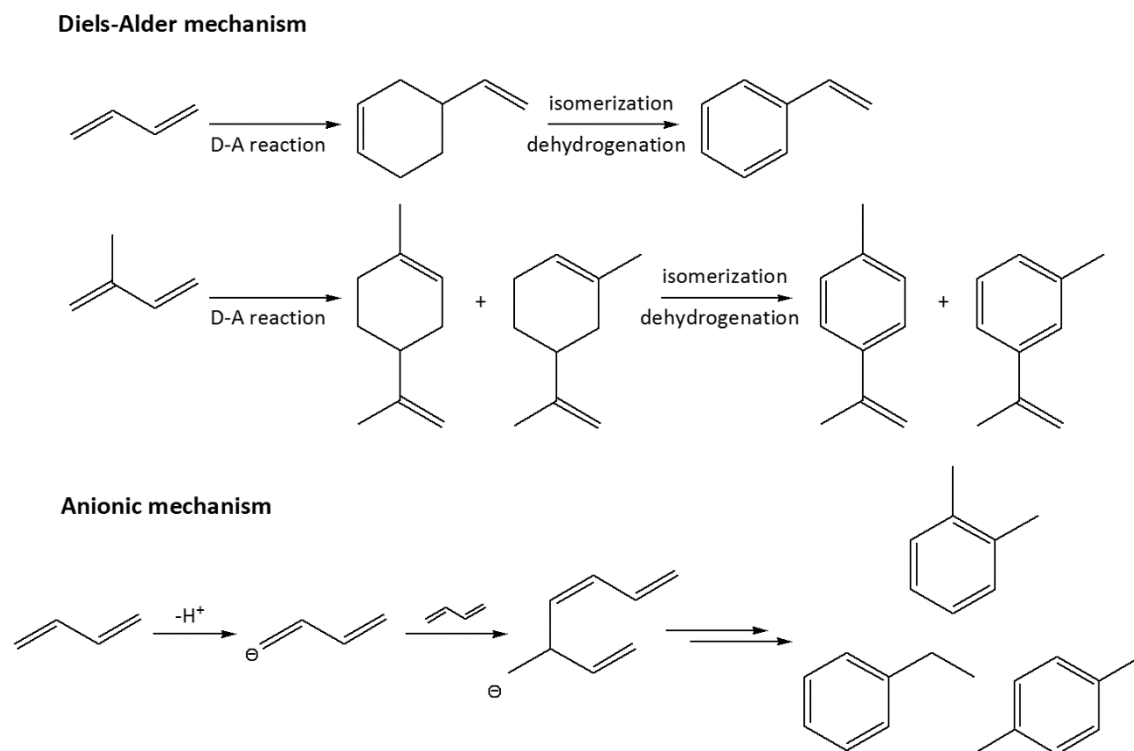
Scheme 3-2. Mechanisms for dehydrocyclodimerization of conjugated dienes.

3.3.5. Alkylation of aromatics compounds

In general, alkylation of aromatics occurs at a ring position over an acidic catalyst, while side chain alkylation takes place over a basic catalyst. Toluene undergoes side chain alkylation with methanol to produce ethylbenzene and styrene over Cs^+ ion-exchanged-X-zeolite.The first step in this reaction is dehydrogenation of methanol to formaldehyde, which undergoes aldol type reaction with toluene to form styrene. Ethylbenzene is formed by hydrogenation of styrene. The basic sites in the zeolite catalyst participate in both the dehydrogenation of methanol and the aldol type reaction[17].

As mentioned in the previous chapter another reaction with several industrial application is the methylation of phenol that indeed could be classified as an alkylation of aromatic compound.The methylation of phenol and phenol derivatives has a high industrial relevance. 2,6-Xylenol is, for example, the monomer for the production of poly-(2,6-dimethyl)phenylene oxide resin, 2-methylphenol (o-cresol) is the monomer for the synthesis of epoxycresol paints, 2,5-dimethylphenol is the intermediate for the synthesis

of dyes, antiseptics, and antioxidants, and 2,3,6-trimethylphenol is the starting compound for the synthesis of vitamin E. The products of ortho-methylation of phenol or anisole and of diphenols, such as guaiacol, are intermediates in the production of skin-protecting agents and food additives.

The ring methylation of phenol to o-cresol is industrially carried out with methanol as alkylating agent over basic catalysts. Typical catalysts are (supported) alkali and alkaline-earth metal oxides, (mixed) transition metal oxides, and combination of both. These catalysts show very high regioselectivity in the methylation of the aromatic ring as well as high chemo-selectivity with only minor amounts reacting via oxofunctionalization.

In this field Cavani et al. have deeply studied the application of MgO as heterogeneous basic catalyst for the gas-phase methylation of phenol. As first pristine MgO is used for the determination of the overall reaction network through the performing of catalytic tests in different conditions of temperature, contact time and also varying the feed substrates; furthermore, IR spectroscopy and DFT calculation strategies have been applied to elucidate the real pathway[18] ().
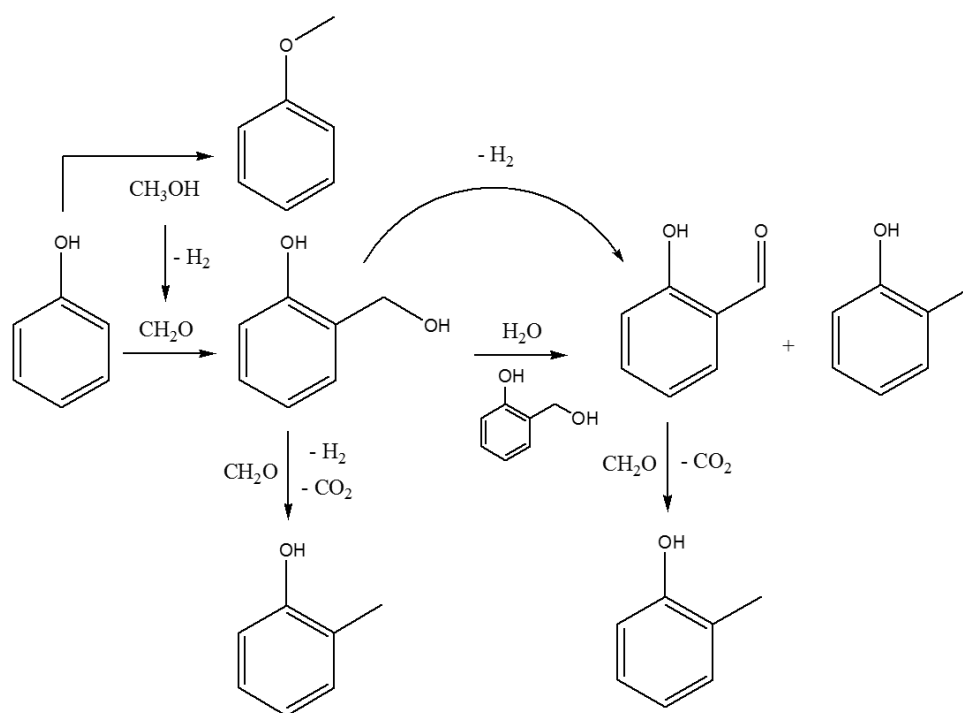
Scheme 3-3. *Overall reaction network for the gas-phase methylation of phenol over MgO catalyst. Adapted from [18]*

62

Under conditions at which the extent of methanol dehydrogenation is low, i.e., low temperature, the main primary products of reaction are anisole and o-cresol. Under conditions more favorable for methanol dehydrogenation, anisole is no longer formed, and o-cresol becomes the only reaction product. 2,6-Xylenol forms in significant concentrations above 350°C and for high phenol conversion. The adsorption of phenol on MgO generates a phenolate species, and the energetically preferred mode of adsorption is on the corner site of MgO, with an almost orthogonal orientation of the aromatic ring with respect to the catalyst surface.

The reaction between adsorbed phenolate and formaldehyde generates salicylic alcohol via hydroxymethylation, which is rapidly transformed to salicylic aldehyde. At low temperature and for very low conversions and short residence time, salicylic aldehyde is one of the primary reaction products. However, the aldehyde is very rapidly transformed into o-cresol.

In a second moment the products distribution for the methylation process of phenol has been studied with mixed Mg/M/O oxides (M = Al^{3+}, Fe^{3+}, Cr^{3+}). Introducing and host heteroatom in the structure of MgO both the acid-base and redox properties are affected and it has been demonstrated that this has a direct consequence on the reactivity in terms of products distribution. For instance, the change of these properties directly affect the methanol activation mechanism over the catalyst surface, changing the ability of the catalyst to de-hydrogenate the latter into formaldehyde, identified as the real alkylating agent. Mg/Cr/O and Mg/Fe/O show a typical basic/dehydrogenating catalytic reactivity, with high chemo- and regio-selectivity and the favor formation of o-cresol as main product. On the other hand, Mg/Al/O exhibits a catalytic behaviour quite similar to that shown by conventional Brønsted-type acid catalysts (e.g., zeolites) bringing to the formation of the O-methylation product, indeed, anisole is detected as main product[19].

3.4. MgO and CaO: heterogeneous basic catalysts for biomass upgrading

In the last years the heterogeneous basic catalysts have found several application in the field of biomass upgrade and renewable feedstock valorization. As just described in the section "2.2.2" heterogeneous systems with basic properties has been reported as high active catalysts for the catalytic transfer hydrogenation reaction for the upgrade of oxygenated building block produced from lignocellulose biomass treating.

Another appealing process in which the heterogeneous basic catalysts have recently found always more application is the production of the FAME, fatty-acid-methyl-esters, considered one of the most valid alternative to the market diesel produced from the oil. Indeed, the non-food vegetable oil is considered one of the biomass resources and is used as a feedstock of an alternative to fossil diesel fuel. The alternative fuel, named as ''Biodiesel'', consists of fatty acid methyl esters produced by the transesterification of vegetable oil with methanol[20]. In addition to the renewable nature peculiar to the biomass resources, biodiesel has another advantage of the good fuel properties: high flash point, good lubricity and so on[21,22]. Moreover, it was reported that emissions of both carbon monoxide and particulate was reduced by fueling the engine with biodiesel[23,24,25].

In 2003, European Community has decided to replace at least 5.75% of the yearly-consumed fossil fuels with biofuels, by the year 2010. This decision accelerated the use of biodiesel and its production has been constantly growing. The total of biodiesel yearly produced in the world was 7.75 million metric tons in 2008[26]. For the existent biodiesel production process, vegetable oil is transesterified with the help of homogeneous base catalysis of alkali hydroxide dissolved in methanol. The base-catalyzed transesterification is faster than the acid-catalyzed one for which sulfonic acid or p-toluenesulfonic acid is employed[27]. Furthermore, the reactants are accessible to the catalytic site in the homogeneous form. Thus, the existent biodiesel production process is characterized by the very fast transesterification. For instance, Freedman et al. reported that the yield of FAME produced from the transesterification of sunflower oil in the presence of 1% sodium hydroxide dissolved into methanol at the temperature of 333 K is above 90% in 10 minutes[28]. 97% conversion of palm oil into its methyl esters is detected by the base-catalyzed transesterification performed at 306 K for 1 h on a continuous-flow reaction

system[29]. It should be noted that methanol is the alcohol appropriate to biodiesel production from an economical and available point of view[30].

However, for the existent process the main drawbacks consist in the massive amount of the waste water, which is due to the purification to wash the homogeneous catalyst off the crude biodiesel with water. And besides, emulsification of biodiesel occurs during the purifying operation, which causes not only obstruction of the process operation but also loss of biodiesel.
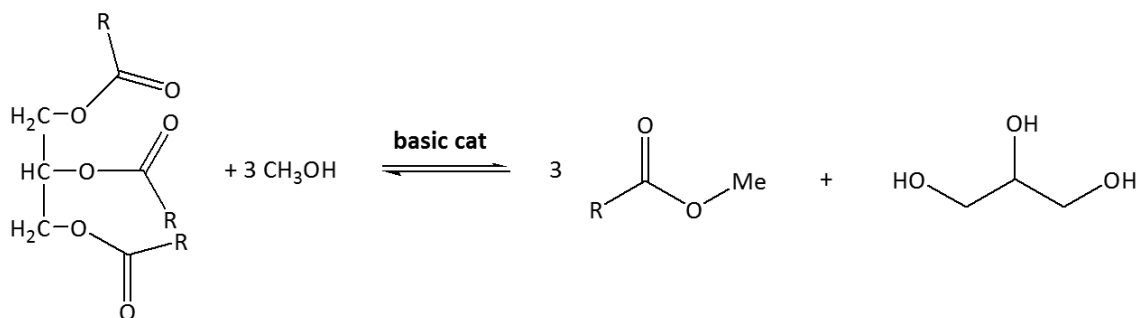
Scheme 3-4. *General reaction pathway for the production of FAME from triglycerides.*

In this view, the use of heterogeneous basic catalysts could be a valid alternative for the FAME production process leading also to a decrease of the biodiesel production cost due to the easier recover and reuse of the catalyst. Oxides of magnesium and calcium (MgO and CaO) have been tried as solid base catalyst owing to their easy availability, low cost, and non-corrosive nature[31].

At the beginning the results obtained with MgO and CaO have been considered not-comparable with those obtained in the same reaction conditions with the homogeneous systems. For instance, when both homogeneous and heterogeneous catalysts are tried for the transesterification of sunflower oil, NaOH (homogeneous catalyst) performed much better than MgO (heterogeneous catalyst) in terms of conversion. 100% conversion is reported to have been achieved in 8 h reaction time and 60°C with NaOH, while only 11% with MgO[31]. The main reason of the low activity showed by the heterogeneous system has been attributed to the low surface area of MgO resulting of an high temperature pretreatment.

More recently MgO has shown to possess catalytic activity for synthesis of biodiesel. A pioneering work on catalytic activity of MgO has been reported by Di Serio et al.[32] where 92% yield has been achieved using 12:1 methanol to oil molar ratio, 5.0 wt.% of the catalyst in 1 h. Dossin et al. reported that MgO is efficient in batch reactor at ambient temperature in the transesterification reaction with production of 500 tonne of biodiesel.

As heating is not required during batch process, and so the overall cost of production of biodiesel is reduced[33].

Furthermore, MgO supported over different mesoporous silicas (MCM-41, SBA-15, and KIT-6), ahows to be quite effective resulting in high conversion. For instance, MgO loaded on SBA-15 shows an interesting 96% of conversion in batch system at 220°C after 5h[34].

Finally, the possibility to support alkaline metal hydroxides or carbonates over MgO, has been considered as a strategy for the production of an active basic heterogeneous catalysts for the synthesis of FAME. KOH loaded on MgO by wet impregnation method shows high conversion (99.36%) and yield (95.05%) of biodiesel from canola oil[35].

Like magnesium oxide, calcium oxide (CaO) has gained attention as heterogeneous basic catalyst for the development of biodiesel production process thanks to its low cost and easy preparation. However this simple basic oxide shows two main drawbacks that could negatively affect its industrial employment. Indeed, it is very sensitive to structural modification, and so to catalytic performance variation, depending on the calcination temperature. Furthermore, it shows several leaching problem due to its solubility in methanol, the most common alcohol used for the transesterification process[31].

Despite these problems. Huaping et al.[36] used CaO as heterogeneous catalyst for biodiesel synthesis from Jatropha curcas oil. They demonstrate that an increase of the basic strength of the pristine CaO could be induced with a pre-calcination treatment with ammonium carbonate solution. This results, after a calcination at 900°C, in 93% of conversion of the oil to the biodiesel at the optimized conditions (70°C temperature, 2.5 h reaction time, 1.5% catalyst amount, and 9:1 methanol to oil molar ratio). They also reported that an high calcination temperature is necessary for the decomposition of the calcium carbonate and for the formation of superficial crystalline structural defects that are crucial for the formation of calcium methyloxide which is a surface intermediate in the transesterification reaction. The catalyst is further reused three times with 92% conversion of jatropha oil[37].

Calcium oxide has also been tried in combination with other compounds to enhance its catalytic activity. For instance, wet impregnation combined with thermal treatment method is used to adhere aqueous solutions of calcium acetate on porous silica such as SBA-15, MCM-41, and fumed silica, and tried as catalyst for biodiesel development from castor and sunflower oils. CaO is incorporated on porous silica after drying and calcining at 60°C and 600°C, respectively. The siliceous support has been demonstrated to have an

important influence on the activity of the catalyst. Among the catalysts, SBA-15 possessed highest thermal stability at a higher calcination temperature of 800°C and not suffer any structural modifications. CaO (14 wt.%) supported on SBA-15 is found to be most active for reaction and thermally resistant. High calcination temperature (800°C) has been reported to transform the calcite phase ($CaCO_3$) and the calcium hydroxide into calcium oxide. An important finding by incorporation of CaO on silica is prevention of lixiviation of the active phase in methanol. CaO and carbonate particles adhere to the surface of the catalyst[38].

Finally, the alkaline metal doping ($LiNO_3$, $NaNO_3$, and KNO_3) of CaO has been studied in order to evaluate an eventual synergetic effect. A correlation is observed between the base strength and the activity of the catalyst. Calcination of the catalyst results in decrease in the surface area of the catalyst from 10 to 1–2 m^2/g. Higher surface area of the catalyst is not even desired as triglycerides are large molecules and would not be able to diffuse into the pores unless a mesoporous substrate is used. Conversion obtained from not-calcined catalysts ($LiNO_3$/CaO, KNO_3/CaO, and $NaNO_3$/CaO) showes to be 85%, 90% and 98%, respectively. With the calcined samples, the conversion reached 99–100%. Leaching of the catalyst has been observed also for these catalysts, representing one of the major constraint for their application as a heterogeneous catalyst[39].

Despite the main drawback consisting in the leaching of the active phase, economic assessment has also favored CaO as heterogeneous catalyst, which can be separated either by hot water purification process or vacuum distillation process when compared with the similar process adopted with homogeneous catalyst (KOH). It is observed that the manufacturing cost of biodiesel from waste cooking oil using CaO as catalyst manufactured in batch process with a plant capacity of 7260 tonne/year with hot water purification process and vacuum distillation process was 584 and 622 \$/tonne of biodiesel. Using KOH as catalyst, the manufacturing cost of biodiesel with same plant capacity utilizing hot water purification process and vacuum distillation process is 598 and 641 \$/tonne of biodiesel[40].

[1] H. Pines, J. A. Veseley, V. N. Ipatieff, *J. Am. Chem. Soc.,* 1955, **77**, 6314

[2] H. Hattori, *Chemical Reviews,* 1995, **95**, 3

[3] S. Coluccia, Proceedines of the 7th International Congress on' Catalysis Tokyo, Japan: 1980; p 1160

[4] H. Hattori, *Stud. Surf. Sci. Catal.,* 1993, **78**, 35

[5] H. Hattori, R. Tanabe, K. Hayano, H. Shirahama, T. Matsumoto, *Chem. Lett.,* 1979, **133**

[6] K. Shimazu, K. Tanabe, H. Hattori, *J. Catal.,* 1977, *45*, 302

[7] G. Suzukamo, M. Fukao, T. Hibi, K. Chikaishi, Acid-Base Catalysis, Kodansha (Tokyo)-VCH (Basel, Cambridge, New York, Weinheim), 1989; p 405

[8] G. Suzukamo, M. Fukao, M. Minobe, *Chem. Lett.,* 1987, **585**

[9] A. Hattori, K. Tanabe, *J. Catal.,* 1980, **65**, 246

[10] A. J. Lundeen, R. J. van Hoozen, Org. Chem., 1967, 32, 3386

[11] Tomatsu. T.: Yoneda. H.: Ohtsuka. H. Yukagaku. 1968, **17**, 23

[12] T. Yamaguchi, H. Sasaki, K. Tanabe, *Chem. Lett.,* 1976, **677**

[13] H. Hattori, Y. Tanaka, K. Tanabe, *J. Am. Chem. Soc.,* 1976, **98**, 4652

[14] T. Yokoyama, T. Setoyama, N. Fujita, M. Nakajima, T. Maki, K. Fukii, *Appl. Catal. A,* 1992, **88**, 149

[15] H. Suzuka, H. Hattori, *Appl. Catal.,* 1989, **48**, L7

[16] H. Suzuka, H. Hattori, *J. Mol. Catal.,* 1990, **63**, 371

[17] P. E. Hathaway, M. E. Davis, *J. Catal.,* 1989, **119**, 497

[18] F. Cavani, L. Maselli, S. Passeri, J. A. Lercher, *Journal of Catalysis,* 2010, **269**, 340

[19] V. Crocellà, G. Cerrato, G. Magnacca, C. Morterra, F. Cavani, S. Cocchi, S. Passeri, D. Scagliarini, C. Flego, C. Perego, *Journal of Catalysis,* 2010, **270**, 125

[20] F. Ma, H. A. Hanna, *Bioresour. Technol.,* 1999, **70**, 1

[21] M. P. Dorado, E. Ballesteros, J. M. Arnal, J. Gomez, F. J. Lopez, *Fuel,* 2003,**82**, 1311

[22] C. Y. Lin, H. A. Lin, L. B. Hung, *Fuel,* 2006, **86**, 1743

[23] S. K. Karmee, A. Chadha, *Bioresour. Technol.,* 2005, **96**, 1425

[24] J. P. Szybist, J. Song, M. Alam, A. L. Boehman, *Fuel Process Technol.,* 2007, **88**, 679

[25] S. G. Micheal, R. L. McCormick, *Prog. Energy Combust. Sci.,* 1998, **24**, 125

[26] G. Knothe, *Top Catal.,* 2010, **53**, 714

[27] D. Nimcevic, R. Puntigam, M. Worgetter, J. R. Gapes, *J. Am. Oil Chem. Soc.,* 2000, **77**, 275

[28] B. Freedman, E. H. Pryde, T. L. Mounts, *J. Am. Oil Chem. Soc.,* 1984, **61**, 1638

[29] V. Mao, S. K. Konor, D. G. B. Boocoke, *J. Am. Oil Chem. Soc.,* 2004, **81**, 803

[30] M. Kouzu, J. S. Hidaka, *Fuel,* 2012, **93**, 1

[31] Y.C. Sharma et al., *Fuel,* 2011, **90**, 1309

[32] M. Di Serio, M. Ledda, M. Cozzolino, G. Minutillo, R. Tesser, E. Santacesaria, *Ind. Eng. Chem. Res.,* 2006, **45**, 3009

[33] T. F. Dossin, M. F. Reyniers, R. J. Berger, G. B. Marin, *Appl. Catal. B: Environ.,* 2006, **67**, 136

[34] E. Li, V. Rudolph, *Energy Fuels,* 2008, **22**, 145

[35] O. Ilgen, A. N. Akin, *Energy Fuels,* 2009, **23**, 1786

[36] Z. Huaping, W. Zongbin, C. Yuanxiong, Z. Ping, D. Shijie, L. Xiaohua, *Chin. J. Catal.,* 2006, **27**, 391

[37] M. L. Granados, M. D. Z. Poves, D. M. Alonso, R. Mariscal, F. C. Galisteo, R. M. Tost, *Appl. Catal. B: Environ.,* 2007, **73**, 317

[38] M. C. G. Albuquerque, I. J. Urbistondo, J. S. González, J. M. M. Roble, R. M. Tost, E. R. Castellón, *Appl. Catal. A: Gen.,* 2008, **334**, 35

[39] C. S. MacLeod, A. P. Harvey, A. F. Lee, K. Wilson, *Chem. Eng. J.,* 2008, **135**, 63

[40] T. Sakai, A. Kawashima, T. Koshikawa, *Bioresour. Technol.,* 2009, **100**, 3268

CHAPTER 4.   Experimental section

4.1. Introduction

The aim of the present PhD thesis has been focused on the synthesis, characterization and evaluation of the catalytic activity of different heterogeneous catalysts, showing different properties, in the gas-phase catalytic transfer hydrogenation of furfural (FU) into the products deriving from the selective reduction of the carbonyl group furfuryl alcohol (FAL) and 2-methylfuran (MF). The catalysts used for this purpose can be divided in two main groups: $FeVO_4$ based catalyst and basic oxides-based catalysts. In this section the synthetic procedure for the preparation of the different heterogeneous systems, the characterization techniques used for the determination of the properties of the solids as well as the characteristics of the lab-scale plant used for the catalytic tests and the analysis for the determination of conversion and yield will be described.

4.2. Raw materials and reagents

Compound	Physical aspect	M.W. (g/mol)	Purity	Supplier
NH_4VO_3	Light yellow powder	117	99	Alfa Aesar
$Fe(NO_3)_3$ nona-hydrate	Light brown solid	404	98	Sigma-Aldrich
$Mg(NO_3)_2$ hexahydrate	White solid	256	98	Alfa Aesar
$Ca(NO_3)_2$ tetra-hydrate	White solid	236	99	Sigma-Aldrich
Li_2CO_3	White solid	74	99	Alfa Aesar
Na_2CO_3 deca-hydrate	White solid	286	99	Sigma-Aldrich
Oxalic acid	White powder	90	99	Sigma-Aldrich
NaOH	White pellets	40	98	Sigma-Aldrich
HNO_3	Colorless liquid	63	65% solution in water	Fluka
NH_3	Colorless liquid	17	33% solution in water	VWR Chemicals
2-furaldehyde (FU)	Light yellow liquid	96	99	Sigma-Aldrich
Furfuryl alcohol (FAL)	Dark orange liquid	98	99	Sigma-Aldrich
2-methylfuran (MFU)	Yellow liquid	82	99	Sigma-Aldrich
2,5-dimethylfuran (DMF)	Dark yellow liquid	96	99	Sigma-Aldrich
2-furyl methyl ketone	Brown solid	110	99	Sigma-Aldrich
(±)-1-(2-Furyl)ethanol	Colorless liquid	112	99	Sigma-Aldrich
Trifluoroacetaldehyde methyl hemiacetal	Colorless liquid	130	99	Alfa Aesar
Methanol	Colorless liquid	32	100	VWR Chemicals
Cyclopentanone (CP)	Colorless liquid	84	99	Sigma-Aldrich
Acetonitrile	Colorless liquid	41	99	VWR Chemicals
Acetone	Colorless liquid	58	99	VWR Chemicals
2-propanol	Colorless liquid	60	99	VWR Chemicals
CH_2O	Colorless liquid	30	37% in water solution with 10÷12% of methanol	Sigma-Aldrich

Table 4-1. *List of the main raw materials and reagents used.*

4.3. Catalysts preparation

The preparation of the catalysts could be divided into two main procedure depending on the type of catalyst:

- FeVO$_4$ bulk catalyst;
- Heterogeneous basic-based catalysts.

4.3.1. Preparation of bulk FeVO$_4$

The FeVO$_4$ catalyst has been prepared by co-precipitation from an aqueous solution containing the corresponding metal precursors, to obtain an atomic ratio Fe^{3+}/V^{5+} equal to 1. For the synthesis of 20 g FeVO$_4$, a solution containing 47.32 g of Fe(NO$_3$)$_3$*9H$_2$O (Sigma Aldrich, 99% purity) in 105 ml of distilled water is usually prepared. A second solution containing 13.70 g NH$_4$VO$_3$ (Sigma Aldrich, 99% purity) in 105 ml of distilled water is prepared and added dropwise under vigorous stirring to the Fe solution. The pH of the resulting solution is then adjusted to the value of 6.8 with an ammonia solution (14%) to precipitate the FeVO$_4$ precursor. After 1 h of aging under stirring, the resulting precipitate is filtered and washed with an excess of water and dried overnight at 110°C. Finally, dried solid is ground and calcined at 650°C in static air for 3 h in order to form the crystalline structure of the mixed iron-vanadium catalyst.

4.3.2. Preparation of heterogeneous basic-based catalysts

The list of the catalysts prepared and grouped in this type of heterogeneous catalyst include numerous systems such as: MgO, CaO, mixed Mg/Fe/O and Ta$_2$O$_5$ supported on MgO.

Pristine MgO and the mixed Mg/Fe/O have been prepared by thermal treatment of hydrotalcite-like precursors. The latter has been synthesized by precipitation, at controlled pH, temperature and stirring rate, from an aqueous solution containing the corresponding metal nitrates Mg(NO$_3$)$_2$·6H$_2$O and Fe(NO$_3$)$_3$·9H$_2$O, Sigma Aldrich) into a solution of Na$_2$CO$_3$. The use of the carbonate is necessary in order to balance the excess of positive charge in the hydrotalcite-sheet deriving from the replacement of Mg^{2+} cations with Fe^{3+} cations. Lastly, the filtered samples are dried at 120 °C overnight and then calcined in air at 500 °C for 6 h. The precursors have been synthesized using a Mg^{2+}/Fe^{3+} molar ratio equal to 2, which is within the range of values at which the corresponding hydrotalcite-like material is formed.

For the preparation of the Lithium-doped MgO catalysts the wet impregnation method has been used. First the high surface MgO is synthesized following the procedure described above. In a second moment a water solution of Li_2CO_3 has been prepared, the amount of the lithium precursor dissolved has been calculated in order to prepare different catalysts with a weight percentage of Li in the range between 1 and 10. Once dissolved the metal precursor the high surface MgO, or the commercial one, is introduced into the solution and stirred for two hours. Then the solvent is eliminated by-means of a rotavapor, the resulting solid has been dried overnight at 120°C and finally calcined in static air at 500°C.

4.4. Catalyst characterization

BET specific surface area. The BET surface area of catalysts has been determined by means of N_2 absorption–desorption at liquid N_2 temperature, using a Sorpty 1750 Fison instrument. 0.3 g of the sample is used for the measurement, and the sample is outgassed at 150°C before N_2 absorption.

X-ray diffraction analyses (XRD). XRD powder patterns of the catalysts have been recorded with Ni-filtered Cu Kα radiation ($\lambda = 1.54178$ Å) on a Philips X'Pert vertical diffractometer equipped with a pulse height analyzer and a secondary curved graphite-crystal monochromator. The acquisition of the diffractograms have been performed in the 2θ degree window between 5÷80° with 0.1° steps each 2 seconds.

Thermogravimetric/differential thermal analyses (TGA/ DTA). TGA/DTA analysis of fresh and spent catalysts have been carried out using a SDT Q 600 instrument, to identify the amount of heavy compounds absorbed on the catalyst surface. 5-10 mg of sample are typically used, from room temperature up to 900°C, with a heating rate of 10°C min^{-1} in air or in nitrogen depending on the catalyst.

Raman spectroscopy. Laser Raman spectra have been recorded at room temperature using a Renishaw 1000 spectrometer equipped with a Leica DLML microscope (5x, 20x, 50x lenses were used) and a CCD detector. Samples are excited with a diode laser beam (782 nm or 514 nm). Raman spectra have been recorded in the spectral window 500-2000 cm^{-1}.

Atomic absorption. The elementary analysis has been carried out with a VARIAN SpectrAA 100 (equipped with a graphite tube atomizer); the solutions resulting from the mineralization process performed with hot aqua regia on both fresh and spent catalysts have been analysed to determine the Fe/V ratio in the mixed iron-vanadium-based catalysts.

In-situ DRIFTS (Diffuse Reflectance Infrared Fourier Transform Spectroscopy) experiment with mass spectrometer. The IR apparatus used is a Bruker Vertex 70 with a Pike DiffusIR cell attachment. Spectra have been recorded using a MCT detector after 128 scans and 2 cm^{-1} resolution. The mass spectrometer used is an EcoSys-P from European Spectrometry Systems. In most cases the catalyst is loaded into the sample holder and the cell is closed and inserted into the DRIFT apparatus. A pretreatment up to 320-450°C in helium flow is then performed to remove any molecules adsorbed on the material, mainly carbon dioxide and water. The sample is then cooled down to 85°C and the spectra of the pure catalyst is recorded and used as a background for the following measurement. In particular the DRIFT characterization has been applied to determine the interaction between methanol and the $FeVO_4$ catalyst. A first set of experiments have been performed at 85°C by feeding methanol in a helium flow and vaporising it using heating strips. Then methanol is stopped and only helium is flowed inside the IR cell. This way, the low-temperature adsorption and desorption process has been monitored. The second set of experiments is performed with a low-temperature adsorption and a programmed temperature desorption during which the following temperatures have been monitored: 125°C, 175°C, 225°C, 275°C, and 320°C.

Thermogravimetric-Mass spectrometry desorption of n-propylamine (NPA TGA-MS). NPA TGA-MS analysis have been carried out on the fresh catalysts with xxx instrument in order to quantify the total amount of acid sites. The irreversible adsorption of light amines, such as n-propylamine, represents an alternative method to the most common NH_3-TPD for the determination of the total amount of the acid sites. Nevertheless, depending on the desorption mechanism of NPA, information related to the strength or to the Lewis/Bronsted nature of the sites could be obtained. Generally, 25-30 mg of powder were saturated with liquid n-propylamine for 30 minutes; after that the sample was treated overnight in a vacuum oven at 30°C in order to remove the excess of physisorbed NPA. Finally, the sample was heated from 40 to 800°C (10°C/min) in a

nitrogen flow (40 ml/min). The exiting stream from the TGA was then transferred to the MS through an heated line.

Acrylic acid irreversible adsorption (A.A. ADS). The A.A. ADS, as well as for the irreversible adsorption of NPA, represents an alternative method to the most common CO_2-TPD for the determination of the total basic sites of a catalyst. In particular this method have been found suitable for the hydrotalcite-type-precursor derived-mixed oxides for which the formation of carbonate species as a consequence of the treatment in CO_2 stream is well known. Generally 20-40 mg of powder was added to 20 ml of ca. 20 mM acrylic acid solution in cyclohexane. The adsorption was performed for 4 h in closed vessels, after that the material was filtered off using syringe filters (Chromafil, PTFE, pore size 0,2 µm). Concentration of acrylic acid in the filtrate was determined by-means of HPLC analysis using an Agilent Technologies 1260 Infinity instrument equipped with a DAD UV-Vis detector and Aminex HPX-87H 300 mm x 7.8 mm column, using a 0,005 M H_2SO_4 solution in water as mobile phase.

Temperature programmed Desorption-Reduction-Oxidation (TPDRO). The reducibility behavior, as well as the total acidity or basicity of the catalysts were determined using a TPD/TPR/TPO Micromeritics instrument equipped with a MKS MS Spectrometer. Generally 15-30 mg of catalyst were pretreated up to 500°C under He flow. After cooling down to 50°C, a mixture of 5% H_2 or 5% O_2 in He was used for the TPR-TPO experiments; after a stabilization time of 20 minutes the temperature was increased from 50 to 800°C (10°C/min) and maintained at 800°C for 30 minutes. For the NH_3-TPD and CO_2-TPD experiment the sample was cooled down to 100°C and 40°C respectively and the adsorption of the probe molecule was performed for 1 h flowing a mixture of 10% NH_3 or 5% CO_2 in He. Then, He flow was used for 30 minutes at the adsorption temperature in order to remove the excess of physisorbed molecule; finally the temperature was increased up to 800°C (10°C/min) and maintained at 800°C for 30 minutes.

4.5. Gas-phase catalytic tests

Catalytic tests have been conducted in a continuous-flow fixed-bed micro-reactor (Pyrex, length 38 cm, internal diameter ⅓ inch) (in **Scheme 4-1** it is reported the flow-sheet of the entire plant used to perform the catalytic tests). The catalyst (30-60 mesh particles) is

usually placed into the reactor in a quantity appropriate for changing the contact time from 0.01 to 2.0 s, and then heated to the desired reaction temperature (200-500°C) under N_2 flow (26÷54 ml min^{-1}). The catalytic reaction starts by the vaporization of the reagents, usually methanol and FU, in a 10/1 molar ratio using nitrogen as the carrier gas. FU has been purified via azeotropic distillation prior to being feed into the flowing gas stream in order to avoid the blockage of the feeding stainless-steel pipe due to the deposition of the oligomers formed during the storage. The total volumetric inlet flow rate has been kept constant at 60 ml min^{-1} and the molar concentrations of FU, methanol, and nitrogen are respectively 1, 10, and 89% in the case of the catalytic tests performed with the mixed iron-vanadium oxide while, for the basic-based materials the molar concentration are respectively 5, 50 and 45%. In all cases, results are taken after 1 h reaction time. Analysis of reactants and products have been carried out as follows: the outlet stream are scrubbed for 1 h in cold acetonitrile, which is maintained at -26°C by a F32 Julabo thermostat. The condensed products are then analyzed by means of HPLC, using an Agilent Technologies 1260 Infinity instrument equipped with a DAD UV-Vis detector and an Agilent POROshell 120 C-18 column (see **Figure 4-1** for an example of the acquired chromatogram). Non-condensable gases (CO, CO_2, CH_4 and H_2) have been analyzed on-line with a PerkinElmer Clarus 500 gas chromatograph equipped with a TCD detector and a Carbosphere® 80/100 mesh column. FU Conversion, product selectivity, and C loss have been expressed as follows:

$$Furfural\ Conversion = \frac{\dot{n}_{furfural}^{in} - \dot{n}_{furfural}^{out}}{\dot{n}_{furfural}^{in}}$$

$$Products\ Selectivity = \frac{\dot{n}_{product}^{out}}{\dot{n}_{furfural}^{in} - \dot{n}_{furfural}^{out}}$$

$$C - Loss = 100 - \sum_{i} Product\ Selectivity$$

Preliminary tests have conducted, making it possible to exclude any problems originating from interparticle and intraparticle diffusion limitations. More specifically, some catalytic tests have been conducted by changing the catalyst particle size for the same catalyst weight/inlet flow ratio; no effect on catalyst performance is observed. The catalytic tests performed while keeping the contact time constant but doubling or halving the total

volumetric flow and catalyst volume, compared to the conditions typically used, showed no performance changes.
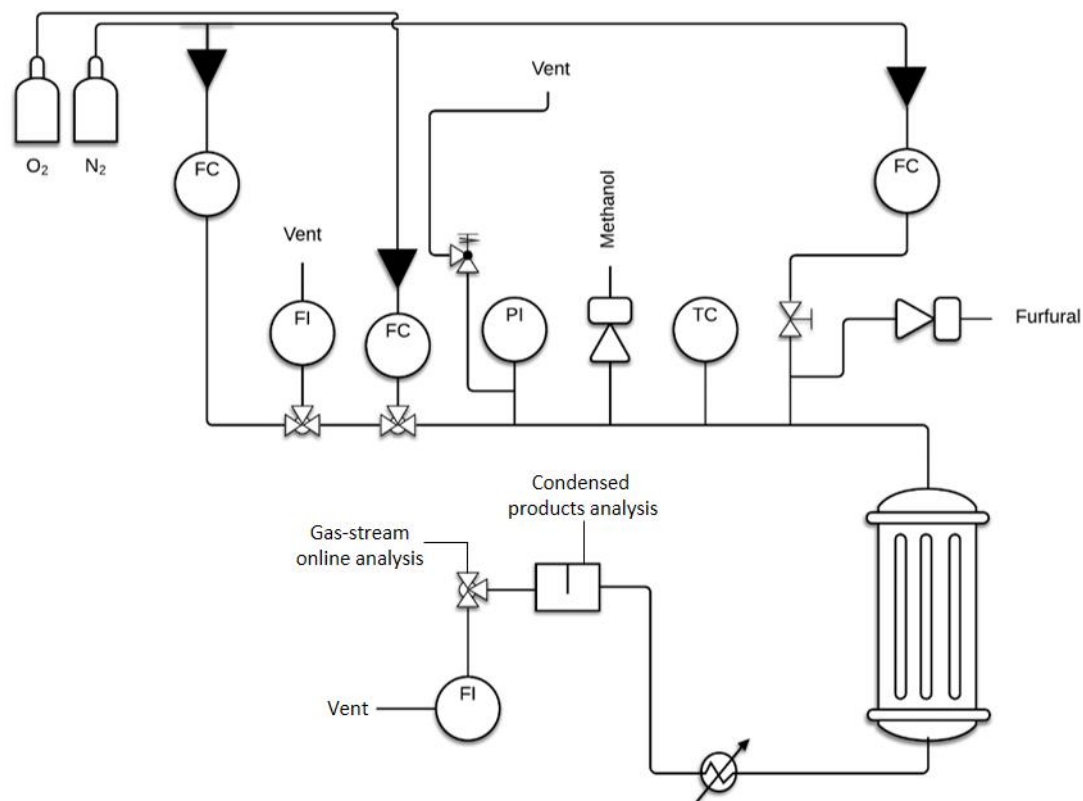
Scheme 4-1. *Gas-phase plant flow sheet.*
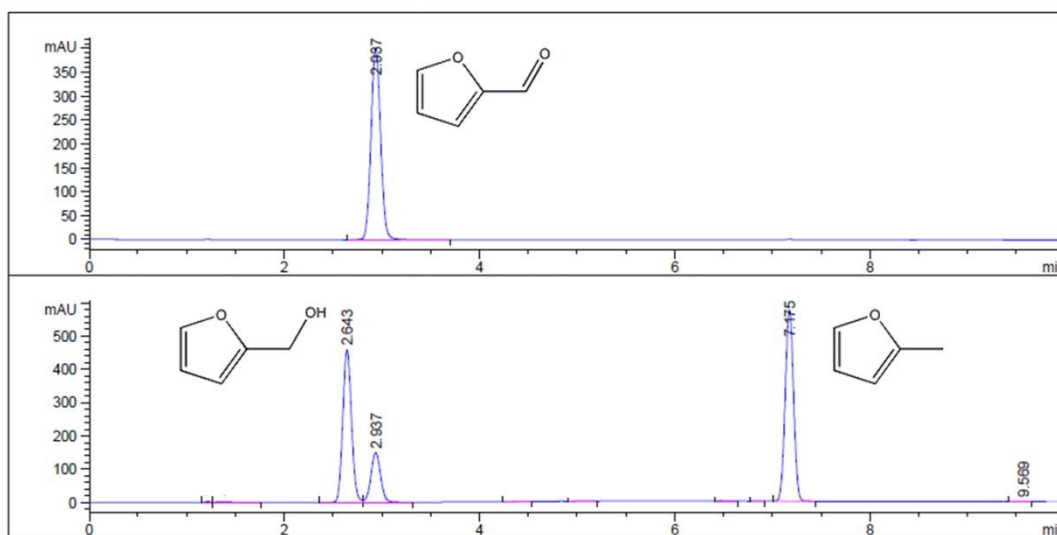
Figure 4-1. *Example of HPLC-chromatogram acquired monitoring two different wavelength (253 and 215 nm).*

CHAPTER 5.   Catalytic transfer hydrogenation over heterogeneous basic-based catalysts

5.1. Introduction

In the present section of the work the results concerning the gas-phase catalytic transfer hydrogenation of furfural (FU) to the corresponding unsaturated alcohol (furfuryl alcohol-FAL) and to the de-oxygenated 2-methylfuran (MF) by-means of methanol as H-transfer reactant and basic oxides-based catalysts have been presented and discussed. Both catalytic performances and details regarding the reaction mechanism for the transformation of FU over different basic-based systems have been considered in order to find a correlation between the catalytic activity and the catalyst properties such as acid-base strength, redox or de-oxygenation properties and de-hydrogenation. The latter properties could be introduced or tuned for a pristine basic catalyst thanks to the introduction of a guest-metal-heteroatoms into the lattice of the basic system (e.g. introduction of Fe^{3+} or Al^{3+} into the structure of MgO through the synthesis of the corresponding hydrotalcite-type precursor). Nevertheless, the basic material could be used as a support for the deposition of a metal oxide having different properties.

As a matter of fact, in the chapter regarding the catalytic transfer hydrogenation (CTH) as a tool for the hydrogenation of the biomass-derived building blocks, it has been highlighted that basic, acid or systems with both properties have been considered the most active and promising for the considered reaction due to the ability to catalyze the formation of the six-membered ring transition state that then evolve into the formation of the hydrogenation products.

In the present PhD project, the investigation of basic-based systems in the CTH reaction for the reduction of biomass-derived building block has been deeply studied both in the liquid-phase and in the gas-phase lab-scale plant layout. In particular the catalytic activity of alkaline-earth metal oxides and mixed or supported transition metal oxides over alkaline-earth metal oxides such as MgO, CaO, mixed Mg/M/O (M = Fe or Al) and $LiCO_3$ supported over MgO have been studied.
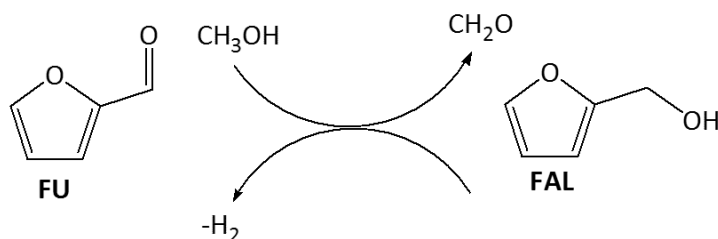
Scheme 5-1. *Selective reduction of FU to FAL by-means of CTH with methanol.*

The first work in this field concerned the liquid-phase selective reduction of FU to FAL using methanol as hydrogen source and high surface MgO as heterogeneous basic catalyst (**Scheme 5-1**). In that work we demonstrated that MgO acted as high active and selective catalyst for the reduction of the carbonyl group of FU. Indeed, in the proper reaction condition, 100% of FU conversion with 100% of FAL yield were obtained[1].

Figure 5-1 shows the effect of the amount of catalyst loaded in the reactor on FU conversion and FAL selectivity. Increasing the amount of MgO progressively increased the conversion of the substrate up to the total conversion obtained loading 1 g of MgO; on the other hand the catalyst showed to be totally selective toward FAL independently from the mass of catalyst.
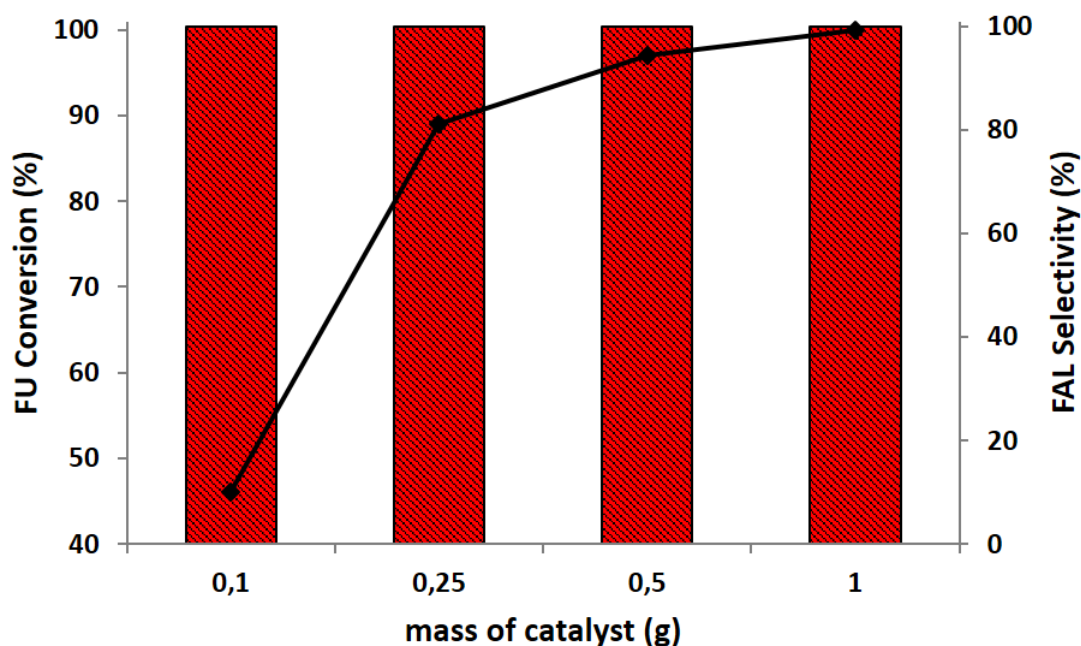
Figure 5-1. *FU conversion and FAL selectivity as a function of the mass of MgO loaded. Reaction conditions: 50 ml of CH₃OH, 1.21 mmol of FU, T = 160°C, t = 3h. Legend: FU conversion (♦), FAL selectivity (■).*

The high surface area MgO (~200 m²/g) showed also to be totally selective toward the formation of FAL as the only reduction product in the catalytic tests performed changing the reaction time. Indeed, at the increase of the latter a progressive increase of both the

substrate conversion and the FAL yield was obtained; furthermore, for all the tested reaction time, the registered FAL yield corresponded always, within the experimental errors, with the values of the conversion (**Figure 5-2**). Moreover, a comparison between the synthesized high surface area MgO and the commercial MgO, having a very low surface area (~10m^2/g), allowed to demonstrate that the surface area, and so the number of the basic site, was a crucial parameter that directly affected the catalyst performance of basic catalyst in the CTH reaction. Thus, the comparison between the trends reported in **Figure 5-2**, clearly showed that the CTH reaction performed with the high surface MgO was much faster if compared to that performed with the commercial sample highlighting another important feature of the synthesized catalyst.
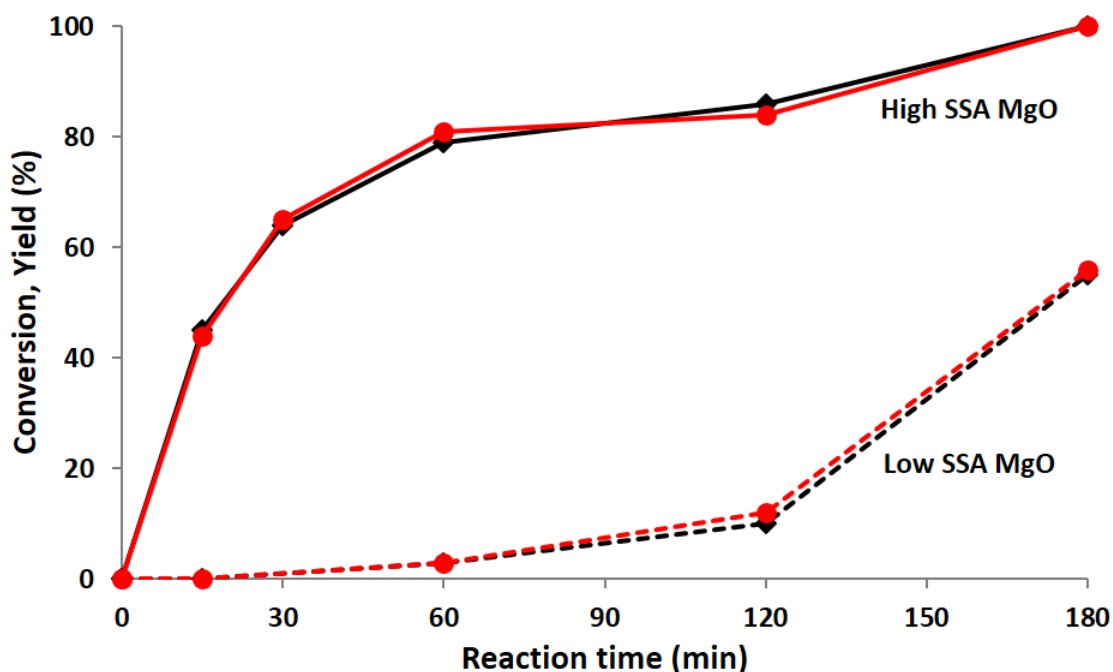
Figure 5-2. FU conversion and FAL yield as a function of the reaction time for the high surface area MgO (bold line) and the commercial low surface area MgO (dotted line). Reaction conditions: 50 ml of CH$_3$OH, 1.21 mmol of FU, T = 160°C, t = 0 ÷ 180 min, 1 g of catalyst. Legend: FU conversion (━), FAL yield (━).

Nevertheless, the synthesized high surface area MgO showed a relevant drawback related to the reusability tests. Indeed, as reported in **Figure 5-3**, the catalyst showed a non-marginal loss in the catalytic activity in the second use performed after a simple separation and drying procedure. That loss in the activity was demonstrated to be related to the formation, over the surface of the catalyst, of carbonaceous deposits deriving from methanol degradation reactions. TGA-DTA analysis over the sample used after the

second use showed a weight loss in the range 200÷350°C coupled with an exothermic peak, confirming the hypothesis of carbonaceous compounds formation. Furthermore, a second use of the catalyst performed after a re-calcination treatment in static air at 450°C, allow to remove the carbonaceous compounds formed and recover almost all the catalytic performance in FU reduction.
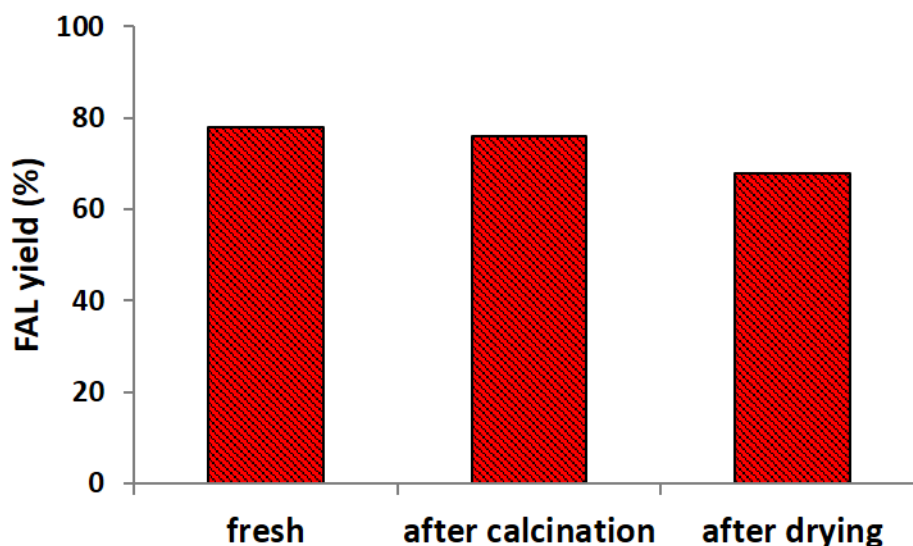
Figure 5-3. *FAL yield in the 2nd use as a function of the post-reaction treatment performed on the spent catalyst. Reaction conditions: 50 ml of CH_3OH, 1.21 mmol of FU, T = 160°C, t = 3h, 1 g of catalyst.*

In a second moment, the liquid-phase catalytic transfer hydrogenation of FU to FAL by-means of methanol as hydrogen source has been examined with Ca-based materials. In that second work it was demonstrated that CaO, despite its very low surface area ($2,4 m^2/g$), was highly active and stable in the studied reaction. Indeed, in the proper reaction conditions, 100% of FU conversion with 100% of FAL yield were obtained.

CaO showed to be very active at a reaction temperature higher if compared to that at which MgO showed its maximum activity. Indeed, the best catalytic performance was obtained at 210°C instead of 160°C, temperature required for MgO.

Another difference between the catalytic activities of the two pure basic oxides consisted in the trend of FU conversion and FAL yield as a function of the reaction time. As reported above, both the FU conversion and the FAL yield increased together with corresponding values with MgO. On the other hand, these trends showed to be very different in the case of CaO (**Figure 5-4**). The latter catalyst showed an high substrate conversion (> 80%) for a very short reaction time coupled with an initial nil production of FAL. Then, the

84

conversion slightly increased up to the total value registered after three hours while, the yield in FAL, progressively increased up to the final value of 93%. The deep difference between the trend of conversion and yield as a function of the reaction time was demonstrated to be ascribable to an initial rapid, but reversible, formation of furan oligomeric species as a consequence of the interaction between FU and catalyst. This was confirmed both from ESI-MS analysis that revealed the presence of high molecular mass species in the low-reaction time solution and also from the color of these. In the box of **Figure 5-4** is reported the comparison between the colors of the reaction solutions obtained increasing the reaction time; it is clear that at low reaction time the solution was colored due to the presence of oligomeric species that is well known to have higher UV-VIS absorption thanks to the high number of conjugated double bonds deriving from the condensation of several furanic molecules[2].
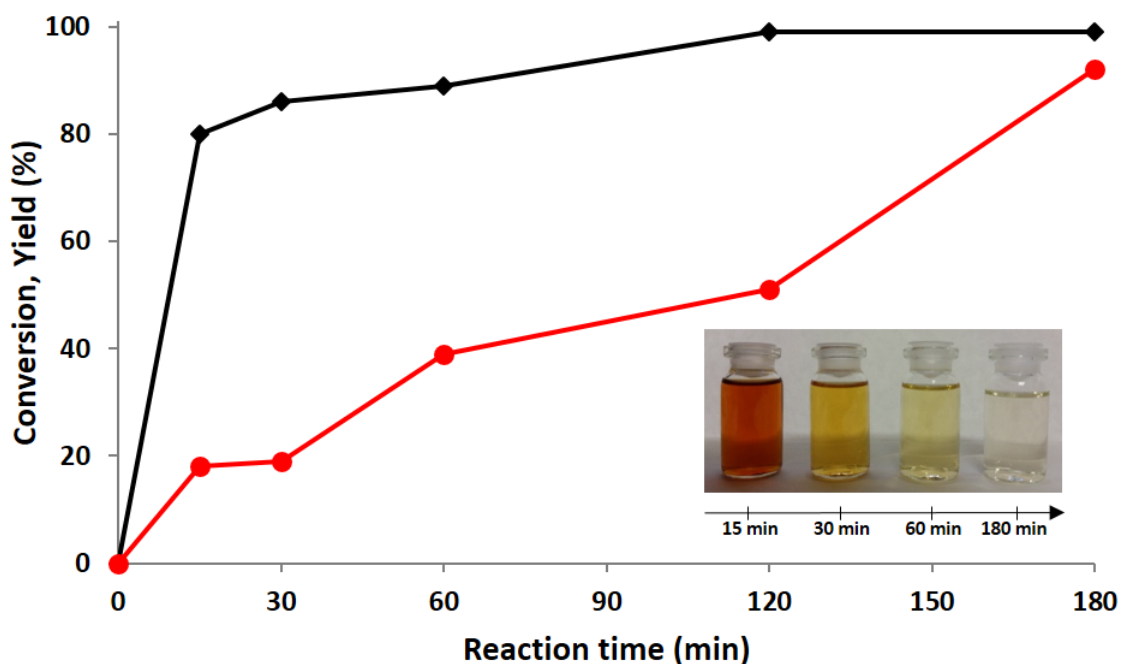
Figure 5-4. FU conversion and FAL yield as a function of the reaction time for the CaO catalyst. Reaction conditions: 50 ml of CH₃OH, 1.21 mmol of FU, T = 210°C, t = 0 ÷ 180 min, 1 g of catalyst. Legend: FU conversion (━), FAL yield (━). In the box were reported the reaction solutions obtained at different reaction time.

Finally, it has to be highlighted that CaO exhibited an important feature if compared to MgO. Indeed, we reported that for the latter it was possible to recover almost all the catalytic activity in a second use only treating it in static air at 450°C, procedure needed to guarantee the removal of carbonaceous compounds formed on the catalyst surface. On the other hand, CaO exhibited an higher stability considering that with a simple drying

work-up procedure it was possible to recover almost all the catalytic activity up to the 5th use (**Figure 5-5**).
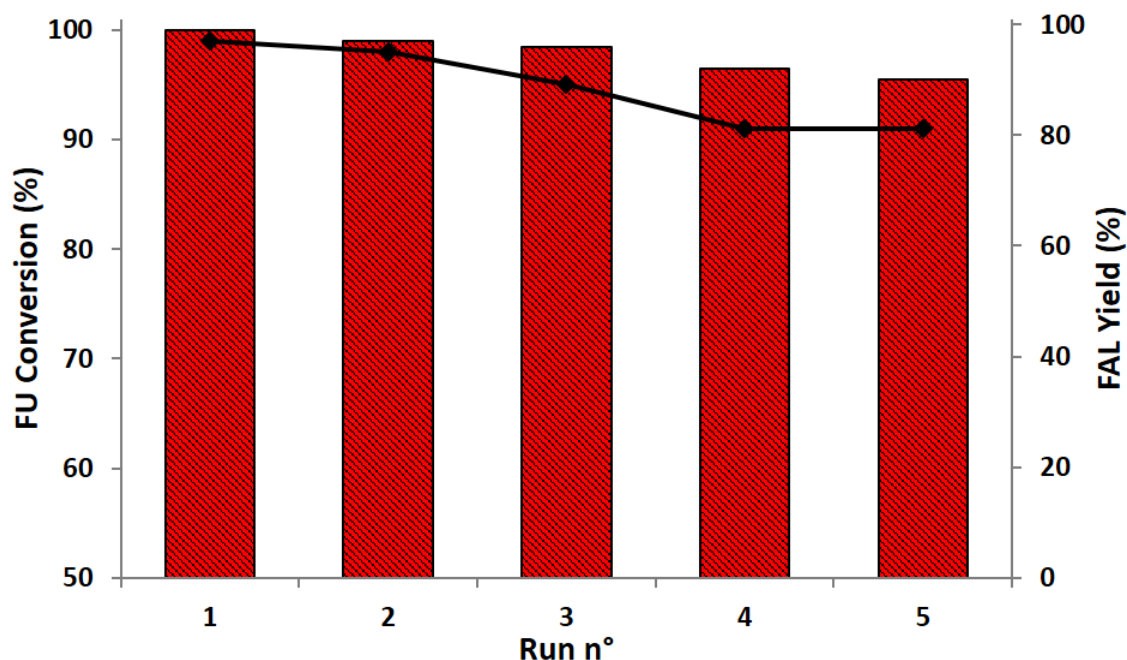
Figure 5-5. *Stability tests for CaO catalyst. Reaction conditions: 50 ml of CH₃OH, 1.21 mmol of FU, T = 210°C, t = 3h, 1 g of catalyst. Legend: FU conversion (♦), FAL selectivity (■).*

Then, the evaluation of the activity of these heterogeneous basic catalysts for the CTH of FU by-means of methanol as hydrogen source, has been continued with the development of a continuous gas-phase lab-scale plant. The possibility to shift the catalytic transfer hydrogenation process to a continuous plant was very attractive from an industrial scale-up point of view. Indeed, passing from a discontinuous liquid-phase process to a continuous gas-phase set-up, an intrinsic higher productivity could be reached; in a second view, it could also be possible to evaluate the catalytic performance of the different heterogeneous catalysts at higher temperature. The liquid-phase process showed some constrain due to the high autogenic pressure of methanol reached inside the batch reactor at the increase of the reaction temperature (~55 bar at 210°C).

In this view the catalytic activity of pristine MgO and that of a mixed Mg/Fe/O, obtained by the thermal decomposition of the hydrotalcite-like precursor (molar ratio Mg^{2+}/Fe^{3+} equal to 2) has been studied as first example. Then the catalytic activity of the pristine CaO basic catalyst has been evaluated.

86
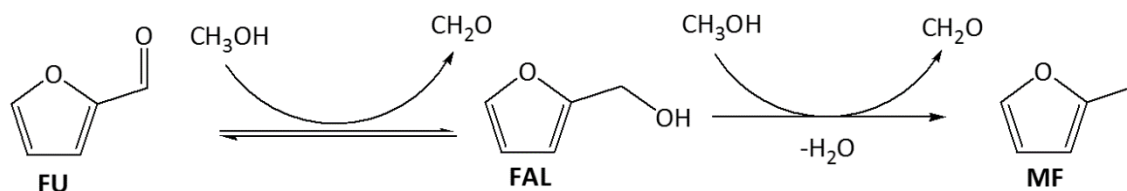
Scheme 5-2. *Gas-phase catalytic transfer hydrogenation of FU to FAL and MF.*

In the vapor-phase catalytic tests performed with the MgO-based catalysts, FAL and MF were the main products detected in the reaction with FU (**Scheme 5-2**); some cyclopentanones (CPs) were identified at very high temperatures (450–500 °C). These by-products resulted from FU rearrangement that occurs under reducing conditions and was previously observed by Hronec and co-workers[3,4] in their studies on FU hydrogenation.

Figure 5-6. *Effect of reaction temperature on FU conversion and product selectivity with the MgO catalyst. Feed composition: 5% FU, 50% CH₃OH, 45% N₂; pressure of 1 atm, overall gas residence time of 1,1 s, reaction time of 1 h. Legend: FU conversion (■), FAL selectivity (■), MF selectivity (■), C-Loss (■).*

With pristine MgO, at low temperature (250 °C), the results obtained in liquid phase were confirmed; the catalytic transfer hydrogenation occurred selectively and FAL was the only molecule produced.

No products of ring hydrogenation or decarbonylation were detected. Moreover, although formaldehyde was supposed to be initially produced, it was never detected in the present experiments; therefore, in addition to the main reaction involving FAL formation, the

process was accompanied by the decomposition of formaldehyde to CO, CO_2, CH_4 and H_2, which were the only co-products detected in the stream exiting from the reactor.

At the increase of the reaction temperature (**Figure 5-6**) an increase of FU conversion from the initial value of ~55% to the ~90% registered at 500°C. Concerning the products distribution, a progressively decrease of FAL selectivity was registered increasing the reaction temperature. Parallel, from 380°C, MF started to be produced reaching a maximum selectivity of ~40% registered at 500°C; unfortunately increasing the reaction temperature increased also the amount of heavy carbonaceous compounds formed on the catalyst surface due to thermal degradation of the furanic species involved in the reaction. Since the catalyst showed to be totally selective toward FAL, 250°C has been chosen as the optimal reaction temperature at which the stability of pristine MgO was evaluated. Monitoring the catalytic performances for six hours it was demonstrated that the formation of carbonaceous species deriving from methanol degradation reactions caused a slight deactivation of the catalysts during the monitored time on stream; TGA-DTA analysis performed on the spent catalyst confirmed the presence of C-species. Despite this deactivation, decrease of conversion from 54 to 35%, the catalyst showed to be always totally selective toward FAL[5] (**Figure 5-7**).

Figure 5-7. *Effect of reaction time on FU conversion and FAL selectivity with the MgO catalyst. Feed composition: 5% FU, 50% CH_3OH, 45% N_2; pressure of 1 atm, T = 250°C, overall gas residence time of 1,1 s. Legend: FU conversion (♦), FAL selectivity (■).*

Then, the catalytic behavior of a mixed Mg/Fe/O has been studied in the gas-phase catalytic transfer hydrogenation of FU using methanol as hydrogen source. The introduction of iron into the lattice of MgO allowed us to tune the acid-base properties of the catalyst, introducing also de-hydrogenating and de-oxygenating characteristics. The mixed iron-magnesium oxides showed to be active in the CTH reaction but the products distribution was deeply different to that obtained with pristine MgO considering that MF was always detected as the main reduction product instead of FAL. Indeed, as showed in **Figure 5-8**, FU conversion reached a maximum at 380°C (~93%), temperature at which the mixed oxide showed also an 80% of selectivity in MF.
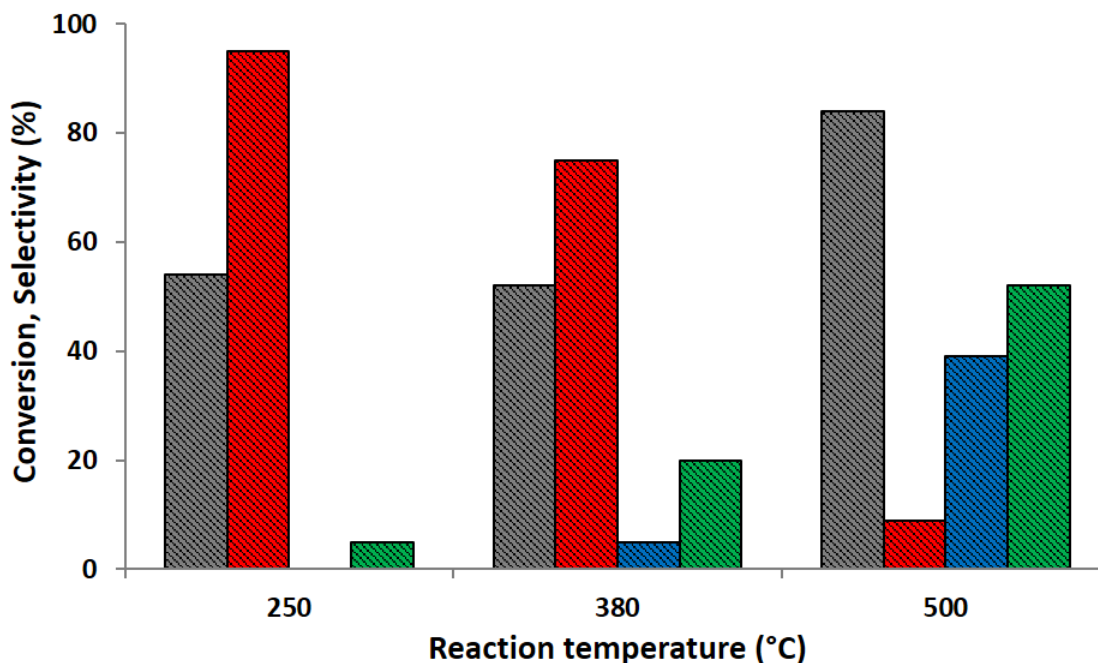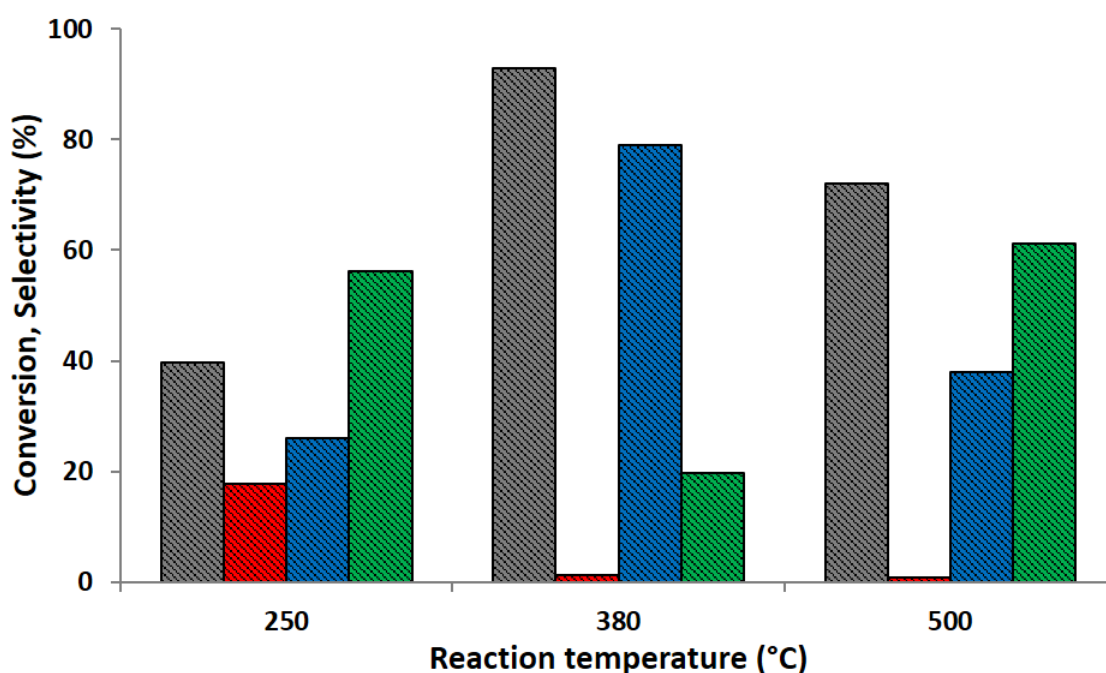

Figure 5-8. *Effect of reaction temperature on FU conversion and product selectivity with the Mg/Fe/O catalyst. Feed composition: 5% FU, 50% CH₃OH, 45% N₂; pressure of 1 atm, overall gas residence time of 1,1 s, reaction time of 1 h. Legend: FU conversion (■), FAL selectivity (■), MF selectivity (■), C-Loss (■).*

Thus, under our conditions, it has been demonstrated that MgO easily carried out the reduction of FU to FAL via the MPV reaction, confirming the data obtained in the liquid phase. In addition, the catalytic activity of MgO for the hydrogenolysis of FAL to MF is significantly enhanced with the addition of Fe. In particular, at 380 °C, MF selectivity increases from 2 to 79%. The previously reported characterization of Mg/Fe/O[6] indicated that this catalyst shows Lewis-type acid features, which were associated with the presence of a guest Fe^{3+} metal cation. Moreover, this material showed a strong dehydrogenating capacity. Therefore, we demonstrated that the excellent performance of Mg/Fe/O in FU

reduction to MF may be correlated with its higher dehydrogenation properties[7] and Lewis acidity, both properties having been introduced in MgO because of Fe addition.

Concerning the stability, the catalytic activity of the mixed iron magnesium oxide has been evaluated increasing the reaction time at the optimal reaction temperature of 380°C, condition at which both FU conversion and MF production were maximized. The iron containing system showed a deep deactivation due to the formation of heavy carbonaceous species over the catalyst surface; that phenomena brought also to a differentiation in the products distribution. Indeed, during the six monitored hours the conversion dropped down to the initial value of 93% to 24%; parallel the selectivity in MF decreased while that of FAL progressively increased (**Figure 5-9**).
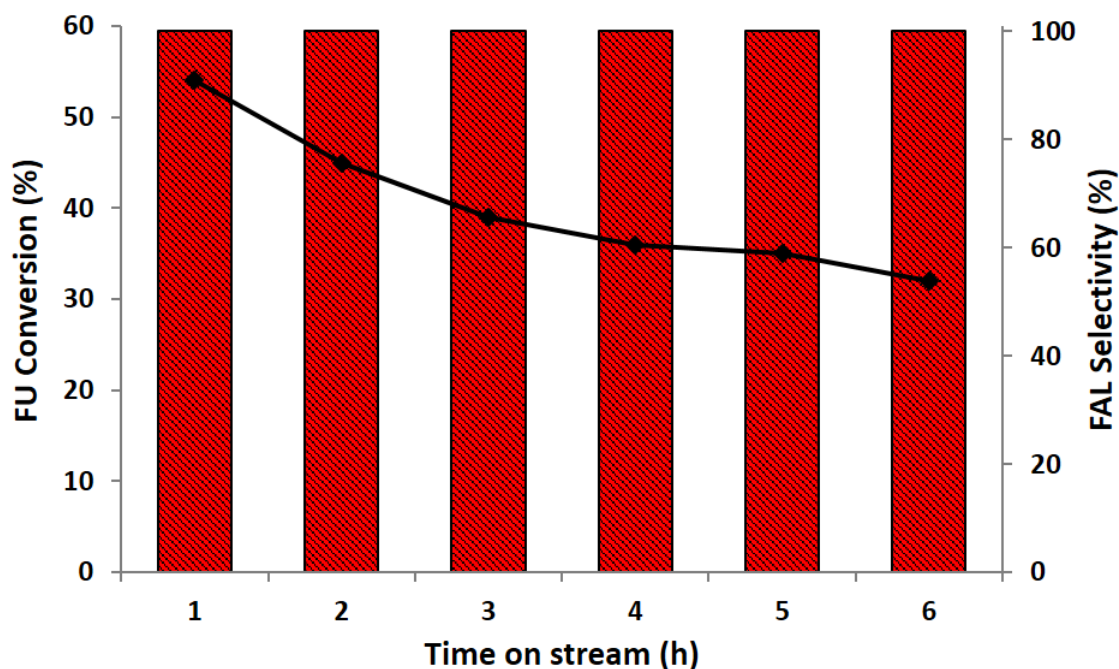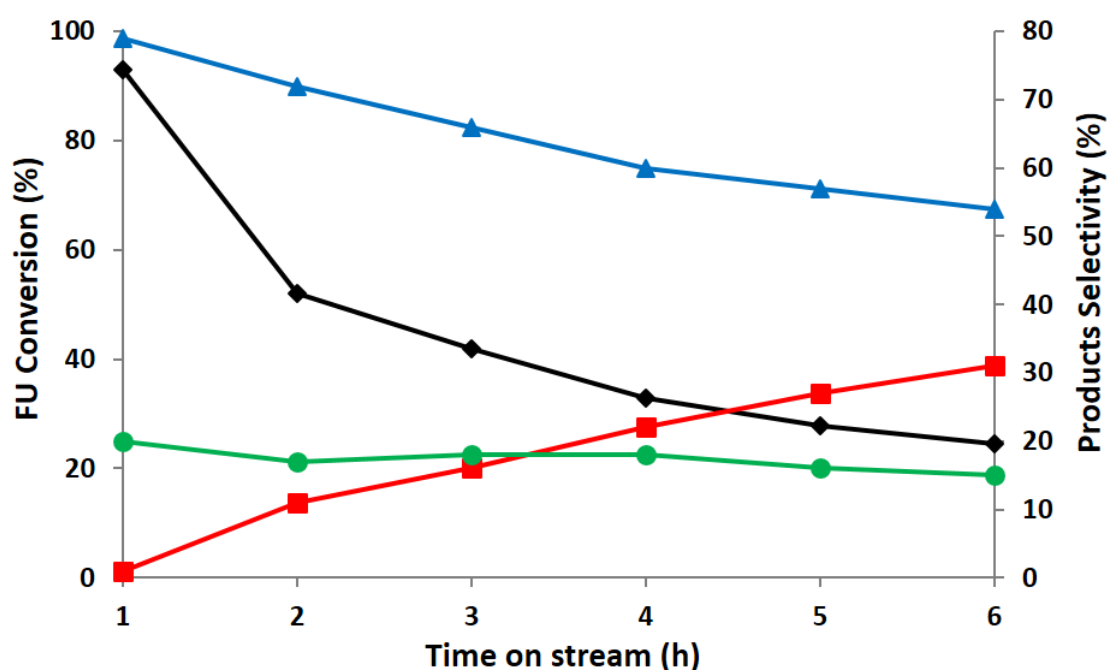

Figure 5-9. *Effect of reaction time on FU conversion and product selectivity with the Mg/Fe/O catalyst. Feed composition: 5% FU, 50% CH$_3$OH, 45% N$_2$; pressure of 1 atm, T = 380°C, overall gas residence time of 1,1 s. Legend: FU conversion (♦), FAL selectivity (■), MF selectivity (▲), C-Loss (●).*

Despite the deep deactivation showed, some regeneration tests with the mixed iron-magnesium catalysts have been performed in order to verify if an in-situ thermal treatment in air at 450°C for 2 h could be enough to promote the removal of the carbonaceous species formed and recover the initial catalyst activity. The data reported (**Figure 5-10**) indicate that the treatment led to an almost complete recovery of the original catalytic performance. The major variation in activity was shown after the 1st use; after the 2nd use,

in fact, both FU conversion and MF selectivity at the start of the next cycle were similar to those observed during the previous cycle.
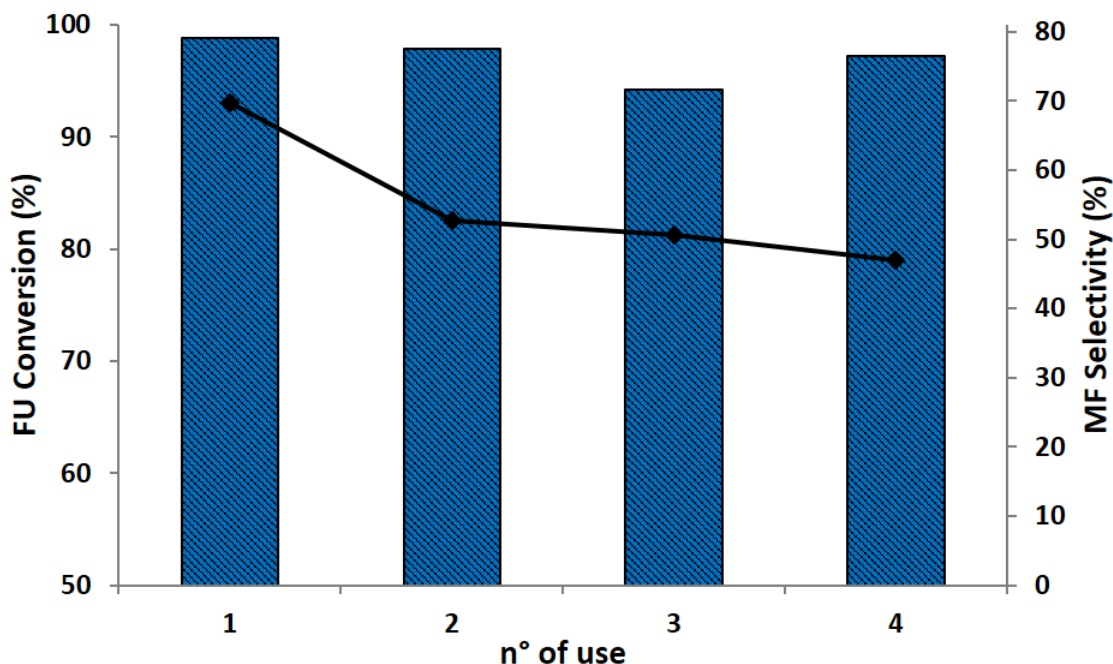
Figure 5-10. FU conversion and MF selectivity in the regeneration tests performed with the mixed Mg/Fe/O catalyst. Feed composition: 5% FU, 50% CH₃OH, 45% N₂; pressure of 1 atm, T = 380°C, overall gas residence time of 1,1 s. Legend: FU conversion (♦), MF selectivity (■).

Summing up the initial part of the work concerning the use of the heterogeneous basic-base catalysts for the catalytic transfer hydrogenation of FU to the corresponding reduced products using methanol as hydrogen transfer reactant it could be briefly concluded that:

- Pristine MgO and CaO showed to be very active and selective toward the formation of FAL as the only reduction product in the liquid-phase process. For CaO it was demonstrated that an higher reaction temperature was required to reach the maximum activity, 210°C instead of 160°C used with MgO. On the other hand CaO showed an higher stability in the recycle tests; a simple drying procedure showed to be enough in order to recover almost all the activity for 5 following run while, with MgO, a re-calcination treatment at 450°C in air was necessary to remove C-species;

- Pristine MgO confirmed, also in the gas-phase tests, to be active and selective toward FAL as the only reduction product at low temperature (250°C). On the contrary, the products distribution obtained with the Mg/Fe/O system was

significantly different, with prevailing 2-methylfuran formation when the reaction was carried out between 300 and 400°C.

Taking into the background concerning the activity of the reported heterogeneous basic catalysts described above, the activity of pristine CaO in the gas-phase CTH of FU will be described in detail in the next section of the present work. In particular, the primary aim to test CaO in the continuous set-up layout was that to evaluate if the higher stability showed in the liquid phase tests, compared to that of MgO, was maintained also in the vapor-phase.

In a second moment, a detailed paragraph will be dedicated to a depth study of the reaction mechanism, with particular regard to the MF formation pathways on the base of the catalyst properties such as acid-base strength and de-hydrogenating/de-oxygenating features. Catalysts characterization and catalytic tests performed feeding different hydrogen sources have been used as a general strategy to gain information regarding the reaction mechanism.

5.2. Gas-phase catalytic transfer hydrogenation of FU with bulk CaO

In this section of the present work the catalytic activity of the heterogeneous Ca-based catalysts in the gas-phase catalytic transfer hydrogenation of FU by-means of methanol as hydrogen source have been described.

5.2.1. Bulk features of the catalyst

The CaO catalyst was obtained by thermal treatment of the synthesized $CaCO_3$ precursor. The latter, as described in the experimental section, was produced from the precipitation at controlled pH, temperature and stirring of the metal precursor ($Ca(NO_3)_2$) into a CO_3^{2-} solution. In order to obtain the formation of the crystalline phase of CaO the precursor was calcined in static air at different temperature: 500°C, 700°C and 900°C.

Calcination Temperature (°C)	Crystalline phase (XRD)	SSA m²/g	Total basicity (mmol/g)[a]	Total basicity (mmol/g)[b]	CO_2 T desorption (°C)	Total acidity (mmol/g)[c]	Total acidity (mmol/g)[d]
120	$CaCO_3$ (Vaterite + Calcite)	1,7	0	-	-	0	0
500	$CaCO_3$ (Calcite)	1,4	0,22	-	-	0	0
700	CaO (Lime)	2,4	2,57	2,49	700	0	0
900	CaO (Lime)	2,3	1,10	1,13	700	0	0

Table 5-1. *Main features of the catalysts depending on the calcination temperature.*

    a.   *Determined by irreversible adsorption of acrylic acid;*

    b.   *Determined by CO_2-TPD;*

    c.   *Determined by irreversible adsorption of n-propylamine (NPA);*

    d.   Determined by NH_3-TPD.

Table 5-1 summarized the main features of the catalysts obtained calcining the synthesized precursor at different temperature. All the prepared samples showed a very low specific surface area, lower than 5m²/g; values in agreement with those reported in

literature in several works employing CaO as solid base catalyst for bio-refinery process such as the methanol transesterification reaction of triglycerides to produce bio-diesel additives such as the fatty acid methyl esters (FAME)[8,9]. In **Figure 5-11** were reported the diffractograms of the samples treated at different calcination temperature. The analysis of the reported XRD pattern and the comparison with JCPD library demonstrated that the as synthesized dried precursor consisted in a mixed phase of two polymorphs of $CaCO_3$, named calcite and vaterite respectively. The former one, from a thermodynamic point of view, was considered the most stable crystalline polymorph of calcium carbonate. On the other hand, vaterite was considered the less stable polymorph and Wolf et al. have reported that a thermal treatment in static air at 330°C allowed the complete structure transition from vaterite to calcite[10]. Indeed, in our case, the sample calcined in air at 500°C showed a perfect calcite structure, confirming the transition from the mixed crystalline structure to the pure polymorph of calcite. In literature it was also reported that calcium carbonate could be present in a third polymorph, named aragonite, itself thermodynamically less stable than calcite, which was never detected in the structure of the catalyst precursor and of the calcined samples. In any case, only for calcination temperatures of 700°C and 900°C the formation of CaO was observed. The diffraction patterns of the samples treated at these temperatures fitted very well with that of the reference pattern of CaO (lime); traces of $Ca(OH)_2$ were detected in the sample calcined at 700°C and then completely disappeared in that treated at 900°C.

The decomposition of $CaCO_3$ for calcination temperature equal or higher than 700°C was in agreement with the results obtained from the thermogravimetric (TGA) analysis performed on the catalyst precursor (**Figure 5-12**). Indeed, the synthesized catalyst precursor, having $CaCO_3$ crystalline structure, showed a weigh loss of 44% in the range of temperature between 550°C and 750°C that corresponded to the theoretical transition from the carbonate specie to the oxide one. Moreover, that specific weight loss was coupled with an endothermic peak, registered by the difference thermal analysis (DTA), characteristic of decomposition process.

Concerning the acid-base properties, both the irreversible adsorption of n-propylamine and the NH_3-TPD experiments confirmed the pure basic features of the Ca-based catalysts. Indeed, none acid sites were detected for the samples treated at the different calcination temperature. Nevertheless, the irreversible acrylic acid adsorption experiments confirmed the basic feature of the systems and, furthermore, a correlation between the calcination temperature and the total amount of the basic sites was observed.

The as synthesized precursor, dried at 120°C and having a mixed crystalline-phase of $CaCO_3$, showed no basic feature while, the sample treated at 500°C, with pure $CaCO_3$ calcite structure, showed a slight increase of the basicity. The latter showed to increase of more than a magnitude order for the samples treated at 700°C and 900°C. Thus, the basic features of the Ca-based systems were demonstrated to be strictly related to the crystalline structure of the samples, in particular the decomposition of calcium carbonate to form the oxide form showed to be essential for obtaining the higher density of basic sites. Similar results were obtained with CO_2-TPD characterization.
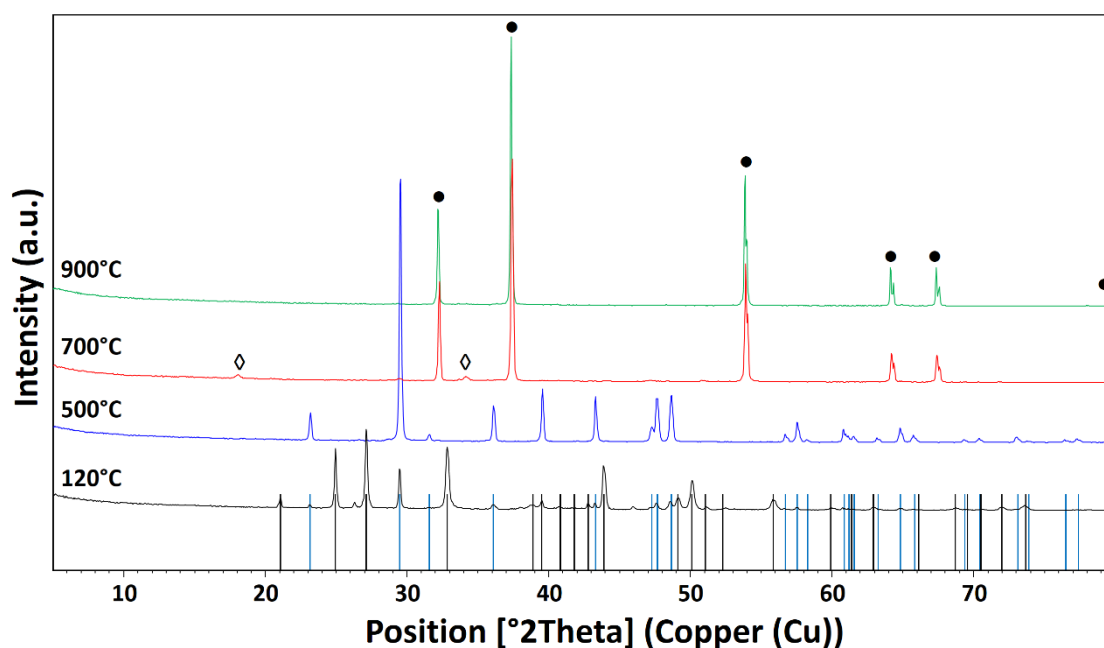
Figure 5-11. *XRD patterns of the dried CaO precursor and that of the samples calcined at different temperature. Reference patterns: (●) CaO, (◊) Ca(OH)₂, (━) CaCO₃ Vaterite, (━) CaCO₃ Calcite.*
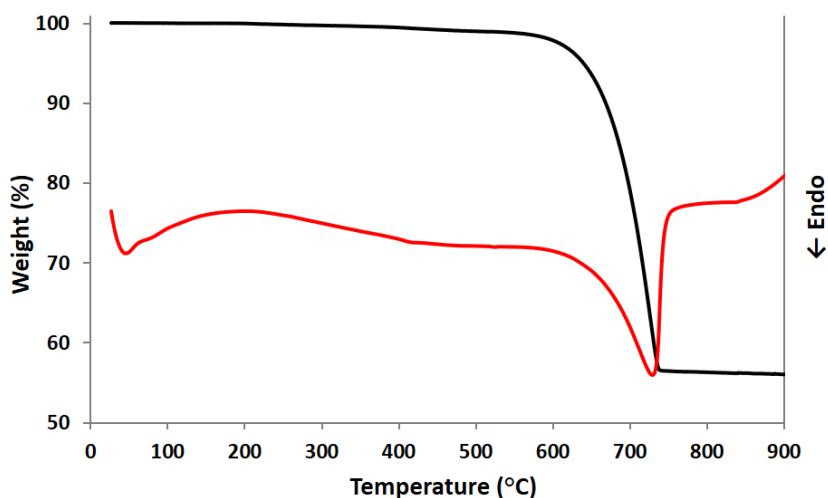
Figure 5-12. *Thermogravimetric and differential thermal analysis performed in air over the synthesized CaCO₃.*

95

5.2.2. Catalytic transfer hydrogenation of FU over CaO catalyst: effect of calcination temperature

The catalytic transfer hydrogenation of FU by-means of methanol as H-transfer reactant was carried out using CaO catalyst as heterogeneous basic catalyst. The interaction between methanol and CaO have been studied, prior to the catalytic tests, through DRIFT experiments (*Diffuse Reflectance Infrared Fourier Transform Spectroscopy*). In these experiments methanol was adsorbed on the catalyst surface at room temperature and then the interaction between the basic catalyst and the hydrogen source have been studied increasing the temperature in order to promote both the desorption of the alcohol and the detection of specific IR band attributable to species formed as a consequence of methanol activation.
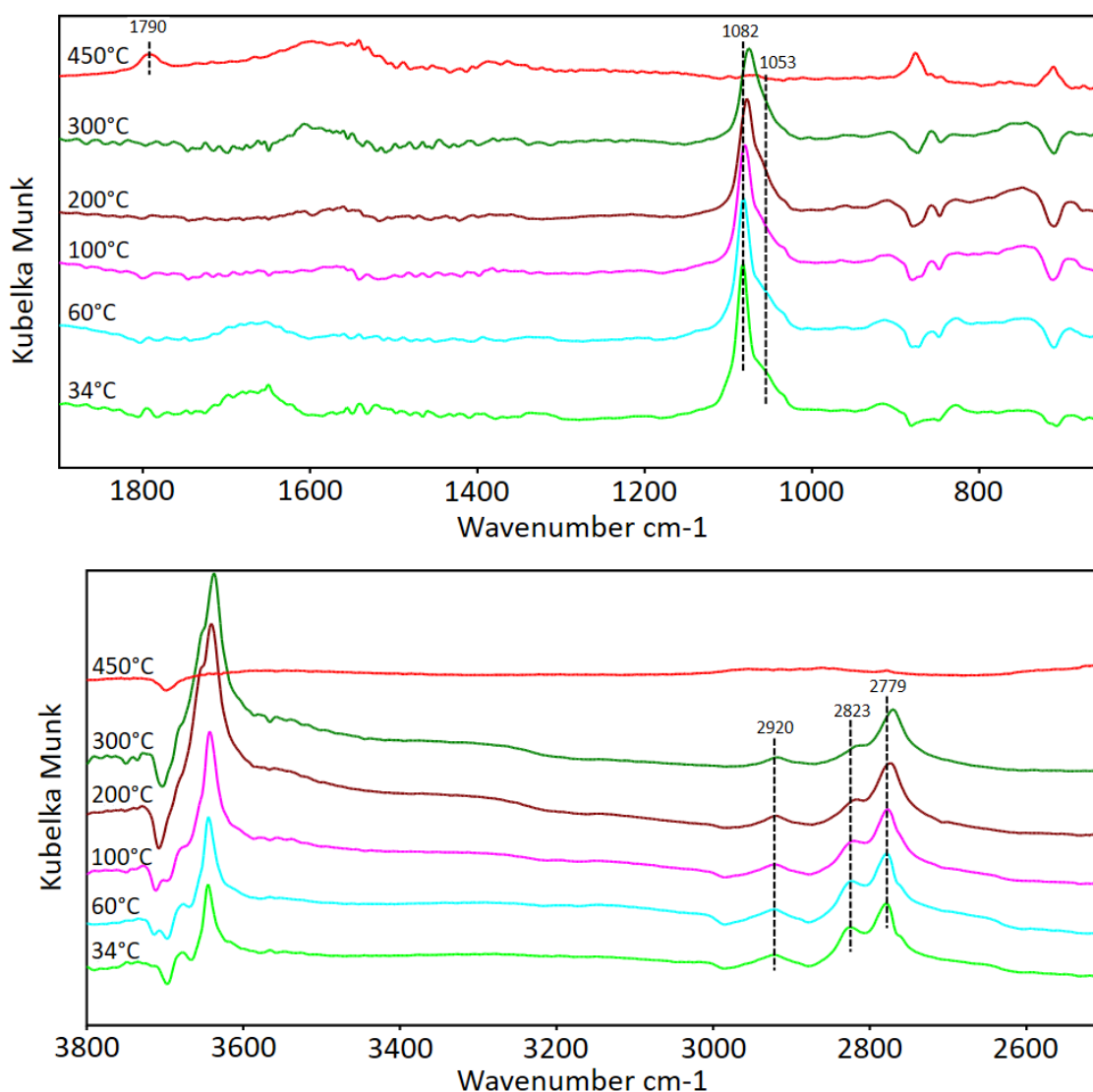
Figure 5-13. *DRIFT spectra registered after methanol adsorption over CaO at different temperatures. Spectral windows 700÷1900 cm^{-1} and 2500÷3800 cm^{-1}.*

In particular, we demonstrated that at room temperature methanol interact with the catalyst through two main route: physi-adsorption or dissociative adsorption. The presence of the physi-adsorbed un-dissociated methanol on the catalyst surface was confirmed by the detection of the characteristic band related to the stretching of the C—O at 1052 cm^{-1} while, the presence of the dissociate chemisorbed methanol, was confirmed by the formation of the characteristic band at 1082 cm^{-1} related to the di-coordinate methoxy specie[11]. At the increase of temperature, the dissociative chemisorption of methanol became the most important interaction and the transition from the methoxy to the aldehyde specie, coupled with the release of molecular hydrogen, was demonstrated to take place on the catalyst surface.

A light surface carbonatation starts at 300°C and it is confirmed by the broad and small band around 1600 cm^{-1}. A band at 1790 cm^{-1} might be related to $v1+v4$ CO_3 or to some carboxylate formation due to carbonates degradation. The bands at 2779, 2823, 2920 cm^{-1} appear due to C-H stretching vibration related to CH_3. Positive band at 3636 cm^{-1} indicates the formation of new surface OH. The negative band is due to the interaction of the terminal surface OH[12].

In our catalytic tests FAL was the main reduction product detected in the reaction with FU and methanol over CaO catalyst, only traces of MF were detected at the higher reaction temperature tested. No ring opening or hydrogenation products were identify for all the performed catalytic tests.

Calcination T (°C)	FU Conversion (%)	Product Selectivity (%)			FAL Yield (%)
		FAL	MF	C-Loss	
500	15	19	0	81	3
700	20	67	1	32	13
900	15	58	1	41	9

Table 5-2. *Effect of calcination temperature of catalyst precursor over FU conversion FAL selectivity and Yield. Feed composition: FU 5%, CH$_3$OH 50%, N$_2$ 45%; Pressure 1 atm, reaction temperature 350°C, overall gas residence time 1.0 s.*
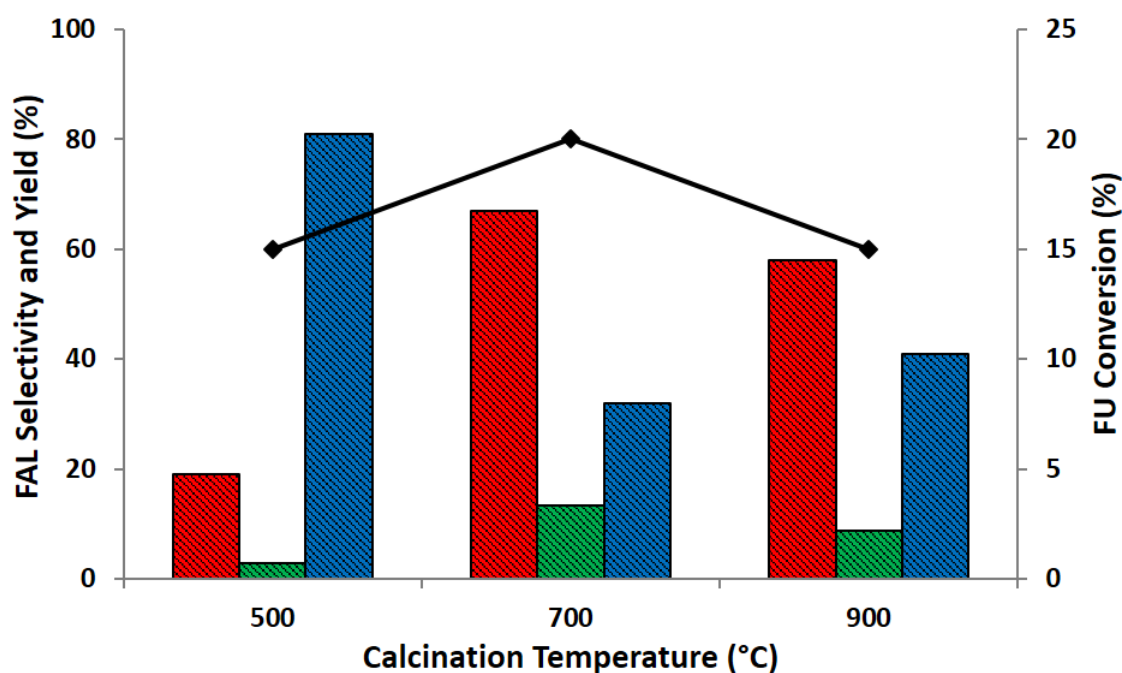
Figure 5-14. *Effect of calcination temperature of catalyst precursor over FU conversion FAL selectivity and Yield. Feed composition: FU 5%, CH₃OH 50%, N₂ 45%; Pressure 1 atm, reaction temperature 350°C, overall gas residence time 1.0 s. Legend: FU conversion (♦), FAL selectivity (■), FAL Yield (■), C-loss (■).*

Since the synthesized Ca-based material was shown to undergoes in a crystalline-phase transition and also to a deep change of basicity as a function of the calcination temperature (**Figure 5-11**), we have first investigated the effect of the latter parameter on the catalytic activity in the CTH reaction of FU.

The sample treated at 500°C, presenting a crystalline structure of $CaCO_3$ calcite and the lower total amount of basic sites, showed to be partially active but not selective in the conversion of the substrate (**Figure 5-14** and **Table 5-2**). Indeed, 15% conversion of furfural was registered with only few percentage point of FAL yield. The most of FU fed during the catalytic test was degraded to heavy carbonaceous deposits formed over the catalyst surface. Increasing the calcination temperature an increase of the catalytic performance was registered in terms of both FU conversion and FAL selectivity and yield. This trend was in agreement with the bulk features of the catalyst described in the former section where it was demonstrated that a calcination temperature at least of 700°C was necessary to decompose the catalyst precursor to form the CaO crystalline structure and to obtain the higher amount of basic sites over the surface. More in detail, the sample treated at 700°C showed the best performances, the higher values of FU conversion, FAL selectivity and yield were obtained (respectively 20% of FU conversion, 67% of FAL

selectivity and 13% of yield). Finally, the catalyst calcined at 900°C showed a better catalytic performances than that obtained with the sample treated at 500°C but worse if compared to that obtained with the sample treated at 700°C. Lower FU conversion, FAL selectivity and yield were registered. In literature, it was generally reported that the activity of a basic catalyst in the hydrogen transfer reaction was related to two main catalyst features. The first was the number of the basic sites present on the surface of the catalyst; that parameter was generally related to the surface area meaning that the higher was the surface area the higher should be the number of basic sites. The second was the number of structural defects on the surface of the solid such as kink, step and corner defective sites; in this case the higher activity was related to the lower coordination of the atoms that composed these particular structures[13,14]. In this view, the lower activity showed by the sample treated at 900°C compared to that treated at 700°C, could be explained by the lower number of basic sites titrated over the surface. Furthermore, an effect related to the lower surface defectivity could not be excluded. It has been demonstrated that the number of defects on the catalyst surface was related to the thermal treatment temperature, the higher was the temperature of the treatment the lower was the number of defects and higher the crystallinity of the solid; the increase of the calcination temperature promote the formation of the most stable thermodynamic structure that was the one with the lower surface defectively sites. In this view, for the sample treated at 700°C, it could be hypothesized the presence of an higher number of defectively sites on the surface compared to the sample calcined at 900°C. As a matter of fact, 700°C was the minimum temperature required for the complete decomposition of $CaCO_3$ to form CaO (**Figure 5-12**); indeed, at this temperature the crystalline transition was just completed and so an higher number of defectively sites on the surface could be present. On the contrary, the sample treated at 900°C could be less defectively because the treatment at high temperature could promote some superficial-reconstruction phenomena the consequence of which were the formation of the lower energy-content structure, identified as the one with the lower number of defectively sites.

Summarizing this part it was possible to conclude that 700°C was the best calcination temperature at which the catalyst performance was maximized both in term of activity and selectivity. Thus, all the catalytic results reported in the further sections were obtained with CaO catalyst calcined at 700°C.

5.2.3. Catalytic transfer hydrogenation of FU over CaO catalyst: effect of reaction temperature

The second reaction parameter investigated was the reaction temperature. In **Figure 5-15** was reported the effect of the reaction temperature over FU conversion, MF selectivity, FAL selectivity and yield. The reported results were related to catalytic tests performed in the range of temperature between 250°C and 400°C at 1,0 s of contact time. Since the catalyst performance showed to be different between the first and the following reaction hours of the monitored time on stream, the plotted results consisted in the average values registered between the 2nd and the 6th hour. Further details regarding the behavior of the catalyst during the time on stream will be given in the following section.
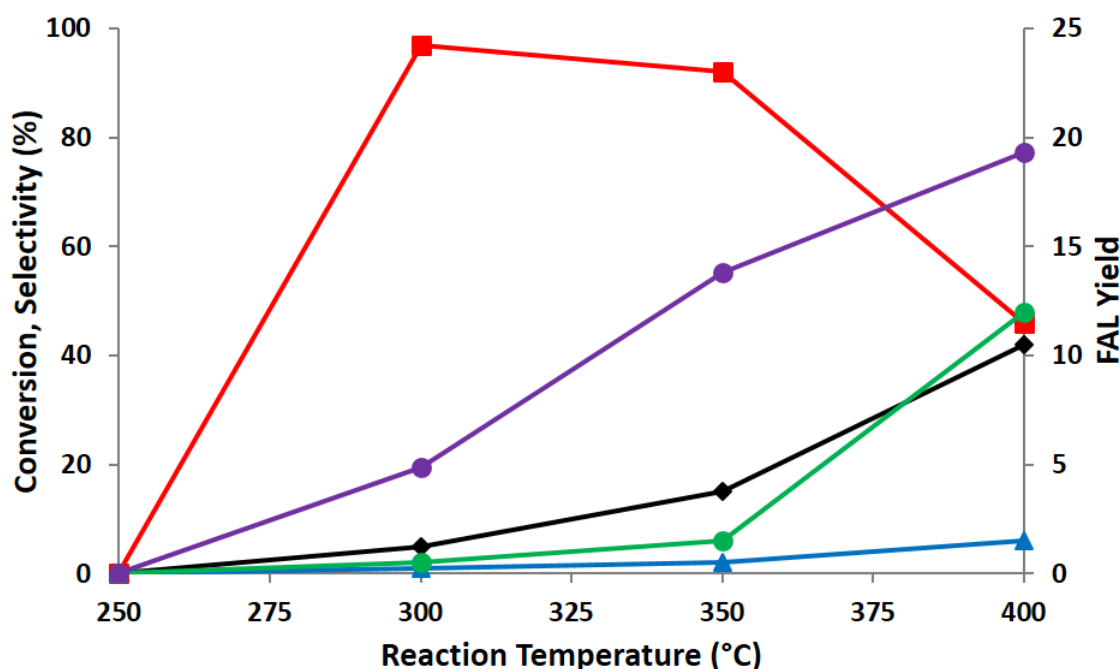
Figure 5-15. *Effect of reaction temperature over FU conversion, products selectivity and FAL yield with CaO catalyst calcined at 700°C. Feed composition: FU 5%, CH₃OH 50%, N₂ 45%; Pressure 1 atm, reaction temperature 250 ÷ 400°C, overall gas residence time 1.0 s. Legend: FU conversion (♦), FAL selectivity (■), FAL Yield (●), MF selectivity (▲), C-loss (●).*

At low temperature the catalyst was not active in the catalytic transfer hydrogenation of FU by-means of methanol. Indeed, at 250°C, nil FU conversion or reduced products formation was detected. Furthermore, it was also demonstrated that FU was stable under these reaction conditions; no thermal degradation, or transformation into by-products, as a consequence of the interaction between FU and catalyst surface, were registered.

Reaction T (°C)	FU Conversion (%)	Product Selectivity (%)			FAL Yield (%)
		FAL	MF	C-Loss	
250	0	0	0	-	0
300	5	97	1	2	5
350	15	92	2	6	14
400	42	46	6	48	19

Table 5-3. *Effect of reaction temperature on FU conversion, product selectivity and FAL yield with CaO catalyst calcined at 700°C. Feed composition: FU 5%, CH₃OH 50%, N₂ 45%; Pressure 1 atm, reaction temperature 250 ÷ 400°C, overall gas residence time 1.0 s.*

At the increase of the reaction temperature the catalyst became active in the catalytic transfer hydrogenation process and a progressive increase of FU conversion was registered. A final value of 42% of FU conversion was registered at 400°C, higher to the 5% and 15% registered at 300 and 350°C respectively. The trend showed by the conversion was in agreement to that obtained in the liquid-phase catalytic transfer hydrogenation of FU with methanol. As reported above, the comparison between CaO and MgO in the liquid-phase process demonstrated that for the former heterogeneous basic catalyst was required an higher reaction temperature to activate the CTH process; 210°C was demonstrated to be the optimal temperature instead of 160°C, the optimal condition for MgO. The same behavior was confirmed also in the gas-phase process in which it was demonstrated that 300°C was the minimal temperature necessary to activate the CTH, instead of the 200°C at which MgO was still active.

Despite the high conversion obtained at 400°C, the catalyst showed to become progressively less selective towards the formation of the selective reduction products of FU when the reaction temperature was increased from 300°C to 400°C. Indeed, CaO showed to be totally selective in the formation of FAL as the only reduction product at 300°C while, increasing the temperature to 350°C and 400°C, the selectivity in the unsaturated alcohol decrease to 92% and 48% respectively.

Concerning the formation of MF, product of the consecutive hydrogenolysis of FAL, only some traces were obtained for temperature equal or higher than 350°C; the highest selectivity was obtained at 400°C and it was equal to 6%. Parallel to the decrease of FAL selectivity an increase of the C-Loss term, in which were enclosed the heavy carbonaceous compounds formed over the catalyst surface was registered. In our previous work concerning the catalytic transfer hydrogenation of FU by-means of methanol as hydrogen source and MgO-based catalysts, we have just demonstrated that the formation

of heavy carbonaceous species was the consequence of thermal degradation processes in which the furanic compounds involved in our reaction undergoes at high temperature. Furthermore, we were able to demonstrate that also the methanol, used as hydrogen source, could form oligomeric species over the catalyst surface. In order to confirm that CaO could show a similar behavior, TGA/DTA analysis were performed over the spent catalyst used in the tests performed varying the temperature.
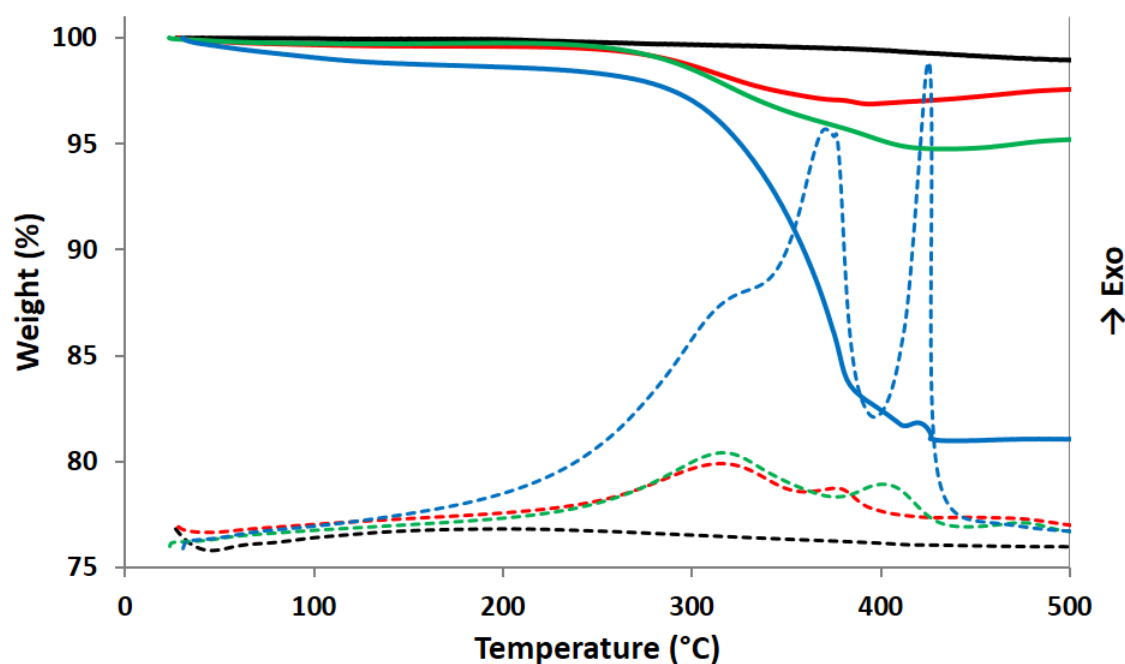
Figure 5-16. *Thermogravimetric (bold line) and differential thermal analysis (dotted line) performed in air over different sample of CaO. Legend: CaO fresh calcined at 700°C (━), CaO used in the catalytic test at 300°C (━), CaO used in the catalytic test at 350°C (━), CaO used in the catalytic test at 400°C (━).*

In **Figure 5-16** were reported the thermograms obtained from the TGA/DTA analysis performed over the catalysts used in the reaction at different temperature. The fresh CaO calcined at 700°C (black line) as expected showed none weight loss in all the monitored temperature range. On the contrary, all the catalysts used in reaction showed non-negligible weight loss that could be related to the removal, through combustion, of the heavy carbonaceous deposits formed during the reduction catalytic tests. In particular, the different TGA profiles collected were related to the catalysts used in the tests performed at 300°C (red line), 350°C (green line) and 400°C (blue line).

The three samples used in reaction showed a weight loss in the temperature range between 250°C and 450°C that, according to the exothermic peaks registered by the differential thermal analysis, could be related to the combustion of the carbonaceous species formed

over the catalyst surface during the catalytic test. Furthermore, it was possible to find a correlation between the registered weight loss and the C-Loss term determined during the catalytic tests. Indeed, as mentioned above, it was observed a progressive increase in the C-loss term at the increase of the reaction temperature and the same trend was observed for the weight loss determined with the TGA analysis. As a matter of fact, an increase of the latter was observed at the increase of the reaction temperature. The sample used in the reaction at 300°C showed a weight loss of 3%, the one used at 350°C lost the 5% of the initial weight while the one used at 400°C showed a weight loss of 19% that was in agreement with the trend of C-Loss (**Figure 5-15**).

The weight loss showed by the catalyst used in the reaction at 300°C seemed to disagree with the C-Loss; indeed at that temperature the carbon balance was closed and a nil carbon loss value, related to the furanic aromatic component, was registered. Therefore, we could hypothesized that the 3 point percentage of weight loss registered were related to the removal of some oligomeric species deriving from methanol degradation. Indeed, we previously demonstrated that formaldehyde, produced as a consequence of methanol dehydrogenation, could form some polyoxomethylene oligomers that were removed for combustion at temperature between 250°C and 350°C.

It has also to be highlighted that increasing the reaction temperature from 300°C to 400°C an increase of the temperature at which the carbonaceous deposits burned was registered. This could be connected to the formation of deposits with much-ordered structures; we have just observed a similar phenomenon in our work concerning the use of MgO-based catalyst. The differential thermal analysis (**Figure 5-16**) supported the former hypothesis. The reported thermograms showed two different peaks, in the case of the samples used at 300°C and 350°C, and three in the case of the sample used in the reaction at 400°C that could be related to the combustion of different carbonaceous species having progressively an higher ordered structure.

Summing up this part, it could be concluded that CaO catalyst showed a reaction temperature (350°C) at which the catalytic performance was maximized in terms of FU conversion, FAL selectivity and yield.

5.2.4. Catalytic transfer hydrogenation of FU over CaO catalyst: effect of contact time

In this part of the present work the effect of the contact time on the catalytic performance of the heterogeneous basic catalyst in the gas-phase catalytic transfer hydrogenation reaction of FU my-means of methanol as the hydrogen source has been investigated. Since in the previous section it has been demonstrated that 700°C was the optimal calcination temperature and 350°C was the best reaction temperature, the influence of the contact time was evaluated at these reaction conditions.
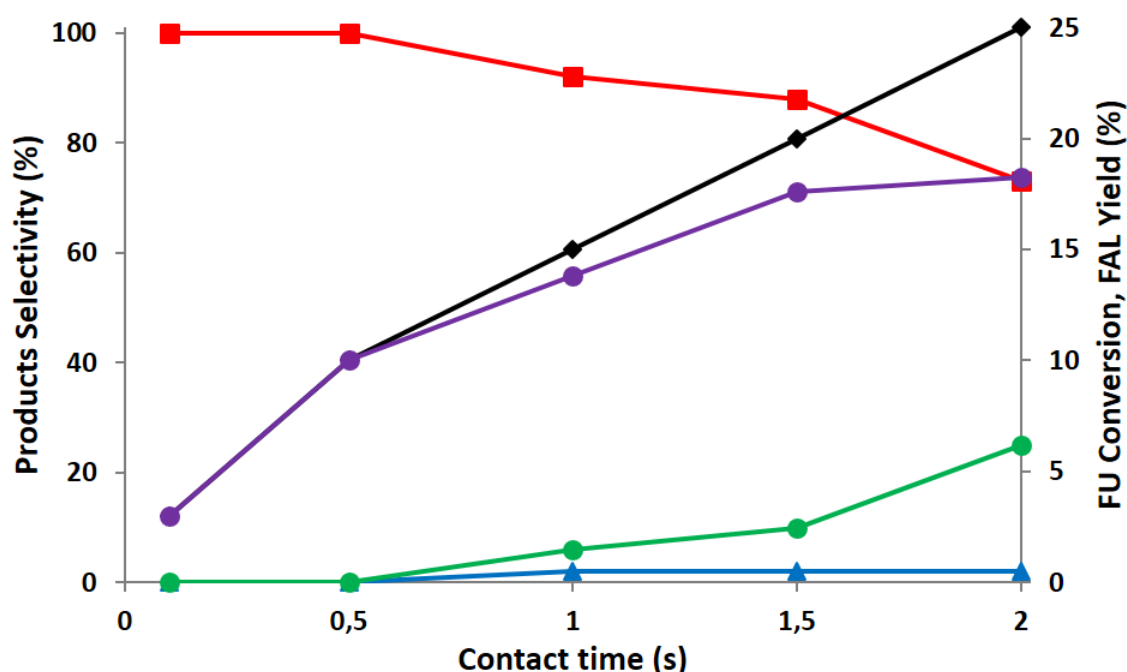
Figure 5-17. *Effect of time over FU conversion, products selectivity and FAL yield with CaO catalyst calcined at 700°C. Feed composition: FU 5%, CH₃OH 50%, N₂ 45%; Pressure 1 atm, reaction temperature 350°C, overall gas residence time 0,1 ÷ 2,0 s. Legend: FU conversion (♦), FAL selectivity (■), FAL Yield (●), MF selectivity (▲), C-loss (●).*

In these catalytic tests the overall gas residence time was varied, changing the volume of the catalyst loaded inside the tubular reactor and keeping fixed the total volumetric flow, from 0,1 s to 2,0 s in order to evaluate the effect over the substrate conversion and the products distribution.

In **Figure 5-17** (**Table 5-4**) was reported the effect of the contact time over FU conversion and products distribution; the plotted results were related to the average values obtained between the 2nd and the 6th hour of the monitored time on stream; as described above for the effect of reaction temperature further detail regarding the possibility to mediate the

results obtained after the first reaction hour will be described in the section regarding the effect of the reaction time.

Contact time (s)	FU Conversion (%)	Product Selectivity (%)			FAL Yield (%)
		FAL	MF	C-Loss	
0,1	3	100	0	0	3
0,5	10	100	0	0	10
1,0	15	92	2	6	14
1,5	20	88	2	10	18
2,0	25	73	2	25	18

Table 5-4. *Effect of contact time on FU conversion, product selectivity and FAL yield with CaO catalyst calcined at 700°C. Feed composition: FU 5%, CH_3OH 50%, N_2 45%; Pressure 1 atm, reaction temperature 350°C, overall gas residence time 0,1 ÷ 2,0 s.*

At low contact time the catalyst showed to be totally selective in the production of FAL as the only reduction product then, at the increase of the overall residence time, the catalyst became always less selective towards the production of the unsaturated alcohol against the progressive increase of the heavy carbonaceous compounds formed over the catalyst surface. Indeed, 100% of FAL selectivity with no C-Loss were obtained at 0,1 and 0,5s while, at 2,0 s the selectivity towards FAL decreased to 73% and the C-Loss increased up to 25%. Concerning the formation of MF, only a slight increase was observed in the contact time windows tested.

In our previous work concerning the evaluation of the catalytic activity of MgO in the same reaction we reported that the heavy deposits formed on the catalyst surface mainly derive from a thermal degradation of the furanic species involved in our reaction, in particular from FU or better from the unsaturated alcohol FAL[5]. As a matter of fact, FAL was a monomer used in the polymer industries for the production of thermostatic resins; thus, could undergoes into oligomerization processes to form heavy compounds over the catalyst's surface[15,16]. The polymerization process of FAL could be considered a consecutive reaction, favored at the increase of the contact time and so in agreement with the increase of the C-Loss term registered as a function of the contact time.

Finally, regarding the conversion of FU, a progressive increase was registered at the increase of the tested contact time. At 0,1s the registered conversion was 3% and then increase up to the value of 25% obtained at 2,0s.

Summarizing the information obtained evaluating the effect of the contact time it was possible to confirm two main aspect related to the catalytic activity of a basic catalyst in the catalytic transfer hydrogenation of furfural by-means of methanol as hydrogen source. The first consisted in the possibility to identify an optimal contact time at which the catalyst showed the best catalytic performance at which the best compromise between substrate conversion, FAL selectivity and yield was reached. In particular 1,5 s was identified as the optimal residence time considering the 20% of FU conversion and the selectivity in FAL next to the 90%.

On the other hand, the obtained results allow to confirm that over a basic catalyst, in condition of low-medium temperature, the catalytic transfer hydrogenation proceed through the classic MPV (Meerwin-Poondorf-Varley) mechanism. In particular the mechanism provide the presence of both the molecules, the carbonyl substrate and the hydrogen source, absorbed and activated simultaneously over the catalyst surface; then, the reduction proceed through the formation of a six-membered ring intermediate that bring to the formation of the product. Furthermore, it was also confirmed that using CaO FAL was the primary reduction product while MF and the oligomer produced from FAL degradation were consecutive products considered that their selectivity increased at the increase of the contact time. In **Scheme 5-3** was reported an overall reaction pathway for the catalytic transfer hydrogenation over CaO that summarized the main information reported.
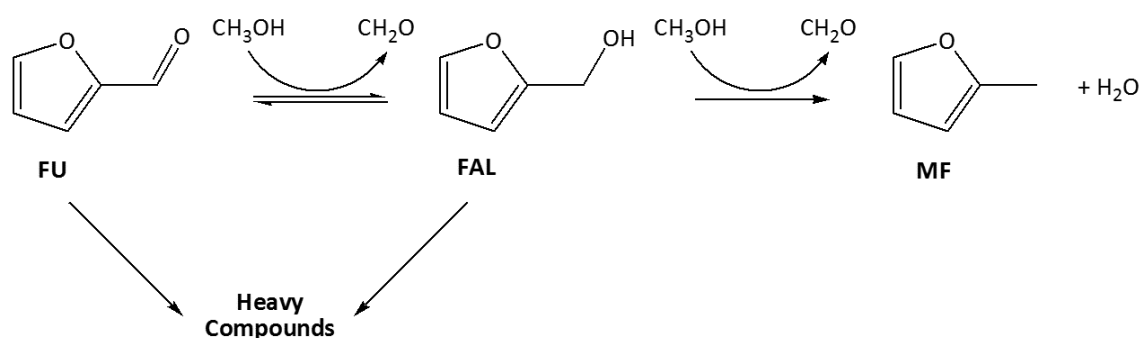
Scheme 5-3. *Overall reaction pathway for the catalytic transfer hydrogenation of FU by-means of methanol over CaO catalyst.*

5.2.5. Catalytic transfer hydrogenation of FU over CaO catalyst: effect of reaction time

The stability of the catalyst in the catalytic transfer hydrogenation reaction has been examined by conducting catalytic tests with the catalyst for 6 h at the optimized reaction condition determined above. In particular, the calcination temperature of the precursor was 700°C, the reaction temperature 350°C and the overall gas residence time 1,5s.

Figure 5-18 showed the effect of the reaction time over FU conversion, products selectivity and FAL yield.

CaO catalyst clearly showed a different behavior both in terms of substrate conversion and in terms of products distribution between the first and the following hours of the monitored time on stream. Indeed, in the first hour, FU conversion was close to the 30% with a selectivity in FAL slightly higher than the 60% and the C-Loss term, related to the formation of carbonaceous deposits over the catalyst surface, attested at 34%. Starting from the second hour of reaction, the catalytic performance changed completely and a lower FU conversion (20%) was registered coupled with a notable increase of FAL selectivity that grew up to the value of 85%, according to this a deep decrease of the C-Loss was observed.

A second important feature showed by the catalyst was the almost stable performance, in terms of conversion and selectivity, registered starting from the second hour. Indeed, both FU conversion and products selectivity showed to be constant, within the experimental errors, during the remaining five monitored hours of reaction.

The stable catalytic performance showed by CaO consisted an important feature if compared to the activity showed by MgO in the same reaction[5]. Therefore, we demonstrated that CaO was a stable and highly selective catalyst for the process of catalytic transfer hydrogenation of FU to produce FAL using methanol while, MgO showed the drawback to suffer of a slight deactivation phenomena at low temperature during the time on stream due to the deposition of heavy compounds over the surface that caused a decreasing of FU conversion.

Furthermore, it that has to be highlighted that, in contrast to the trend of FAL selectivity, a stable yield toward the unsaturated alcohol was obtained starting from the first hour of reaction. Thus, considering the higher FU conversion and the lower FAL selectivity in the first hour, it could be concluded that during the first 60 minutes the higher amount of

furfural converted, compared to that transformed in the other hours, was degraded to heavy compounds.
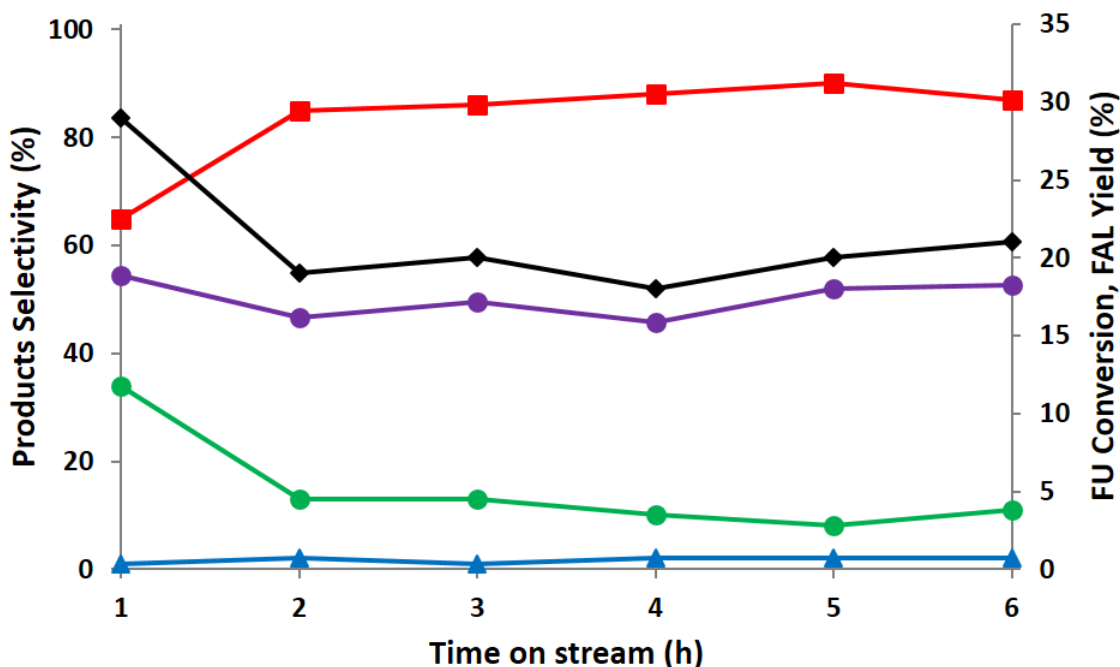
Figure 5-18. *Effect of reaction time over FU conversion, products selectivity and FAL yield with CaO catalyst calcined at 700°C. Feed composition: FU 5%, CH₃OH 50%, N₂ 45%; Pressure 1 atm, reaction temperature 350°C, overall gas residence time 1,5 s. Legend: FU conversion (♦), FAL selectivity (■), FAL Yield (●), MF selectivity (▲), C-loss (●).*

Time on stream (h)	FU Conversion (%)	Product Selectivity (%)			FAL Yield (%)
		FAL	MF	C-Loss	
1	29	65	1	34	19
2	19	85	2	13	16
3	20	86	1	13	17
4	18	88	2	10	16
5	20	90	2	8	18
6	21	87	2	11	18

Table 5-5. *Effect of reaction time over FU conversion, products selectivity and FAL yield with CaO catalyst calcined at 700°C. Feed composition: FU 5%, CH₃OH 50%, N₂ 45%; Pressure 1 atm, reaction temperature 350°C, overall gas residence time 1,5 s.*

The catalytic tests performed at 350°C, with different contact time, confirmed the different behavior showed by the catalyst during the time on stream. As an examples in **Figure 5-19** were reported the trends of FU conversion and FAL selectivity for the catalytic tests performed at 350°C at 1,0-1,5-2,0s respectively. For all the tested

conditions a notable decrease of FU conversion was observed between the first and the following hours; furthermore, starting from the second hour the performance became stable. Concerning the selectivity toward FAL the tests performed at 1,0 s and 2,0 s showed the same trend of the test performed at 1,5 s; after an initial low selectivity registered in the first hour a notable increase was observed from the second hour. These results suggested that the catalyst probably undergoes in a change during the first hour of reaction.
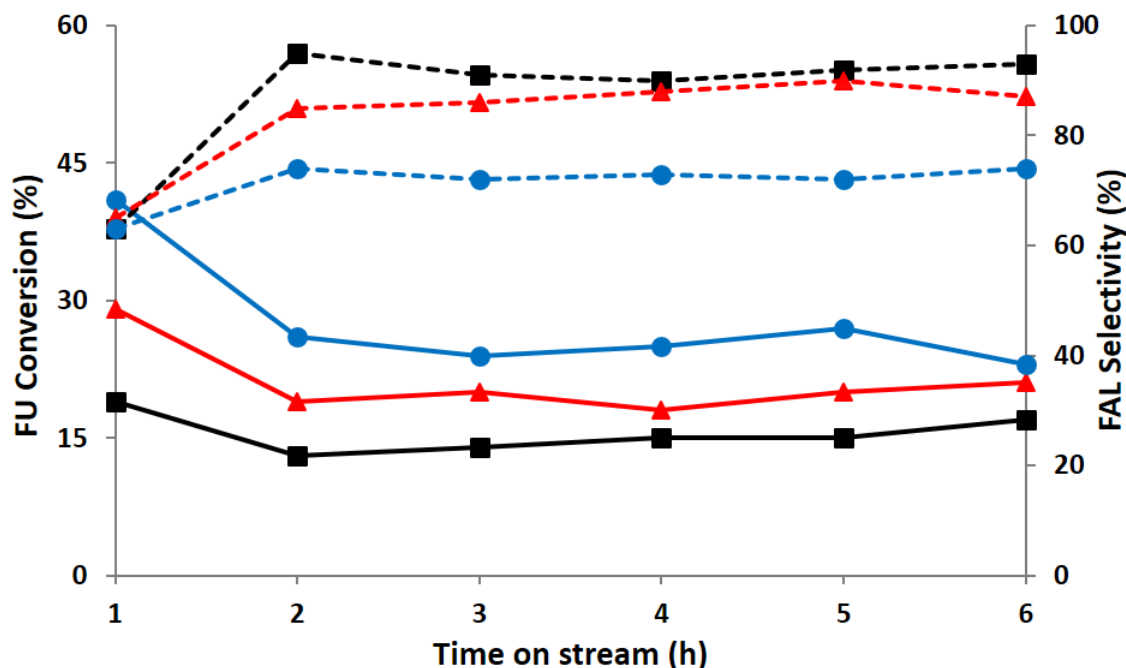
Figure 5-19. *Effect of reaction time, at different contact time, over FU conversion and FAL selectivity with CaO catalyst calcined at 700°C. Feed composition: FU 5%, CH₃OH 50%, N₂ 45%; Pressure 1 atm, reaction temperature 350°C, overall gas residence time 1,0 ÷ 2,0 s. Legend: contact time 1,0 s (▬), contact time 1,5 s (▬), contact time 2,0 s (▬); FU conversion (bold line), FAL selectivity (dotted line).*

$$CH_3OH \rightarrow H_2CO + H_2 \tag{1}$$

$$CH_2O \rightarrow CO + H_2 \tag{2}$$

$$CO + H_2O \rightarrow CO_2 + H_2 \tag{3}$$

$$2\ CH_2O \rightarrow CH_3O\text{-}C(O)H \tag{4}$$

$$CH_3OC(O)H \rightarrow CO_2 + CH_4 \tag{5}$$

$$2\ CH_2O + H_2O \rightarrow CH_3OH + HCOOH \tag{6}$$

$$HCOOH \rightarrow CO_2 + H_2 \tag{7}$$

$$CH_3OH + H_2O \rightarrow CO_2 + 3H_2 \tag{8}$$

Scheme 5-4. *Summary of main reactions occurring to methanol in the catalytic transfer hydrogenation reaction with FU.*

In order to gain more information about the different behavior showed by the catalyst during the time on stream, the trend of the light compounds in the outlet stream exiting from the reactor have been monitored. Indeed, in several our previous works, we have demonstrated that in our typical reaction condition methanol could be subjected to various reactions, summarized in **Scheme 5-4**, that finally bring to the formation of only light compounds such as CO, CO_2, CH_4 and H_2. Briefly, regarding the main reaction reported in **Scheme 5-4**, methanol could de-hydrogenate into H_2 and formaldehyde, while the decomposition of the latter bring to the formation of CO and H_2 (Reaction 1 and 2). Alternatively, two adsorbed CH_2O may disproportionate to formate and a methoxy species yielding methylformate (reaction 4) (the latter can also be formed by Tishchenko dimerization), which decomposes at high temperatures to CH_4 and CO_2 (reaction 5). In the presence of water in the feed, formaldehyde may also produce formic acid and methanol through the Cannizzaro reaction (reaction 6), with formic acid then easily decomposing to CO_2 and H_2 (reaction 7) Moreover, the role of water in WGS (reaction 3) or methanol reforming (reaction 8) cannot be disregarded.

According to that described above, in our catalytic tests the only light compounds detected were CO, CO_2, CH_4 and H_2; the amount of these, formed as a function of the time on stream at the residence time of 1,5 s and 350°C, were reported in **Figure 5-20**. It was clear that the trend of the lights reflected the same behavior observed for the organic compounds collected and analyzed after each hour of reaction. Indeed, the analysis of the plotted results, clearly highlighted that the catalyst suffered of some modification during the first hour of reaction. As a matter of fact, the amount of the light compounds, formed as a consequence of methanol and formaldehyde degradation, showed a different trend between the first and the following reaction hour confirming what previously obsereved for FU conversion and products distribution.

Taking the catalytic test performed at the residence time of 1,5s as an examlpe, it has to be highlighted that in the first hour of reaction H_2 was the main light compound produced, it was detected in amount about ten times higher compared to other lights that were produced in a very low quantity. Then, starting from the second hour, the trend of the lights was completely overturned; the molecular hydrogen production dropped down but, despite this, H_2 was still the light with the higher production but, if compared to the value registered in the first hour, the difference with other gaseous products decreased many times. CO and CH_4 were almost produced in the same quantity of the first hour while CO_2 progressively increased. According to the reaction set reported in **Scheme 5-4** carbon

dioxide could be mainly produced as a consequence of the methylformate decomposition or as a co-product of the Tishchenko reaction in which traces of water in the feed as impurities reacts with formaldehyde.

A further confirmation of the initial high production of H_2 and of the progressively increase of the CO_2 detected starting from the second hour of reaction was obtained from the monitoring of these light compounds in the catalytic tests performed at 350°C and overall gas residence time of 1,0 s and 2,0 s respectively (**Figure 5-21**). The comparison between the moles of H_2 and CO_2 produced, on the base of reacion time, at the different contact time allowed also to demonstrate that increasing the latter an overall increase of both H_2 and CO_2 moles was observed.
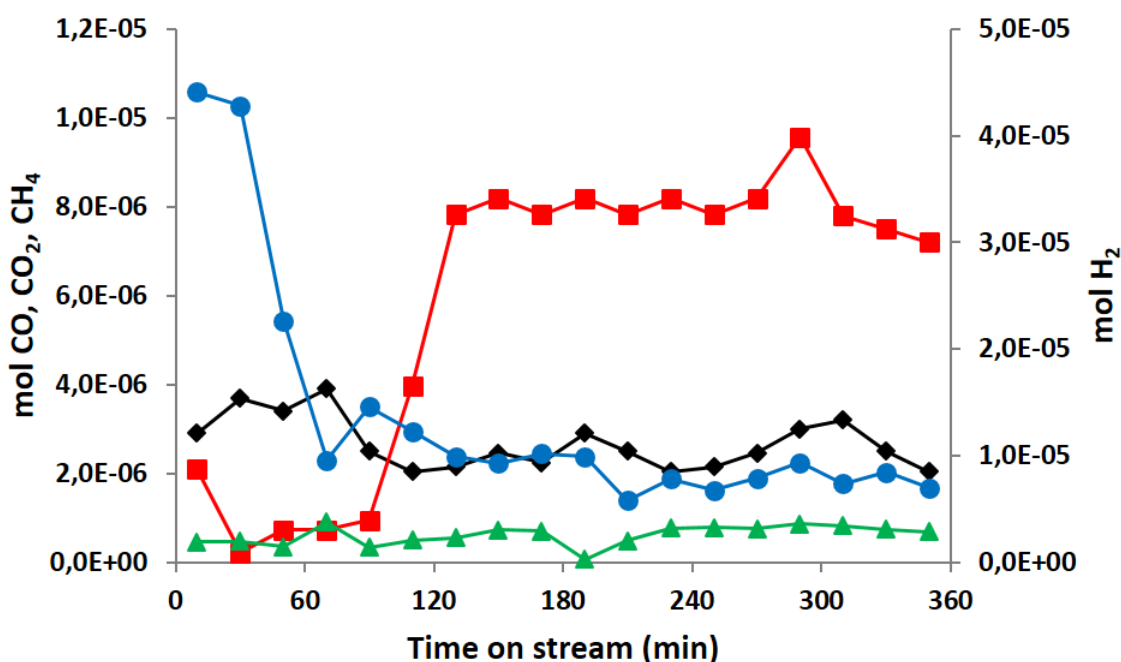
Figure 5-20. *CaO catalyst. Number of moles of gas formed, based on the time, in the reaction of FU reduction with methanol. Feed composition: FU 5%, CH_3OH 50% , N_2 45% ; Pressure 1 atm, T = 350°C, overall gas residence time 1,5 s. Legend: CO (♦), CO_2 (■), CH_4 (▲), H_2 (●).*
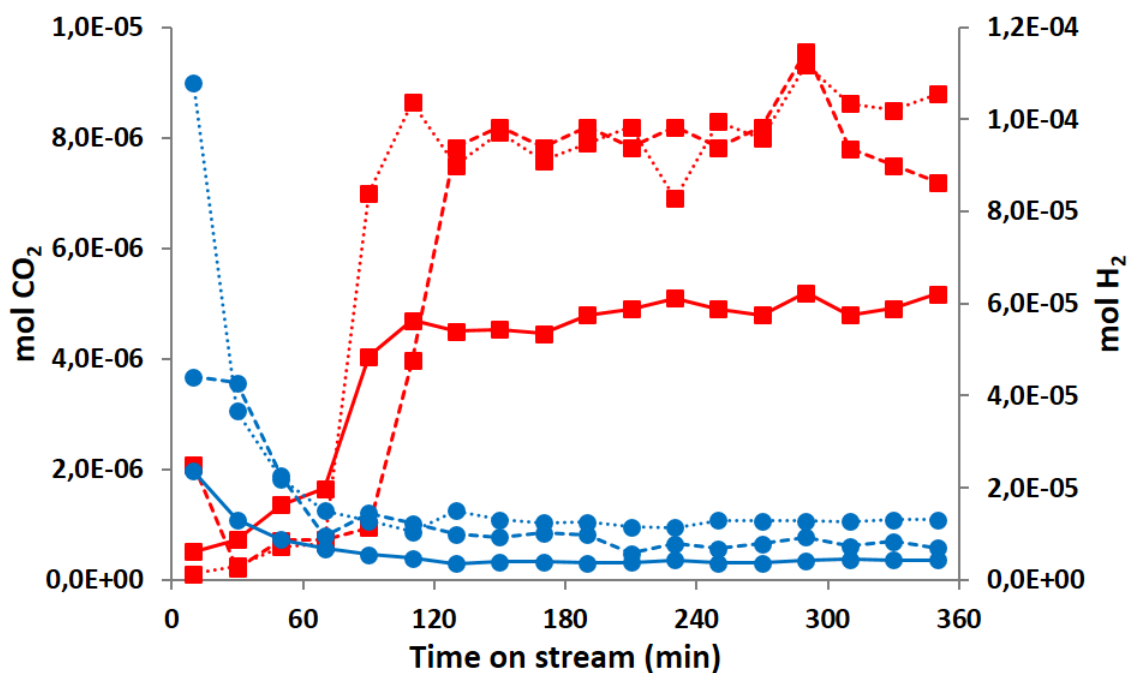
Figure 5-21. *Comparison between the moles of CO_2 and H_2 produced, based on the time, in the reaction of FU reduction with methanol over CaO calcined at 700°C. Feed composition: FU 5%, CH_3OH 50%, N_2 45% ; Pressure 1 atm, T = 350°C. Legend: CO_2 (■), H_2 (●); bold line τ = 1,0 s; dotted line τ = 1,5 s; punctuated line τ = 2,0 s.*

In the present work it has been demonstrated that CaO acted as an heterogeneous basic catalyst, furthermore, in the former part, it was determined that its precursor consisted in $CaCO_3$ and that, once calcined at the proper temperature to form the oxide phase, the latter was able to interact with CO_2 to reform the carbonate specie. Thus, it could be hypothesized that the interaction between the calcined CaO and the in-situ produced CO_2 was the main cause for the different catalytic behavior showed by the catalyst in the first reaction hour. In order to gain evidence that supported the formulated hypothesis XRD and TGA/DTA characterization over the spent catalysts were performed.

In **Figure 5-22** was reported the comparison between the diffraction patterns of the fresh CaO calcined in static air at 700°C and that of the samlpe used in the catalytic transfer hydrogenation test performed at 350°C and contact time of 1,5s. It was clear that the two patterns showed to be different. Indeed, as described above, the sample calcined at 700°C showed the lime CaO structure while, the sample used in reaction, showed an higher number of reflexes that was demonstrated to agree with those of $CaCO_3$ (calcite). Thus, it could be concluded that the used catalyst consisted in a mixed crystalline phase of CaO (lime) and $CaCO_3$ (calcite).

112

In order to gain more information about the phenomena just described, the spent catalysts used in reaction were also characterized with TGA/DTA analysis. In **Figure 5-23** were compared the thermograms and the differential thermal analysis performed over the spent catalysts and the precursor. All the spent catalysts showed two main weight loss in the analized range of temperature. The former, between 200°C and 450°C, considering the exothermic peaks registered at the differential thermal analysis could be assigned to the removal of the carbonaceous deposits formed over the catalyst surface during the reaction. The second was instead observed in the range between 600°C and 750°C, considering the endothermic peaks at the DTA and the temperature corresponding to that of the catalyst's precursor decomposition, could be related to the decomposition of the partial carbonate phase formed during the reaction.

Furthermore, it could be also concluded that the re-carbonatation of CaO was partial and not affected all the bulk of the solid. Indeed, XRD analysis showed that the most intense reflex detected were the ones related to the calcite phase; in addition the weight loss in the region of carbonate decomposition was lower than 15% for the catalysts used in reaction instead of the 44% registered in the case of the decomposition of the precursor.
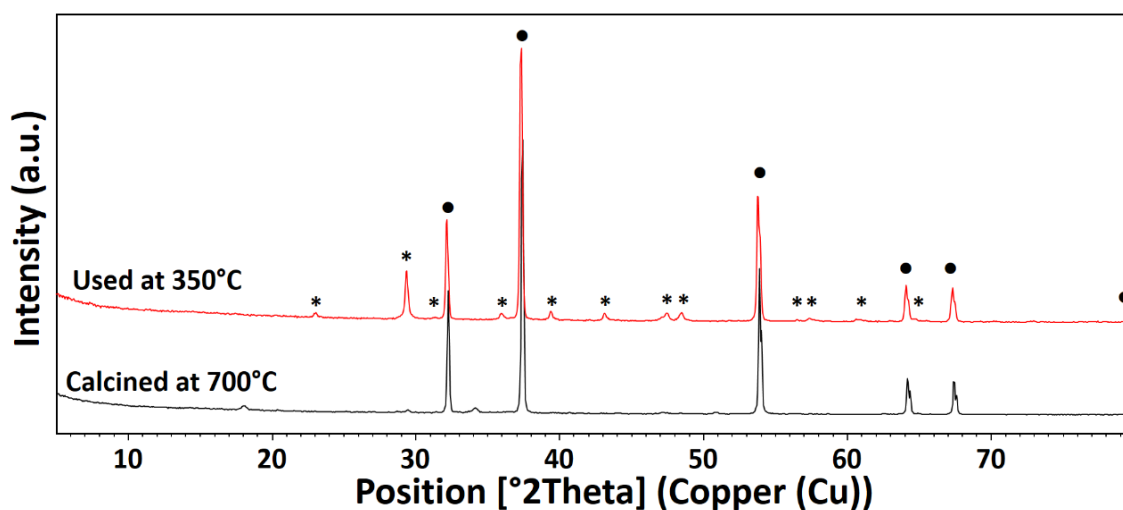
Figure 5-22. *XRD patterns of the fresh CaO sample calcined at 700°C and that of the spent used in the catalytic test at 350°C. Reference patterns: (●) CaO, (*) CaCO$_3$ Calcite.*
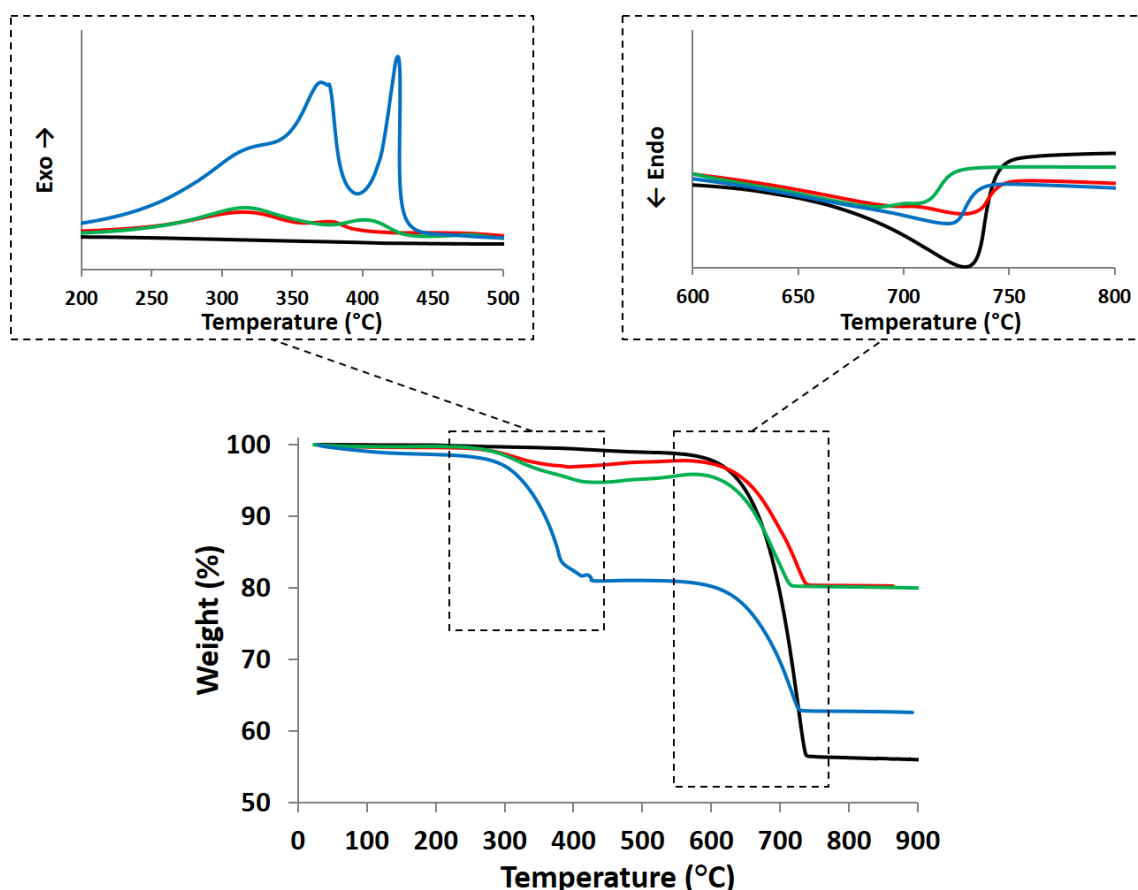
Figure 5-23. *Thermogravimetric and differential thermal analysis performed in air over different sample of CaO. Legend: CaO precursor (━), CaO used in the catalytic test at 300°C (━), CaO used in the catalytic test at 350°C (━), CaO used in the catalytic test at 400°C (━).*

Since it was demonstrated that the catalyst suffered of a structural change during the first hour of reaction due to the interaction with the reagents, it could be also concluded that the different catalytic perfomances, in terms of conversion and products distribution, showed by the catalyst between the first and the following hours of reaction was connected to the carbonatation process.

Furthermore, it has also to be highlighted that the mixed phase obtained after the re-carbonatation process was much more selective in the hydrogen transfer process considered the minimization of the heavy compounds formed and the higher FAL selectivity obtained starting from the 2nd hour. As well as the high H_2 production in the first hour could be related to a low efficiency of the catalyst in the hydrogen transfer mechanism. Indeed, in literaure it was reported that the mechanism for the hydrogen transfer reaction over basic catalyst follow the MPV mechanism for which, the reduction proceed through a concerted step that involve the contemporary adsorption and activation of both the carbonyl and the hydrogen source molecule to form a six-membered ring

intermediate that then evolved to the desortion of the products. Thus, considering the concerted reaction mechanism, the lower was the amount of molecular hydrogen produced during the process the higher was the efficiency of the catalyst in hydrogen transfer mechanism.

5.2.6. Catalytic transfer hydrogenation of FU over CaO catalyst: effect of feed composition

The effect of the feed composition has been investigated in order to evaluate if the catalytic activity of the basic CaO catalyst could be influenced by the amount of the organic content present in the feed. The reasons why the effect of the feed composition, in particular in term of the total organic content, has been investigated were mainly two. The former was related to the low surface area showed by the catalyst while, the second, was related to the possibility to further improve the catalytic performance in terms of FU conversion and FAL selectivity, yield and productivity.

Concerning the low surface area it was reported above that CaO calcined at 700°C had a specific surface area of 2,4 m^2/g. In our previous work concerning the same process performed using $FeVO_4$ as heterogeneous catalyst with low surface area (12 m^2/g), it was demonstrated that an overall improvement of the catalytic performance was obtained decreasing the organic content present in the feed[17]. In the case of the mixed vanadium-iron oxide decreasing the total organic content from 55% molar (5% molar of FU and 50% molar of methanol) to 11% molar (1% molar of FU and 10% molar of methanol), an overall increase of FU conversion from the few percentage points obtained in the condition of high organic content to the complete conversion with yield in MF up to the 90% in the condition of low organic content was obtained.

Taking into account these information the effect of the organic content in the feed on the catalytic activity was evaluated following the same strategy applied for the mixed iron-vanadium oxide. The catalytic tests were performed at the optimized reaction conditions (calcination temperature 700°C, reaction temperature 350°C, overall gas residence time 1,5 s), decreasing the total organic molar content in the feed from 55% (5% mol FU + 50% mol CH_3OH) to 11% (1% mol FU + 10% mol CH_3OH), keeping constant the relative methanol to furfural molar ratio.

Entry	Feed composition (%mol)			Total organic content (%)	CH₃OH/FU mol ratio	FU Conversion (%)	Selectivity (%)			FAL Yield (%)
	FU	CH₃OH	N₂				FAL	MF	C-Loss	
1	1	10	89	11	10	35	45	1	54	20
2	5	50	45	55	10	20	88	2	10	18
3	5	5	90	10	1	4	46	0	54	2
4	5	25	70	30	5	10	50	0	50	5
5	5	75	20	20	25	20	97	1	2	19

Table 5-6. *Effect of the feed composition on FU conversion and products distribution for CaO catalyst. Feed composition: variable, Pressure 1 atm, reaction temperature 350°C, overall gas residence time 1,5 s.*

The results obtained were reported in **Table 5-6** (Entries 1 and 2). At a first analysis the results seemed to be in opposition to what previously observed. Indeed, in the test performed feeding the low amount of organic, only a slight increase of FU conversion, from 20% to 35%, was registered in comparison to that obtained with the high organic content. Moreover, the trend showed by FAL selectivity was much more surprisingly, considering that the value obtained with the low organic condition was about the half, 45% instead of 88%. Furthermore, the lower selectivity in FAL was accompanied by an increase of the C-Loss and, in general, a poorer carbon balance was registered.

Considering the results obtained in the condition of low organic content, a possible phenomenon of FU preferential adsorption over the catalyst surface towards methanol was hypothesized to explain the lower FAL selectivity and the slight increase of FU conversion.

In order to find evidence to support the formulated hypothesis several catalytic tests have been performed keeping constant the molar percentage of FU in the feed, equal to 5%, and varying progressively the molar percentage of methanol, in the range between 5% and 75%; thus resulted also in a change of the relative methanol to furfural molar ratio. Therefore, if a progressive increase of both FU conversion and FAL selectivity would be observed at the increase of the methanol to furfural molar ratio, the hypothesis of FU preferential adsorption over the catalyst surface could be demonstrated.
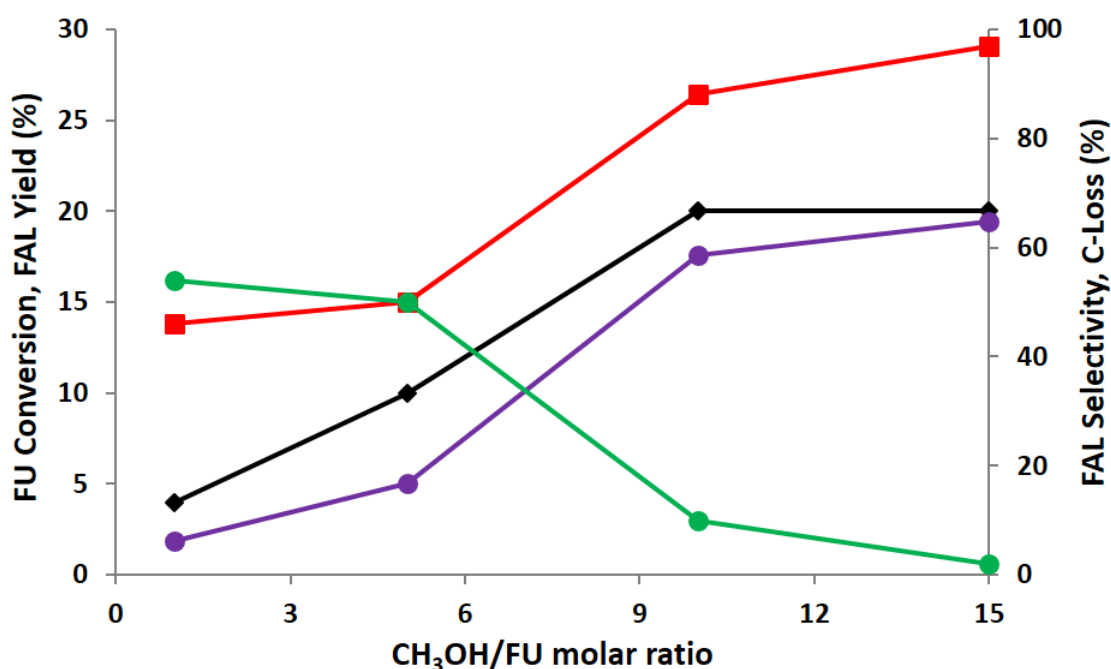
Figure 5-24. *Effect of feed composition over FU conversion, products selectivity and FAL yield with CaO catalyst calcined at 700°C. Feed composition: FU 5%, CH₃OH 5 ÷ 50%, N₂ 20 ÷ 90%; Pressure 1 atm, reaction temperature 350°C, overall gas residence time 1,5 s. Legend: FU conversion (♦), FAL selectivity (■), FAL Yield (●), C-loss (●).*

In **Figure 5-24** were reported the results of these catalytic tests. The results obtained showed to be in agreement with the formulated hypothesis of a preferential absorption of FU towards methanol over the catalyst surface. Indeed, at the increase of the methanol to furfural molar ratio in the feed a progressive increase of the conversion of FU from the 4% obtained with the unitary molar ratio to the 20% detected at the higher molar ratio was registered (**Table 5-6** Entries 2, 3, 4 and 5). A second evidence that supported the formulated hypothesis was the trend showed from both the FAL selectivity and the C-Loss. As a matter of fact, the progressively increase of the conversion at the increase of the methanol to furfural molar ratio was accompanied with the rapid increase of the selectivity in the unsaturated alcohol and a drop of the heavy carbonaceous compounds formed as a consequence of degradation phenomena. In particular, FAL selectivity grew up from the 45% obtained with the unitary molar ratio to the 97% detected in the condition of the larger excess of methanol in the feed. The greater excess of methanol could be a drawback in the case of a possible scale up to bigger plant; despite this, considering the boiling points of the main involved compounds (b.p. FU = 96°C, b.p. FAL = 170°C, b.p. methanol = 65°C), an easy recycle, after a separation by distillation, of the unreacted methanol and FU could be possible, increasing the feasibility of the scale up.

Summarizing this part it was possible to demonstrate that the composition of the feed, both in terms of total organic content and relative methanol to furfural molar ratio, was a parameter that directly affected the catalytic activity of CaO in the catalytic transfer hydrogenation process. Furthermore, it was demonstrated that FU had a preferential absorption towards methanol over the surface of the catalyst. Finally, tuning the reaction conditions in terms of methanol to substrate molar ratio, a condition in which the catalyst showed to be totally selective in the formation of FAL as the only reduction product was found; thus, an improvement of the catalytic performance has been reached.

5.2.7. Conclusions regarding the use of bulk CaO as heterogeneous basic catalyst for the gas-phase catalytic transfer hydrogenation of FU to FAL

CaO was shown to be active in the gas-phase catalytic transfer hydrogenation of the biomass-derived FU using methanol as the hydrogen source. 350°C was demonstrated to be the optimal reaction temperature at which the selectivity toward FAL was maximized and the formation of the heavy compounds formed, on the catalyst surface, as a consequence of thermal degradation involving FU and FAL in our reaction conditions was minimized. Furthermore, it was demonstrated that FU undergoes in a preferential adsorption toward methanol over the surface of the catalyst. The understanding of this phenomena allow also to tune the reaction conditions, in terms of total organic content in the feed and relative methanol to furfural molar ratio, in order to improve the catalyst performance and the possibility to produce FAL with total selectivity was observed feeding a relative methanol to furfural ratio equal to 15. Moreover, considering that FAL was the only reduction product obtained with CaO, it was demonstrated that the catalytic transfer hydrogenation process proceed through the classic MPV mechanism that involve the formation of the six-membered ring intermediate.

Due to the high selectivity, CaO offers an alternative to FAL production from FU without the need for H_2 at high pressure and precious metal catalysts.

5.3. MgO and CaO: a comparison between the catalytic activity of two heterogeneous basic catalysts in the gas-phase catalytic transfer hydrogenation of FU to FAL using methanol as H-transfer reactant

In the present section of the work, a comparison between the activity of the basic materials MgO and CaO in the gas-phase catalytic transfer hydrogenation of FU by-means of methanol as the hydrogen source has been examined. Indeed, in our previous work, we reported on the activity of MgO in the mentioned process. Briefly, in that work it was demonstrated that at low temperature the magnesium-based catalyst was completely selective toward the production of FAL as the only reduction product; despite this, the catalyst showed to suffer of limited deactivation phenomena during the time on stream due to the deposition of oligomeric carbonaceous species over the surface. On the other hand, in the present work, we reported that also CaO, in the proper reaction condition, could be totally selective in the production of FAL. Thus, a comparison between the two catalysts has been performed in order to find an explanation able to correlate the very similar catalytic activity and the deep difference of surface area showed by the two metal oxides considering that the latter has been identified as one of the main feature that directly affected the activity of a basic catalyst in the catalytic transfer hydrogenation process.

In **Table 5-7** were reported the main features at which the two catalysts showed the best performance in the studied reaction. In addition to the deep difference of specific surface area the two systems showed several different characteristics. First of all, a different calcination temperature was required to decompose the precursor and form the oxide phase. Indeed, $Mg(OH)_2$, precursor of MgO, decomposed in the temperature range between 250°C and 400°C; thus the magnesium precursor was treated at 500°C in order to keep a stable structure with an high surface area. On the other hand, for $CaCO_3$, precursor of CaO, only calcination temperature equal or higher than 700°C allow to form the oxide structure.

Entry	Feature	MgO	CaO
1	**Specific surface area (m²/g)**	200,0	2,4
2	**Calcination Temperature (°C)**	500	700
3	**Total Basicity (mmol/g) [a]**	7,05	2,57
4	**Basicity surface density (mmol/m²) [a]**	0,0353	1,0708
5	**Total Basicity [b]**	7,51	2,35
6	**FU molar % in the feed**	5	5
7	**CH₃OH molar % in the feed**	50	75
8	**N₂ molar % in the feed**	45	20
9	**CH₃OH/FU molar ratio**	10	15
10	**Reaction Temperature (°C)**	250	350
11	**Contact Time (s)**	1,5	1,5
12	**FU Conversion (%)**	60	20
13	**FAL Selectivity (%)**	100	97
14	**MF Selectivity (%)**	0	2
15	**C-Loss**	0	1
16	**FAL Yield (%)**	60	19
17	**FAL Production (mol FAL produced/h)**	3,97E-3	1,34E-3
18	**FAL Specific Productivity (mol FAL/h*m²)**	1,98E-5	5,37E-4
19	**CaO/MgO specific productivity ratio**	27	

***Table 5-7.** Main characteristics of MgO and CaO. The reported catalytic performance are related to the gas-phase reduction process.*

> a. *Determined by irreversible adsorption of acrylic acid;*
> b. *Determined by CO_2-TPD.*

The total basicity (**Table 5-7** Entry 3), determined by-means of the irreversible adsorption of acrylic acid, showed that MgO was characterized by the presence of an higher number of basic sites compared to CaO. Despite this, taking also into account the difference of specific surface area, the number of basic sites characterizing the surface of CaO was not so low. Thus means that the density of the basic sites on the surface was clearly higher for CaO (**Table 5-7**Entry 4). In order to gain more insight regarding the total basicity of the solids as well as the strength of the basic sites, CO_2-TPD analysis were performed over the analyzed systems. The amount of the basic sites determined using CO_2 as the

probe molecule were very similar to the ones titrated with acrylic acid for both the catalysts used; in particular the presence of an higher number of basic sites for MgO, 7,51 instead of the 2,35 observed for the calcium-based oxide, was confirmed. Regarding the strength of the sites, the analysis of the CO_2-desorption curve demonstrated that CaO basic-sites were stronger compared to the ones of MgO. Indeed, for the latter the desorption of the CO_2 was in the temperature range between 50 and 500°C while for CaO the desorption took place at higher temperature (500÷750°C). Another important difference between the two catalysts was the composition of the feed, both in term of total organic content and in term of relative methanol to furfural molar ratio, at which the best catalytic performance was obtained. With CaO the best performance was obtained feeding a methanol to furfural molar ratio equal to 15 instead of the 10 necessary with MgO. The higher methanol amount needed with CaO was related to the preferential absorption phenomena that FU showed to have towards methanol over the catalyst surface.

Concerning the reaction temperature, MgO showed the maximum of activity at 250°C while for CaO 350°C was identified as the optimal condition; the latter catalysts was indeed completely not active at 250°C. This trend confirmed the data obtained in the liquid phase catalytic transfer hydrogenation of FU by-means of methanol. Indeed, as reported in the former part of the present chapter, an increase of the reaction temperature from 160°C to 210°C was necessary with CaO in order to obtain the same catalytic performance showed by MgO at the lower temperature (100% of FAL yield).

FU conversion, FAL selectivity and the FAL specific productivity calculated on the base of the surface area of the catalysts were reported in **Figure 5-25** (**Table 5-7** Entries 13, 14 and 19). Both the systems showed to be almost totally selective toward the production of FAL as the only reduction product; with MgO 100% of FAL selectivity was registered while, with CaO, 97% of FAL selectivity was detected with the addition of MF traces. Concerning FU conversion (**Table 5-7** Entry 13), with MgO the 60% of substrate conversion was registered instead of the 20% showed by CaO.

In the previous paragraphs of the work it was mentioned that the number of basic sites present over the surface and so, in the most of the cases, the specific surface area of the catalyst, was a key parameter directly affecting the activity of a basic catalyst in the process of catalytic transfer hydrogenation. Nevertheless, also the number of the defective sites over the surface play an important role on the catalyst's activity. In this view, considering the deep difference of surface area between the two catalysts (SSA of MgO

~ 80 times of SSA of CaO), the 20% of FU conversion obtained with CaO could be considered an unexpected value if compared to the 60% observed with MgO. Indeed, with a specific surface area 80 times lower a conversion of "only" one third was obtained.

In order to gain more insight about this phenomenon, a specific FAL productivity based on the surface area of the catalysts was calculated for both the sample (**Table 5-7** Entry 19). For CaO this value was about 27 times higher compared to that of MgO, suggesting that the basic active sites of the former were more active in the catalytic transfer hydrogenation reaction. In addition, the superficial basic-sites density, calculated referring the total number of the basic sites to the specific surface area (**Table 5-7** Entry 4), seemed also to play a direct role in the explanation of the higher specific activity of CaO. That value was indeed more than one magnitude order higher of that showed by MgO indicating that the basic-sites density directly affected the activity. Furthermore, the strength of the basic sites must not be disregarded.
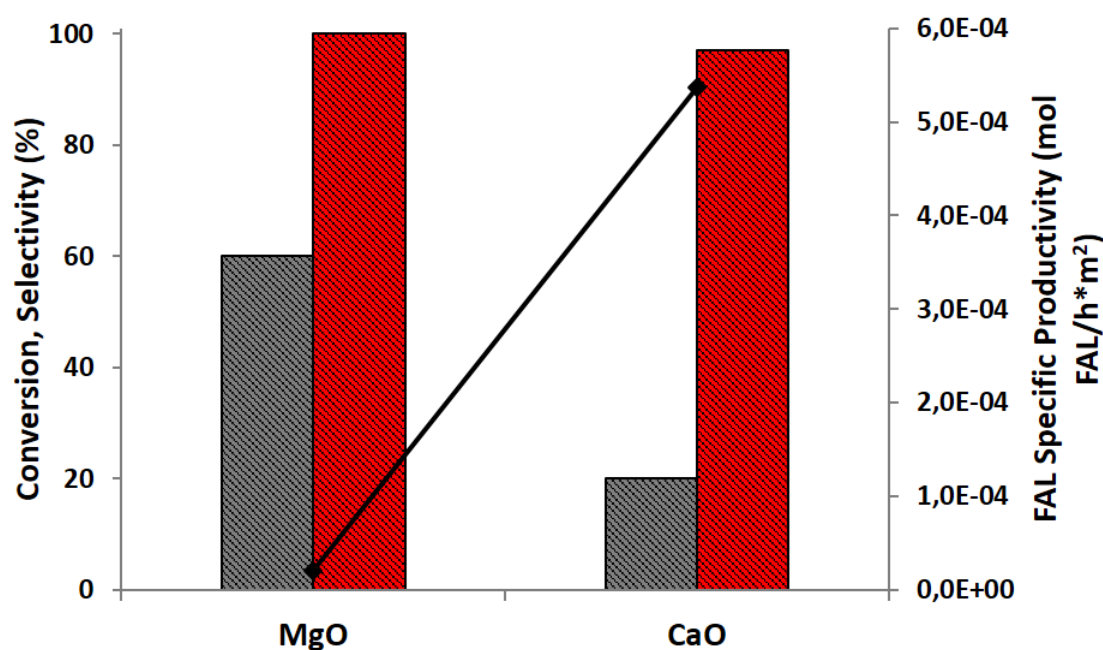
Figure 5-25. *Comparison of the catalytic performances of MgO and CaO at their best reaction conditions. Legend: FU conversion (■), FAL selectivity (■), FAL specific productivity (━).*

Summing up this part, it could be concluded that the limited difference in term of catalytic activity between MgO and CaO in the gas-phase catalytic transfer hydrogenation of FU for the production of FAL, was related to particular basic features of the latter catalyst that make up for the deep difference of specific surface area. In particular, it could be concluded that both the higher superficial basic-sites density as well as the higher strength of the basic sites characterizing the bulk CaO compared to that of MgO were the responsible for the high specific activity of the calcium-based material.

5.4. Study of the CTH reaction network over heterogeneous basic-based catalysts

In the last paragraph of the present chapter, the study of the catalytic transfer hydrogenation reaction network has been conducted in order to summarize and explain the main differences highlighted by the used catalysts. Indeed, as deeply discussed above, the reaction of FU reduction to produce FAL and MF has been studied with two different plant-layout strategies. The former consisted in a discontinuous liquid-phase plant in which it was demonstrated that, in the proper condition of reaction temperature, both MgO and CaO could be used as stable and reusable heterogeneous basic catalysts for the selective production of FAL. As a matter of fact, both the catalysts showed to produce FAL as the only reduction product with 100% of yield.

In a second moment, considering the interesting results obtained in the liquid-phase process, a continuous gas-phase plant in which were evaluated the catalytic performances of the pristine MgO and that of the mixed oxide Mg/Fe/O in the catalytic transfer hydrogenation process was developed. In that work it was confirmed that at low temperature (250°C) MgO was totally selective in the production of FAL as the only reduction product while, with the mixed magnesium-iron oxide, at 380°C, the 75% of yield in MF was detected[5].

It was clear and it was also reported in literature[7], that the introduction of the iron into the lattice of the MgO caused a modification of the acid-base, de-hydrogenating, de-oxygenating and redox properties of the catalyst. The key point was to investigate and understand if these properties, introduced by the insertion of iron, could be used to explain the difference MF production showed by the two magnesium-based catalysts. Furthermore, considering that the introduction of iron lead to the introduction of both acid and redox properties, due to the redox couple Fe^{3+}/Fe^{2+}, a mixed Mg/Al/O system was tested in the same reaction in order to gain more insight about the effect deriving by the introduction of a pure acid guest cation into the lattice of MgO. The aluminum-containing system showed higher FU conversion compared to the pristine MgO and lower than that obtained with the iron-containing system (**Table 5-8**), highlighting that the introduction of aluminum could increase the activity of MgO towards the CTH reaction but, at the same time, it was confirmed that the major increase in activity was obtained with the iron-system. Concerning the products distribution, the introduction of aluminum lead to a

decrease of FAL selectivity with a parallel increase of MF production if compared to MgO; on the other hand, a lower MF production was registered if the iron-containing systems was considered as the reference catalyst. Moreover, the poorest carbon balance was obtained.

Finally, we also reported on the activity of CaO in the gas-phase CTH reduction of FU to FAL. It was demonstrated that the calcium-based catalyst was totally selective towards the formation of FAL as the only reduction product exhibiting a catalytic activity similar to that showed by MgO.

Entry	Catalyst	FU Conversion (%)	Selectivity (%)			Yield (%)	
			FAL	MF	C-Loss	FAL	MF
1	MgO [a]	52	75	5	20	39	3
2	CaO [b]	20	97	2	1	19	< 1
3	Mg/Fe/O [a]	93	1	80	19	1	75
4	Mg/Al/O [a]	63	41	22	37	26	14

Table 5-8. *FU conversion, products selectivity and yield obtained with the different basic-based catalysts. Reaction conditions:*

   a. *Feed composition: 5% FU, 50% CH₃OH, 45% N₂; pressure of 1 atm, T = 380°C, overall gas residence time of 1,1 s, reaction time 1 h;*

   b. *Feed composition: 5% FU, 75% CH₃OH, 20% N₂; pressure of 1 atm, T = 350°C, overall gas residence time of 1,5 s, reaction time 1 h.*

Thus, with the aim to further investigate the reaction mechanism of the CTH reduction of FU to produce FAL and MF over the pristine basic catalysts MgO and CaO and the mixed $Mg/M^{3+}/O$ (M^{3+} = Fe or Al) using methanol as hydrogen source we tried to verify the involvement of the formaldehyde, produced as a consequence of the methanol de-hydrogenation in our typical reaction condition, for the production of MF. The methanol to formaldehyde de-hydrogenation reaction was indeed strongly influenced, for the magnesium-based catalysts, by the insertion of heteroatoms such as Fe^{3+} or Al^{3+} into the lattice of pristine MgO.

Indeed, in our previous work concerning the gas-phase methylation of phenol over MgO-based catalysts[18] , we have demonstrated that a direct disproportion reaction, involving salycilic aldehyde, or salycilic alcohol, and the formaldehyde produced from methanol, with the parallel release of CO_2, could be a possible reaction pathways for the direct formation of o-cresol (**Scheme 5-5**). This work also demonstrated that salycilic alcohol

was the primary product derived from nucleophilic attack of formaldehyde on the activated orto position of the aromatic ring. Furthermore, it was established that the salycilic aldehyde could be produced as a consequence of the disproportion process in which two salycilic alcohol molecules were respectively converted into one molecule of salycilic aldehyde and one of o-cresol. Important experimental evidence that supported the involvement of the direct disproportion reaction involving formaldehyde in the formation of high quantity of o-cresol was the detection of a high amount of CO_2 in the outlet stream. Indeed, the amount of the latter was higher to that expected considering the main reaction of methanol decomposition over MgO-based catalysts.
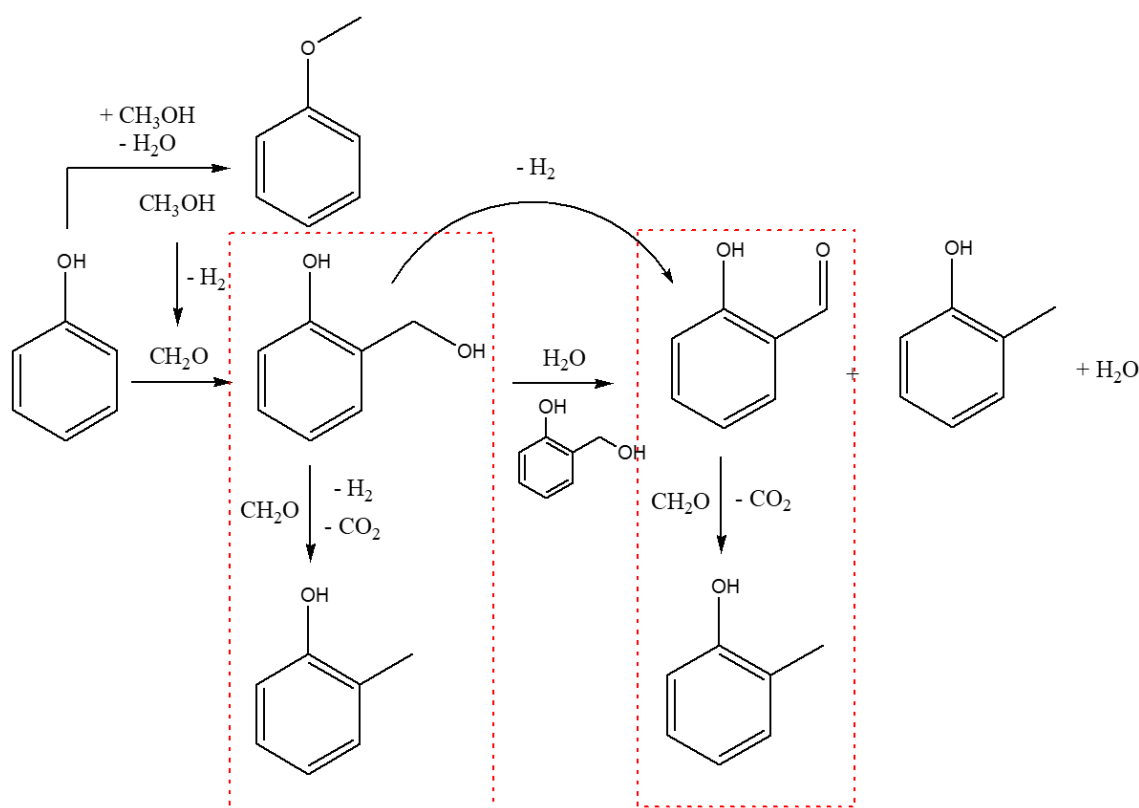
Scheme 5-5. *Overall reaction pathway of phenol alkylation with methanol over MgO-based catalysts. In dashed square were highlighted the two possible disproportion reactions involving salycilic alcohol or salycilic aldehyde and formaldehyde.*

In order to gain more information about the reaction mechanism for the formation of FAL and MF and to evaluate the possible involvement of the formaldehyde in a direct disproportion reaction, similarly to that reported above for the alkylation of phenol, several catalytic tests with MgO, CaO, Mg/Fe/O and Mg/Al/O feeding both FU and FAL as reducible substrates and different hydrogen sources such as methanol, formaldehyde, isopropanol, acetone and acetaldehyde have been performed. In particular, these catalytic tests were performed with the aim to demonstrated if the acid-base features, but also de-hydrogenating and de-oxygenating properties of the tested catalysts and, furthermore, the ability to activate the formaldehyde as a reducing agent could play a direct role in the conversion of FU to FAL and MF.

Prior to the catalytic tests the different systems have been characterized with BET, XRD, irreversible adsorption of acrylic acid and n-propylamine, CO_2 and NH_3-TPD, H_2-TPR in order to gain information on the relative acid, basic and redox properties. In **Table 5-9** are summarized the main characteristics of the catalysts used.

Table 5-9 summarizes the main features of the catalysts. First, it has to be highlighted that different calcination temperatures are necessary in order to allow the formation of the active phase between the Mg-based systems and CaO. For the latter 700°C has been identified as the optimal condition at which the carbonate precursor is transformed into the oxide specie while, for the former catalysts, 500°C is enough to decompose the hydrotalcite-type precursor. The XRD pattern collected over the calcined samples confirmed the formation of the active phases; CaO shows a calcite crystalline structure while MgO a single well-defined periclase phase. Conversely, the dried Mg/Fe/O and Mg/Al/O showed a hydrotalcite-like structures, leading after calcination to broad XRD lines, corresponding to a quasi-amorphous MgO phase. The latter XRD pattern well agrees with those reported in the literature[19,20,21] for the formation of a Mg/Fe and Mg/Al mixed oxide, in which incorporation of a trivalent Fe^{3+}, or Al^{3+}, cation into the MgO lattice generates cationic defects and produces a low degree of crystallinity. No appreciable shifts of XRD reflexes have been observed, because the ionic radius of the Fe^{3+} (0.69 Å) cation is similar to the radius of Mg^{2+} (0.65 Å) and the one of Al^{3+} is lower (0.50 Å).

Entry	Feature	Catalyst			
		MgO	**CaO**	**Mg/Fe/O**	**Mg/Al/O**
1	M^{2+}/M^{3+} molar ratio	-	-	2	2
2	Calcination T (°C)	500	700	500	500
3	Crystalline phase (XRD)	MgO (periclase)	CaO (lime)	MgO-like mixed oxide	MgO-like mixed oxide
4	SSA (m²/g)	200	2,4	140	132
5	Total basicity (mmol/g) [a]	7,05	2,57	3,89	4,87
6	Surface basic-site density (mmol/m²) [a]	0,0353	1,0708	0,0278	0,0369
7	Total basicity (mmol/g) [b]	7,51	2,35	3,72	4,48
8	Total acidity (mmol/g) [c]	0	0	0,087	0,224

Table 5-9. *Main characteristics of the basic-based catalysts.*

a. *Determined by irreversible adsorption of acrylic acid;*

b. *Determined by CO_2-TPD;*

c. *Determined by NH_3-TPD;*

Concerning the trend showed by the surface area the deep difference showed between the calcium- and the magnesium-based materials well agrees with the general values reported in literature[8,9]; the lower surface area showed by CaO is mainly related to the higher temperature required to decompose the precursor and form the oxide phase. Nevertheless, the decrease of surface area observed in the Mg/Fe/O and Mg/Al/O compared to that exhibited by pristine MgO could be related to the distortion of the crystalline structure of the material deriving from the introduction of the trivalent cations into the lattice of MgO. The determination of the total amount of basic sites was performed by means of two different techniques: the irreversible adsorption of acrylic acid and the CO_2 temperature programmed desorption. The results obtained with the two different probe molecules well agree one with each other (**Table 5-9** Entries 5 and 7) confirming the basic feature of the studied catalysts. Getting more into the details, pristine MgO shows the higher number of basic sites while, according to the introduction of the acid cations iron and aluminum, a decrease of the basicity has been observed for the mixed oxides Mg/Fe and Mg/Al. Indeed, the higher electronegativity which characterized both Fe^{3+} and Al^{3+} with respect

to Mg^{2+} decreases the charge density and makes the O^{2-} less electrophilic than in pure MgO; the iron containing mixed oxide, which is characterized by a number of basic sites between 3,7 and 3,9 mmol/g, resulted the sample with the lower basicity in the Mg-based family. On the other hand CaO was found to be characterized by the lower amount of basic sites, equal to 2,57 mmol/g. Despite this it has to be highlighted once more, as reported in the former section of the chapter, that the number of basic sites characterizing CaO material has to be referred to the lower specific surface area, resulting in the higher surface basic-sites density (**Table 5-9** Entry 6).

Furthermore, the CO_2-TPD analysis allow to get more insight about the strength of the basic sites. In literature is indeed generally reported that, based on the CO_2 desorption temperature, the curve could be divided into three regions each of that represents different basic sites[22]. The classification could be resumed as follows:

- weak basic sites (surface hydroxyl groups): CO_2 desorption in the temperature range 25÷125°C;
- medium basic sites (oxygen atoms in Mg^{2+}-O^{2-} pairs): CO_2 desorption in the temperature range 125÷225°C;
- strong basic sites (low coordinated oxygen anions in superficial defectively sites): CO_2 desorption at temperature higher than 225°C.

The analysis of the CO_2 desorption profiles reported in **Figure 5-26** demonstrates that the catalysts are mainly characterized by medium and strong basic sites; furthermore, the introduction of iron and aluminum into the lattice of MgO seems to mainly decrease the number of the strong basic sites.
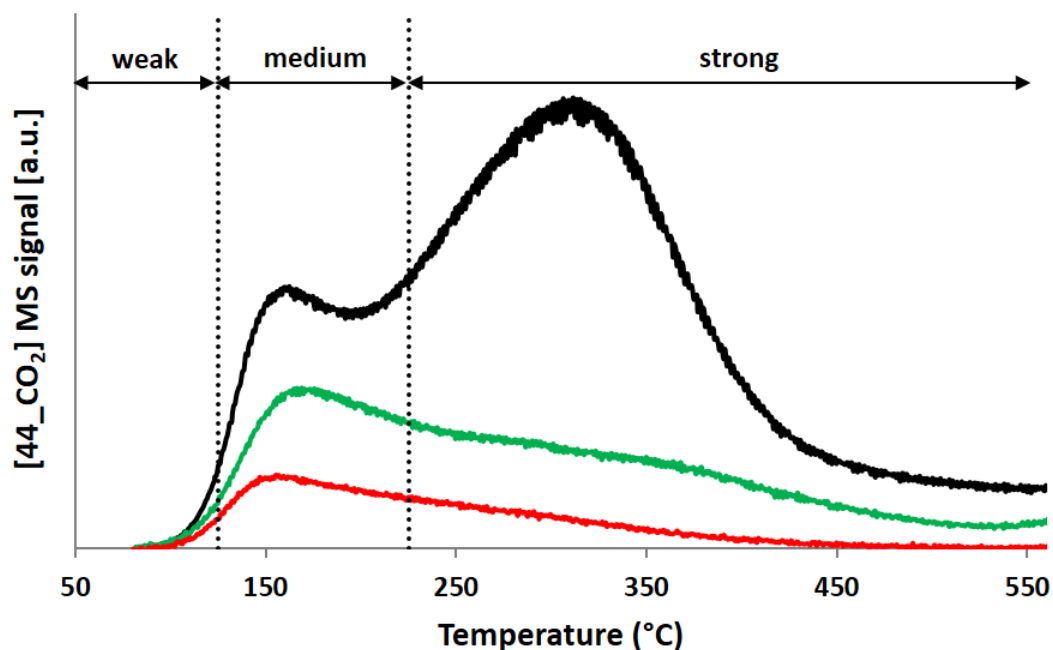
Figure 5-26. *Example of CO_2-TPD analysis performed over the MgO-based catalysts. Legend: MgO (—), Mg/Al/O (—), Mg/Fe/O (—).*

The determination of the acid features of the catalysts, performed by-means of NH_3-TPD desorption (**Table 5-9** Entry 8), demonstrated that the pristine oxides MgO and CaO do not exhibit any acidic behavior while, for the mixed oxides Mg/Fe/O and Mg/Al/O, the presence of acid sites has been confirmed. According to that reported in literature by Di Cosimo et al.[23] the introduction of aluminum into the lattice of MgO brings to the formation of the higher number of Lewis acid sites. Furthermore, it has to be highlighted that the introduction of Al is generally reported to be crucial only for the formation of Lewis acid sites while, the introduction of iron allow the formation of both acid and redox properties[6]. The ammonia desorption profiles (**Figure 5-27**) also demonstrated that the strength of the acid sites introduced with aluminum and iron were similar; both the doped MgO-systems showed an ammonia desorption peak in the range between 125 and 450°C.
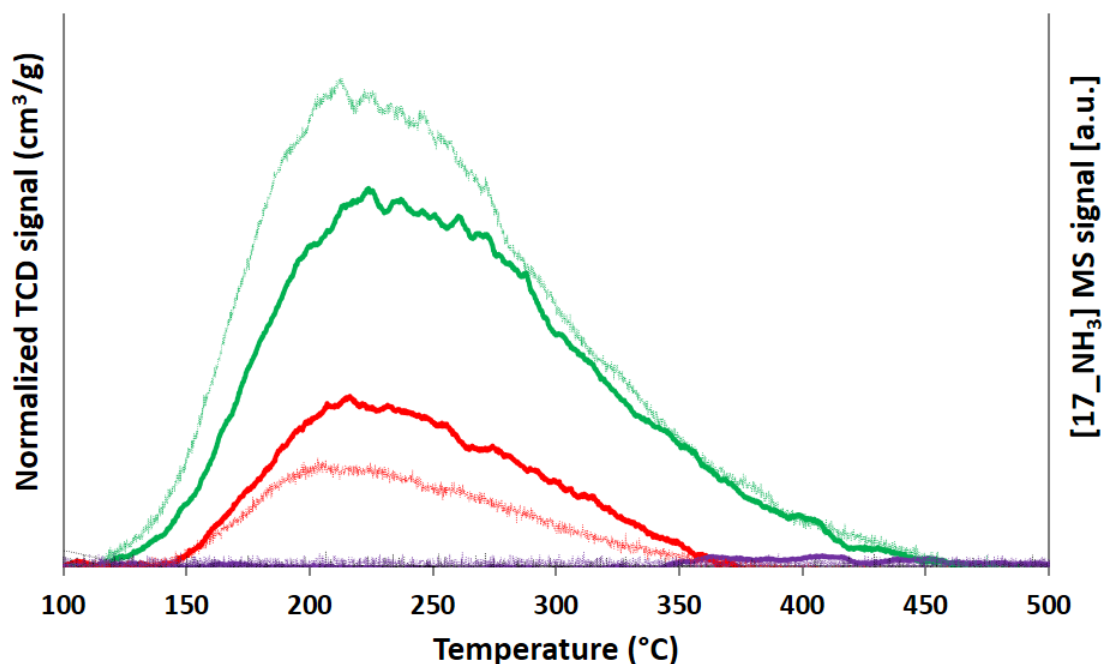
Figure 5-27. *Example of NH₃-TPD analysis performed over the MgO-based catalysts. Legend: MgO (━), Mg/Al/O (━), Mg/Fe/O (━), CaO (━); TCD signal (bold line), NH₃-MS signal (dotted line).*

In order to gain more insight about the redox properties of the studied systems H_2-TPR characterization have been performed. **Figure 5-28** reported the hydrogen signal registered at the mass detector. According to the information reported in literature the only catalyst exhibiting redox features was the iron-containing one. Indeed, for MgO, CaO as well as for the magnesium-aluminum mixed oxide, nil hydrogen consumption was observed up to 900°C; on the contrary, the iron containing system showed the consumption of hydrogen in the temperature range between 300 and 600°C.

The typical Fe_2O_3 (hematite) TPR pattern shows two peaks at 500 °C and 650 °C and a broad reduction feature at temperature higher than 700°C. Based on literature data, these peaks can be assigned to the reduction of Fe_2O_3 to Fe_3O_4, Fe_3O_4 to FeO and FeO to metallic iron, respectively[24,25,26]. Compared to pure hematite the co-precipitated Mg/Fe/O mixed oxide showed a significant shift to lower temperature of the peaks related to reduction of hematite to magnetite and the following to FeO. Furthermore, the separation of the two peaks was not observed indicating that the iron containing system was characterized by the presence of iron-species with higher reducibility behavior.

130
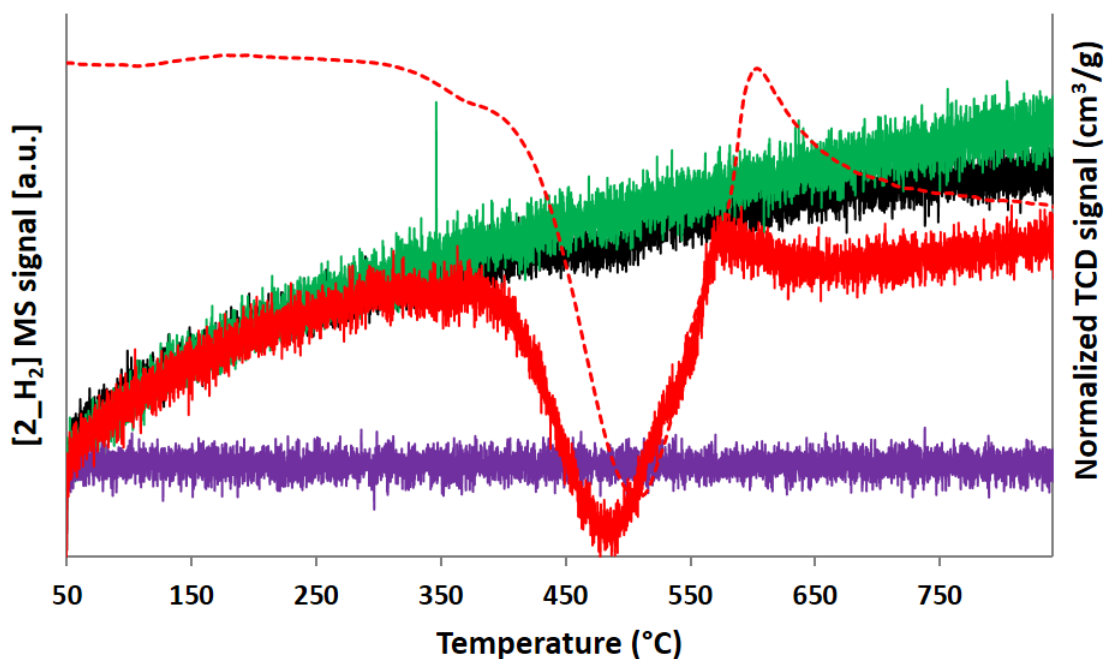
***Figure 5-28.** H_2-TPR profile of the studied catalysts. H_2-MS signal legend: MgO (━), Mg/Al/O (━), Mg/Fe/O (━), CaO (━); TCD signal for Mg/Fe/O (dotted line).*

In light of the above, the analysis of the catalytic performances in the catalytic transfer hydrogenation reaction of FU (**Table 5-8**) clearly shows that a simple correlation between the acid-basic features of the catalysts, deriving from the introduction of the guest cations Fe and Al, and the products distribution, in terms of de-oxygenation properties towards the formation of MF, is not present.

In the literature, the hydro-deoxygenation ability of a catalyst is generally associated with the Lewis acid sites present in the system; typical example are niobium oxide and zeolite which are used in liquid phase reactions. Indeed, the acid functionality catalyzes the dehydration of alcohol to form intermediates which will be substituted by surface hydride. On metal oxides, it is reported that the electron rich oxygen anions show basic properties and electron donating character, while the electron deficient metal cations show acidic character[27,28].

Nevertheless, in the case of the magnesium-based catalysts the modulation of acidity by-means of the introduction of iron and aluminium as guest cations brings to different results to that expected. Indeed, the higher acidity showed by the mixed oxide Mg/Al/O is not reflected into higher MF production that is instead obtained with the iron-containing catalyst. In order to better clarify the effect of acid-base properties over the catalytic activity the trend for MF Yield and C-Loss as a function of the total acidity as well as the trend of FAL Yield as a function of the total basicity showed by the different systems

have been reported in **Figure 5-29**. The analysis of the reported results further confirms that a direct correlation between the total acidity showed by the catalyst and the yield in MF is not present; despite this, it has to be highlighted that only with the mixed oxides Mg/Fe/O and Mg/Al/O MF is produced in appreciable amount. Thus, allow to hypothesized once more that the introduction of acidity could play a direct role in the mechanism of MF formation but, at the same time, that this characteristic is not the only and probably the most relevant to enhance the de-oxygenating feature of the catalyst.

On the other hand, a direct relationship between the total acidity and the formation of heavy carbonaceous compounds as a consequence of degradation reactions in which mainly FU and FAL undergoes in our reaction conditions is demonstrated. The higher is the acidity the higher is the C-Loss term; in the case of pristine MgO the carbon balance loss registered in the test at 380°C is mainly related to the thermal degradation of the species involved in the reaction; indeed, decreasing the temperature at 250°C nil loss is registered confirming the high selectivity towards the formation of FAL as the only reduction product.

Regarding the production of the latter compound a direct relationship with the total basicity has been highlighted. Indeed, for the pure basic systems MgO and CaO, the higher is the basicity the higher is the yield in FAL.

Thus, the overall comparison of the catalytic performance showed by the catalysts and the features of these it has been possible to further confirm that the acidity feature tuned with introduction of a guest cations into the lattice of a pristine basic catalyst is not the only characteristic that play a direct role in the mechanism of MF formation. This suggestion further confirms the necessity to investigate on the role of the in-situ generated formaldehyde that could be involved in a direct disproportion reaction with FU and FAL similarly to that previously demonstrated in the phenol methylation process (**Scheme 5-5**).

Therefore, to gain more information related to the former hypothesis, a complete series catalytic tests changing the hydrogen source have been performed.
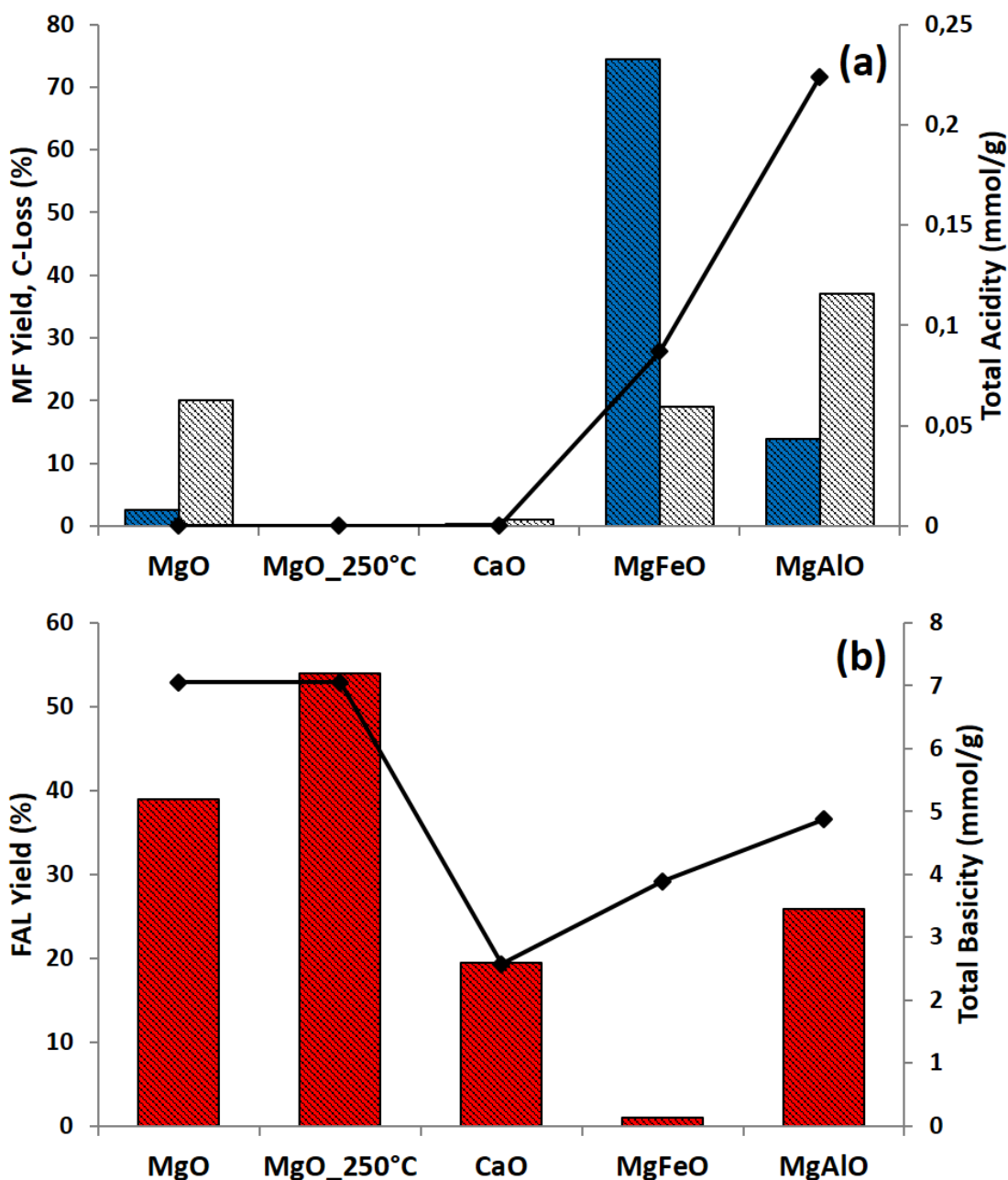
Figure 5-29. *(a) MF Yield and total amount of heavy carbonaceous species formed over the catalyst surface (C-Loss) as a function of the total acidity for the different catalysts. (b) FAL Yield as a function of the total basicity for the different catalysts. Legend: MF Yield (■), C-Loss (■), FAL Yield (■), total acidity/total basicity (━). Reaction conditions:*

- *MgO-based catalysts. Feed composition: 5% FU, 50% CH_3OH, 45% N_2; pressure of 1 atm, T = 380°C (or 250°C in the case of the second result reported for pristine MgO), overall gas residence time of 1,1 s, reaction time 1 h;*

- *CaO. Feed composition: 5% FU, 75% CH_3OH, 20% N_2; pressure of 1 atm, T = 350°C, overall gas residence time of 1,5 s, reaction time 1 h.*

Entry	Catalyst	Substrate	H-source	Reaction T (°C)	FU conversion (%)	Selectivity (%)		
						FAL	MF	C-Loss
1	MgO [a]	FU	CH₃OH	250	54	100	0	0
2				380	52	75	5	20
3			2-propanol	200	100	100	0	0
4				250	100	100	0	0
5				380	100	93	2	5
6			acetone	250	33	0	0	100
7				380	40	0	0	100
9			CH₂O	380	8	0	0	100
10			H₂	250	0	0	0	-
11				380	0	0	0	-
12	CaO [b]	FU	CH₃OH	350	20	97	2	1
13			2-propanol		57	98	2	0
14			acetone		19	0	0	100
15			CH₂O [c]		0	0	0	-
16			H₂		0	0	0	-

Table 5-10. *Catalysts MgO and CaO. FU conversion and products distribution as a function of the hydrogen-source molecule used at different reaction temperature. Reaction conditions:*

a. *MgO catalyst: Feed composition: 5% FU, 50% CH₃OH, 45% N₂; pressure of 1 atm, T = 380°C, overall gas residence time of 1,1 s, reaction time 1 h;*

b. *Feed composition: 5% FU, 75% CH₃OH, 20% N₂; pressure of 1 atm, T = 350°C, overall gas residence time of 1,5 s, reaction time 1 h;*

c. *CH₂O from formalin solution in water: 37% w/w CH₂O, 7-8% w/w CH₃OH.*

The first sets of experiments were performed feeding furfural as substrate over the pure basic oxides MgO and CaO using different molecules as hydrogen source (methanol, isopropanol, formaldehyde, acetone and acetaldehyde). In **Table 5-10** were reported FU conversion and products distribution as a function of the hydrogen source molecule used at different reaction temperature. The trend observed using MgO and methanol has been previously described[5]; briefly both at 250°C and 380°C (**Table 5-10** Entries 1 and 2) the catalyst showed 50% FU conversion and total selectivity towards FAL at the lower temperature. On the contrary, at 380°C the FAL selectivity decreased to 75% due to the formation of heavy carbonaceous compounds deriving from thermal degradation

processes involving the unsaturated alcohol. Furthermore, MgO at the higher temperature, lead to the formation of traces of MF (5% of selectivity).

Figure 5-30. *Effect of reaction time over FU conversion and FAL selectivity with MgO catalyst with different H-source. Feed composition: FU 5%, CH₃OH or isopropanol 50%, N₂ 45%; Pressure 1 atm, reaction temperature 250°C, overall gas residence time 1,1 s. Legend: FU conversion with CH₃OH (bold line), FU conversion with isopropanol (dotted line).*

Using a different hydrogen source, such as isopropanol, very efficient in the H-transfer process[13], the activity of MgO was strongly affected (**Table 5-10** Entries 3, 4 and 5). Indeed, complete FU conversion and almost total yield in FAL were registered at very low temperature (200°C). The higher conversion and FAL yield obtained feeding isopropanol instead of methanol supported the occurrence in the reaction of the classical H-transfer pathway mediated by a basic catalyst. Indeed, the intermolecular hydride transfer of the β-H in the alcohol to the carbonyl group, following the Meerwein−Ponndorf−Verley (MPV) mechanism, was favoured by secondary alcohols that were stronger reductants than primary ones. Furthermore, using isopropanol as the H-source, a higher stability during the time on stream was observed. Indeed, total conversion and total yield in FAL (100% of selectivity) were obtained for all the monitored time on stream while, using methanol, a slight and continue deactivation was observed due to the deposition of carbonaceous species deriving from methanol degradation (**Figure 5-30**).

Replacing isopropanol with acetone (**Table 5-10** Entries 6 and 7) very low activity was registered, both at 250°C and at 380°C, due to the absence of β-H acting as a hydrogen donor and a nil FAL production was obtained. The whole FU converted was transformed into heavy deposits over the catalyst surface. Furthermore, the effect as reducing agent of the molecular hydrogen produced in-situ as a consequence of the methanol dehydrogenation on the catalyst surface was investigated (**Table 5-10** Entries 10 and 11); the results of the catalytic tests confirmed that MgO, at both the temperature tested, was not able to activate H_2 as reducing agent.

The results obtained performing the same set of catalytic tests, replacing MgO with CaO, validated the ones observed with the former catalyst. Indeed, an increase of FU conversion from 20 to 57% was obtained feeding isopropanol instead of methanol as the hydrogen source, validating the former hypothesis for which the use of a more activated alcohol as hydrogen source allow to improve the catalyst performance. In the test performed using the secondary alcohol (**Figure 5-31**) was also observed that the catalyst kept a stable activity during the monitored time on stream. Nevertheless, it was also confirmed that a pure basic catalyst was not able to catalyze the following hydrogenolysis step to convert FAL into MF. Finally, CaO, as demonstrated above for MgO, was not able to activate both the formaldehyde and the molecular hydrogen produced in situ from methanol hydrogenation.

In conclusion, the results obtained with pristine MgO and CaO, demonstrated the hypothesis for which the gas-phase reduction of FU with methanol over the pure basic catalysts followed the classic mechanism of the catalytic transfer hydrogenation. The latter, as reported in literature, involved the formation of a six-membered transition state over the catalyst surface as the consequence of the simultaneous absorption and activation of the carbonyl specie and the hydrogen donor, this mechanism occurred in a concerted step, in which the H transferred never adsorbed onto the surface of the catalyst, that than evolve into the desorption of the reduced specie[29].
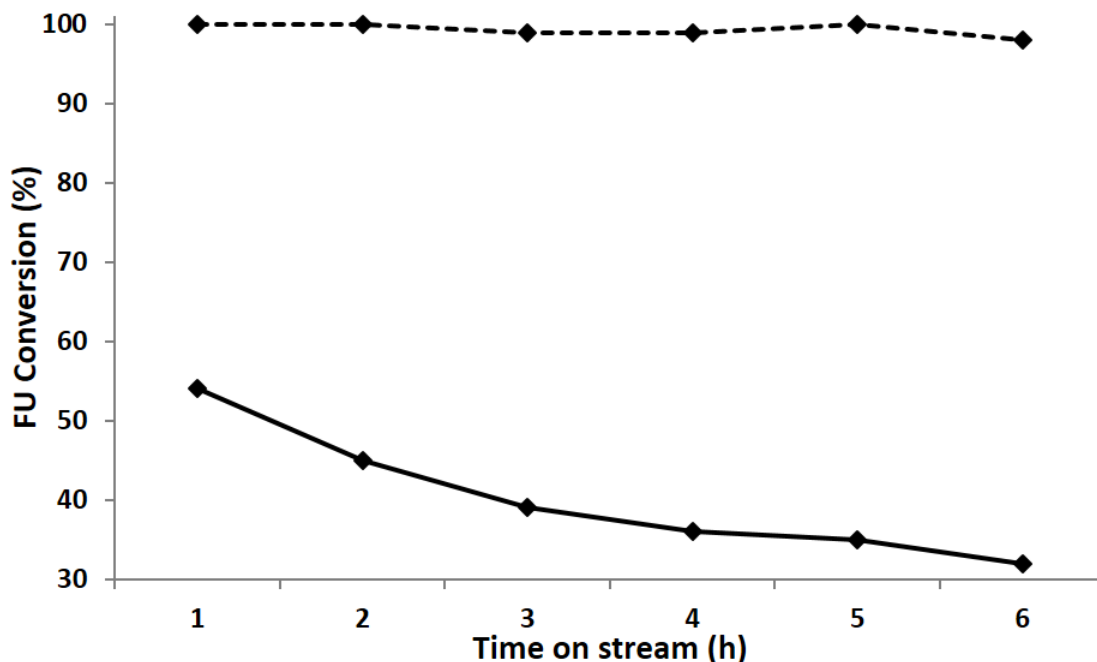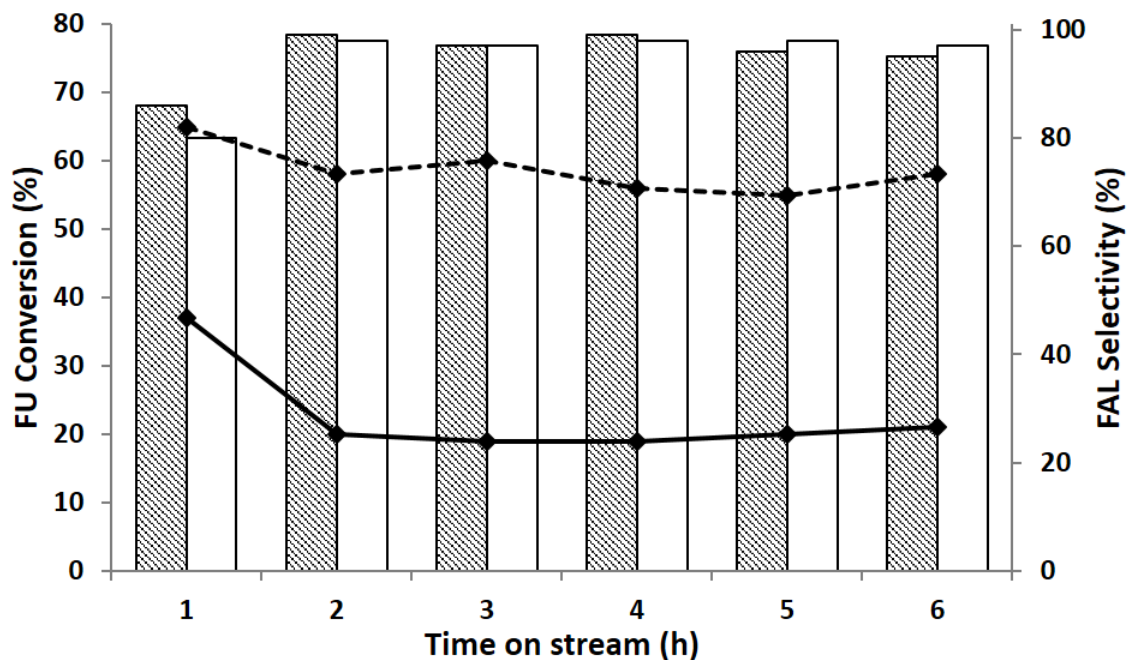
Figure 5-31. *Effect of reaction time over FU conversion and FAL selectivity with CaO catalyst with different H-source. Feed composition: FU 5%, CH_3OH or isopropanol 75%, N_2 20%; Pressure 1 atm, reaction temperature 350°C, overall gas residence time 1,5 s. Legend: FU conversion with CH_3OH (bold line), FU conversion with isopropanol (dotted line), FAL selectivity with CH_3OH (■-left/full bar), FAL selectivity with isopropanol (■-right/empty bar).*

The second sets of experiments were performed feeding FU or FAL as substrates over the mixed oxides Mg/Fe/O and Mg/Al/O at the fixed contact time of 1,1 s and 380°C as reaction temperature. These experiments were performed in order to find more insight about the mechanism for the formation of MF and gain more information to explain the deep different catalytic performance showed between the pristine basic catalysts and that containing iron or aluminum as guest cations (**Table 5-8**). Specifically, the intention was to evaluate if the formaldehyde, produced from methanol dehydrogenation, could act as "reducing agent" for a direct disproportion reaction in which FU or FAL were transformed into MF with the parallel release of CO_2 (**Scheme 5-6**) with a mechanism similar to that demonstrated for the gas-phase methylation of phenol (**Scheme 5-5**).
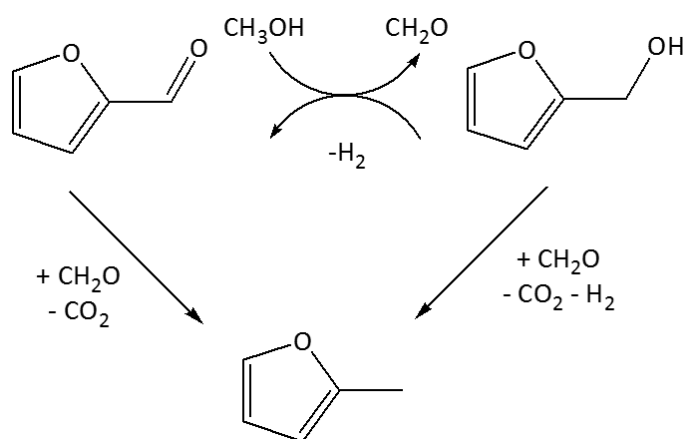
Scheme 5-6. *Possible reaction pathway for the direct production MF from FU and FAL as a consequence of the direct disproportion reaction involving the in-situ generated formaldehyde.*

As reported above the mixed Mg/Fe/O and Mg/Al/O were characterized by similar basic feature while, the acidity of the aluminium containing system was about three times higher to the one of the former. On the other hand, the iron containing catalyst showed redox properties, related to the Fe^{3+}/Fe^{2+} couple, that the aluminium one did not display. In **Table 5-11** were reported FU or FAL conversions and products distribution as a function of the used hydrogen source molecule with the two Mg/M/O mixed oxides. Considering at first the activity of the mixed Mg/Fe/O system, the catalytic test performed using methanol as the hydrogen source bring to the formation of the highest MF yield (**Table 5-11** Entry 1). The latter was also higher than to that obtained feeding isopropanol (**Table 5-11** Entry 2), a hydrogen transfer reactant much more active of methanol.

n°	Catalyst	Substrate	H-source	Conversion (%)		Selectivity (%)				MF yield (%)
				FU	FAL	FU	FAL	MF	C-loss	
1			CH$_3$OH	93	-	-	1	80	19	75
2			2-propanol	69	-	-	18	55	27	38
3	**Mg/Fe/O**	FU	acetone	20	-	-	0	0	100	0
4			acetaldehyde	15	-	-	22	0	78	0
5			CH$_2$O [a]	34	-	-	14	39	47	13
6			H$_2$	20	-	-	0	25	75	5
7			CH$_3$OH	63	-	-	41	22	37	14
8			2-propanol	89	-	-	81	18	1	16
9	**Mg/Al/O**	FU	acetone	43	-	-	0	0	100	0
10			CH$_2$O [a]	29	-	-	26	40	34	12
11			H$_2$	15	-	-	0	0	100	0
12			CH$_3$OH	-	55	16	-	60	26	33
13			2-propanol	-	68	9	-	74	17	50
14			acetone	-	77	12	-	10	78	8
15	**Mg/Fe/O**	FAL	acetaldehyde	-	60	15	-	16	69	10
16			CH$_2$O [a]	-	83	48	-	40	12	33
17			No source	-	34	25	-	40	35	14
18			H$_2$	-	100	5	-	42	53	42
19			CH$_3$OH	-	55	21	-	33	46	18
20			2-propanol	-	59	2	-	33	65	19
21	**Mg/Al/O**	FAL	acetone	-	52	26	-	29	45	15
22			CH$_2$O [a]	-	88	64	-	13	23	11
23			H$_2$	-	58	20	-	18	62	10

Table 5-11. *Catalysts Mg/Fe/O and Mg/Al/O. FU or FAL conversion and products distribution obtained using different molecules as the hydrogen-source. Reaction conditions: 5% FU or FAL, 50% hydrogen source, 45% N$_2$, pressure of 1 atm, T = 380°C, 1 atm, overall gas residence time 1,1s, reaction time 1h.*

a. *CH$_2$O from formalin solution in water: 37% w/w CH$_2$O, 7-8% w/w CH$_3$OH.*

These results could suggest that formaldehyde, formed from methanol dehydrogenation, but not from isopropanol, could be directly involved in the mechanism of MF formation. Indeed, using isopropanol, acetone instead of formaldehyde was released in the reaction mixture; lower FU conversion and lower yield in MF compared to that obtained with methanol were obtained.

In addition, the results obtained using isopropanol with FAL (**Table 5-11** Entry 13), suggested that with iron containing catalyst, the FAL hydrogenolysis to produce MF could proceed through the classic hydrogen transfer mechanism. Indeed, the results obtained feeding FAL with methanol and isopropanol indicated that the reduction process became more efficient in the case of the test conducted using isopropanol (higher FAL conversion and MF yield).

The direct involvement of formaldehyde in the mechanism of MF formation was also suggested by the comparison between the quantities of MF formed respectively from FU and FAL using methanol as the hydrogen donor (**Table 5-11** Entries 1 and 12). Indeed, using the alcohol a significantly lower production of MF respect to FU feeding was detected. This could lead to the hypothesis that the formation of MF from FU proceed through two parallel mechanisms. The first was identified as the classic catalytic transfer reduction of FU to produce FAL as the primary reduction specie that was subsequently reduced to MF; the second pathway was identified in the direct disproportion reaction involving formaldehyde and FU to produce MF and CO_2.

The feeding of FU or FAL in the presence of formaldehyde at 380°C over the mixed oxide Mg/Fe/O validates the former hypothesis. In fact, feeding formaldehyde with FU (**Table 5-11** Entry 5), a mixture mainly composed of MF and FAL (39 and 14% selectivity respectively) was obtained while, in the test performed feeding FAL in the presence of formaldehyde (**Table 5-11** Entry 16), an equimolar amount of FU and MF was obtained. The obtained results seemed to confirm that the mixed Mg-Fe catalyst was able to activate the in-situ generated formaldehyde for the direct disproportion reaction involving the light aldehyde and FU to produce both FAL and MF with the parallel release of CO_2. Nevertheless, the results suggested that the same disproportion process between formaldehyde and FAL was not catalyzed. In this view, the formation of an equimolar amount of FU and MF in the test performed feeding FAL with formaldehyde could be explained as the consequence of a different disproportion reaction in which two molecules of FAL undergoes, over the catalyst surface, to produce one molecule of MF and one of FU. The same behaviour was observed in the process of phenol alkylation in which two

140

molecules of salycilic alcohol disproportionate into one of o-cresol and one of salycilic aldehyde.

In order to gain more information about the ability of the iron-containing catalyst to activate a light aldehyde, such as formaldehyde, as alternative hydrogen source for the selective reduction of FU to FAL, two catalytic tests have been performed using acetaldehyde instead of formaldehyde (**Table 5-11** Entries 4 and 15).

The obtained results confirmed the formulated hypothesis. Indeed, feeding FU, none MF production and FAL traces were detected. On the contrary, feeding FAL instead of FU, equimolar amount of FU and MF were obtained, as a consequence of the disproportion process in which two FAL molecules undergoes. These latter results confirmed the ability of the catalyst to partially activate an aldehyde as H-donor for the reduction of the carbonyl group to the alcoholic function but not for the consecutive step of hydrogenolysis.

Finally, the effect as reducing agent of the in-situ produced molecular H_2 has been evaluated. The obtained results (**Table 5-11** Entries 6 and 18) suggested that a direct involvement of the latter must not be excluded as one of the possible pathways for the formation of MF starting from FU. Indeed, according to the TPR profile reported in **Figure 5-28**, which demonstrated the ability for the iron containing system to partially activate molecular hydrogen starting from temperature slight higher than 350°C, both FU and FAL showed to be converted into MF when H_2 was fed instead of methanol as reducing agent. The conversion of the unsaturated alcohol was higher in comparison to that of FU and an overall yield in MF of 42% was obtained.

On the other hand, the results obtained with the Mg/Al/O allow to demonstrate that the acidic properties of the iron containing system, reported in literature to be the key factor necessary to enhance the de-oxygenation activity of a pure basic system in the catalytic transfer hydrogenation reaction, was not the only factor responsible for the high MF yield observed. As a matter of fact, the aluminium catalyst, characterized by an higher acidity compared to the iron one, showed to produce the 14% of MF yield instead of the 75% obtained with the latter.

Replacing methanol with the more active hydrogen source isopropanol it was demonstrated that the doping of MgO with a pure Lewis guest cation such as Al increased the activity of the resulting system towards the classic MPV reaction pathway, which was supposed to be the mechanism for the transformation of FU to FAL. Indeed, feeding FU in the presence of isopropanol (**Table 5-11** Entries 7 and 8) the overall activity of the

catalyst was enhanced compared to that observed using methanol. Higher FU conversion and FAL yield were registered while, the amount of MF produced resulted comparable, suggesting that with aluminium, on the contrary to that observed with iron, the involvement of the in-situ produced formaldehyde could be less important in the mechanism of MF formation. The result obtained feeding FAL with isopropanol supported even more the one observed feeding FU; the same amount of MF was indeed produced indicating that the addition of Al increased only the activity towards the reduction of FU to FAL and left unaltered the ability of the catalyst in the following hydrogenolysis step.

Two catalytic tests have been performed feeding FU and FAL in the presence of formaldehyde (**Table 5-11** Entries 10 and 22). The results were surprising considering that the activity showed by the Al-doped system was only a bit lower to the Fe-doped one when FU was used as reducible substrate. On the other hand, when FAL was fed with formaldehyde on the aluminium system the resulting MF yield, deriving from the disproportion reaction involving two FAL molecules, was lower than in case of the iron system. Finally, according to the inability of the Mg/Al/O catalyst to activate hydrogen (**Figure 5-28**), nil MF formation was observed feeding FU with molecular hydrogen while, the low amount produced replacing FU with FAL derived once again from the disproportion mechanism in which two FAL molecules undergoes (**Table 5-11** Entries 11 and 23).

Summarizing the information collected using different hydrogen sources and the two mixed oxides it was possible to demonstrate that the higher acidity of the Al-containing system, compared to that of the Fe one, generally considered the key factor to generate an higher de-oxygenating activity, was not true in the process of FU reduction using methanol as hydrogen source. Indeed, the higher de-oxygenating activity of the Mg/Fe/O was related to three main features not characterizing the aluminium containing system:

- the iron containing catalyst showed an higher activity to catalyze the disproportion reaction involving the in-situ produced formaldehyde and furfural which produce MF with the parallel release of CO_2;
- the iron containing catalyst was also demonstrated to catalyze the reduction of FU to FAL and the following hydrogenolysis step to produce MF activating the in-situ produced molecular hydrogen;

- finally, the contribution of the disproportion reaction involving two FAL molecules to produce equimolar amount of MF and FU, resulted much more important with the iron system.

Finally, summing up the information described above, an overall reaction mechanism for the gas-phase catalytic transfer hydrogenation of FU by-means of methanol as hydrogen source over the basic-based systems has been proposed (**Scheme 5-7**). When pristine heterogeneous basic catalyst was used, such as MgO and CaO, the catalytic transfer hydrogenation proceed through the classic MPV reaction mechanism reported in literature, which involve the formation of a six-membered ring reaction intermediate over the catalyst surface after the simultaneous adsorption and activation of the hydrogen source and the reducible substrate. In this case the reaction resulted highly selective towards the reduction of FU to FAL which was produced with selectivity next to the 100%. On the other hand, over the mixed Mg/M/O (M = Fe or Al) catalysts, in addition to the classic mechanism, a direct disproportion reaction involving the in-situ produced formaldehyde and FU to produce MF with the parallel release of CO_2 it was demonstrated to play a direct role in the production of MF with high yield. Furthermore, a disproportion mechanism involving two adsorbed FAL molecules to produce equimolar amount of FU and MF took place. Finally, the activation of the in-situ produced molecular hydrogen as reducing agent for the transformation of FU to FAL and for the following hydrogenolysis to produce MF it was demonstrated to be another possible pathway for the production of MF.

Considering the comparison between Fe and Al it was also demonstrated that the lower MF yield obtained with the latter guest cation was mainly related to the poorer activation of the in-situ produced formaldehyde toward the disproportion reaction with FU as well as the lower activity toward the FAL disproportion and the complete lack of molecular hydrogen activation as reducing agent. In this view, the trend of the released CO_2 moles together with the obtained MF yield (**Figure 5-32**), further support the hypothesis for which, introducing iron or aluminium into the lattice of MgO, the increase of MF yield could be related to the disproportion reaction between formaldehyde and FU. It was indeed clear that the higher was the ability of the catalyst to activate that disproportion mechanism the higher was the MF yield and the parallel CO_2 released into the stream exiting from the reactor.
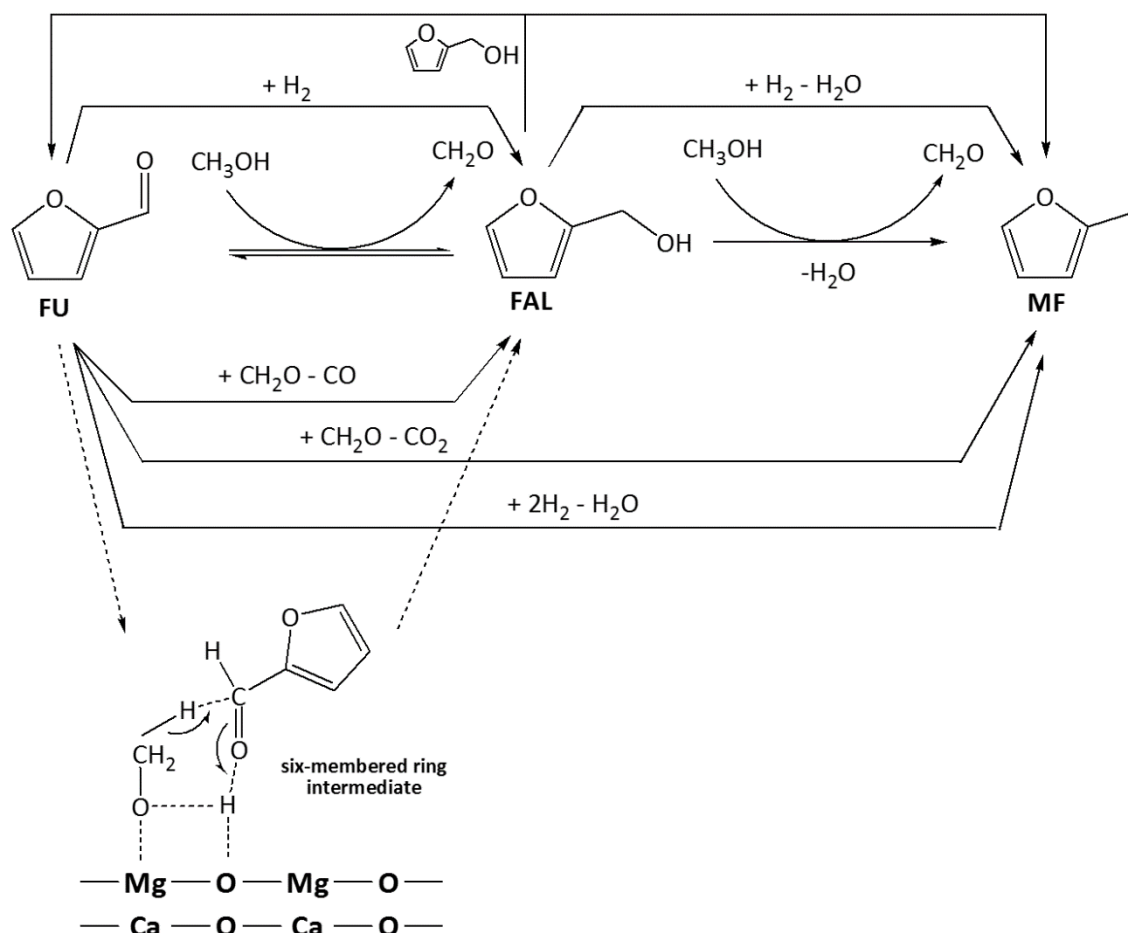
Scheme 5-7. *Overall proposed reaction pathway for the gas-phase catalytic transfer hydrogenation of FU using methanol as the hydrogen source and basic-based catalysts.*
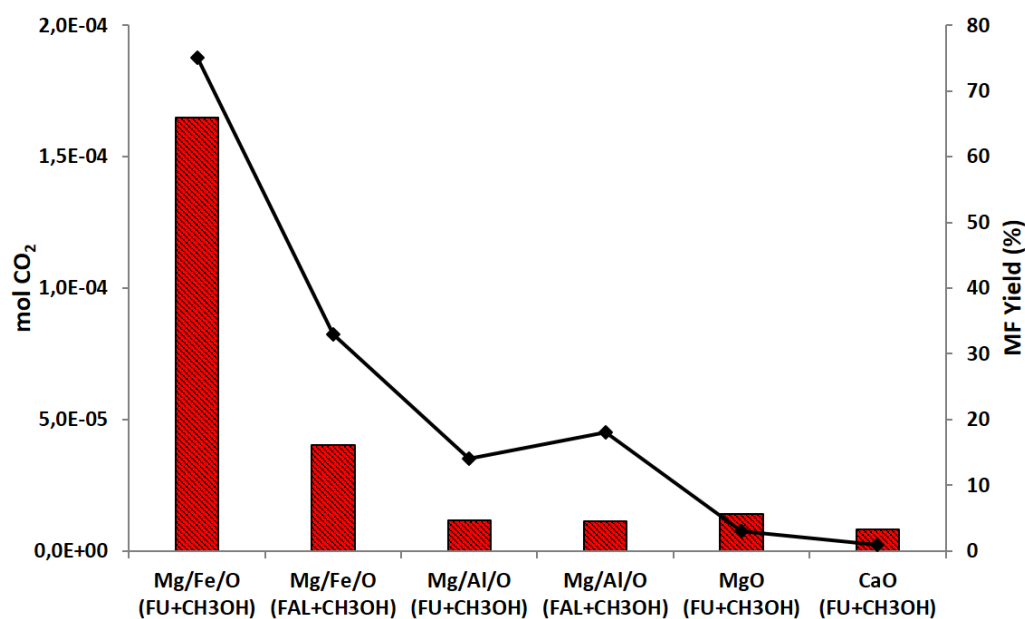

Figure 5-32. *Moles of CO_2 produced and obtained MF yield in the catalytic tests performed feeding FU or FAL in the presence of methanol as the hydrogen source over the different basic-based catalyst.*

[1] T. Pasini, A. Lolli, S. Albonetti, F. Cavani, M. Mella, *J. Catal.,* 2014, **317**, 206

[2] A. Lolli, S. Albonetti, L. Utili, R. Amadori, F. Ospitali, C. Lucarelli, F. Cavani, *Applied Catalysis A: General,* 2015, **504**, 408

[3] M. Hronec, K. Fulajtarová and T. Liptaj, *Appl. Catal., A,* 2012, **437**, 104

[4] M. Hronec, K. Fulajtarova, I. Vavra, T. Sotak, E. Dobrocka and M. Micusik, *Appl. Catal., B,* 2016, **181**, 210.

[5] L. Grazia, A. Lolli, F. Folco, Y. Zhang, S. Albonetti and F. Cavani, *Catal. Sci. Techn.,* 2016, **6**, 4418

[6] V. Crocellà, G. Cerrato, G. Magnacca, C. Morterra, F. Cavani, L. Maselli and S. Passeri, *Dalton Trans.,* 2010, 8527

[7] N. Ballarini, F. Cavani, L. Maselli, A. Montaletti, S. Passeri, D. Scagliarini, C. Flego and C. Perego, *J. Catal.,* 2007, **251**, 423

[8] H. Petitjean, C. Chizallet, J. M. Krafft, M. Che, H. L. Pernot and G. Costentin, *Phys. Chem. Chem. Phys.,* 2010, **12**, 14740

[9] Y.H. Taufiq-Yap, H.V. Lee, M.Z. Hussein and R. Yunus, *Biomass and Bioenergy,* 2011, **35**, 827

[10] G. Wolf, E. Königsberger, H. G. Schmidt, L.-C. Königsberger and H. Gamsjäger, *J. Therm. Anal. Cal.*, 2000, **60**, 463

[11] G. Busca, *Catalysis Today,* 1996, **27**(3), 457

[12] G. Busca et al., *Journal of the American Chemical Society,* 1987, **109**(17), 5197

[13] F. Cavani, S, Albonetti, F. Basile and A. Gandini, (eds.) *"Chemicals and Fuels from Bio-Based Building Blocks"* 2016, ISBN 978-3-527-33897-9 Wiley-VCH, Weinheim;

[14] .H. Hattori, *Chemical Reviews,* 1995, **95**, 3

[15] J.P. Lange et al.; *ChemSusChem,* 2012, **5**, 150

[16] M. López Granados et al., *Energy Environ. Sci.,* 2016, **9**, 1144

[17] L. Grazia, D. Bonincontro, A. Lolli, T. Tabanelli, C. Lucarelli, S. Albonetti and F. Cavani, *Green Chemistry,* 2017, **19**, 4412

[18] F. Cavani, L. Maselli, S. Passeri, J. A. Lercher, *Journal of Catalysis,* 2010, **269**, 340

[19] J. S. Valente, F. Figueras, M. Gravelle, P. Kumbhar, J. Lopez and J. P. Besse, *J. Catal.,* 2000, **189**, 370

[20] T. Sato, T. Wakahayash and M. Shimada, *Ind. Eng. Chem. Prod. Res. Dev.,* 1986, **25**, 89

[21] D. Tichit, M. H. Lhouty, A. Guida, B. H. Chiche, F. Figueras, A. Auroux, D. Bartalini and E. Garrone, *J. Catal.,* 1995, **151**, 50

[22] F. Wang, N. Ta, W. Shen, *Applied Catalysis A: General,* 2014, **475**, 76

[23] J.I. Di Cosimo, V.K. Díez, M. Xu, E. Iglesia, C.R. Apesteguía, *Journal of Catalysis,* 1998, **178**, 499

[24] G.K. Reddy, P. Boolchand, P.G. Smirniotis, *The Journal of Physical Chemistry C,* 2012, **116**, 11019

[25] P. Chandramohan, M.P. Srinivasan, S. Velmurugan, S.V. Narasimhan, *Journal of Solid State Chemistry,* 2011, **184**, 89

[26] O. Vozniuk, S. Agnoli, L. Artiglia, A. Vassoi, N. Tanchoux, F. Di Renzo, G. Granozzi, F. Cavani, *Green Chemistry,* 2016, **18**, 1038

[27] Y. Shao, Q. Xia, X. Liu, G. Lu, Y. Wang, *ChemSusChem,* 2015, **8**, 1761

[28] D.-Y. Hong, S.J. Miller, P.K. Agrawal, C.W. Jones, *Chemical Communications,* 2010, **46**, 1038

[29] M. J. Gilkey, B. Xu, *ACS Catal. 2016,* **6**, 1420

CHAPTER 6.   FeVO$_4$ bulk catalyst

6.1. Introduction

In the former chapter it was demonstrated that the catalytic transfer hydrogenation reduction of FU to FAL and MF using methanol as the H-transfer reactant and heterogeneous basic catalysts could proceed through two main pathways depending on the catalyst's features. The systems exhibiting pure basic feature, such as MgO and CaO, were mainly active in the selective reduction of FU to FAL through the classic MPV reaction mechanism, which involved the formation of a six-membered ring reaction intermediate over the catalyst's surface. On the other hand, the mixed magnesium-iron catalyst, which was characterized by different acid-base properties and higher de-hydrogenating/de-oxygenating features compared to the pristine MgO, it was demonstrated to catalyze the formation of high MF quantity through a reaction mechanism consisting in more parallel pathways. Indeed, in addition to the classic MPV mechanism, the addition of iron into the lattice of the pristine MgO allow the activation of the in-situ produced formaldehyde for a direct disproportion reaction with FU to produce both FAL and MF with the parallel release of CO and CO$_2$.

On the base of the obtained results, the evaluation of the catalytic activity of a catalyst, which was active in the production of formaldehyde, could represent a valid option to gain further information on the involvement of the latter in the direct transformation of FU to MF.

In this view, the vanadium based catalysts such as bulk vanadium oxide, supported vanadium oxide or as mixed vanadium oxide with metal of the first two transition state as well as rare earth element has become always more important. Indeed, many researchers have focused their attention over the synthesis of these materials and their application as catalysts for the removal of NO$_x$ form the exhaust gas (Selective Catalytic Reduction plant), in the selective oxidation of methanol to formaldehyde and, as a general rule, in the selective oxidation reactions[1,2,3].

In the last years the metal-vanadate compounds became always more attractive from a catalytic point of view due to the lower toxicity compared to that of the pristine vanadium oxide, the higher thermal and chemical stability in the classic operating reaction

conditions and medium and a catalytic performance very similar. Thus, in the next future the bulk vanadium oxide could be replaced by the more appealing metal-vanadate.

More specifically, $FeVO_4$, showed to be one of the most stable and active vanadate gaining always more attention also from an industrial point of view.

6.2. Catalytic application of FeVO₄

As mentioned above in the last years the metal-vanadates have been considered one of the main alternative to the use of the bulk vanadium oxide thank to the quite similar catalytic activity showed and the numerous advantages such as the lower toxicity, the higher thermal and chemical stability. The latter is understood in the terms of a lower vanadium-loss, as a consequence of volatilization phenomena, that took place especially in the methanol involved process.

The chemical process in which $FeVO_4$ has been studied as catalyst can be divided in three main groups, the same in which the pristine vanadium oxide find nowadays application:

- Selective Catalytic Reaction (SCR) process for the removal of NO_x form exhaust gas;
- Selective oxidation of methanol to formaldehyde;
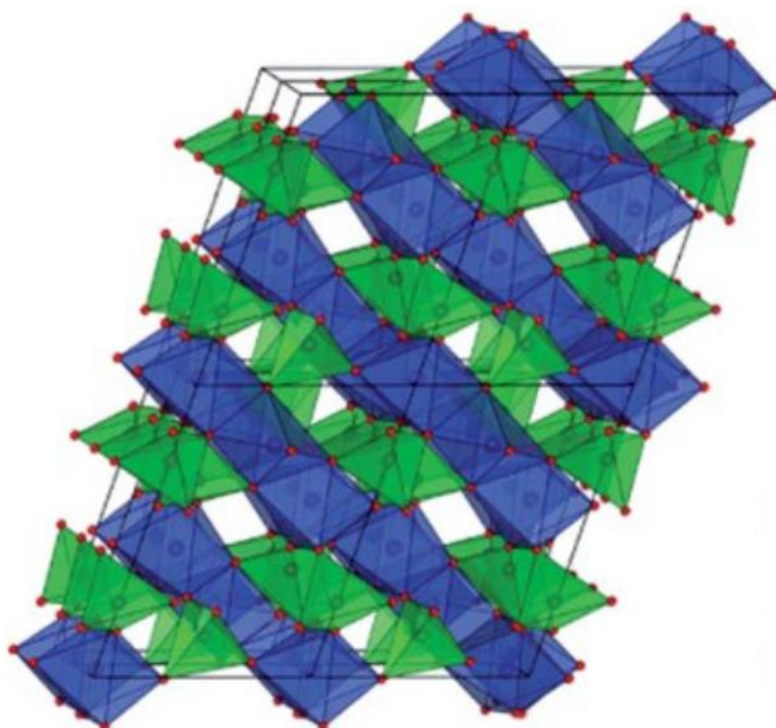- Gas-phase phenol alkylation using methanol as alkylating agent.

Figure 6-1. *Structure of FeVO₄. Adapted from [4].*

148

Lehnen et al. has deeply studied the structure changes occurred during the synthesis of porous $FeVO_4$ nanorods. It is demonstrated that the as-prepared samples, dried overnight at 90°C in static air oven, assume a fervanite-like monoclinic structure ($FeVO_4*1.1H_2O$). In the latter the Fe^{3+} cations are located only in octahedral positions to form $Fe_2O_9(H_2O)$ domains, vanadium cations are mainly present as $VO_3(OH)$ tetrahedron domains while water could be incorporated both in axial positions of edge connected iron octahedral and vanadium tetrahedron. The thermal treatment up to 650°C induces a structural change in iron-vanadate material from the fervanite-like monoclinic structure to the triclinic $FeVO_4$ structure (**Figure 6-1**). In triclinic $FeVO_4$, the iron atoms are located in three different sites: two distorted FeO_6 octahedron and one distorted FeO_5 trigonal bipyramid. The FeOx polyhedra are connected with their edges leading to doubly-bent chains, which are interconnected by VO_4 tetrahedron[5] (**Figure 6-1**).

6.2.1. FeVO₄ as catalyst for the Selective Catalytic reduction (SCR) of NO_x

The selective catalytic reduction (SCR) of NO_x by ammonia (NH_3) is to date the worldwide most efficient post-treatment method for reducing nitrogen oxide emissions from stationary sources. The harmful NO_x gases react with injected NH_3 to form nitrogen and water according to the following reaction[6]:

$$4\ NO + 4\ NH_3 + O_2 \rightarrow 6\ H_2O + 4\ N_2$$
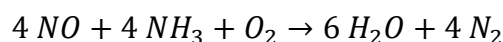
The technology is well-established in industrial removal of NO_x in stationary applications. Vanadium-based SCR catalysts of the type $V_2O_5/WO_3/TiO_2$ have been the most established systems for decades. For mobile sources such as heavy-duty engines, a urea solution is used as a nonpoisonous NH_3 source and with the most recent NO_x emission standards, NH_3-SCR becomes a promising technology also for light-duty engines. Mobile sources demand more efficient catalysts which fulfill new and different requirements. The SCR catalyst has to operate under dynamic conditions and has to work properly in extreme cases, such as low temperature due to cold starts or short city driving. It can also be exposed to high temperature (>600°C) due to the coupled particulate filter which is often located upstream of the SCR catalyst that undergoes periodic regeneration. Therefore, future catalysts will have to exhibit both high N_2 selectivity and high-temperature stability over a broader operation temperature window[7,8,9,10].

Present industrial vanadium-based-SCR catalysts consist of a sub-monolayer of VO_x (0.5−3 wt % V_2O_5) usually supported on 10 wt % WO_3/TiO_2[2,11]. An optimal loading of supported active material is essential for the performance and thermal stability of a SCR catalyst. A low vanadium loading is beneficial for the temperature stability while high loading is responsible for high activity[12]. Vanadium is deposited on the support by wet impregnation in order to homogeneously disperse the active species[13]. Depending on the loading and the preparation procedure, the VO_x species form monomers, polymers, or V_2O_5 crystallites[14].

Recent studies show that various metal vanadates ($MeVO_4$), such as $FeVO_4$, $ErVO_4$, or $TbVO_4$ demonstrate promising NH_3−SCR activity[15,16,17]. The high melting point of e.g. $FeVO_4$ (ca. 850°C) compared to V_2O_5 (ca. 690°C) makes them attractive as high temperature stable SCR catalysts[10,18]. Casanova et al. reported that metal vanadates and mixtures thereof such as $Fe_xEr_{1−x}VO_4$ (0 ≤ x ≤ 1) supported on WO_3 (9 wt %)/TiO_2 modified with 10 wt % SiO_2, exhibit excellent temperature stability and good SCR activity[17]. The origin of the temperature stability was interpreted as a result of the lack of free vanadium species on the surface of the catalyst, which is responsible for the undesired anatase to rutile phase transformation above 700°C. SiO_2 is often added as promoter to the support material for vanadia based catalysts. SiO_2 enhances the surface acidity, the structural strength, and the retention of BET surface area upon high temperature treatment[19,20].

Liu et al. investigated $FeVO_4$ deposited by co-impregnation from $Fe(NO_3)_3$ and NH_4VO_3 on TiO_2. The catalyst with 9 wt % $FeVO_4/TiO_2$ showed an excellent NO_x conversion for calcination temperatures below 600°C. Above this temperature, a severe NH3−SCR activity loss was observed. The deactivation was correlated to the phase transformation of TiO_2, leading to a loss of surface area. The $FeVO_4$ phase was identified by extended X-ray absorption fine structure (EXAFS) spectroscopy and was stable up to 800°C.

6.2.2. FeVO₄ as catalyst for the Selective oxidation of methanol to formaldehyde

Production of formaldehyde from methanol and air is done with either methanol-rich (36% to 40%) or methanol-lean (8.5% to 9.5%) feed using the silver process and the oxide process, respectively. Historically, the silver process has been preferred over the oxide

process mainly due to lower investment costs[21,22], but since the methanol price has almost been doubled over the last five years[23] the more selective oxide process has been favored considerably. For new formaldehyde capacities, the oxide process is the most common choice today. The commercial MoO$_3$/Fe$_2$(MoO$_4$)$_3$ catalyst used in the oxide process is in many aspects superb, showing very high selectivity (> 93%) at almost complete conversion of methanol. However, at the reaction conditions the molybdenum is volatile, resulting in lowered activity and poorer selectivity of the catalyst with time on stream as well as increased pressure drop over the catalytic bed[24,25,26,27]. Owing to the deactivation, the catalyst has to be replaced every 1 to 2 years depending on the operating conditions. Higher temperature and methanol partial pressure favour the molybdenum loss, making it difficult to increase the plant capacity by increasing the methanol concentration. Since the far largest production cost is that of methanol, alternative more stable catalysts are of interest provided that they show comparable selectivity to formaldehyde[27].

In the area of alternative catalysts for methanol oxidation, several studies have been reported on vanadium-based catalysts including pure vanadium oxide, mixed oxides, and supported vanadium oxide[3,28,29,30]. In particular, vanadates with Ni, Fe, Co, Mg, Cr, Mn, Al, Ag, Cu, and Zn have been found to have selectivities >90% to formaldehyde at high methanol conversion[31,32,33]. According to Wachs et al.[33], the vanadium in bulk metal vanadates is not volatile in methanol oxidation, although XPS analysis before and after use of the samples in methanol oxidation indicated some structural changes in the surface and near surface layers during catalysis. Indeed, since vanadium is toxic and because of increasing environmental concerns, low vanadium volatility is desirable not only to improve the catalyst life time, but also to minimize the spread of V inside the plant and in nature. Use of supported vanadium catalysts with loads in the monolayer range can be one approach both to decrease the amount of toxic vanadium being used and to improve the stability of the vanadium through its interaction with the support.

Häggblad et al. have recently compared the activity of bulk FeVO$_4$ with that of TiO$_2$, Al$_2$O$_3$ and SiO$_2$ supported FeVO$_4$, the catalytic activity of these vanadates has also be compared with VO$_x$/SiO$_2$[34]. Considering both activity and selectivity to formaldehyde, the most interesting catalysts on each support are those with the highest load of vanadium. At 80% methanol conversion, these samples show a selectivity to formaldehyde in the range 80% to 88%, a value which decreases in the order FeVO$_4$/TiO$_2$ > FeVO$_4$/Al$_2$O$_3$ > FeVO$_4$/SiO$_2$ > V$_2$O$_5$/SiO$_2$ and that is always lower if compared with the 90% obtained with bulk FeVO$_4$.

In terms of vanadium and molybdenum volatility during the reaction time on stream, a comparison have been performed between a commercial-type iron molybdate bulk catalyst, the bulk FeVO$_4$ and the supported vanadates. For the supported Fe-V-oxide, the volatilization of V is severer considering the limited vanadium content on the support. After operation at 300°C for 5 days in methanol oxidation with an approximately constant composition of 10 vol.% each of methanol and oxygen, depending on the load of vanadium and iron not less than about 40% to 80% of the total amount of vanadium in the TiO$_2$ and Al$_2$O$_3$ supported catalysts has volatilized. For the silica supported samples, the volatilization is even worse. On the other hand, the iron and vanadium volatilization in the bulk FeVO$_4$ showed to be lower than that of molybdenum in the commercial-type catalyst. Thus, the supported metal vanadate, in particular supported FeVO$_4$, could be hardly considered as valid alternative to the bulk molybdates. On the contrary, bulk FeVO$_4$, showing similar catalytic performances and lower metal volatilization, could be an alternative catalyst for the selective oxidation of methanol into formaldehyde, also at industrial-scale plant, thanks to its high stability and low deactivation.

6.2.3. FeVO$_4$ as catalyst for the methylation of phenol

The alkylation of phenols is a very important industrial reaction. Olefins, alcohols and alkyls halides might be used as alkylating agents. Preferred alkylating agents for industrial purposes are methanol and dimethylcarbonate. More conventional reactants, such as methylchloride and dimethylsulphate, although still employed industrially, are less attractive nowadays due to environmental concerns[35]. Phenol methylation process consists in the alkylation of phenol with methanol. It is used to produce mainly *o*-cresol, 2,6-xylenol and traces of 2,4,6-trimethylphenol. Reaction conditions can, in some cases, be adjusted to promote the selectivity for one of the products. Industrially the phenol methylation process is carried out by means of three main types of processes: i) liquid-phase methylation; ii) fixed-bed liquid-phase methylation; iii) gas-phase methylation. When the reaction is carried out in the liquid phase it gives numerous products and their separation is very difficult and complicated. On the contrary, gas-phase alkylation is simpler, more selective and doesn't require complicated separation of products. Classically gas phase methylations produce mainly 2,6-xylenol, while liquid phase methylations yield *o*-cresol as the main product. The other products being *p*-cresol, 2,4-

and 2,6-xylenols in a typical 7:5:2 ratio, respectively. Yields of up to 98% (based on phenol) have been reported for the gas phase reaction. Common side products include heavy compounds, methane gas, carbon monoxide and carbon dioxide. This process is currently used worldwide to produce almost the entire supply of 2,6-xylenol.

Several studies have been performed in order to gain information about the real alkylating agent in the gas-phase methylation process. The general conclusion is that formaldehyde, produced as a consequence of methanol de-hydrogenation, acts as alkylating specie by-means as an electrophilic attack on the activated aromatic ring of phenol[35].

Since the in-situ formation of formaldehyde from methanol has been identified as the key-step for the gas-phase alkylation of phenol, the catalysts that shows an high activity in the selective oxidation of methanol to formaldehyde could also be considered as good candidates for the methylation process. As described in the previous paragraph, the metal-vanadates, in particular the bulk FeVO₄, has been reported to be very active in the mentioned reaction.

For example, Asahi Company reported that FeVO₄ is a very active and stable catalyst for the gas-phase methylation of phenol to *o*-cresol using methanol as alkylating agent[36]. It has been demonstrated that the strong de-hydrogenating properties of the catalyst allow the in-situ formation of high quantity of formaldehyde that is the real (hydroxyl)alkylating agent.

Considering the several and potential industrial application of the mixed iron-vanadium oxide, which mainly involved the production of formaldehyde, in the present section of the work the catalytic activity of the mixed oxide in the gas-phase catalytic transfer hydrogenation of FU using methanol as the H-source has been evaluated with the aim to gain more information related to the direct involvement of the formaldehyde in the production of MF.

6.3. Results and discussion

The catalyst was characterized via different techniques such as BET surface area, atomic absorption, X-ray diffraction, and Raman spectroscopy. After calcination at 650°C, the catalyst showed a specific surface area of 12 m^2g^{-1}, a value in agreement with that reported by other authors[37,38].

XRD patterns of the dried precursor and the calcined material are compared in **Figure 6-2**. The dried sample showed an amorphous structure: no reflection was registered, while the calcined catalyst presented a well-defined FeVO₄ triclinic structure with traces of segregated iron oxide phase (hematite).
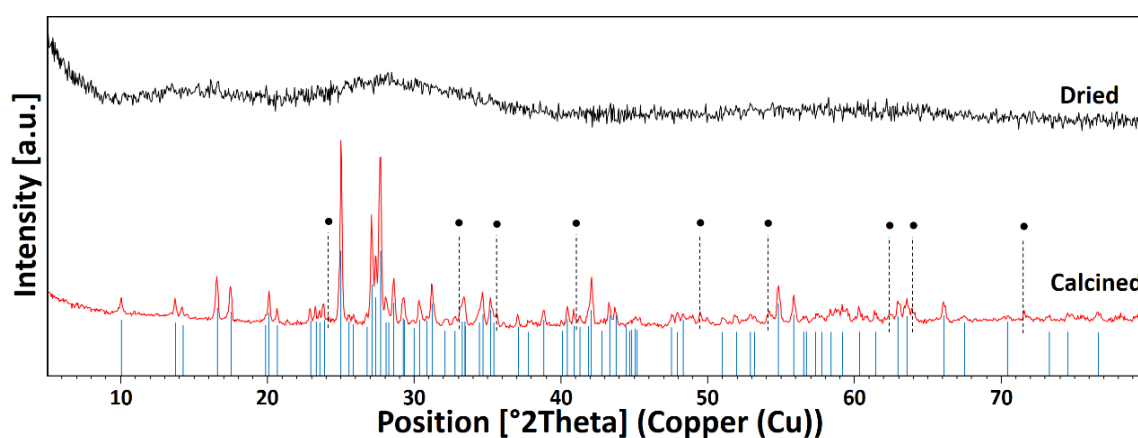
Figure 6-2. *XRD patterns of the dried (black) and calcined (red) FeVO₄. Reference patterns: (━) FeVO₄, (●) Fe₂O₃.*

The Raman analysis confirmed these results. The spectrum reported in **Figure 6-3** can be divided into four spectral regions which agree well with those reported in literature for crystalline FeVO₄[37]:

- (i) at Raman shift 1050-880 cm^{-1}, there are bands attributable to terminal V=O bond stretching;
- (ii) at 880-700 cm^{-1}, to V—O--Fe bond stretching;
- (iii) at 700-550 cm^{-1} to V—O--Fe and V--O--Fe stretching;
- (iv) at < 550 cm^{-1}, to the deformation of V—O—V bonds and Fe—O stretching;
- in addition to these bands, at 1300 cm^{-1} a weak broad band can be attributed to α-Fe₂O₃[39], indicating the possible segregation of a small quantity of hematite.

154
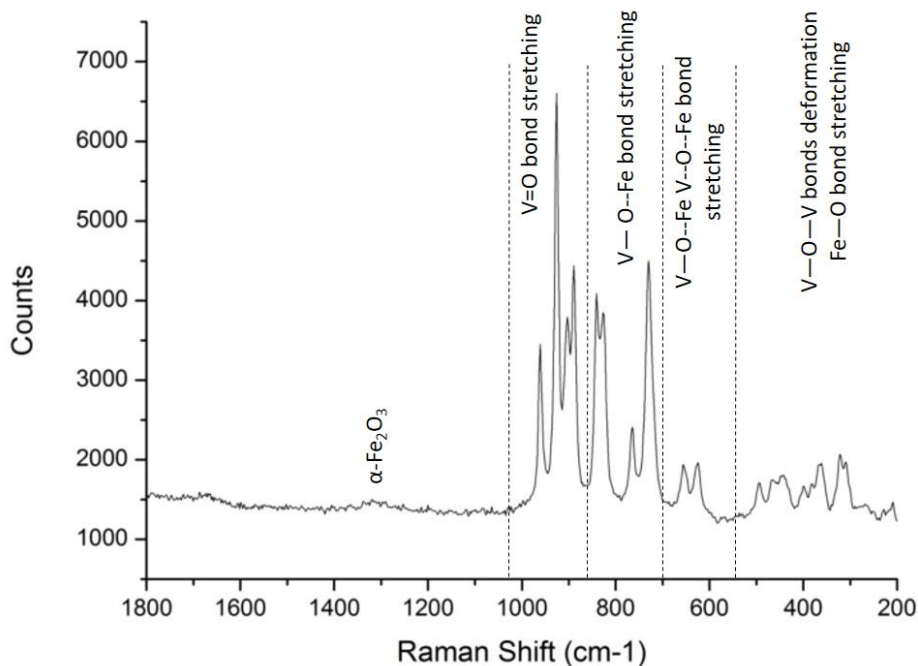
Figure 6-3. *Raman spectrum of calcined FeVO₄.*

The elemental analysis indicated the presence of a Fe/V molar ratio equal to 1.09±0.02 in fresh catalyst. This value is slightly higher than the theoretical one, thus highlighting the possible loss of some vanadium during catalyst synthesis. Indeed, the analysis of the solution obtained after filtration and washing of the catalyst showed the presence of a small vanadium quantity, thus justifying the slight excess of iron in the solid.

6.3.1. Hydro-deoxygenation of FU with FeVO₄ catalyst: effect of reaction temperature

The gas phase hydrodeoxygenation of FU was carried out using methanol as the hydrogen source.

The strong interaction between methanol and FeVO₄ was demonstrated by means of in-situ DRIFTS (Diffuse Reflectance Infrared Fourier Transform Spectroscopy) experiments. Indeed, by feeding continuously the alcohol during the adsorption at low temperature (**Figure 6-4**), we demonstrated that methanol was mainly physi-adsorbed as methoxy species (IR bands at 2930 and 2828 cm-1)[40,41]; an evidence of the physi-nature of the adsorption of methanol over the surface consisted in the rapid disappearing of the bands related to the methoxy species after the end of the feeding of the alcohol.
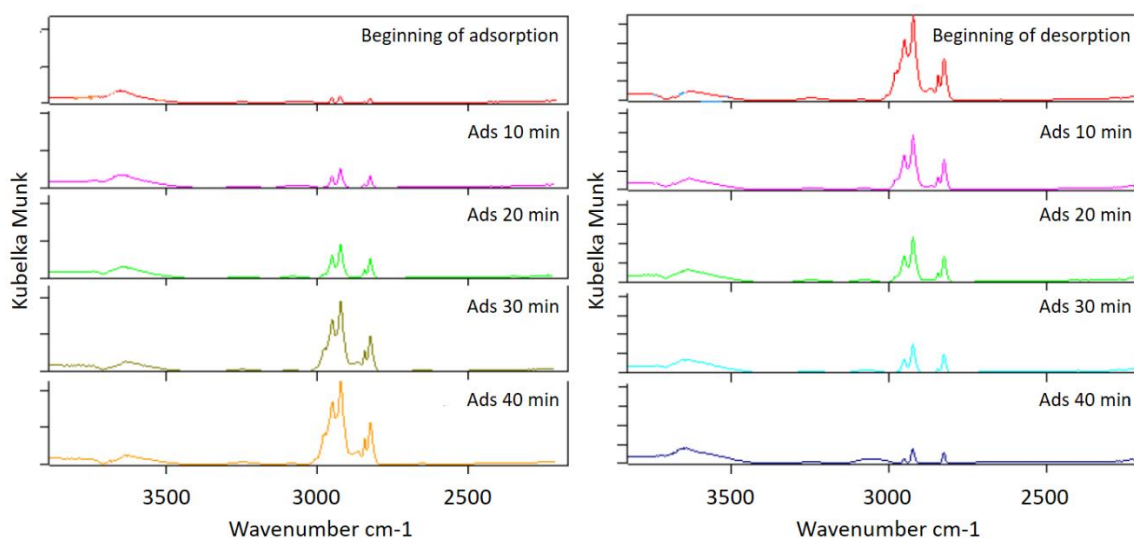
Figure 6-4. *DRIFT spectra recorded during methanol adsorption (left) and desorption (right) over FeVO₄ catalyst at 85°C.*
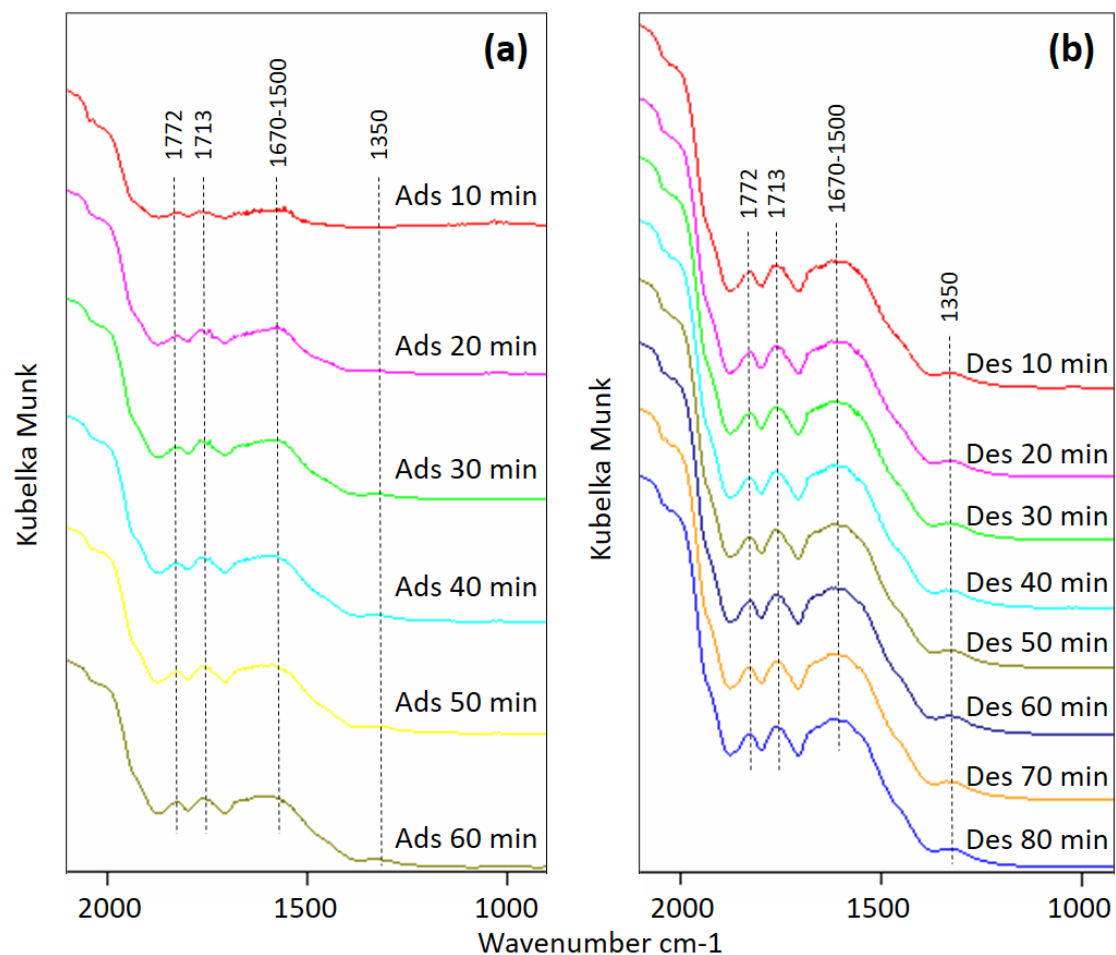
Figure 6-5. *DRIFT spectra recorded after methanol adsorption and desorption at the temperature of 320°C. During adsorption methanol was continuously fed over the catalyst while, during desorption, only He was fluxed. Legend: (a) DRIFT spectra registered during methanol adsorption, (b) DRIFT spectra registered during methanol desorption.*

The same behaviour was also confirmed at high temperature, but for very short time only (**Figure 6-5**); during adsorption, the main IR bands relating to the presence of both methoxy and molecular physi-adsorbed methanol were identified. For prolonged adsorption-desorption times, the appearance of broad bands at 1670-1500 cm^{-1}, 1350-1300 cm^{-1} and 1713-1772 cm^{-1} could be attributed to C-O vibration of molecular formaldehyde[42], providing evidence for the formation of chemi-adsorbed formate and formaldehyde species, thus confirming the ability of the catalyst to activate and dehydrogenate methanol at this temperature. Furthermore, the intensity of the IR bands remained unchanged during desorption, indicating that the interaction between activated methanol and catalyst was strong.

At first the influence of the reaction temperature has been studied in order to evaluate the optimal temperature at which the catalyst showed the best catalytic performance. In these catalytic tests, MF was the main product detected, with small amounts of 2,5-dimethylfuran (DMF) and 2-vinylfuran (VINFU).


Figure 6-6. *Effect of reaction temperatures on FU conversion and product selectivity in the second hour of reaction, catalyst FeVO₄. Feed composition: FU 1%, CH₃OH 10%, N₂ 89%; Pressure 1 atm, overall gas residence time 1.0 s. Symbols: ♦ FU conversion, ■ MF selectivity, ■ DMF selectivity, ■ VINFU selectivity, ■ C loss.*

Since the product selectivity changed significantly between the first and the following monitored hour of reaction (further details concerning this behavior will be given in the section regarding the effect of reaction time), catalyst performances were compared at the second hour. **Figure 6-6** (and **Table 6-1**) shows FU conversion and product selectivity based on temperature (range 250-400°C).

At a low temperature (250°C), the hydrogenation of FU to MF occurred with very low efficiency. Indeed, the conversion of FU was lower than 50% and the overall selectivity to the identified products was around 25% ($\approx$ 20% selectivity to MF). The low selectivity to MF and the high C loss indicate the poor ability of the catalyst to activate methanol for temperatures lower than 300°C. Indeed, the C loss could be ascribed to the formation of heavy carbonaceous compounds deriving from the degradation of FU.

When the temperature was increased up to 300-350°C, the efficiency of the H-transfer increased significantly. In this temperature range, we registered a notable increase in FU conversion and a remarkable enhancement of the overall selectivity to reduction products to up to approximately 75% ($\approx$ 65% selectivity to MF). The formation of heavy compounds, due to FU degradation, was less than 20-30%.

The presence of the oligomeric compounds adsorbed on the used catalyst surface was confirmed by Raman spectroscopy (**Figure 6-7**), with the characteristic D3 band at 1600cm^{-1}, which is ascribable to the presence of amorphous carbon species[43]. Furthermore, no products of ring hydrogenation or decarbonylation were formed.

Reaction T (°C)	FU Conversion (%)	Product Selectivity (%)					MF Yield (%)
		FAL	MF	DMF	VINFU	C-Loss	
250	45	0	22	1	2	75	10
300	93	0	68	3	6	23	63
320	98	0	68	3	6	23	67
350	90	0	63	2	6	29	57
400	100	0	62	1	3	34	62

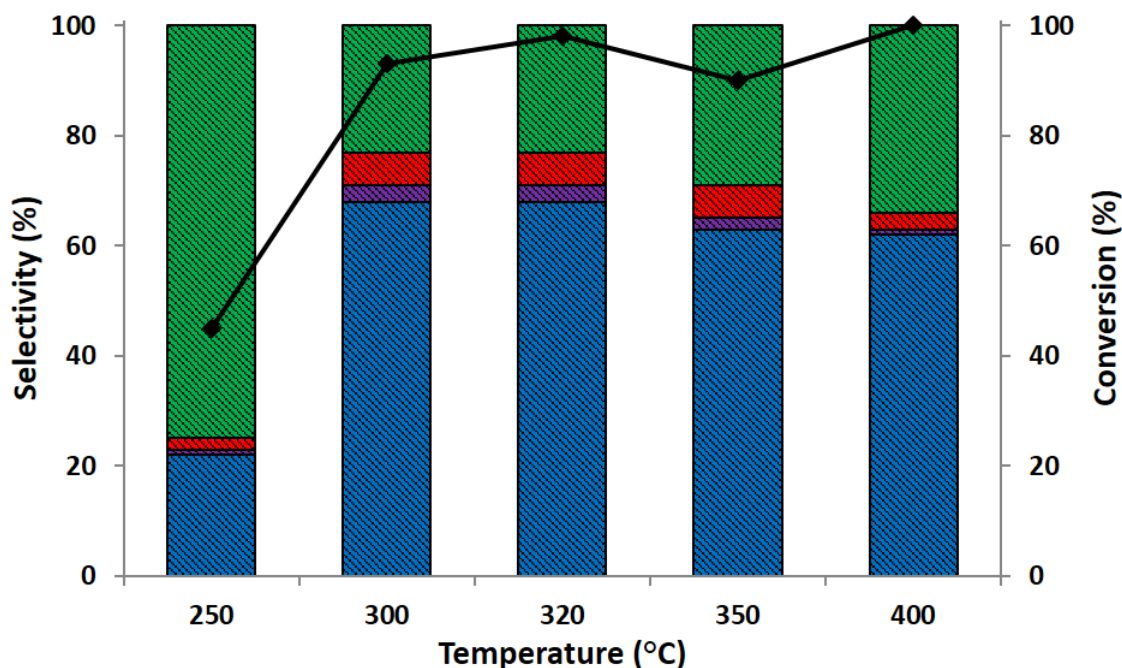**Table 6-1.** *Effect of reaction temperatures on FU conversion and product selectivity in the second hour of reaction, catalyst FeVO₄. Feed composition: FU 1%, CH₃OH 10%, N₂ 89%; Pressure 1 atm, overall gas residence time 1.0 s.*
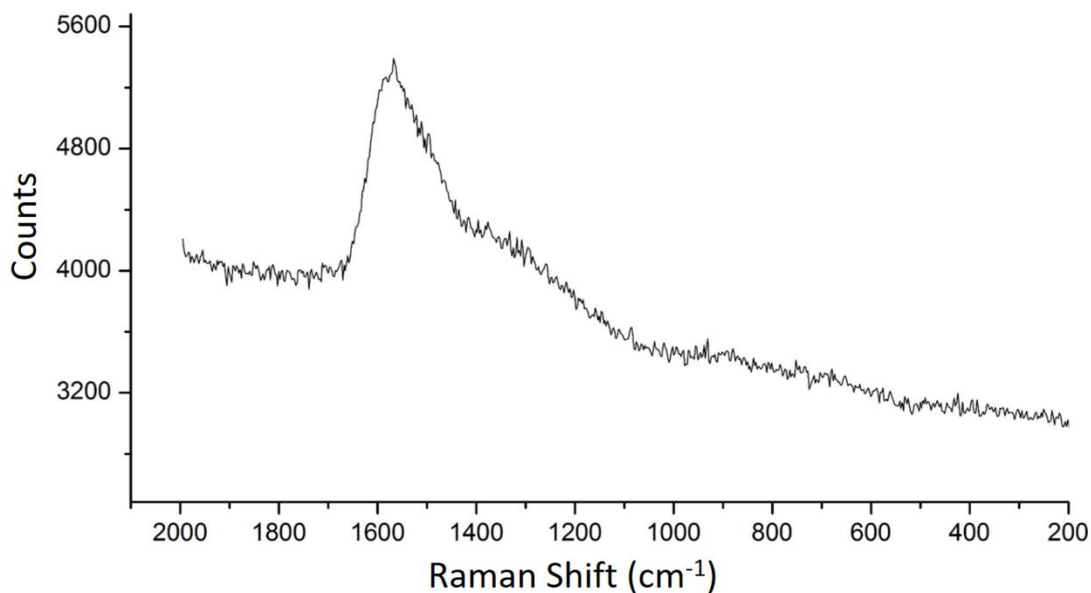
Figure 6-7. *Raman spectra collected over the spent FeVO₄ used in the catalytic test performed at 320°C.*

The ability of $FeVO_4$ to activate methanol for temperatures higher than 300°C was confirmed by the results in **Figure 6-8**, which shows the number of moles of light compounds formed, based on time, at 250°C and 320°C. The negligible amount of CO, CO_2, CH_4, and H_2 produced at 250°C agrees with the results in **Figure 6-6**. As a matter of fact, in addition to the main reaction involving the H-transfer to MF, the process was accompanied by the decomposition of formaldehyde, which is produced by methanol dehydrogenation, into light gaseous compounds, CO, CO_2, CH_4, and H_2. In a previous work, we demonstrated that in similar reaction conditions formaldehyde was decomposed following the formal set of reactions reported in **Scheme 6-1**[35,36,18].

$$CH_2O \rightarrow CO + H_2 \qquad\qquad (1)$$
$$CO + H_2O \rightarrow CO_2 + H_2 \qquad\qquad (2)$$
$$2\ CH_2O \rightarrow CH_3O\text{-}C(O)H \qquad\qquad (3)$$
$$CH_3OC(O)H \rightarrow CO_2 + CH_4 \qquad\qquad (4)$$
$$HCOOH \rightarrow CO_2 + H_2 \qquad\qquad (5)$$
$$HCOOH \rightarrow CO + H_2O \qquad\qquad (6)$$
$$CH_3OH + H_2O \rightarrow CO_2 + 3H_2 \qquad\qquad (7)$$
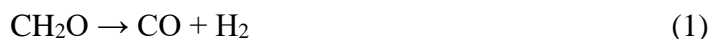
Scheme 6-1. *Summary of main reactions involving methanol in the catalytic H-transfer of FU[35,36].*

159

Figure 6-8. *FeVO₄ catalyst. Number of moles of gas formed, based on time, in the reaction of FU reduction with methanol at 320°C (bold line) and 250°C (dashed line). Feed composition: FU 1%, CH₃OH 10%, N₂ 89%; Pressure 1 atm, overall gas residence time 1,0 s. Legend: ♦ CO, ■ CO₂, ▲ CH₄, ● H₂.*

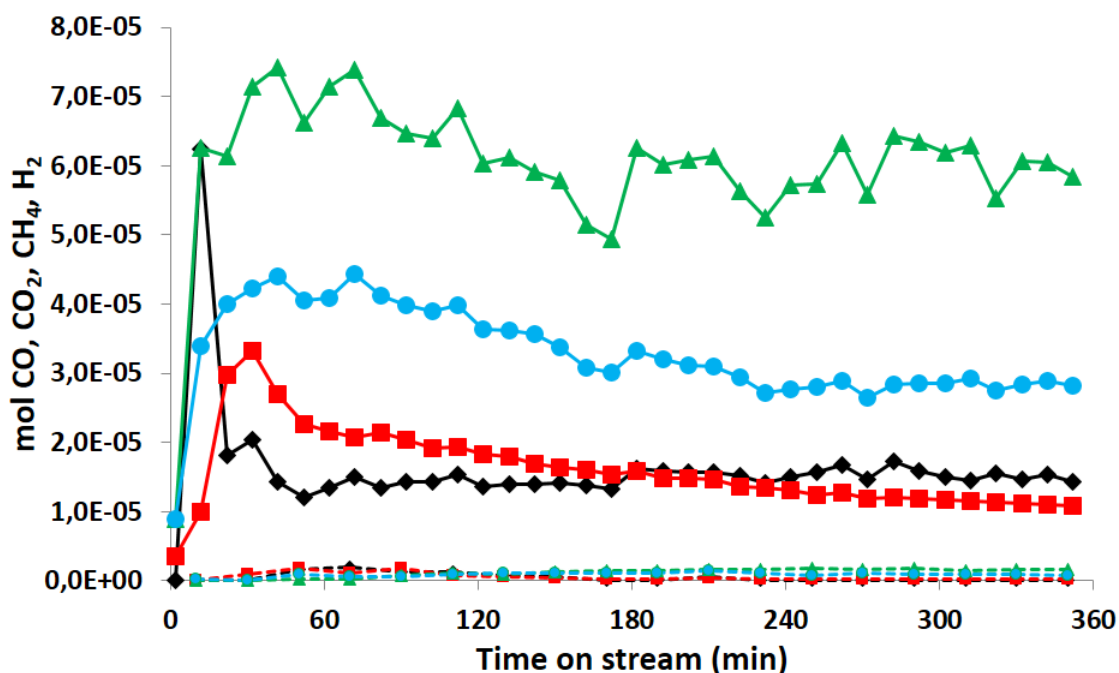The formaldehyde generated as the co-product of H-transfer decomposes, leading to the formation of CO and H_2 (Reaction 1). Alternatively, two adsorbed CH_2O molecules may disproportionate to formate and a methoxy species, yielding methylformate (reaction 3) (the latter can also be formed by Tishchenko dimerization), which decomposes at high temperatures to CH_4 and CO_2 (reaction 4). Formic acid may also form through the oxidation of formaldehyde by Fe^{3+}, and decompose to CO_2 and H_2 (reaction 5) or CO and H_2O (reaction 6). Moreover, water gas shift (WGS) (reaction 2) or methanol reforming (reaction 7) cannot be disregarded.

The high amount of CH_4 produced, higher than that of CO_2, suggests the occurrence of a disproportionation involving two methanol molecules to yield an equimolar amount of methane, formaldehyde, and water. Ueda et al. have recently reported similar results over vanadium and molybdenum oxides, using various alcohols, including methanol and ethanol, to produce the corresponding alkanes and aldehydes in equimolar ratio[44,45].

Lastly, when FU was reduced with methanol at 400°C, the total conversion of the substrate was registered. The main product detected was MF with a selectivity of 62%. However, a lower carbon balance was registered due to the degradation of FU to carbonaceous compounds.
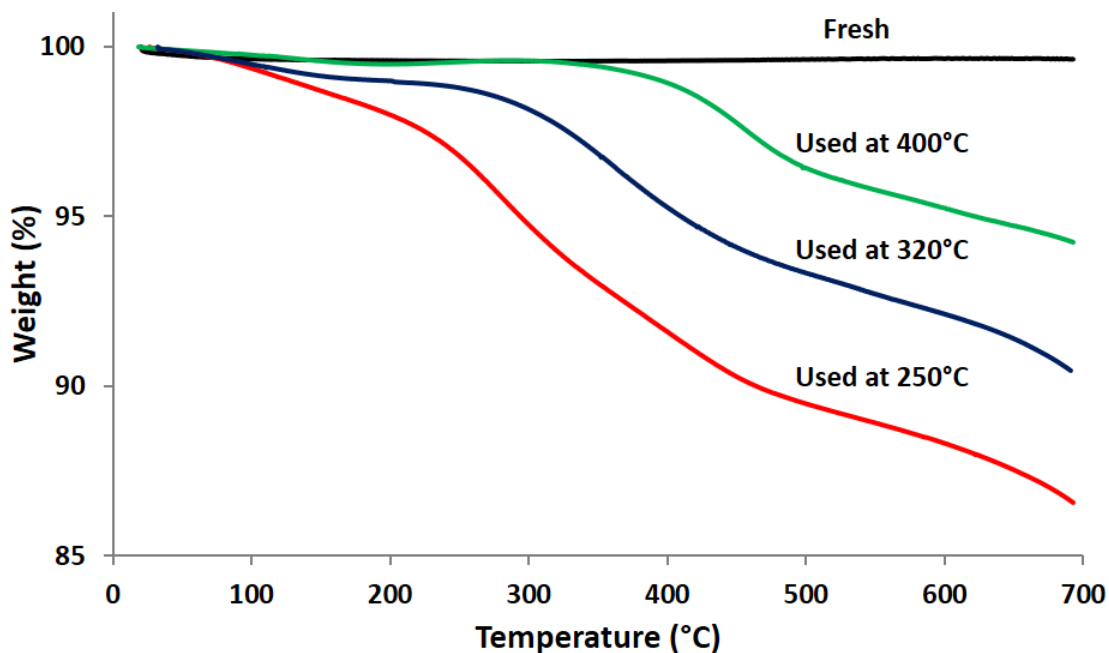
160

Figure 6-9. *Thermogravimetric analysis (TGA) in nitrogen: (—) fresh FeVO₄ calcined at 650°C; FeVO₄ used in catalytic test (—) at 250°C, (—) at 320°C and (—) at 400°C.*

With the aim of studying the effect of reaction conditions on the amount of carbonaceous deposits, TGAs were carried out on the spent catalysts (**Figure 6-9**).

Thermograms were obtained by heating up the samples in a nitrogen flow, instead of air, in order to avoid the re-oxidation of the catalyst that would invalidate the results. Thus, it is necessary to take into account that some carbonaceous compounds could remain on the catalyst after TGA due to the anaerobic condition utilized (see the section concerning the effect of reaction time on catalyst structure).

As expected, the fresh catalyst calcined at 650°C (black line) did not show any weight loss. Conversely, all the used catalysts showed a weight loss that could be related to the desorption/decomposition of the amorphous carbon deposited during reactivity tests; however, the weight loss was a function of the temperature used for FU reduction. In fact, after heating up to 150-170°C, samples showed a common and marginal initial weight loss (2-3 wt %) which is related to the desorption of some physisorbed water. However, upon increasing the temperature, an evident weight loss ($\approx$ 10 wt %), in the range 200-450°C, was observed for the sample used at 250°C; a further and limited weight loss ($\approx$ 3-4 wt %) was then registered while heating up the sample to 700°C. This latter weight loss could be related to the removal of the heavier oligomeric carbonaceous species, whereas that registered at lower temperatures could be connected to the desorption of

lower molecular mass deposits. It may be hypothesized that the catalyst oxidises carbonaceous residua, while being itself reduced because of anaerobic conditions.

It is also shown that, in the case of the sample used at 250°C, the formation of the lighter carbonaceous deposits was largely improved. The sample used at 320°C showed a lower weight loss (≈5-6 wt %) in the range 200-450°C, and a similar weight loss in the high temperature region. These results can be correlated to the trend of C loss observed in function of reaction temperature (**Figure 6-6**). Indeed, the formation of heavy carbonaceous deposits (oligomeric species deriving from the condensation of several furanic species) could represent the main contribution to C loss.

Lastly, it should be pointed out that increasing the reaction temperature from 250°C to 400°C significantly increased the temperature at which carbonaceous deposits were eliminated. This could be connected to the formation of compounds with more ordered structures.

These results confirm that the catalyst has the best performance in the temperature range between 300 and 350°C. In particular, at 320°C a conversion higher than 95% was registered, with a selectivity to MF of around 70%; moreover, a fairly good C balance was obtained (C loss 25%).

6.3.2. Hydro-deoxygenation of FU with FeVO₄ catalyst: effect of reaction time

The stability of the catalyst was examined by conducting tests for 6 h at the optimized reaction temperature (320°C) (**Figure 6-10** and **Table 6-2**). FU conversion proved to be almost constant during the first 3 hours of reaction, with only a slight decrease; then, starting from the 4th hour, a rapid decrease was observed and a final conversion of 55% was reached. This drop in conversion may be correlated to the previously discussed accumulation of heavy C residues (**Figure 6-7** and **Figure 6-9**).

With regard to the products formed, a notable difference in selectivity was observed between the first and following hours of reaction, thus highlighting a different catalyst behavior over time. Indeed, in the first hour of reaction, a C loss of 63% and a selectivity to MF of 32% only were registered; starting from the second hour, the C loss dropped to 25%, with a significant increase in MF (66%), DMF and VINFU yields.

Figure 6-10. *Effect of reaction time on FU conversion and product selectivity for FeVO₄ catalyst. Feed composition: FU 1%, CH₃OH 10%, N₂ 89%; Pressure 1 atm, 320°C, overall gas residence time 1.0 s. Legend: ♦ FU conversion, ■ MF selectivity, ■ DMF selectivity, ■ VINFU selectivity, ■ C loss.*

A further evidence of the change in catalytic behaviour occurring during the first hour can be inferred from **Figure 6-8**, showing the light gaseous compound amounts. CO and CO₂ exhibited an initial rapid increase up to a maximum value at 15 and 30 minutes,

respectively. After this maximum, their concentration rapidly decreased. The high amounts of CO and CO_2 initially produced are probably due to the oxidation of methanol by the catalyst.

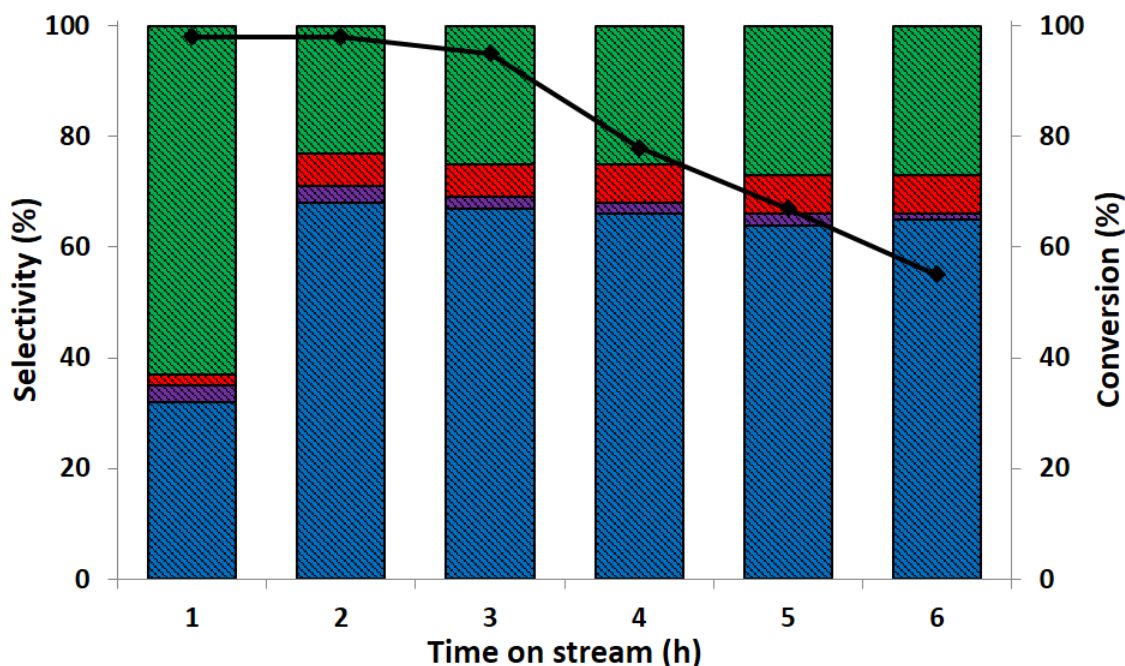| Time on stream (h)	FU Conversion (%)	Product Selectivity (%)					MF Yield (%)
		FAL	MF	DMF	VINFU	C-Loss	
1	98	0	32	3	2	63	31
2	98	0	68	3	6	23	67
3	95	0	67	2	6	25	64
4	78	0	66	2	7	25	51
5	67	0	64	2	7	27	43
6	55	0	65	1	7	27	36

Table 6-2. *Effect of reaction time on FU conversion and product selectivity, catalyst FeVO₄. Feed composition: FU 1%, CH₃OH 10%, N₂ 89%; Pressure 1 atm, 320°C, overall gas residence time 1.0 s.*

The same behavior was shown by the catalyst also for the other reaction temperature tested confirming that a change in the catalytic activity took place in the first hour. In **Figure 6-11** (**Table 6-3** and **Table 6-4**) were reported the results of the catalytic tests performed at 300 and 350°C respectively. For both the temperature tested was confirmed the different catalyst performance, in terms of products distribution. Indeed, a poor carbon balance coupled with low selectivities in the reduction products has been detected in the first hour, values that were completely overturned from the second hour.

Time on stream (h)	FU Conversion (%)	Product Selectivity (%)					MF Yield (%)
		FAL	MF	DMF	VINFU	C-Loss	
1	98	0	50	3	4	43	49
2	93	0	69	3	6	23	63
3	85	0	66	2	5	27	56
4	69	0	61	1	6	32	42
5	57	0	63	1	6	30	36
6	52	0	62	2	6	30	32

Table 6-3. *Effect of reaction time on FU conversion and product selectivity, catalyst FeVO₄. Feed composition: FU 1%, CH₃OH 10%, N₂ 89%; Pressure 1 atm, 300°C, overall gas residence time 1.0 s.*

Time on stream (h)	FU Conversion (%)	Product Selectivity (%)					MF Yield (%)
		FAL	MF	DMF	VINFU	C-Loss	
1	97	0	40	2	3	55	39
2	90	0	63	2	6	29	57
3	80	0	53	2	6	39	42
4	68	0	67	2	8	23	46
5	57	0	58	3	7	32	33
6	56	0	59	1	8	32	33

Table 6-4. *Effect of reaction time on FU conversion and product selectivity, catalyst FeVO₄. Feed composition: FU 1%, CH₃OH 10%, N₂ 89%; Pressure 1 atm, 350°C, overall gas residence time 1.0 s.*
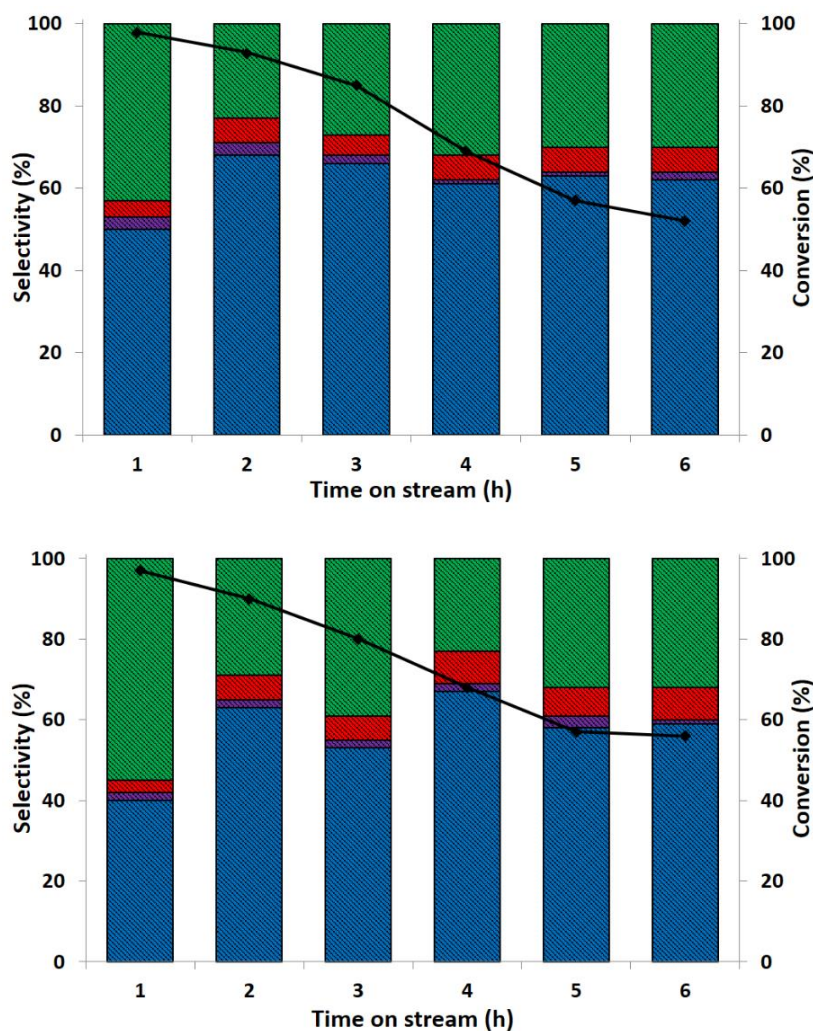

Figure 6-11. *Effect of reaction time on FU conversion and product selectivity for FeVO₄ catalyst at 300°C (top) and 350°C (bottom). Feed composition: FU 1%, CH₃OH 10%, N₂ 89%; Pressure 1 atm, overall gas residence time 1.0 s. Legend: ♦ FU conversion, ■ MF selectivity, ■ DMF selectivity, ■ VINFU selectivity, ■ C loss.*

In order to gain better insight into this hypothesis, the oxidation of methanol by-means of catalyst reduction, we performed a catalytic test in which only methanol was fed at 320°C for 1h. **Figure 6-12** shows the number of moles of light compounds formed, based on the time; methanol and furfural were then fed under usual conditions. The trend of light compounds, obtained by feeding methanol alone, was very similar to that registered in the test performed by co-feeding methanol and FU (**Figure 6-8**). Therefore, during the first hour of reaction, methanol preferentially reacts with the catalyst, thus decreasing the amount of methanol available as the H source for the reduction of FU. In these conditions, FU was mainly degraded, leading to the high C loss registered.
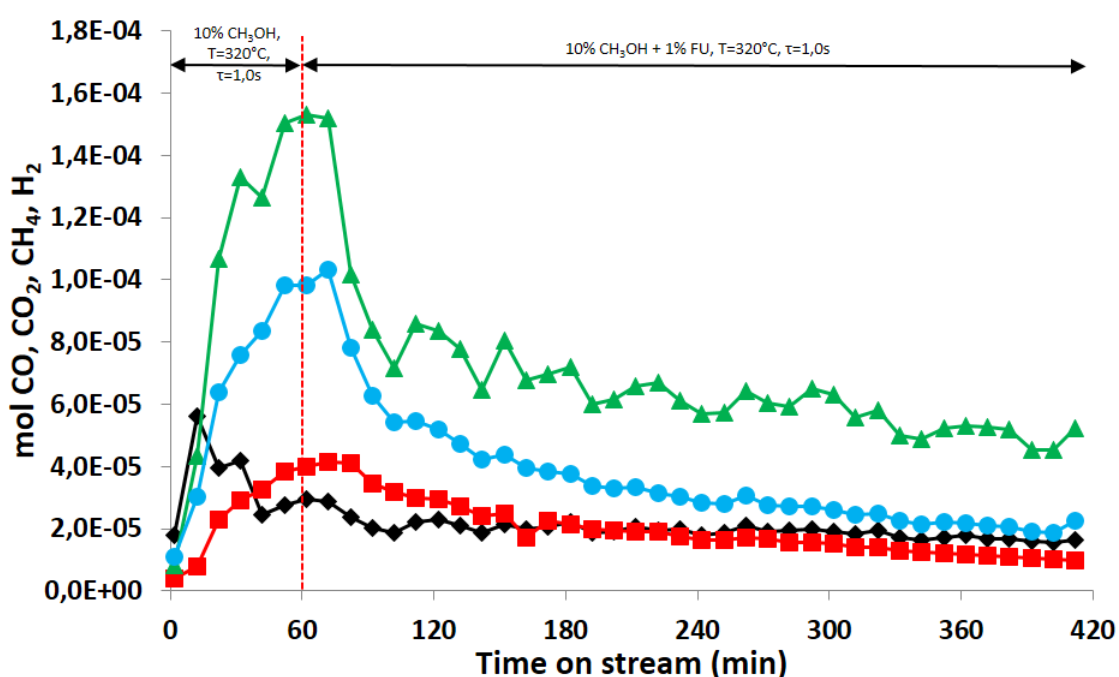

Figure 6-12. *FeVO₄ catalyst. Number of moles of gas formed, based on the time, in the reaction of methanol decomposition at 320°C (first hour) and in the reaction of FU reduction with methanol at 320°C. Feed composition: FU 1%, CH₃OH 10% , N₂ 89% ; Pressure 1 atm, overall gas residence time 1,0 s. Legend:* ♦ *CO,* ■ *CO₂,* ▲ *CH₄,* ● *H₂.*
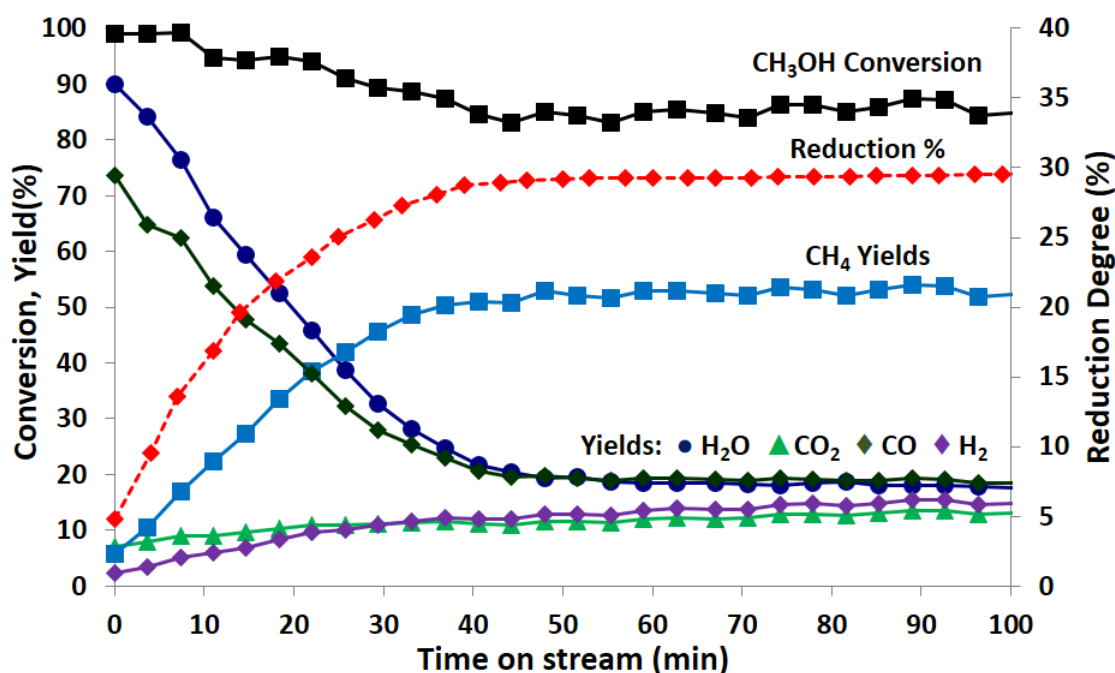
Figure 6-13. *FeVO₄ catalyst. Methanol conversion, light compounds yield and reduction degree, based on the time, in the reaction of methanol decomposition at 320°C. Legend: ■ CH₃OH conversion, ♦ CO, ▲ CO₂, ■ CH₄, ♦ H₂, ● H₂O, reduction degree (dotted line).*

In order to further validate this hypothesis and evidence modifications to $FeVO_4$ occurring during the first hours of reaction, we characterized samples subjected to different treatments by means of XRD and elemental analysis. The analysis of the catalysts used, either during FU reduction or with methanol alone, showed a very similar Fe/V atomic ratio (1.08), a value very close to that of the fresh sample (1.09), thus ruling out any loss of vanadium or iron during the first hour of reaction.

Furthermore, a test carried out by feeding methanol only over a fresh $FeVO_4$ catalyst was performed in order to evaluate the reduction degree of the sample; the latter was calculated by taking into account reaction stoichiometries and yields to all products. In fact, the O content in the outlet stream was higher than that contained in the inlet methanol stream, an evidence that confirmed the release of O^{2-} from the catalyst because of metal ions reduction. The experimental reduction degree estimated with this method was 30% (**Figure 6-13**). The patterns of the two used samples, after reaction with either methanol alone or with the FU/methanol mixture (**Figure 6-14**), were very similar and, at the same time, different from that one of the fresh catalyst.

The analysis of the diffraction pattern confirms the formation of a pure spinel structure. However, the only two known spinels containing iron and vanadium are Fe_2VO_4 and FeV_2O_4 (so called coulsonites), and neither of them completely match with the pattern of

our spent catalyst; in coulsonites, iron can be present either as Fe^{3+} or Fe^{2+}, and vanadium as V^{3+} or V^{2+}.

Overall, the analysis of the used catalyst confirmed the same Fe/V ratio as for the fresh one, and showed the formation of a single spinel structure with a reduction extent of 30%. All this led us to conclude that the composition of the spinel in the used catalyst was $Fe^{II}Fe_{0,5}^{III}V_{1,5}^{III}O_4$. Nevertheless, further in-situ studies are currently being carried out in order to confirm this hypothesis.

Summing up this part, by the analysis of the catalytic results in terms of substrate conversion, products distribution and trend of the light compounds exiting from the reactor it was possible to demonstrate that the catalyst was reduced as a consequence of the interaction with methanol at high temperature. Thus, the different catalytic behavior of the catalyst between the first and the following monitored hours of reaction was attributed to the lack of activated methanol as hydrogen source over the surface.
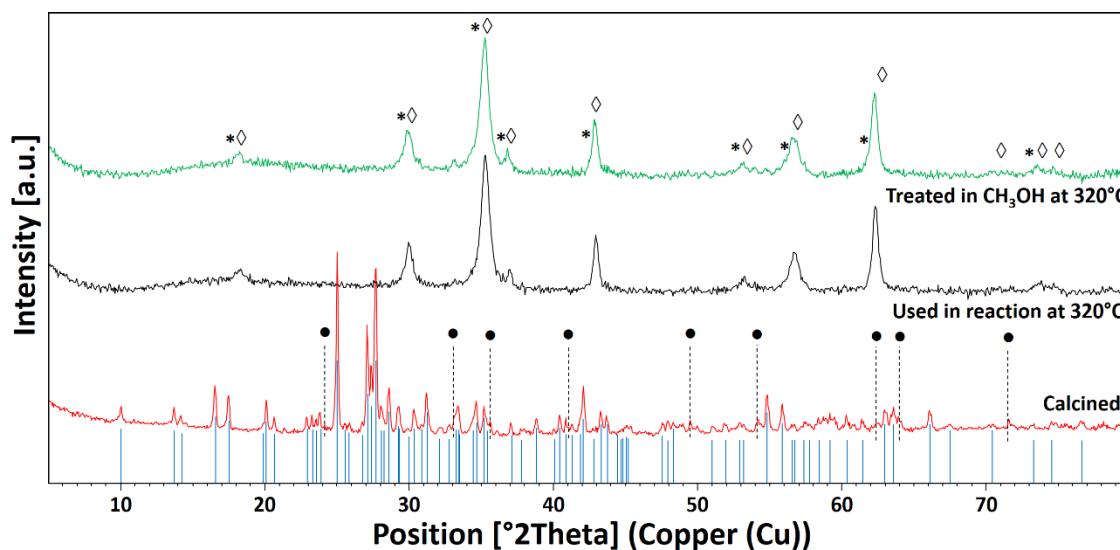

Figure 6-14. *XRD patterns of different FeVO₄ samples. Reference patterns: (—) FeVO₄, (●) Fe₂O₃, (◊) Fe₂VO₄, (*) FeV₂O₄.*

6.3.3. Effect of catalyst pre-reduction

Since catalyst characterization demonstrated that $FeVO_4$ was reduced by methanol during the first hour of reaction, the effect of catalyst pre-reduction was studied in order to check whether it can affect catalytic properties. In particular, catalyst pre-reduction was obtained by feeding methanol alone for 1 h at 320°C; then FU and methanol were fed again and activity was monitored as usual for 6 h. Results (**Figure 6-15** and **Table 6-5**) demonstrated that catalyst pre-reduction improved the performance. In fact, it was not just a higher MF selectivity compared to the untreated catalyst that was registered during the first hour of reaction, but also a greater stability with lower deactivation extent during the 6 h reaction time.

Accordingly, a notably lower C loss was observed and a final value of 80% conversion was registered after 6 h. With the fresh catalyst, final conversion was just 55%. The improved catalyst stability was due to the lower amount of heavy carbonaceous compounds formed with the pre-reduced sample during the initial period, the latter being due, in turn, to the catalyst's higher efficiency in methanol activation for H-transfer.
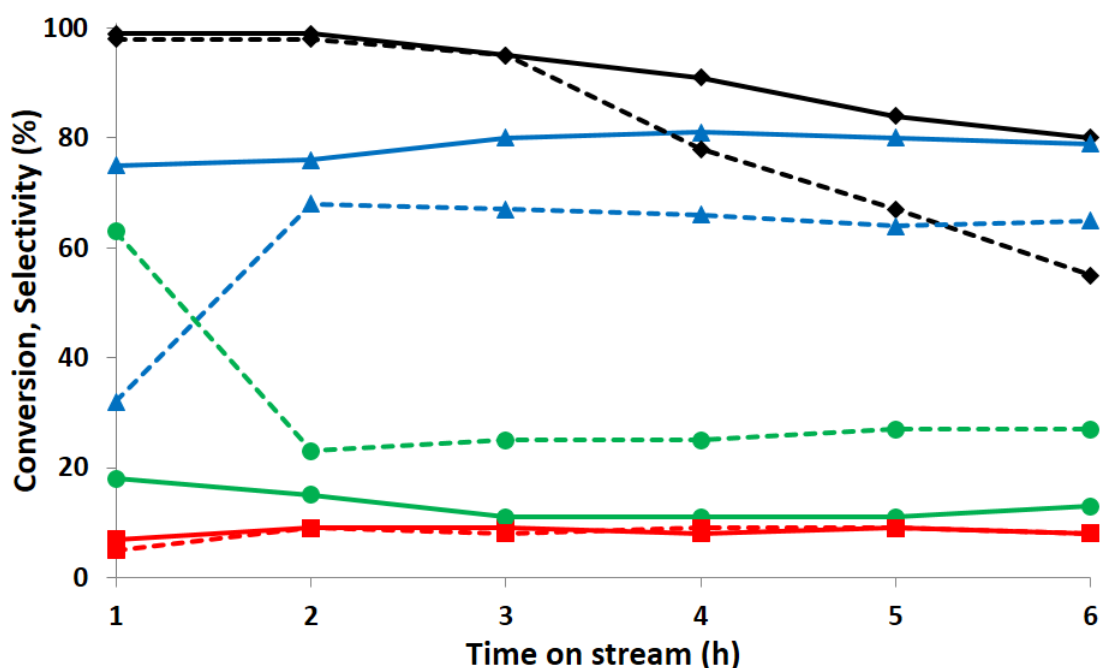
Figure 6-15. Effect of reaction time on FU conversion and product selectivity for pre-reduced FeVO₄ catalyst, feeding only methanol at 320°C for 1 h (bold line), and non-pre-reduced catalyst (dotted line). Feed composition: FU 1%, CH₃OH 10%, N₂ 89%; Pressure 1 atm, overall gas residence time 1.0 s. Legend: ♦ FU conversion, ▲ MF selectivity, ■ sum of DMF and VINFU selectivity, ● C loss.

Time on stream (h)	FU Conversion (%)	Product Selectivity (%)					MF Yield (%)
		FAL	MF	DMF	VINFU	C-Loss	
1	99	0	75	5	2	18	74
2	99	0	76	3	6	15	75
3	95	0	80	3	6	11	76
4	91	0	81	2	6	11	74
5	84	0	80	2	7	11	67
6	80	0	79	2	6	13	63

Table 6-5. *Effect of reaction time on FU conversion and product selectivity for the pre-reduced FeVO₄. Feed composition: FU 1%, CH₃OH 10%, N₂ 89%; Pressure 1 atm, 320°C, overall gas residence time 1.0 s.*

6.3.4. Study of the reaction network

In this section of the work will be reported the results of several experiments that have been conducted aimed to elucidate the reaction network. More specifically, the aim was to investigate the reasons why FAL was never detected, which was supposed to be the intermediate for MF formation starting from FU.

First, the effect of contact time over the catalytic performances has been studied (**Figure 6-16** and **Table 6-6**). Results were taken at the optimized temperature (320°C), having pre-reduced the catalyst with methanol and changing the contact time from 0.01 to 1.0 s. FU conversion increased from 16% at 0.01 s contact time up to 100%. At 0.01 s, MF was the main product with 32% selectivity; however VINFU and FAL, the latter with 2% selectivity, were also formed. Upon increasing FU conversion, MF selectivity increased up to 75% when contact time was set at 1 s. At the same time a lower C-loss was observed, from 63% down to 18%. DMF and VINFU were produced in low amounts ($\approx 5\%$) while FAL was no longer formed at contact times higher than 0.01 s, due to its consecutive transformation.

Contact time (s)	FU Conversion (%)	Product Selectivity (%)				
		FAL	**MF**	**DMF**	**VINFU**	**C-Loss**
0.01	16	2	32	0	3	63
0.1	59	0	61	2	5	32
0.5	95	0	71	3	5	21
1.0	99	0	75	5	2	18

Table 6-6. *Effect of contact time on FU conversion and product selectivity for FeVO₄ catalyst. Feed composition: FU 1%, CH₃OH 10%, N₂ 89%; Pressure 1 atm, Temperature 320°C, overall gas residence time 1.0 s.*
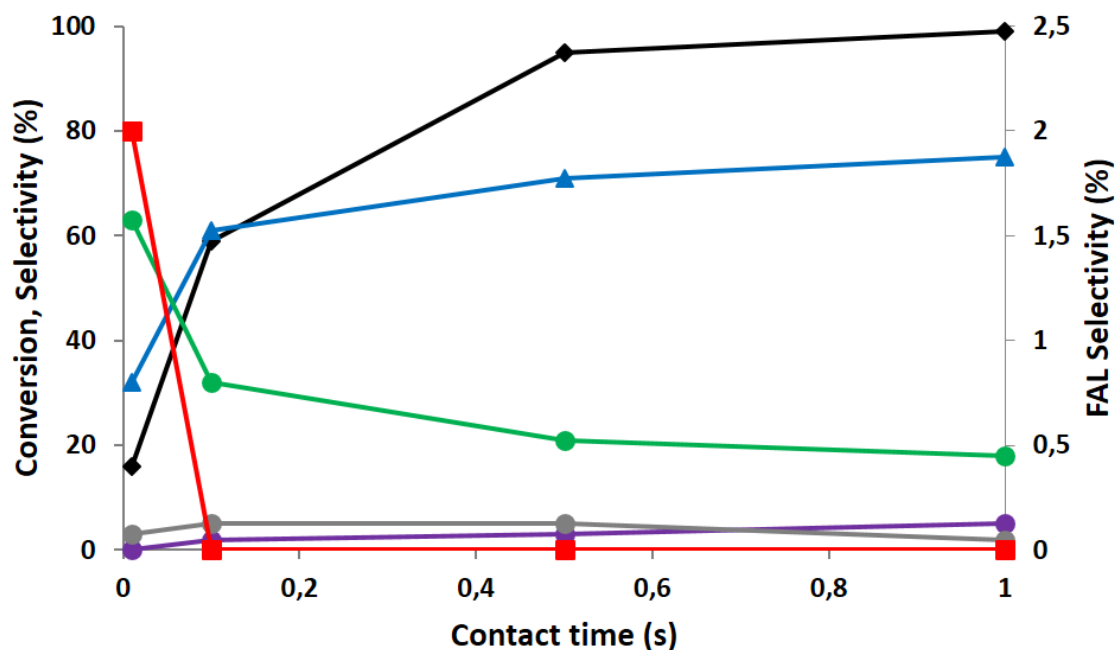
Figure 6-16. *Effect of contact time on FU conversion and product selectivity for FeVO₄ catalyst.*
Feed composition: FU 1%, CH₃OH 10%, N₂ 89%; Pressure 1 atm, Temperature 320°C, overall
gas residence time 1.0 s. Legend: ♦ FU conversion, ■ FAL selectivity ▲ MF selectivity, ● DMF
selectivity, ● VINFU selectivity, ● C loss.

Entry	Substrate	Conversion (%)	Products Selectivity (%)					
			FU	FAL	MF	DMF	VINFU	C-Loss
1	FU + CH₃OH [a]	99	-	0	75	5	2	18
2	FAL + CH₃OH [a]	100	2	-	60	4	0	34
3	FU [a]	31	-	0	21	0	0	79
4	FU [b]	35	-	0	0	0	0	100
5	FAL [a]	85	5	-	25	0	0	70
6	FAL [b]	56	6	-	6	0	0	88
7	MF + CH₃OH [a]	21	0	0	-	42	0	58
8	MF [a]	0	0	0	-	0	0	0
9	DMF + CH₃OH [a]	13	0	0	0	0	0	100
10	DMF [a]	0	0	0	0	-	0	0

Table 6-7. *Reactivity experiments carried out by feeding different reactants: FU or FAL or MF*
or DMF 1%, CH₃OH 10% , N₂ 89% or 99%; pressure 1 atm, temperature 320°C, overall gas
residence time 1,0 s, reaction time 1 h.

a. *Catalyst pre-reduced by feeding methanol at 320°C for 1 h;*

b. *Catalyst calcined in static air at 650°C.*

172

Some catalytic tests were conducted using different substrates (FU, FAL, MF, and DMF) as starting reagents, at 320°C, with both pre-reduced and fresh FeVO₄ (**Table 6-7**).

Entry 1 is the result obtained in the standard catalytic test after 1 h reaction time, using the pre-reduced catalyst. This can be compared with the result obtained by feeding FAL with methanol (entry 2). Also with FAL, the total conversion of the substrate was registered; MF and DMF were produced with 60% and 4% selectivity, respectively: values very similar to those obtained by feeding FU. This further supports the hypothesis that in FU reduction to MF, FAL is the reaction intermediate. It is also important to highlight that starting from FAL the formation of VINFU is not detected.

FU and FAL were then made to react, in the absence of methanol, on the pre-reduced catalyst (**Table 6-7** – entries 3 and 5). These experiments demonstrate that, in the absence of the H-transfer reactant, these substrates undergo degradation; indeed, the C loss registered was 70% or higher in both cases. However, also in this case we observed the formation of MF from FU and FAL, despite the absence of methanol. The analysis of the gas stream (**Figure 6-17**) showed the presence of CO_2, CH_4, and H_2. Therefore, it can be hypothesized that during the first half hour of reaction some adsorbed methanol, deriving from the previous catalyst reduction treatment, was available as the H source for the reduction of FU or FAL to MF.

Figure 6-17. *FeVO₄ catalyst. Number of moles of gaseous products formed, based on the time, for the catalytic test performed feeding only FU over pre-reduced catalyst. Feed composition: FU 1%, N₂ 99% ; Pressure 1 atm, Temperature 320°C, overall gas residence time 1,0 s. Legend: ♦ CO, ■ CO₂, ▲ CH₄, ● H₂.*
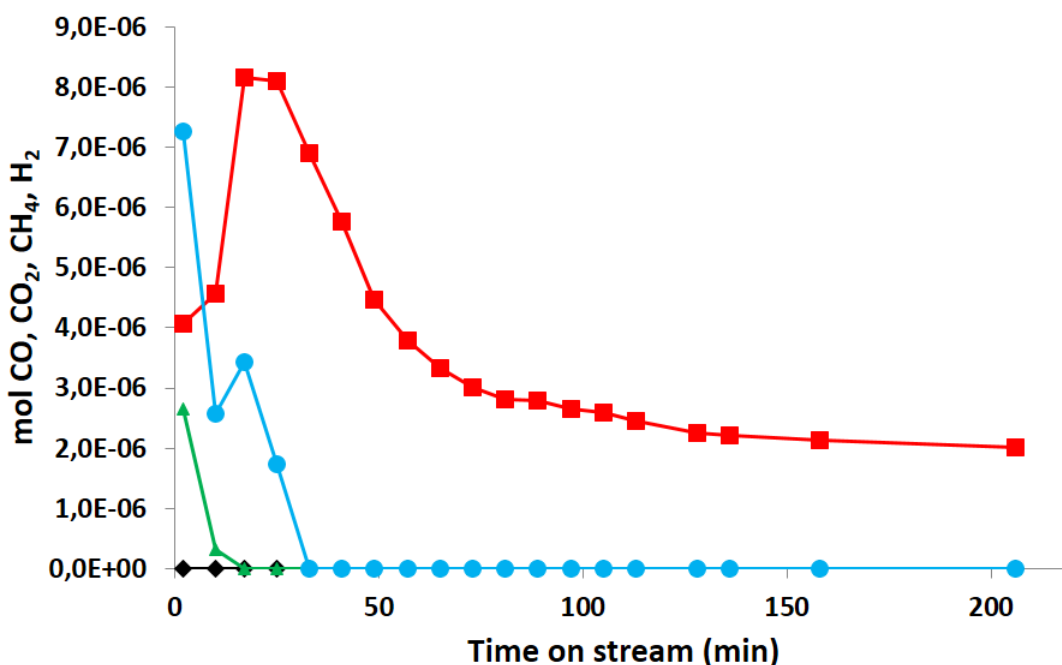
The same catalytic tests were performed by feeding FU and FAL, in the absence of methanol, with the fresh FeVO$_4$ (**Table 6-7** – entries 4 and 6). In these conditions, only small amounts of FU and MF formed from FAL (both with 6% selectivity) and C loss was very high. The equimolar formation of FU and MF could be due to FAL disproportionation; this reaction might contribute to MF and FU formation also with the pre-reduced catalyst (entry 5). TG/DT analysis of the spent catalyst (**Figure 6-18**) in air showed a weight loss of ≈ 3% in the temperature range 290-360°C which, coupled with an exothermic DTA peak, demonstrated the combustion of carbonaceous deposits. The absence of MF in FU reduction with the fresh catalyst confirms the hypothesis that the formation of MF with the pre-reduced catalyst (entries 3 and 5) was due to the presence of pre-adsorbed methanol.
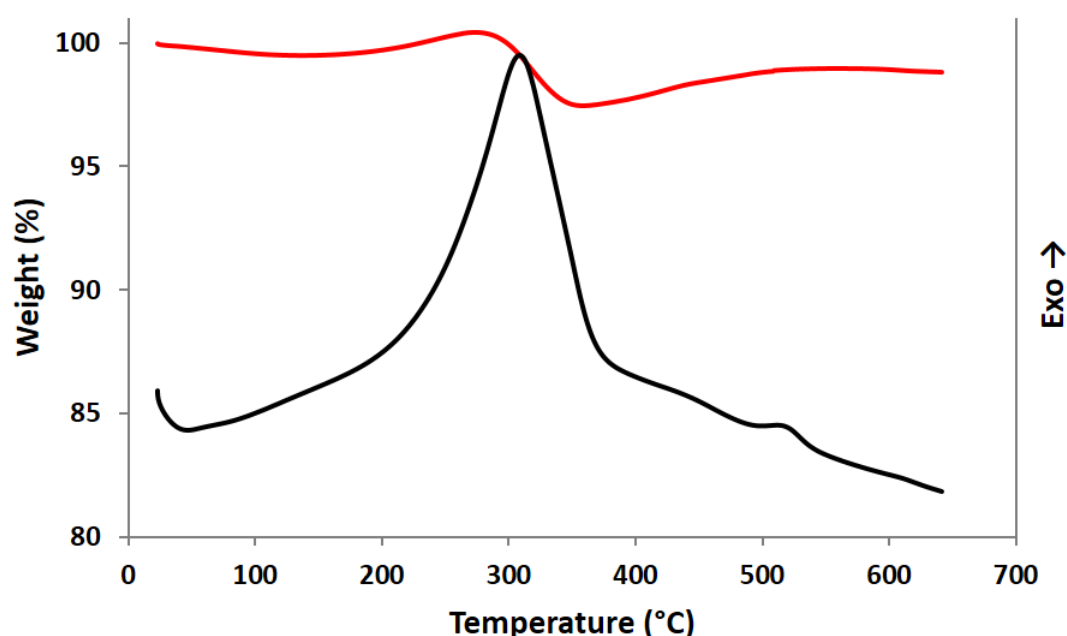
Figure 6-18. *Thermogravimetric (━) and differential thermal (━) analysis (TGA/DTA) in air of spent FeVO₄ (not pre-reduced with methanol before the reaction) used in the catalytic test performed feeding only 1% mol of FAL at 320°C.*

The catalytic tests performed by feeding MF and methanol (**Table 6-7** – entry 7) showed that the reduced catalyst is able to convert MF into DMF through a hydroxyalkylation process that involves MF and formaldehyde, the latter having been formed by methanol dehydrogenation. Furthermore, some experiments carried out by feeding MF and DMF without methanol (**Table 6-7** – entry 8 and 10) demonstrated that both compounds are stable and did not undergo consecutive degradation reactions.

Indeed, no substrate conversion was registered in the catalytic tests performed by feeding either MF or DMF. However, in the presence of methanol, DMF was converted by the 13% (**Table 6-7** – entry 9) and completely transformed into heavy carbonaceous compounds adsorbed over the catalyst surface; this behaviour was probably ascribable to the in-situ formation of formaldehyde that favours consecutive reactions on DMF.

Based on this study, it is possible to conclude that:

i)   FAL is the intermediate for the transformation of FU into MF; however, FAL is very reactive, and is very rapidly reduced to MF without desorbing in the gas phase; indeed, it was observed only in traces at a very low contact time (0.01s);

ii)   MF can be transformed into DMF by reacting with the in-situ-generated formaldehyde; the intermediate 2-methyl-5-hydroxymethylfuran, deriving from the electrophilic attack of formaldehyde, is also rapidly reduced to DMF;

iii) VINFU formed only from FU in the presence of methanol (**Table 6-7** – entry 1).

Entry	Substrate	H-source	Conversion, Selectivity (%)					C-Loss	MF Yield (%)
			FU	FAL	MF	DMF	VINFU		
1	FU	CH₃OH	99	0	75	5	2	18	74
2		2-propanol	93	0	60	0	0	40	56
3		acetone	58	0	8	0	0	92	5
4		CH₂O [a]	79	0	70	4	0	26	55
5		H₂	55	0	17	0	0	83	9
6	FAL	CH₃OH	2	100	60	4	0	34	60
7		2-propanol	2	97	58	0	0	40	56
8		CH₂O [a]	1	97	60	8	0	31	58
9		H₂	1	100	33	0	0	66	33

Table 6-8. *FU/FAL conversion and product distribution as a function of the hydrogen source used. Reaction conditions: 1% FU or FAL, 10% H source, 89% N₂, 1 atm, temperature 320°C, overall gas residence time 1.0s, reaction time 1h. Pre-reduced catalyst.*

a. CH₂O from formalin solution in water: 37% w/w CH₂O, 7-8% w/w CH₃OH.

We then tested the reactivity of FU and FAL on the pre-reduced catalyst with different H sources: formaldehyde, isopropanol, acetone, and hydrogen. **Table 6-8** shows the results of these experiments, collected during the first hour of reaction and compared with the results obtained with methanol as the H source.

It is interesting to note that the use of methanol (**Table 6-8** – entry 1) led to the formation of MF with a yield (74%) which was even higher than that registered with isopropanol (**Table 6-8** – entry 2), despite the latter being considered a much more active H-transfer reactant than methanol. It may be hypothesized that formaldehyde could also be directly involved in the mechanism of MF formation from FU. Conversely, with the much more reactive FAL, similar yields to FU were obtained with methanol and isopropanol (**Table 6-8** – entries 6 and 7).

The direct involvement of formaldehyde in MF formation with the co-production of CO_2 through a disproportionation involving the two aldehydes, in a way similar to that previously reported for salicylic aldehyde reduction[35] was demonstrated by reacting FU and FAL with formaldehyde (entries 4 and 8); the same reaction occurred only at a minor extent with acetone, the co-product of FU reduction with isopropanol (entry 3).

The results of the experiments carried out with H_2 (**Table 6-8** – entries 5 and 9) confirmed the higher reactivity of FAL, and showed that substrate reduction may also occur with H_2; the yield to MF, however, was much lower than that obtained with methanol. Nevertheless, these results demonstrate that a contribution to MF formation deriving from the in-situ generated H_2 should be also taken into account.

It is also worth noting that DMF formed in experiments conducted with methanol and formaldehyde, whereas VINFU formed exclusively with methanol. This confirms that the formation of the former compound involves the aldehyde, via an hydroxyalkylation step, whereas the latter forms only by reaction between FU and methanol.

A possible mechanism for VINFU formation might occur by the formation of the intermediate furfural methyl hemiacetal, as shown in **Scheme 6-2**. Hemiacetal could then be dehydrated into the corresponding enol, which would rapidly rearrange to furyl-methyl ketone; the latter is reduced by methanol to the corresponding alcohol, which is finally dehydrated to VINFU.

In order to support the mechanism proposed, we conducted an experiment entailing a direct feed of furylmethyl ketone and methanol onto the FeVO₄ catalyst at 320°C. The GC-MS analysis of the products revealed the formation of VINFU and ethylfuran; the

latter may form by hydrogenolysis of the alcohol. When the same experiment was conducted without methanol, no VINFU formed.

The formation of the hypothesized ketone was demonstrated by reacting a hemiacetal, trifluoroacetaldehyde methyl hemiacetal (unfortunately, the hemiacetal formed by reaction between furfural and methanol is not commercially available), without methanol. Hemiacetal was readily dehydrated to the ketone (in this case, trifluoroacetone).

These tests support the hypothesized mechanism for the formation of VINFU.
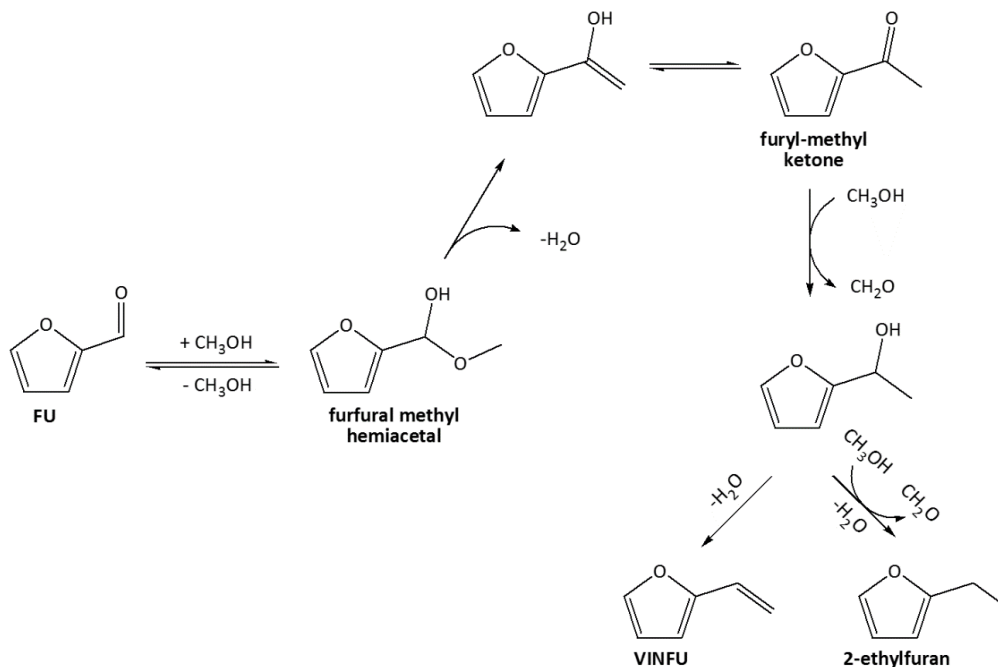
Scheme 6-2. *Possible reaction pathways for the formation of VINFU from FU in the presence of methanol on FeVO₄ catalyst.*

The overall network for the vapour-phase reduction of FU with methanol and the FeVO₄ catalyst is summarized in **Scheme 6-3**. MF can form via three different routes:

i.   the classic H-transfer two-step mechanism with the reduction of FU to FAL and of FAL to MF. Indeed, under normal conditions FAL is not isolated as an intermediate, because of its very high reactivity, also because of the possible involvement of formaldehyde (co-product of the MPV reaction) in the immediate reduction of FAL to MF (see the following point);

ii.   the disproportionation reaction involving the in-situ-generated formaldehyde, with reduction of FU to MF and co-production of CO_2;

iii. the hydrogenation of FU and FAL to MF involving the in-situ-generated H_2.

DMF forms by the hydroxyalkylation of MF with formaldehyde, and the reduction of the alcohol. VINFU forms by reaction between FU and methanol to the corresponding hemiacetal, which is then dehydrated to furylmethyl ketone and finally reduced again via H-transfer.
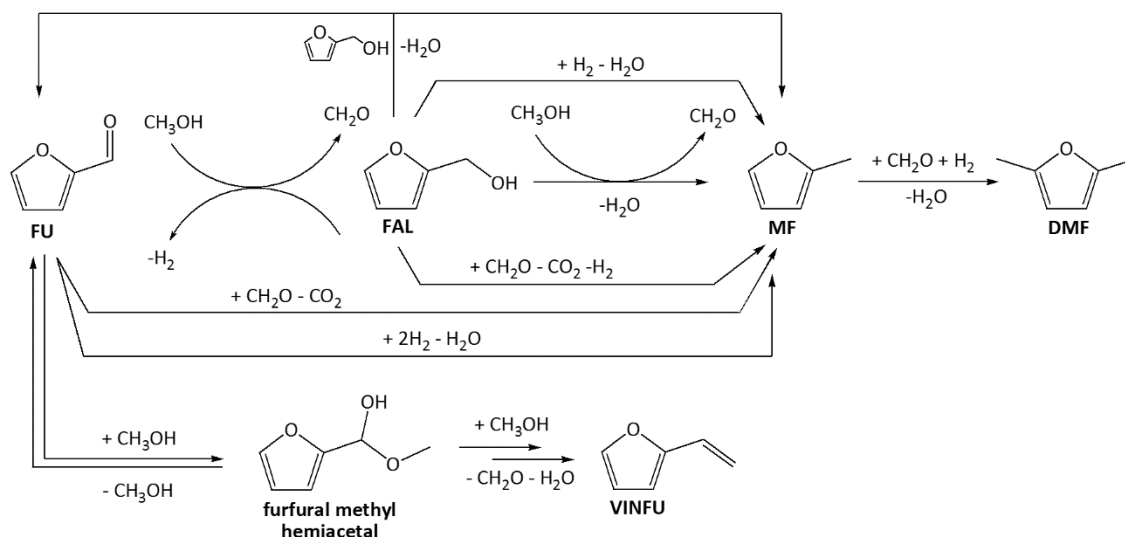
Scheme 6-3. *Overall reaction pathways for the transformation of FU on FeVO₄ catalyst in the presence of CH₃OH as H-source.*

6.7. Conclusions regarding FeVO₄ as bulk catalyst for the gas-phase catalytic transfer hydrogenation of FU to MF

FeVO$_4$ is a very active catalyst in the gas-phase production of 2-methylfuran from biomass-derived furfural using methanol as the H-transfer reactant. 320°C was the optimum reaction temperature at which the selectivity to MF was the highest and, at the same time, the formation of heavy carbonaceous residues was minimized. The deposition of the latter was the main cause of catalyst deactivation.

A simple procedure of FeVO$_4$ pre-reduction with methanol increased both catalyst stability and MF selectivity. Indeed, it was demonstrated that the catalyst was reduced by methanol to form a reduced oxide with spinel structure.

Due to its high activity, FeVO$_4$ offers an alternative to MF production from FU with a high yield without the need for H$_2$ at high pressure and precious metal catalysts. The formation of MF occurred via three different reaction pathways. In addition to the classic H-transfer mechanism, the in-situ-generated formaldehyde and H$_2$ played a direct role in the formation of MF. Furthermore, it has to be highlighted that the mixture of MF, DMF and VINFU could be directly used as fuel-additive thanks to the high energy content, high RON (higher than that of ethanol and 95-RON commercial gasoline), excellent auto-ignition behavior.

[1] J. Haber, *Catal. Today*, 2009, **142**, 100

[2] P. Forzatti, *Appl. Catal. A Gen.*, 2001, **222**, 221

[3] P. Forzatti, E. Tronconi, A. S. Elmi and G. Busca, *Appl. Catal. A Gen.*, 1997, **157**, 387

[4] T. Lehnen, M. Valldor, D. Nižňanský and S. Mathur, *J. Mater. Chem. A*, 2014, **2**, 1862

[5] H. Ma, X. Yang, Z. Tao, J. Liang and J. Chen, *CrystEngComm,* 2011, **13**, 897

[6] M. Koebel, M. Elsener, M. Kleemann, *Catal. Today,* 2000, **59**,335

[7] I. Nova, E. Tronconi, Urea-SCR Technology for DeNO$_x$ After Treatment of Diesel Exhausts; Springer: New York, 2014

[8] D. M. Chapman, *Appl. Catal. A,* 2011, **392**, 143

[9] M. Casanova, K. Schermanz, J. Llorca, A. Trovarelli, *Catal. Today,* 2012, **184**, 227

[10] F. Liu, H. He, Z. Lian, W. Shan, L. Xie, K. Asakura, W. Yang, H. Deng, *J. Catal.,* 2013, **307**, 340

[11] S. Djerad, L. Tifouti, M. Crocoll, W. Weisweiler, *J. Mol. Catal. A: Chem.,* 2004, **208**, 257

[12] G. Madia, M. Elsener, M. Koebel, F. Raimondi, A. Wokaun, *Appl. Catal. B,* 2002, **39**, 181

[13] M. A. L. Vargas, M. Casanova, A. Trovarelli, G. Busca, *Appl.Catal. B,* 2007, **75**, 303

[14] I. E. Wachs, *Dalton Trans.,* 2013, **42**, 11762

[15] A. Sagar, A. Trovarelli, M. Casanova, K. Schermanz, *SAE Int. J. Engines,* 2011, **4**, 1839

[16] K. Schermanz, A. Sagar, A. Trovarelli, M. Casanova, Transition-metal-vanadate or mixed transition-metal/rare earth-vanadate based catalyst composition for selective catalytic reduction of exhaust gases. Patent WO2010121280 A1, 2010

[17] M. Casanova, J. Llorca, A. Sagar, K. Schermanz, A. Trovarelli, *Catal. Today,* 2015, **241** (Part A,), 159

[18] J. Walczak, I. Rychłowska-Himmel, *Thermochim. Acta,* 1994, **239**, 269

[19] D. Chapman, G. Fu, S. Augustine, J. Crouse, *e. a. SAE Int. J. Fuels Lubr.,* 2010, **3**, 643

[20] Y. Peng, C. Liu, X. Zhang, J. Li, *Appl. Catal. B,* 2013, **140**, 276

[21] G. Reuss, W. Disteldorf, A.O. Gamer, A. Hilt, Ullmann's Encyclopedia of Industrial Chemistry, seventh ed., vol. A11, Wiley-VCH, Weinheim, 2008, pp. 619

[22] B. Crichton, in: Informally Speaking (newsletter from Perstorp Formox, <www.perstorpformox.com>), spring/summer 2003, pp. 12

[23] Methanex Corporation, Vancouver, Canada (methanol prices from 2002 to 2008, <www.methanex.com>)

[24] N. Burriesci, F. Garbassi, M. Petrera, G. Petrini, N. Pernicone, in: B. Delmon, G.F. Froment (Eds.), Catalyst Deactivation, Elsevier, Amsterdam, 1980, pp. 115

[25] A.P.V. Soares, M.F. Portela, A. Kiennemann, J.M.M. Millet, *React. Kinet. Catal. Lett.,* 2002, **75**, 13

[26] A.P.V. Soares, M.F. Portela, A. Kiennemann, L. Hilaire, *Chem. Eng. Sci.,* 2003, **58**, 1315

[27] A. Andersson, M. Hernelind, O. Augustsson, *Catal. Today,* 2006, **112**, 40

[28] T. Kim, I.E. Wachs, *J. Catal.,* 2008, **255**, 197

[29] G. Deo, I.E. Wachs, *J. Catal.,* 1994, **146**, 323

[30] S. Lim, G.L. Haller, *Appl. Catal. A,* 1999, **188**, 277

[31] R. Malinski, *React. Kinet. Catal. Lett.,* 1976, **5**, 265

[32] R. Malinski, M. Akimoto, E. Echigoya, *J. Catal.,* 1976, **44**, 101

[33] L.E. Briand, J.-M. Jehng, L. Cornaglia, A.M. Hirt, I.E. Wachs, *Catal. Today,* 2003, **78**, 257

[34] R. Häggblad, M. Massa, A. Andersson, *Journal of Catalysis,* 2009, **266**, 218

[35] N. Ballarini, F. Cavani, L. Maselli, A. Montaletti, S. Passeri, D. Scagliarini, C. Flego, C. Perego, *J. Catal.,* 2007, **251**, 4238

[36] Nakajima et Al., United State Patent 3937669, 1976

[37] K. Routray, W. Zhou, C. J. Kiely, I. E. Wachs, *ACS Catal.,* 2011, **1**, 54

[38] N. Dhachapally, V. N. Kalevaru, A. Brückner, A. Martin, *Appl. Catal. A: General,* 2012, **443–444**, 111

[39] L. A. de Faria, S. V. Silva, M. T. T. de Oliveira, *J. Raman Spectrosc.*, 1997, **28**, 873

[40] G. Busca, *J. Mol. Catal.,* 1989, **50**, 241

[41] L. J. Burcham, G. Deo, X. Gao, I. E. Wachs, *Topics in Catal.,* 2000, **11/12**, 85

[42] G. Busca, *Catal. Today,* 1996, **27**, 457

[43] C. Lucarelli, G. Pavarelli, C. Molinari, S. Albonetti, W. Mista, D. Di Domenico, A. Vaccari, *Int. J. Hydrogen Energy,* 2014, **39**, 1336

[44] Y. Nakamura, T. Murayama, and W. Ueda, *ChemCatChem,* 2014, **6**, 741

[45] Y. Nakamura, T. Murayama, W. Ueda, *J. Mol. Catal. A Chem.,* 2014, **394**, 137

APPENDIX A   Lithium-doped MgO: an highly active catalyst for the liquid-phase catalytic transfer hydrogenation process

A.1. Introduction

In the present section the results concerning the liquid-phase catalytic transfer hydrogenation of furfural (FU) and 5-hydroxymethylfurfural (HMF) to the corresponding unsaturated alcohols (furfuryl alcohol-FAL and 2,5-bishydroxymethylfuran-BHMF) by-means of methanol as H-transfer reactant and Lithium-doped MgO have been presented and discussed.

In a previous section of this work it was indeed reported that an high surface area MgO acted as active and selective catalyst for the reduction of the carbonyl group of FU and HMF. Indeed, in the proper reaction condition, 100% of substrate conversion with 100% of yield into the corresponding unsaturated alcohol was obtained[1].

Figure A-1 shows the effect of the amount of catalyst loaded in the reactor on FU and HMF conversion and selectivity towards the corresponding unsaturated alcohol. Increasing the amount of MgO progressively increased the conversion of the substrate up to the total value obtained loading 1 g; on the other hand, independently from the loaded mass, the catalyst showed to be always totally selective toward both FAL and BHMF.

Despite this, MgO exhibited the drawback to suffer of a slight deactivation in the following stability tests performed treating it with a simple work-up procedure of separation and drying. The formation of carbonaceous deposits over the catalyst surface deriving from methanol degradation process in our reaction condition was identified as the main cause of the deactivation. Furthermore, a work-up procedure consisting in a thermal treatment in static air at 450°C allow the complete removal of the carbon deposits and the recovery of the initial activity.

On the base of the obtained results with pristine MgO, the aim of the present section of the work is to evaluate the effect deriving from the doping of MgO with Lithium. Indeed, in literature is reported that the activity of MgO in the reaction of methane oxidative coupling could be increased by lithium doping.
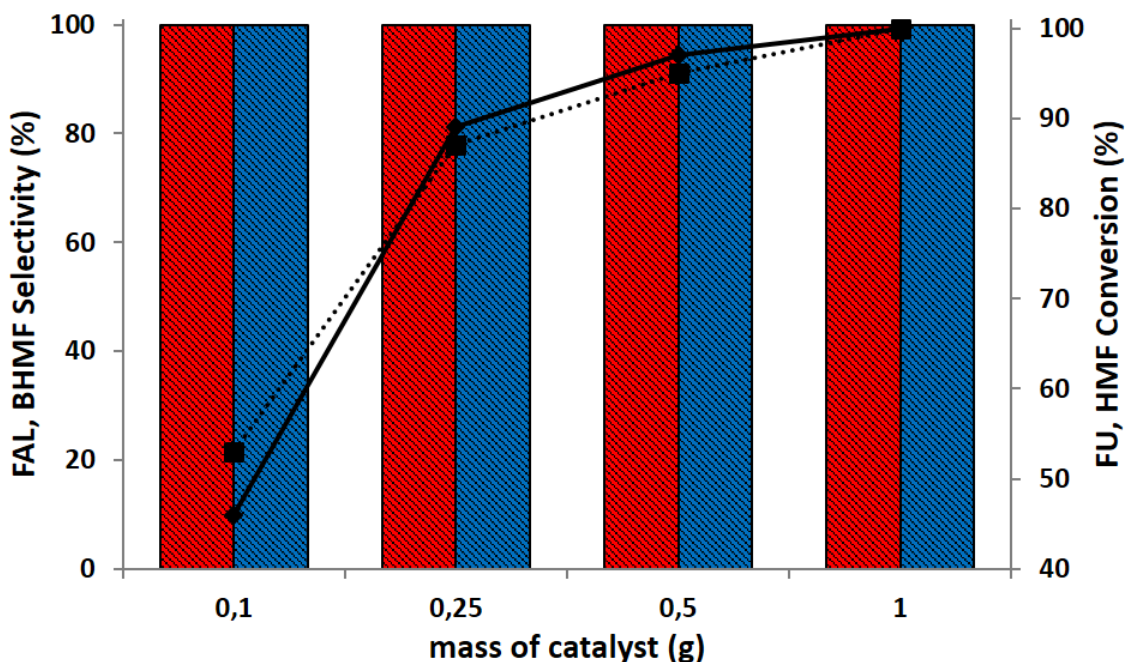
183

Figure A-1. *Substrate conversion and unsaturated alcohol selectivity as a function of the mass of MgO loaded. Reaction conditions: 50 ml of CH₃OH, 1.21 mmol of FU or HMF, T = 160°C, t = 3h, 1 g of MgO. Legend: FU conversion (♦-bold line), HMF conversion (■-dotted line), FAL selectivity (■), BHMF selectivity (■).*

A.2. Lithium-doped MgO

Research on the oxidative coupling of methane (OCM) has increased in intensity over the past decade due to the potential for converting natural gas directly to higher value chemicals, such as ethylene[2,3]. Indeed, methane, one of the main component of natural gas, is highly underutilized due to two problems: the conversion into value added products is difficult, because CH_4 is the most stable hydrocarbon and therefore difficult to activate; difficulties in transporting natural gas from the source to the consumer.

The oxidative coupling of methane (OCM), could overcome these problems and therefore, it is a reaction of great industrial interest. However, this reaction showed some drawbacks that make not possible the development of industrial plants. The main ones are the high temperature at which this process runs and the lack of activity and selectivity of the catalysts.

The simplest catalysts for this reaction, among a large number of complex solid oxides, is Li-doped MgO[4]. Early, Lunsford proposed that the active sites are $O^{\bullet-}$ radicals neighbored to Li^+, with $Li^+O^{\bullet-}$ formally replacing $Mg^{2+}O^{2-}$ [5] and that the C—H bond is activated by homolytic splitting involving hydrogen atom transfer to the $O^{\bullet-}$ sites[6].

184

Lunsford et al. correlated electron paramagnetic resonance (EPR) signals with the methyl radical formation rate, concluding that a [Li$^+$O$^-$] defect is the active center.

It has become a widely accepted fact, even so contradictory results exist in the literature. Mirodatos et al. found that a tight interface between Li$_2$CO$_3$ and MgO is necessary for a good catalytic performance but it only occurs after pretreatment at temperatures allowing the liquefaction of Li$_2$CO$_3$[7,8].

Due to the high initial selectivity and activity of this system, Li/MgO was long the main comparison for any OCM study. However, while catalyst stability was rarely probed in the earlier studies, it has become a key component of the OCM literature, since the Li/MgO catalyst was found to deactivate rapidly during time on stream experiments due to Li volatility[9,10].

However, there is also evidence that the Li$^+$O$^{\bullet-}$ site may not be the active site and that the C—H bond activation may be through heterolytically split[11]. Recently, crucial ENDOR experiments showed that in none of the powder catalysts that were run under an OCM atmosphere Li$^+$O$^-$ centers could be found[12,13] although they were detectable in Li-doped MgO single crystals prepared by arc fusion of MgO/Li$_2$CO$_3$. On the other hand, by careful multi-method characterization[13,14], Li addition was found to lead to restructuring of the MgO surface exposing steps and corner sites and high-index crystallographic surfaces compared to pristine MgO.

Kwapien et al. Recently demonstrated that the higher catalytic performances of the Li-doped MgO is related to possibility to create more defectively sites in the doped materials compared to the pristine one[15]. Quantum chemical calculations and temperature programmed reaction experiments support this conclusion. Indeed, on both Li-doped MgO and pure MgO catalysts conversion of CH$_4$ and O$_2$ starts at about 410°C and formation of C2 species at about 540°C. The difference is that in this initial phase of the reaction Li-MgO is far more active and selective in forming C2 coupling products than pure MgO. We conclude that the reaction pathways are the same for both materials and that the same active sites are present. The role of Li-doping is increasing the number of active sites, which is most likely due to changes of the morphology connected with the formation of a larger number of low-coordinate O^{2-} ions at edges, corners, and kinks.

Further confirmation of the strong morphological promotion of MgO by Li was also predicted by using atomistic and density functional theory approaches by Watson and co-workers[16]. Watson calculated that a particularly stable configuration was achieved when one surface Mg^{2+} ion on the 50% vacant surface Mg layer of the {111} MgO surface was

substituted for two Li ions, leading to a 100% surface layer composed of Li. They finally predicted a transition from the cubic morphology of un-doped MgO to {111} truncated cubes and finally octahedrons at high Li concentrations.

Finally Zavyalova and co-workers demonstrated, thanks to a systematic characterization procedure involving several techniques such as XRD, BET and pore size analysis, SEM/TEM electron microscopy, IR and thermogravimetric mass spectroscopy (TG-MS) in combination with XRD, Diffuse reflectance UV/Vis (DR-UV/Vis) and electron paramagnetic resonance (EPR), that the effect of Li addition on MgO could be rationalized as a roughening of the MgO surface on an atomic level, leading to exposition of more low coordinated O^{2-} surface ions and higher index planes such as fourfold and threefold coordinated surface O^{2-} ions, O^{2-}_{4c} and O^{2-}_{3c}[17].

Therefore, the aim of this part of the work is to evaluate if the lithium-doping of MgO could positively affects the activity of the catalyst in the liquid-phase catalytic transfer hydrogenation of FU and HMF to the corresponding unsaturated alcohols FAL and BHMF by-means of methanol as H-transfer reactant.

The effect of the lithium addition has been evaluated over two MgO support: the high surface synthesized MgO (MgO-HSA) and the commercial MgO with low surface area (MgO-C). At first the catalytic activity of the pristine supports and that of the doped systems have been compared preparing two doped material containing the 2% weight of lithium and testing it in the reduction of both FU and HMF. In a second moment the effect of the lithium doping has been evaluated with the commercial support.

A.3. Results and discussion

A.3.1. Bulk features of the catalysts

The lithium-doped catalysts were synthesized following the wet-impregnation methodology described by Arndt et al.[18]; after the dissolution in water of the right amount of lithium precursor (Li_2CO_3) the support was added and the resulting suspension was stirred for two hours at room temperature. Then, the water was evaporated by-means of a rotavapor; the obtained white solid was dried at 120°C overnight and then calcined at 500°C in static air for 5h.

n°	Catalyst	Li content (wt%)	Calcination Temperature (°C)	Crystalline phase (XRD)	SSA m²/g	Total basicity (mmol/g)ᵃ	Total basicity (mmol/g)ᵇ	Total acidity (mmol/g)ᶜ
1	MgO-HSA	0	500	MgO (periclase)	200	7,05	7,51	0
2	2-Li/MgO-HSA	2	120	$Mg(OH)_2$ + Li_2CO_3	-	-	-	-
		2	500	MgO + Li_2CO_3	200	6,94	7,43	0
3	MgO-C	0	-	MgO (periclase)	14	0,44	0,39	0
4	2-Li/MgO-C	2	120	MgO + Li_2CO_3	-	-	-	-
		2	500	MgO + Li_2CO_3	13	1,45	0,92	0
5	5-Li/MgO-C	5	500	MgO + Li_2CO_3	11	1,86	1,65	0
6	10-Li/MgO-C	10	500	MgO + Li_2CO_3	9	1,95	1,84	0

***Table A-1.** Main features of the Li-doped catalysts.*

    a. *Determined by irreversible adsorption of acrylic acid;*

    b. *Determined by CO_2-TPD;*

    c. *Determined by NH_3-TPD.*

Table A-1 summarizes the main features of the synthesized materials using both the MgO-HSA and the MgO-C as support for the deposition of lithium. At first only doped catalysts containing a fixed Li-content equal to the 2% weight were prepared in order to check the effect deriving from the addition of the alkaline metal in a series of preliminary tests.

The two materials used as support showed the same well defined MgO periclase crystalline structure (**Table A-1** Entries 1 and 3). The main difference characterizing the two samples of magnesium oxide consisted in the specific surface area and in the amount of the total basic sites. Concerning the former parameter, the synthesized material showed a surface area of 200 m^2/g while, for the commercial one, that value was many times lower (14 m^2/g). Different synthesis method or different calcination temperature used for the preparation of the commercial sample could be the explanation for the difference. The lower surface area showed by the latter sample was also reflected by the number of basic sites detected by means of the irreversible adsorption of acrylic acid and CO_2-TPD as probe molecules. Indeed, the commercial materials showed a lower amount of total basic sites if compared to the synthesized one. Nevertheless, both the materials showed the complete absence of acidity confirming their basic feature.

Concerning the surface area of the lithium-doped materials, the addition of the 2 weight % of dopant seemed to leave unaltered that parameter. Indeed, for both the supports used, the surface area measured for the calcined materials obtained after the addition of lithium showed to be, within the experimental errors, very similar. A very limited decrease of surface area was indeed observed for the samples prepared loading the 5 and 10 weight % of lithium over the commercial support.

In **Figure A-2** are collected the X-ray diffraction patterns of the dried and calcined materials obtained after the addition of lithium. In the case of the synthesized MgO-HSA the consequence of the wet impregnation procedure used for the deposition of lithium was the crystalline phase transition from the original MgO periclase structure to the one of Mg(OH)$_2$ brucite. That transition was the consequence of a well-known property of magnesium oxide and hydrotalcite-like materials named memory effect, which consisted in the ability to hire back the structure of their precursor if exposed to water or carbon dioxide[19]. Despite this phase change, the periclase structure was formed again after the calcination treatment at 500°C. According to the literature[17] it was demonstrated that the alkaline metal was present on the support's surface as Li$_2$CO$_3$ also after the high

temperature treatment, demonstrating that the latter was not strong enough to decompose it to the oxide form.

The same structural features were confirmed for the materials obtained using the MgO-C as support for the lithium deposition. Indeed, the calcined sample showed a well-defined magnesium oxide periclase structure with the addition of Li_2CO_3; furthermore, the reflexes related to the latter structure showed a progressively increase in the intensity at the increase of the lithium content. The main difference with the sample synthesized using the high surface magnesium oxide consisted in the structure of the dried sample obtained after the impregnation procedure. In the case of the catalyst obtained using the commercial support the phase transition due to the memory effect was only partial, the reflexes related to the brucite phase were indeed observed but their intensity was very low; a possible higher calcination temperature used to stabilize the periclase crystalline phase in the industrial production process could be the reason.
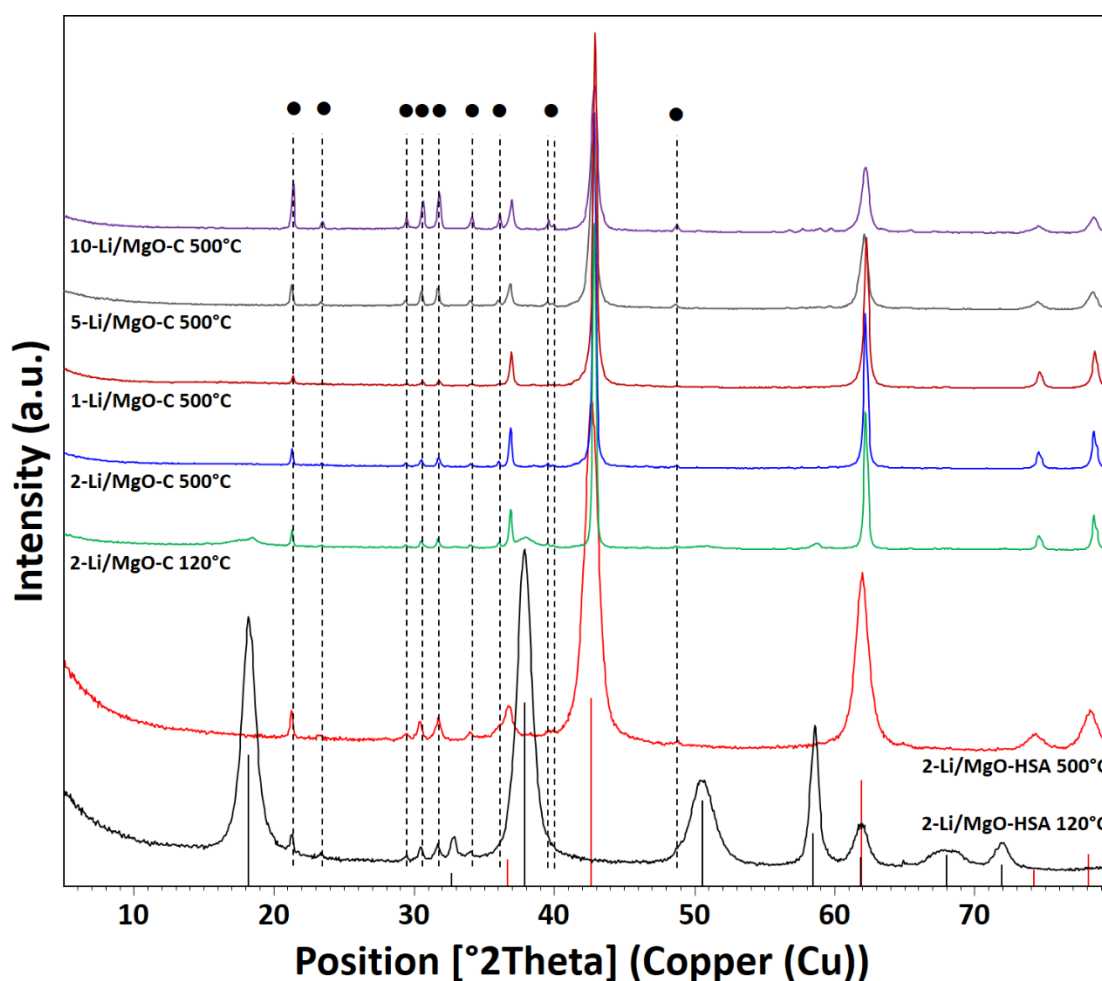

Figure A-2. *XRD patterns of the dried and calcined samples obtained after the addition of Li by-means of wet impregnation over the supports MgO-HSA and MgO-C. Reference patterns: (━) Mg(OH)₂ brucite, (━) MgO Periclase, (●) Li₂CO₃.*

Concerning the basicity of the synthesized lithium doped catalysts, the irreversible adsorption of acrylic acid demonstrated the existing of basic features for all the prepared systems; nevertheless, the addition of lithium differently influenced that parameter depending on the used support. The doping of the MgO-HSA (**Table A-1** entries 1 and 2) left unaltered, within the experimental errors, the total amount of basic sites detected while, for the series of the doped Li/MgO-C materials a correlation between the total amount of the basic sites and the lithium loading was observed. Indeed, a progressively increase of the basicity, in term of sites number, was observed at the increase of the amount of lithium loaded over the commercial support, leading to a value of 1,95 mmol/g for the sample containing the 10% wt of lithium. Nevertheless, the basicity of the doped Li/MgO-C catalysts was always lower to that of the MgO-HSA synthesized material, indicating that the synthetic procedure used for the preparation of the latter allow the production of a material with higher surface area and higher amount of basic sites.

A further confirmation of the existing relationship between the lithium addition and the change of the basic features in the doped Li/MgO-C materials compared to the un-doped one has been found in the CO_2-TPD results that well agree with those determined by-means of the irreversible adsorption of acrylic acid. The analysis of the CO_2 desorption profiles (**Figure A-3**) allow also to find information related to the strength of the basic sites. In literature is indeed generally reported that, based on the CO_2 desorption temperature, the curve could be divided into three regions each of that represent different basic sites: the weak basic sites correspond to the CO_2 desorbed in the temperature range between 25 and 125°C, the medium sites to that desorbed in the range 125÷225°C while, the strong basic sites, were correlated to the CO_2 desorbed at temperature higher than 225°C[20].

The investigation of the basic sites distribution demonstrated that the number of weak basic sites, related to the presence of hydroxyl groups over the surface of the catalyst, was very low for all the tested catalysts, indicating the almost total absence of the –OH groups that were completely removed during the calcination process. All the materials resulted mainly characterized by the presence of strong basic sites but, a correlation between the lithium doping and the strength distribution seemed to be present. As a matter of fact, increasing the amount of lithium a progressive shift to lower temperature for the CO_2 desorption peak was observed indicating that the doping with lithium decreased the strength of the sites. The pristine support showed indeed the desorption peak centered around 380°C while, the samples containing the 2, 5 and 10% of lithium were

characterized by a shift for the maximum of the desorption curve to 340 and 260°C respectively. Thus, the doping of the commercial magnesium oxide with lithium allow to generate an higher basicity in the material; the higher was the amount of lithium added the higher was the resulting basicity. At the same time, the new basic sites generated over the surface as a consequence of the lithium addition were characterized by a lower strength if compared to the ones characterizing the pristine MgO-C.
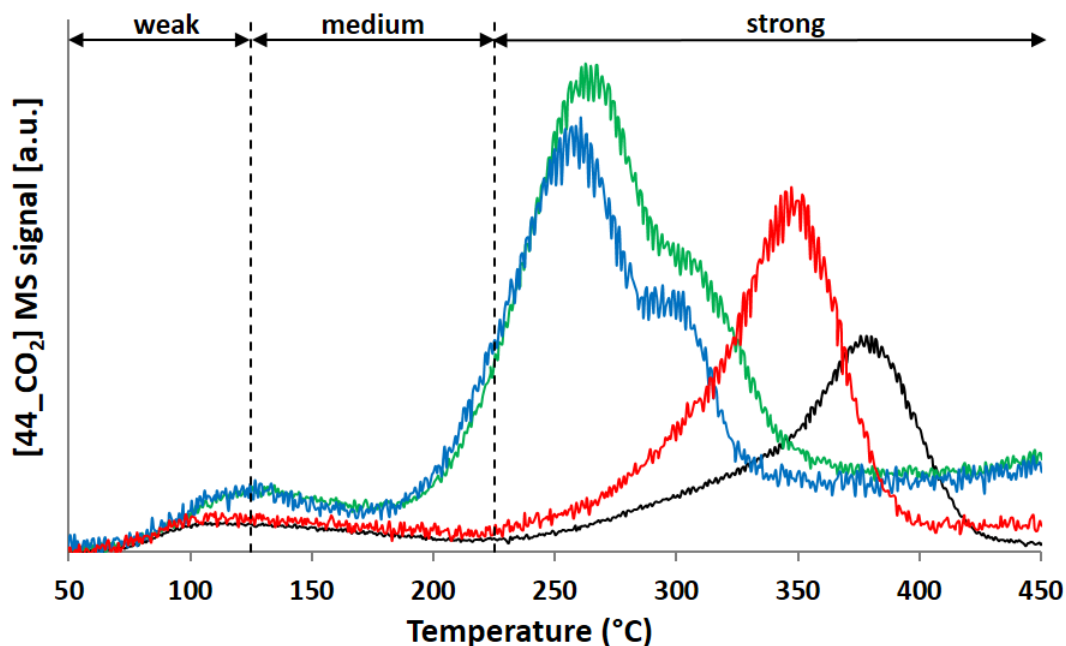

Figure A-3. Example of CO$_2$-TPD profile for the Li/MgO-C catalysts. CO$_2$-MS signal legend: MgO-C (━), 2-Li/MgO-C (━), 5-Li/MgO-C (━), 10-Li/MgO-C (━).

Finally, in order to gain more information related to the superficial morphology, TEM characterization over the Li/MgO-C catalysts were performed. Indeed, Zavyalova and co-workers demonstrated with the same technique that the addition of lithium over MgO caused a roughening of the MgO surface on an atomic level, leading to exposition of more low coordinated O^{2-} surface ions and higher index planes such as fourfold and threefold coordinated surface O^{2-} ions, O$^{2-}_{4c}$ and O$^{2-}_{3c}$[21]; which were responsible for the formation of the basic sites.

The TEM images collected over the synthesized Li/MgO-C samples (**Figure A-4**) confirmed that increasing the lithium content increased the roughening of the surface. The images related to the un-doped MgO-C showed indeed a well-defined and squared shape for the crystallites while, at the increase of the lithium content, the shape of these became progressively less defined and characterized by an higher number of crystallites

with smaller dimension demonstrating once again that the introduction of lithium induced a superficial reconstruction leading to the formation of an high number of defective sites and so to an increase of the total basicity of the catalyst.
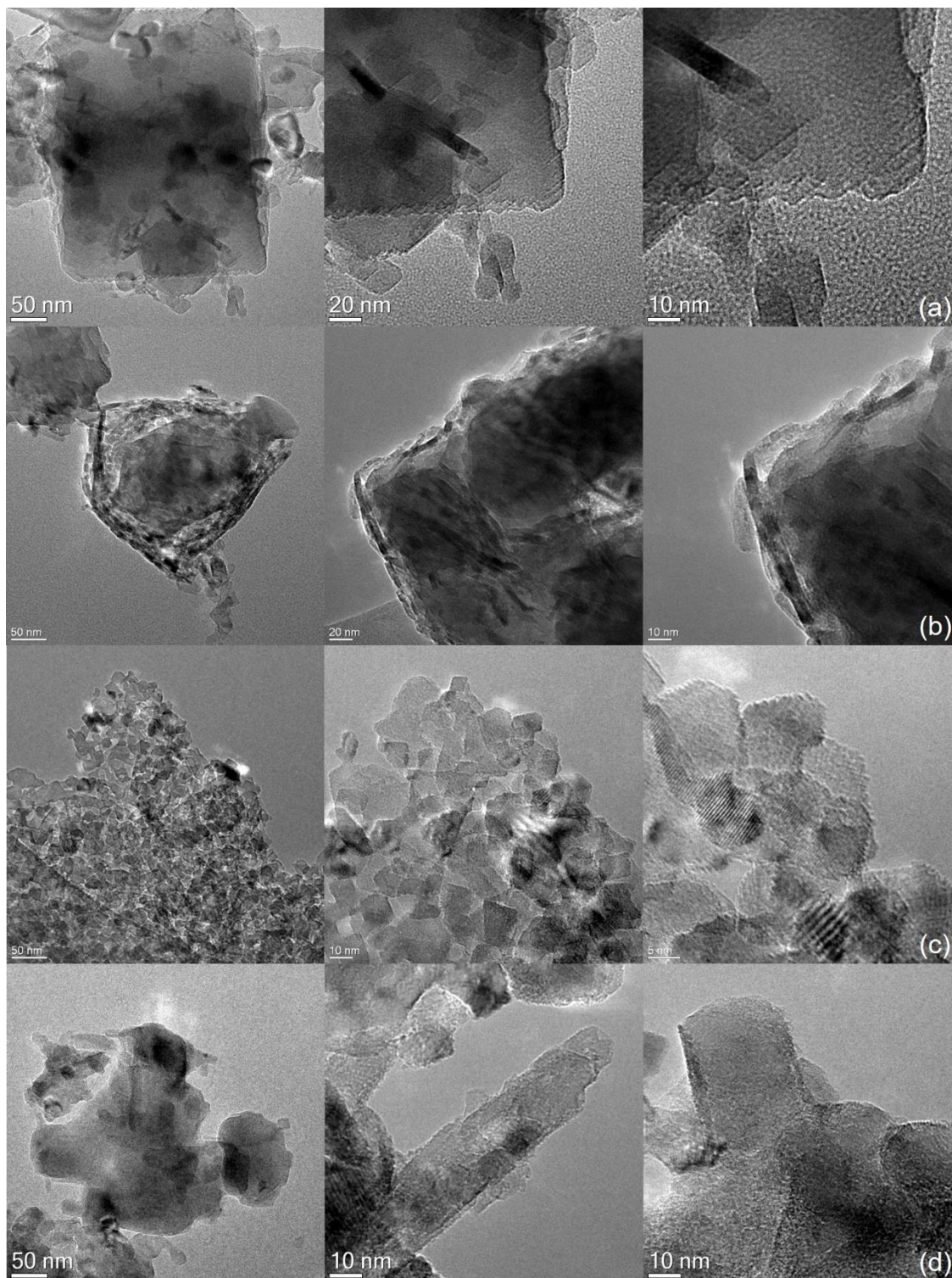

***Figure A-4.** TEM images of the lithium-doped catalysts based on MgO-C as support. Legend: (a) MgO-C, (b) 2-Li/MgO-C, (c) 5-Li/MgO-C, (d) 10-Li/MgO-C.*

A.3.2. Liquid-phase catalytic transfer hydrogenation of HMF over Li-doped MgO catalysts

In the present section of the work the preliminary catalytic tests aimed to evaluate the effect deriving from the addition of lithium as dopant to increase the activity of MgO as basic catalyst for the liquid-phase catalytic transfer hydrogenation have been performed using HMF as the reducible substrate and methanol as the hydrogen source. In particular these preliminary tests were performed to make a comparison between the catalytic activity of the pristine supports, MgO-HSA and MgO-C, and the corresponding doped materials containing the 2% weight of Lithium.

In the chapter concerning the description of the catalytic transfer hydrogenation reaction (CTH) as a tool for the valorization of the biomass-derived building block was indeed reported that in literature the activity of a basic catalyst in the CTH has been related to two main features of the materials: the number of the basic sites, and so in the most of the cases, to the surface area considering that the higher was the latter the higher was generally the number of basic sites; the number of defectively sites over the surface.

On the base of these information and considering that in the former part of the present chapter it was reported that the doping of MgO with lithium could increase the number of the defective sites and the resulting activity of the doped systems in the oxidative coupling of methane reaction, the aim was to evaluate if the same increase in activity could be obtained in the CTH reaction.

Entry	Catalyst	HMF Conversion (%)	BHMF Yield (%)	C-Loss (%)
1	MgO-C	5	5	0
2	2-Li/MgO-C	87	14	73
3	MgO-HSA	100	100	0
4	2-Li/MgO-HSA	100	95	5
5	Li_2CO_3	100	0	100

Table A-2. *HMF conversion and BHMF yield obtained with the different catalysts used for the preliminary tests. Reaction conditions: 50 ml of CH_3OH, 1.21 mmol of HMF, T = 160°C, t = 3h, 1 g of catalyst.*

Figure A-5. *HMF conversion and BHMF yield obtained with the different catalysts used for the preliminary tests. Reaction conditions: 50 ml of CH₃OH, 1.21 mmol of H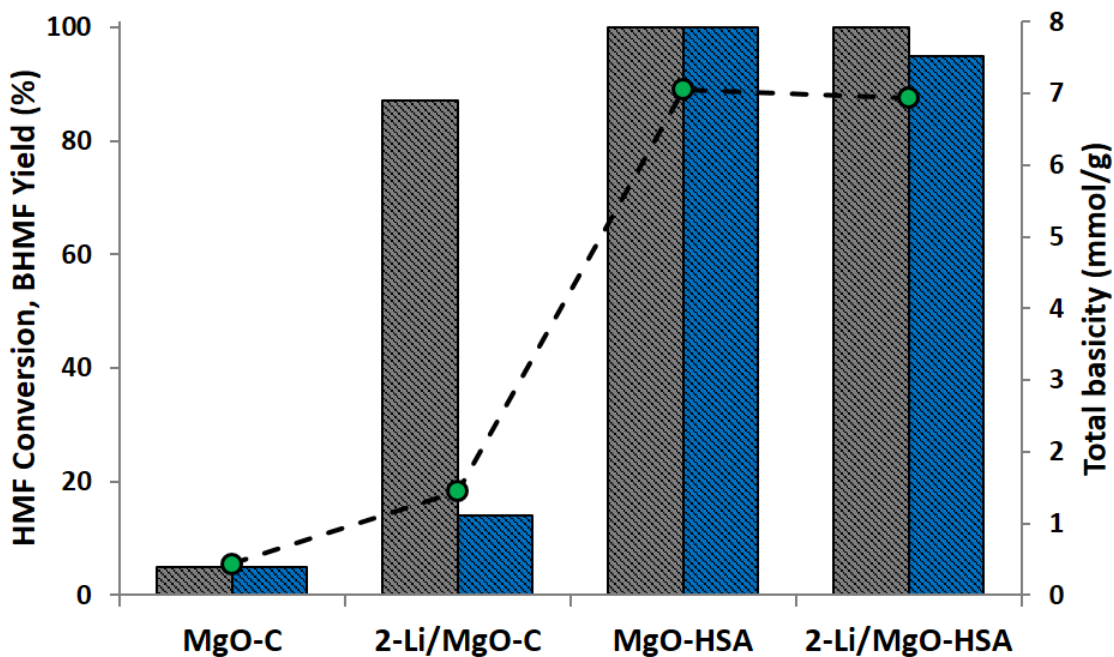MF, T = 160°C, t = 3h, 1 g of catalyst. Legend: HMF conversion (■), BHMF yield (■), total basicity determined by irreversible adsorption of acrylic acid(●).*

The results reported in **Table A-2** and **Figure A-5** demonstrated that both the pristine supports were active and totally selective towards the production of the unsaturated alcohol BHMF as the only reduction product. According to that reported above the two systems, characterized by different basic features and surface area, exhibited conversion values very different after three hours of reaction. With the synthesized MgO-HSA total conversion of HMF was obtained instead of the few percentage point displayed from the commercial sample.

The addition of lithium brought to different effect depending on the nature of the support used. If the alkaline metal, that was demonstrated to be deposit in the form of Li_2CO_3 over the surface of the doped systems, was added to the MgO-HSA the resulting catalytic performance was comparable to that of the un-doped material; indeed, total conversion of the substrate with 95% yield in BHMF were detected. These results well agree with the similar amount of basic sites determined for both the doped and un-doped materials based on the MgO-HSA. On the other hand, if the lithium was added on the MgO-C support, the resulting activity showed to deeply change in comparison to that of the pristine support. The 2-Li/MgO-C catalyst showed indeed an higher conversion, 87% instead of 5% of the un-doped material, but, despite the high activity, the selectivity

towards the formation of BHMF was very low considering the 14% of yield registered. Thus, the most of the HMF was converted to humin and degradation compounds that were observed in the form of black fouling on the reactor's walls at the end of the reaction. Considering the basic feature of the catalysts and taking into account that HMF was reported to undergoes into humin formation in basic environment, such as sodium hydroxide solution or in the presence of strong basic catalysts[22], it has been hypothesized that the higher basicity of 2-Li/MgO-C, in terms of total number of basic sites, compared to that of the un-doped material could be the cause for the substrate degradation in our reaction conditions. The latter hypothesis was then rejected considering that the MgO-HSA, characterized by 7,05 mmol/g of basic sites instead of the 1,45 mmol/g observed for the 2-Li/MgO-C, showed nil humin formation.

The degradation of HMF to humin compounds with 2-Li/MgO-C was then hypothesized to be related to the presence of lithium in the form of Li_2CO_3 (**Figure A-2**) that was the only difference with the pristine commercial support. Considering that HMF usually undergoes into humin formation in strong basic environment two degradation tests were performed preparing a water suspension of HMF with both the doped and un-doped catalysts prepared with MgO-C that was stirred for three hours. The pH of the solution as well as the conversion of HMF were monitored as a function of the time (**Figure A-6**) demonstrating that the higher pH registered using the lithium doped material could be identify as the main cause responsible for humin formation. Indeed, with the un-doped catalyst nil HMF conversion was observed for all the monitored time while, with the lithium containing sample, an increase of HMF conversion, coupled with a progressively darkening of the solution, was observed at the increase of the time confirming the formation of humin.

A final evidence confirming the direct involvement of Li_2CO_3 in the process of humin formation was found performing a catalytic test using it as catalyst (**Table A-2** Entry 5); total HMF conversion with nil BHMF formation were registered while humin compounds were find in the reactor confirming that the addition of Li_2CO_3 mainly enhance the ability of the commercial support to catalyze HMF degradation reactions.

Taking into account the degradation phenomena highlighted using HMF, the evaluation of the catalytic activity for the Li-doped catalysts and the comparison with that of the un-doped materials was continued changing the reducible substrate to furfural, that showed stronger resistance to humin formation and degradation reactions.
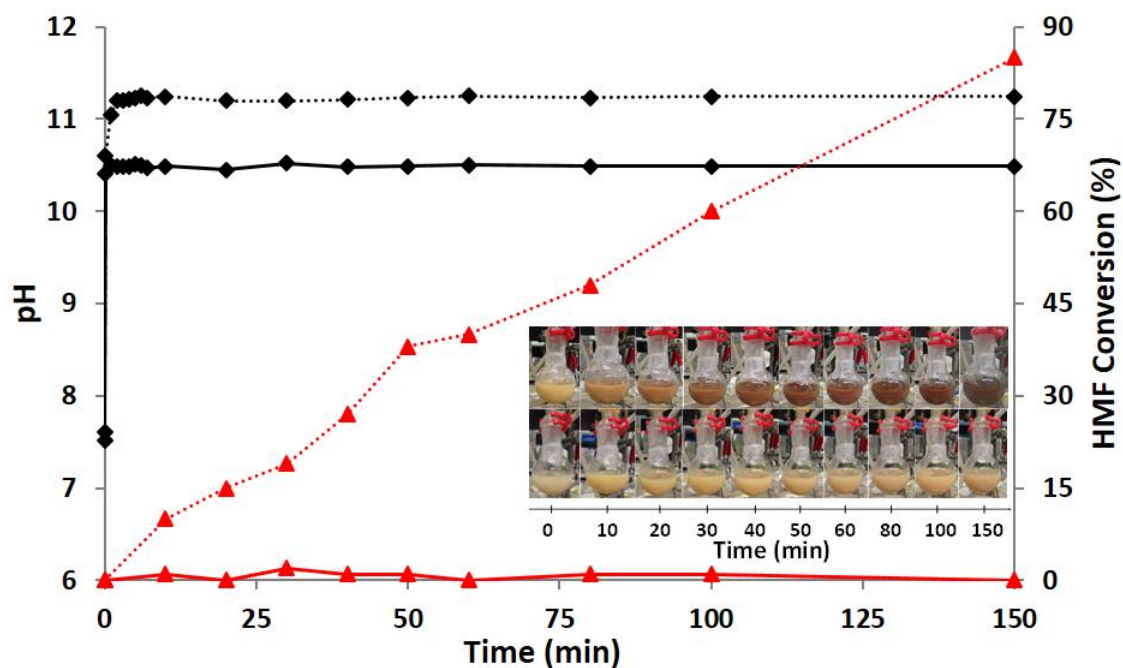
Figure A-6. *pH values and HMF conversion as a function of the time obtained during the HMF degradation tests performed with the pristine MgO-C and the doped 2-Li/MgO-C catalysts; in the square is reported the pictures of the solution at the increase of the time. Degradation test conditions: 50 ml of water, 1g of catalyst, 1.21mmol HMF, T = 90°C, 150 min. Legend: pH (━) MgO-C (bold line), 2-Li/MgO-C (dotted line), HMF conversion (━) MgO-C (bold line), 2-Li/MgO-C (dotted line).*

A.3.3. Liquid-phase catalytic transfer hydrogenation of FU over Li-doped MgO catalysts

In the former paragraph it was demonstrated that a change in the catalytic activity deriving from the addition of lithium on the surface of both the MgO-HSA and the MgO-C could not be possible using HMF as reducible substrate due to the easy propensity of this to undergo in degradation process to form humin compounds. For this reason FU has been identified as alternative substrate due to the stronger resistance to humin formation and degradation reactions.

The results reported in **Table A-3** and **Figure A-7** demonstrated once more that both the pristine supports were active and totally selective towards the formation of the unsaturated alcohol FAL as the only reduction product. Despite this, unlike to that previously reported using HMF, in the case of the tests performed using FU the difference in term of substrate conversion between the two supports was lower considering the total conversion registered with the MgO-HSA and the 55% obtained with the commercial sample instead of the 90% point of difference displayed with HMF. Thus, an higher reactivity of FU compared to HMF in the catalytic transfer hydrogenation reaction has been demonstrated. Nevertheless, the higher activity of the MgO-HSA compared to that of the MgO-C could be once more explained on the base of the difference, in terms of both total number of basic sites and surface area, displayed by the two systems.

The addition of lithium brought to different effect depending on the nature of the used support also in the tests carried out using FU as substrate. If the alkaline metal was added to the MgO-HSA the resulting catalytic performance was comparable to that of the un-doped material considering that with both the catalysts total conversion and total yield were observed. The same behavior was further confirmed in the tests performed decreasing the reaction time to 1 h (**Table A-3** Entries 5 and 6), condition at which both the Li-doped and the un-doped catalyst displayed the same performance, confirming that the addition of lithium to the high surface area MgO did not improve the catalytic activity of the latter; once more the obtained results well agree with the similar basicity displayed by the doped and un-doped catalyst. A possible explanation could be find in the high surface area and high number of basic sites, related to the presence of defective sites, for the synthesized support that make not relevant the effect deriving from lithium addition. Indeed, as reported above, the increase in the activity of MgO as a consequence of the Li-doping was mainly ascribable to superficial reconstruction phenomena deriving by the

deposition of the alkaline metal the consequence of which was the formation of an higher number of defective sites. In the case of the high surface material these phenomena could be marginal, or limited to a low fraction of the entire surface area of the catalyst, making the variation not detectable considering also that the pristine support had itself an high activity in the studied reaction.

On the other hand, if the lithium was added on the MgO-C support, an improvement of the catalytic activity was registered. With the doped 2-Li/MgO-C catalyst an increase of more than 30% for both the substrate conversion and the yield towards FAL were obtained compared to the un-doped material. Unlike to that highlighted above in the case of HMF reduction, in which the addition of lithium to the commercial support brought to an increase of activity and a drop in the unsaturated alcohol yield due to humin formation, using FU as reducible substrate, the increase of FAL yield well agree with the increase of conversion, confirming the high selectivity of the catalyst. The enhancement of the catalytic activity displayed by the doped catalyst was in agreement with the increase of the basicity (**Table A-1** Entries 3 and 4) that could be considered the main reason for the better performance registered.

On the base of these preliminary tests that showed a change in the catalytic activity between the doped and un-doped material only for the MgO-C support, it could be concluded that the effect of the lithium doping could be evaluated only if the alkaline metal was added over the low surface area support. Thus, the work was continued focusing the attention over the effect of the reaction time and on the lithium loading using only the commercial oxide as support and making a comparison between the different doped materials with the activity of both the materials used as supports, MgO-C and MgO-HSA.

Entry	Catalyst	Reaction time (h)	FU Conversion (%)	FAL Yield (%)	C-Loss (%)
1	MgO-C	3	55	54	1
2	2-Li/MgO-C	3	88	86	2
3	MgO-HSA	3	100	100	0
4	2-Li/MgO-HSA	3	100	100	0
5	MgO-HSA	1	79	79	0
6	2-Li/MgO-HSA	1	83	82	1

Table A-3. *FU conversion and FAL yield obtained with the different catalysts used for the preliminary tests. Reaction conditions: 50 ml of CH₃OH, 1.21 mmol of HMF, T = 160°C, 1 g of catalyst.*
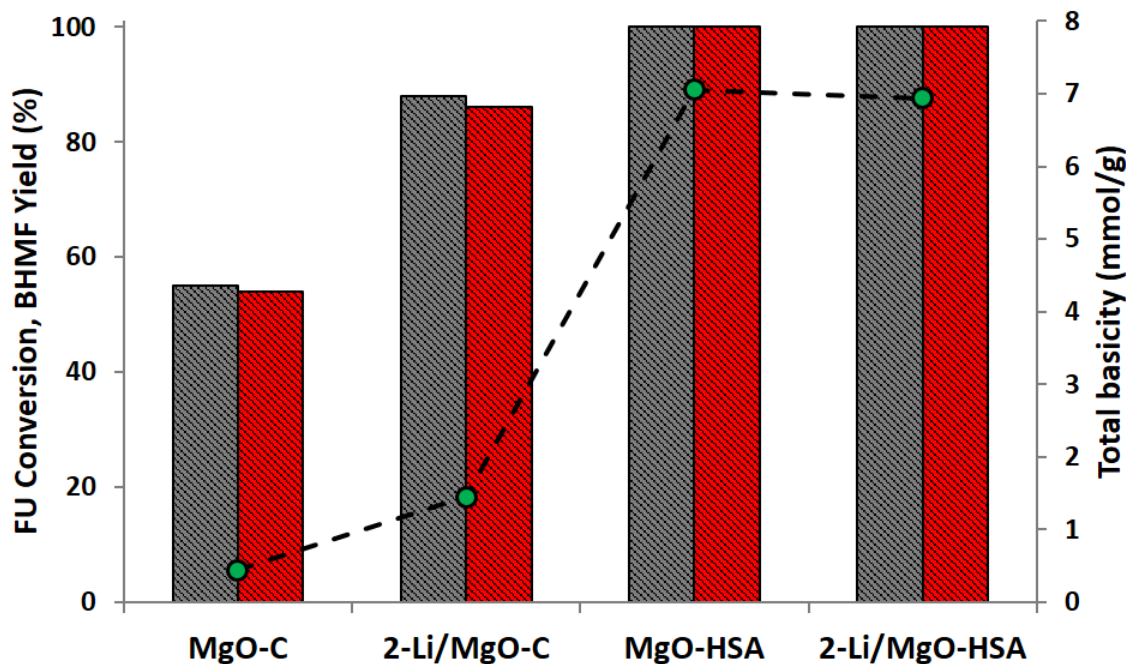
Figure A-7. *FU conversion and FAL yield obtained with the different catalysts used for the preliminary tests. Reaction conditions: 50 ml of CH₃OH, 1.21 mmol of FU, T = 160°C, t = 3h, 1 g of catalyst. Legend: FU conversion (■), FAL yield (■).*

The results obtained changing the reaction time in the range 15÷180 minutes (**Figure A-8** and **Table A-4**) further validated the former hypothesis for which the addition of lithium over the commercial support brought to an enhancement of the catalytic activity. Indeed, for all the studied reaction time both the FU conversion and the FAL yield registered with the doped material were higher than that obtained with the un-doped one. Furthermore, considering short reaction time, such as 30 and 60 minutes, the difference of activity was much more relevant considering that after one hour of reaction the un-doped commercial support showed only 3% of FU conversion while, with the doped sample the 71% of substrate conversion was obtained. Nevertheless, according to the basic feature of the systems the activity of the 2-Li/MgO-comm sample was always lower than that exhibited by the MgO-HSA. Finally, a general comment concerning the trend of the conversion and the yield exhibited by the three catalysts as a function of the reaction time was necessary. Indeed, regardless the difference in the activity, all the catalysts showed to be totally selective towards the formation of FAL as the only reduction product for all the reaction time tested; furthermore, for each of them a general increase of FU conversion was registered at the increase of the reaction time.
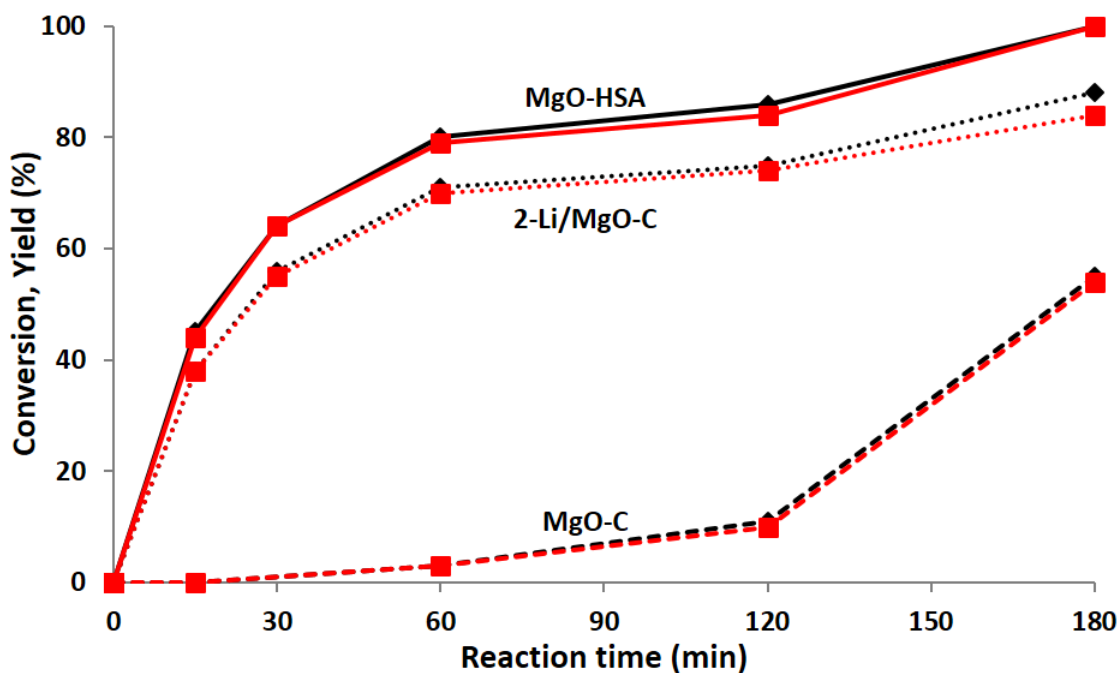
Figure A-8. *FU conversion and FAL yield as a function of the reaction time with the different catalysts used for the liquid-phase catalytic transfer hydrogenation. Reaction conditions: 50 ml of CH₃OH, 1.21 mmol of FU, T = 160°C, t = 0 ÷ 180 min, 1 g of catalyst. Legend: FU conversion (▬), FAL yield (▬); MgO-HSA (bold line), MgO-C (dotted line), 2-Li/MgO-C (pointed line).*

Entry	Catalyst	Reaction time (min)	FU Conversion (%)	FAL Yield (%)	C-Loss (%)
1		15	0	0	0
2	MgO-C	60	3	3	0
3		120	11	10	1
4		180	55	54	1
5		15	38	38	0
6		30	56	55	1
7	2-Li/MgO-C	60	71	70	1
8		120	75	74	1
9		180	88	84	4
10		15	45	44	1
11		30	64	64	0
12	MgO-HSA	60	80	79	1
13		120	86	84	2
14		180	100	100	0

Table A-4. *FU conversion and FAL yield as a function of the reaction time with the different catalysts used for the liquid-phase catalytic transfer hydrogenation. Reaction conditions: 50 ml of CH₃OH, 1.21 mmol of FU, T = 160°C, t = 0 ÷ 180 min, 1 g of catalyst.*

Finally the effect of the lithium loading on the catalytic activity of the commercial support has been investigated; for this purpose catalysts containing 5 and 10 weight % of Li were prepared by-means of the same procedure described above for the preparation of the 2-Li/MgO-C sample and named 5-Li/MgO-C and 10-Li/MgO-C respectively. In the former part of the chapter (**Table A-1**) it was already reported that the acid-base characterization demonstrated the total absence of acidic properties for all the doped catalysts while, concerning the basic properties, a correlation between the lithium addition and the number of the basic sites was demonstrated; the higher was the lithium content the higher were the number of basic sites.

Furthermore, considering also that the largest difference in terms of catalytic activity between the doped and un-doped catalyst was obtained for reaction time between 30 and 60 minutes, the trends for FU conversion and FAL yield for the catalysts containing different lithium loading were compared in the range of 60 minutes.

In **Figure A-9 (a)** are reported the values of FU conversion as a function of the reaction time for the catalysts synthesized with different lithium loading; the performance of both MgO-C and MgO-HSA are reported as the reference trends. First, it has to be highlighted that for all the tested catalysts, both the doped and un-doped one, a progressively increase of FU conversion was registered at the increase of the reaction time; furthermore, the systems showed to be always totally selective towards the formation of FAL as the only reduction product (for this reason only the trends for the conversion were reported on the graph).

Concerning the effect of the lithium addition, the tests performed confirmed a relevant enhancement of the catalytic activity for the doped materials if compared to the pristine support.

Despite this, only for very short reaction time, equal to 15 minutes, a difference between the systems containing different lithium loading could be observed. Indeed, for the tests performed at 30 and 60 minutes none appreciable difference was observed for the samples containing the 2, 5 and 10% of lithium respectively; these catalysts displayed catalytic performances very similar, making difficult the identification of an activity trend based on the lithium content. Furthermore, for the considered reaction time, the activity towards the conversion of FU to FAL for the Li-doped materials was always lower if compared to that of the MgO-HSA.

On the other hand, the comparison at the fixed time of 15 min (**Figure A-9 (a)** and **Table A-5**) make the difference between the different systems more appreciable, allowing the

identification of a correlation between the activity and the lithium loading. The higher was the lithium content the higher were both the FU conversion and the yield in FAL. Indeed, starting from the un-doped commercial support that showed nil substrate conversion, with the increase of lithium content to 2, 5 and 10 weight % a progressively increase of FU conversion was registered, up to the a final value of 47% obtained with the catalyst loaded with the highest lithium quantity; surprisingly the latter value was also higher to the one obtained with the MgO-HSA.

These results provided further evidence confirming the existence of a relationship linking together the amount of lithium loaded on the commercial catalyst with the amount of basic sites formed as a consequence of the superficial reconstruction phenomena and the resulting catalytic activity of the doped MgO-C catalysts in the liquid-phase catalytic transfer hydrogenation of FU. The correlation, for very short reaction time, between the catalytic activity of the different doped catalysts and the number of basic sites generated is reported in **Figure A-9 (b)**. It was clear that the higher was the number of basic sites the higher was the catalytic activity.
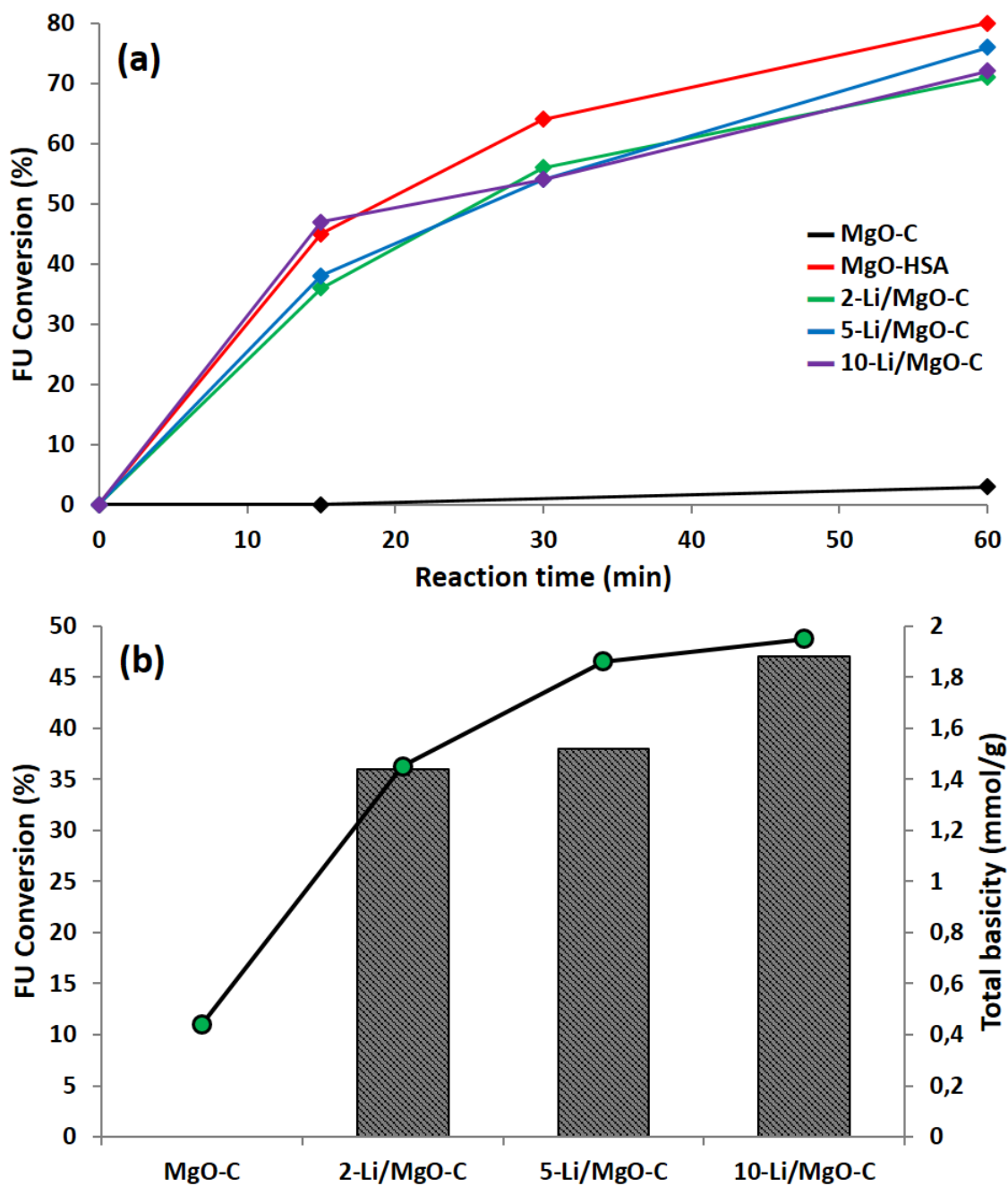
Figure A-9. *(**a**) Comparison of FU conversion obtained as a function of the reaction time with the catalysts prepared with different lithium loading over the MgO-C support. (**b**) FU conversion values obtained with the different catalysts at the fixed reaction time of 15 min. Reaction conditions: 50 ml of CH₃OH, 1.21 mmol of FU, T = 160°C, t = 0 ÷ 60 min, 1 g of catalyst. Legend: MgO-C (▬), MgO-HSA (▬), 2-Li/MgO-C (▬), 5-Li/MgO-C (▬), 10-Li/MgO-C (▬).*

Entry	Catalyst	FU Conversion (%)	FAL Yield (%)	Total basic sites (mmol/g)[a]	TON[b]	TOF (h[-1])[c]
1	MgO-C	0	0	0,44	0	0
2	2-Li/MgO-C	36	37	1,45	0,309	1,24
3	5-Li/MgO-C	38	37	1,86	0,241	0,96
4	10-Li/MgO-C	47	45	1,95	0,279	1,12
5	MgO-HSA	45	44	7,05	0,076	0,30

Table A-5. *FU conversion and FAL yield obtained with the catalysts prepared with different lithium loading at the fixed reaction time of 15 minutes. Reaction conditions: 50 ml of CH$_3$OH, 1.21 mmol of FU, T = 160°C, t = 15 min, 1 g of catalyst.*

a. *Determined by irreversible adsorption of acrylic acid;*
b. *TON expressed as mol of FAL produced per basic site; the number of basic sites was assumed to coincide with the acrylic acid moles adsorbed during the basicity determination test;*
c. *TOF = TON/reaction time.*

In **Table A-5** were also reported the values of TON and TOF for the catalysts prepared with the different lithium content, calculated by assuming that the surface basic sites, previously determined by means of the irreversible adsorption of acrylic acid, are the main sites contributing to the reaction. The reported values reflected the relevant increase observed for the substrate conversion for the doped catalysts compared to the un-doped commercial support. The MgO-C catalysts showed indeed a nil TOF in agreement with the nil registered conversion while, for the lithium doped materials based on this support, an increase of the TOF values in the range between 0,96 and 1,24 was registered confirming the deep increase in the activity towards the catalytic transfer hydrogenation for the low surface area lithium doped catalysts.

Although a correlation between the amount of lithium, the generated strong basic sites and the catalytic performance of the doped materials compared to that of the commercial sample has been demonstrated, some points remained still not well understood. Indeed, the addition of lithium in high quantities clearly generated an increase of the basic sites but these were at least the five times, for the sample containing the 10%, of the ones detected in the commercial sample, value not enough to explain the deep increase of activity. Furthermore, the doped materials obtained using the MgO-C as support showed all a catalytic performance similar, or higher in certain case, to the MgO-HSA for which

the number of strong basic sites was many times higher to that detected for the doped materials.

A second consideration, which was directly linked to the former one, was related to the structural defects generated as a consequence of the lithium addition. It was reported above that the enhancement of the catalytic activity for the doped materials could be rationalized as a roughening of the MgO surface on an atomic level, leading to exposition of more low coordinated O^{2-} surface ions and higher index planes such as fourfold and threefold coordinated surface O^{2-} ions, O^{2-}_{4c} and O^{2-}_{3c}. In this view it could be hypothesized that the new defective sites generated over the surface, the presence of which was demonstrated with TEM analysis in **Figure A-4**, could not be entirely titrated using acrylic acid or CO_2 as probe molecules and that the number of the basic sites remain underestimate. On the other hand, the defectively sites were generally considered to be able to catalyze the catalytic transfer hydrogenation reaction. For this reason the enhancement of the superficial defectively due to the lithium doping, confirmed by TEM analysis, could be considered a possible explanation in addition to the higher basicity generated to justify the higher reactivity of the doped materials.

A.4. Conclusions

The lithium doped-MgO catalysts were synthesized by-means of the wet impregnation procedure using both the commercial sample characterized by a low surface area and the high surface area prepared by thermal decomposition of the hydrotalcite-like precursor. The addition of the alkaline metal was demonstrated to affect the bulk features of the catalysts, mainly in terms of the total basic sites as well as of the superficial defectively, in the case of the commercial sample doping while, no relevant change in the properties of the high surface area MgO was observed after the addition of lithium. The doped materials prepared using the commercial magnesium oxide as support showed indeed an overall increase of the total amount of basic sites but, analyzing the strength distribution of these by means of CO_2-TPD, it was demonstrated that a general decrease of the strength for the generated sites took place at the increase of lithium content.

According to the catalysts characterization, for which the addition of lithium demonstrated to leave unaltered the basicity of the high surface area support, none enhancement of catalytic activity was observed for the doped Li/MgO-HSA in

comparison to the pristine support in the liquid-phase catalytic transfer hydrogenation reaction using both FU and HMF as the reducible substrates and methanol as the H-transfer reactant.

On the other hand, for the doped Li/MgO-C series a relevant enhancement of the catalytic activity towards the CTH reaction was observed. Despite this, only for the tests performed using FU as reducible substrate the increase of the activity was clearly observed. Indeed, in the case of the tests performed with HMF the formation of humin due to the higher strength of the basic sites in the lithium doped material was the main catalyzed process. The tests performed with FU demonstrated the existing of a relation between the amount of lithium loaded, the basic sites and the resulting catalytic activity; for very short reaction time, equal to 15 minutes, the lithium doped materials showed a catalytic activity many times higher to that of the un-doped and the catalyst containing the 10% of lithium showed the better activity.

Due to their high reactivity the lithium doped materials offered an alternative to FAL production from FU with a high selectivity and high TOF without the need for H_2 at high pressure and precious metal catalysts.

[1] T. Pasini, A. Lolli, S. Albonetti, F. Cavani, M. Mella, *J. Catal.,* 2014, **317**, 206

[2] C. Mesters, *Annu. Rev. Chem. Biomol. Eng.,* 2016, **7**, 223

[3] R. Horn, R. Schlögl, *Catal. Lett.,* 2015, **145**, 23

[4] J. H. Lunsford, *Angew. Chem.,* 1995, **107**, 1059; *Angew.Chem. Int. Ed. Engl.,* 1995, **34**, 970

[5] D. J. Driscoll, W. Martir, J. X. Wang, J. H. Lunsford, *J. Am. Chem. Soc.,* 1985, **107**, 58

[6] T. Ito, J.Wang, C. H. Lin, J. H. Lunsford, *J. Am. Chem. Soc.,* 1985, **107**, 5062

[7] C. Mirodatos, V. Perrichon, M.C. Durupty, P. Moral, *Stud. Surf. Sci. Catal.,* 1987, **34**, 183

[8] C. Mirodatos, G.A. Martin, J.C. Bertolini, J. Saint-Just, *Catal. Today,* 1989, **4**, 301

[9] S. Arndt, U. Simon, S. Heitz, A. Berthold, B. Beck, O. Görke, J.-D. Epping, T. Otrembe, Y. Aksu, E. Irran, G. Laugel, M. Driess, H. Schubert, R. Schomäcker, *Top. Catal.,* 2011, **54**, 1266

[10] S. Arndt, G. Laugel, S. Levchenko, R. Horn, M. Baerns, M. Scheffler, R. Schlögl, R. Schomäcker, *Catal. Rev. Sci. Eng.,* 2011, **53**, 424

[11] E. V. Kondratenko, M. Baerns, *Handbook of Heterogeneous Catalysis, Vol. 6* (Ed.: H. K. G. Ertl, F. Sch_th, J. Weitkamp), Wiley-VCH, Weinheim, 2008

[12] P. Myrach, N. Nilius, S. V. Levchenko, A. Gonchar, T. Risse, K. P. Dinse, L. A. Boatner, W. Frandsen, R. Horn, H. J. Freund, R. Schlçgl, M. Scheffler, *ChemCatChem,* 2010, **2**, 854

[13] U. Zavyalova, G. Weinberg, W. Frandsen, F. Girgsdies, T. Risse, K. P. Dinse, R. Schloegl, R. Horn, *ChemCatChem,* 2011, **3**, 1779

[14] U. Zavyalova, M. Geske, R. Horn,G.Weinberg,W. Frandsen, M. Schuster, R. Schlçgl, *ChemCatChem,* 2011, **3**, 949

[15] K. Kwapien, J. Paier, J. Sauer, M. Geske, U. Zavyalova, R. Horn, P. Schwach, A. Trunschke, and R. Schlçgl, *Angew. Chem. Int. Ed.,* 2014, **53**, 8774

[16] G. W. Watson, *Radiat. Eff. Defects Solids,* 2002, **157**, 773

[17] U. Zavyalova, G. Weinberg, W. Frandsen, F. Girgsdies, T. Risse, K. P. Dinse, R. Schloegl, R. Horn, *ChemCatChem,* 2011, **3**, 1779

[18] S. Arndt, U. Simon, S. Heitz, A. Berthold, B. Beck, O. Gorke, J. -D. Epping, T. Otremba, Y. Aksu, E. Irran, G. Laugel, M. Driess, H. Schubert, R. Schomacker, *Top Catal,* 2011, **54**, 1266

[19] S. J. Palmer, R. L. Frost, T. Nguyen, *Coordination Chemistry Reviews,* 2009, **253**, 250

[20] F. Wang, N. Ta, W. Shen, *Applied Catalysis A: General,* 2014, **475**, 76

[21] U. Zavyalova, G. Weinberg, W. Frandsen, F. Girgsdies, T. Risse, K. P. Dinse, R. Schloegl, R. Horn, *ChemCatChem,* 2011, **3**, 1779

[22] A. Lolli, S. Albonetti, L. Utili, R. Amadori, F. Ospitali, C. Lucarelli, F. Cavani, *Applied Catalysis A: General,* 2015, **504**, 408

RINGRAZIAMENTI

Dai eccomi qua, come al solito non mantengo mai le promesse, ma lo sanno in tanti e ne sono cosciente anche io, parlo, parlo e straparlo, tanto che anche i muri mi direbbero di stare zitto a volte; ma anche quando scrivo non scherzo. Mi ero ripromesso di scrivere un qualcosa più corto di quanto fatto alla magistrale per il semplice motivo di non tediare i "numerosi lettori", ovviamente mettendoci tutto l'impegno ho scritto parecchio in più. Ma va beh sono gli imprevisti, diciamo che non sono stato colpito dal blocco dello scrittore.

Lasciando le cavolate da parte mi sembra ieri quando sono entrato per la prima volta in Aula 1, e ne sono uscito più o meno un mese fa per l'ultima volta dopo una delle tante proclamazioni di Laurea, uno di quei momenti che rendono la nostra facoltà una grande famiglia, ma, forse, quell'ultima è stata diversa dalle altre, speciale. Sono passati 8 anni da quel primo giorno, 8 lunghi e velocissimi anni che mi hanno fatto crescere e diventare grande ("uomo" sarebbe un parolone), 8 anni durante i quali ho conosciuto tante persone ma soprattutto trovato tanti amici e amiche, persone "vere" che mi hanno dato tanto e con cui ho condiviso tutto quello che significa e rappresenta "Viale del Risorgimento 4, 40136, Bologna". Lo so, non sembro neanche io, sarà che mentre sto scrivendo queste parole sono già a Bergamo lanciato da una catapulta in una nuova vita, sono più sentimentale del solito.
Ma è ora di iniziare a ringraziare un po' di quelle tante persone che ho incrociato in questo lungo cammino, cercherò di non farlo ma di sicuro mi dimenticherò qualcuno…scusate!!!!

Mamma, Papà, Marty grazie veramente di cuore per tutto quello che avete fatto per me in questo periodo, ci siete sempre stati, magari silenziosamente, lasciandomi rimuginare senza dir niente, perché so di essere un testardo e difficilmente ho chiesto il vostro aiuto, anche quando probabilmente mi sarebbe servito…mi conoscete e sapete che sono fatto così…mi raccomando scimmia tieni botta perché lo so, sono a Bergamo, sto facendo finta di diventare grande, ma è come se fossi li!!!

Dicono che di mamma ce ne sia una sola…però è che come se in questi ultimi anni ne avessi avute due!! Ahahahahah no, non sono diventato matto, un grazie grande come una casa, ma di quelle belle grandi…tipo villa di Holliwood…lo voglio fare a Stefania, che mi ha preso a lavorare con lei in questi anni ed è sempre stata più una mamma, un'amica

piuttosto che un capo. Le mie bacchettate me le sono prese ma è sempre stata disponibile a parlare e consigliarmi su tutto, specialmente su cose extra chimica (…donne???!!...).

Un grazie enorme va anche a Fabrizio, babbo Cavani, che molte volte mi ha aiutato a trovare il bandolo scientifico della matassa da sbrogliare, che mi ha permesso di giocare per il posto in cui sono adesso. Grazie mille a lei prof. ed ai tanti selfie (Belgio-Italia 0-2, Europei 2016, Catprep-Vogué, compagni del Belgio presi per i fondelli in sessione plenaria la mattina dopo, come dimenticare).

Amici, compagni, colleghi, giovani studenti Padawan è arrivato il vostro momento. Dai va, andiamo per ordine.

A tutti i miei giovani Padawan, se sono stato capace di scrivere questa tesi una buona parte del merito è vostro, Danilo, Tito, Matteo, Depa, grazie di cuore perché abbiamo lavorato tanto, fatto tante cazzate ma soprattutto ci siamo divertiti. Un grazie particolare lo voglio fare a Danilo e Tito che da semplici studenti sono diventati veri amici con cui condividere tutto, e per riprendere le parole di Tito "...la fine di un viaggio è solo l'inizio di un altro...", questa volta sono io a ringraziarvi per avermi accompagnato.

Ciccio, Taba, Mattia, Carlo, Vasso, Sara, Macs, Faso, Patatone, Ste, Cla, Ali, Dodo, Erica, Culo, Nine...siete stati fantastici in lab, fuori dal lab, ai congressi, alle feste, a far schifo...insieme a tutti voi le mille ore passate in lab sono volate!! Grazie in particolare a Ciccio, anche se per questioni esterne ci sono stati alti e bassi tra di noi, ti considero uno dei miei più fidati amici, non dimenticherò mai le chiacchierate fino a tarda sera in lab a parlare di stronzate e di cose serie, tutte le feste e le mille balle allucinanti che abbiamo preso insieme, grazie veramete di tutto. Un mega grazie anche a te Sara, adesso starai conquistando gli USA insieme a Roger ma ho trovato in te una vera amica con cui confidarmi e parlare di tutto.

A tutti i miei amici del paesello, quella Sanpi Beach che rimarrà sempre un punto di riferimento, grazie mille perchè ci conosciamo da quando siamo nati e ho sempre potuto contare su di voi.

La famiglia della palla a spicchi..."Innanzitutto GRAZIE"...grazie a tutti voi in giro per l'Italia, Fede, Chiaru, Bart, Marci, Zuzzu, Edo, Leprottino, Bonni & Bonni, Zanco, Pellicagna e tutti gli altri.

È il momento del Jolly Roger e del Tridente d'Attacco. Marco, Luca, Mattia, Fede, Joe, Max. In voi ho trovato amici veri e una famiglia, grazie di tutto, più di questo non dico perchè l'amicizia che ci lega è tutto.

Beh che dire...anche nei ringraziamenti sono stato lungo...sembra un deja-vù ma mi è rimasta ancora una persona da ringraziare, una persona che per mille ragioni è diventata un punto di riferimento su cui contare e una delle persone più importanti per me...vedremo futuro e destino cos'avranno in serbo, cosa scriveranno su quella tela...per il momento...grazie Sara!!